*L*aboratoire de *M*écanique des *F*luides et d'*A*coustique
LMFA UMR 5509

Physics of turbulent flow

Christophe Bailly

Centrale Lyon – MOD 3rdYear & MSc. – version 13-12-2023

Outline

Turbulent flows

- unsteady aperiodic motion
- unpredictable behaviour
- presence of a wide range of time and space scales

Turbulence appears when the source of the kinetic energy which drives the fluid motion is able to overcome viscosity effects, that is the Reynolds number must be sufficiently large

- astrophysics, geophysical flows including ocean circulation, climate, weather forecast, hydrology, dispersion of aerosols
- external aerodynamics for aeronautics & ground transportation, internal flows in mechanical engineering, biomechanics, biological flows
- noise of turbulent flows (aeroacoustics), sound propagation (atmosphere, ocean), fluid-solid interaction and vibroacoustics

Non-linearity of Navier-Stokes' equations

$$\rho\left(\frac{\partial \boldsymbol{u}}{\partial t}+\boldsymbol{u}\cdot\nabla\boldsymbol{u}\right)=-\nabla p+\mu\nabla^2\boldsymbol{u}$$

The non-linear nature of the convective acceleration $\boldsymbol{u}\cdot\nabla\boldsymbol{u}$ is at the origin of the development of a large range of space and time scales, that are observed in a turbulent flow.

A (too) simple example illustrating the generation of harmonics is based on the simplified equation $\partial_t\boldsymbol{u}+\boldsymbol{u}\cdot\nabla\boldsymbol{u}=0$, with $\boldsymbol{u}=(u_1,u_2)$ in 2-D. By assuming that at time t_0,

$$\begin{cases} u_1(x_1,x_2,t_0)=A\cos(k_1x_1)\sin(k_2x_2)\\ u_2(x_1,x_2,t_0)=B\sin(k_1x_1)\cos(k_2x_2)\end{cases}$$

with $Ak_1+Bk_2=0$ to satisfy the incompressibility condition $\nabla\cdot\boldsymbol{u}=0$

Non-linearity of Navier-Stokes' equations (cont.)

A Taylor series of the velocity $\boldsymbol{u}$ around t_0 provides

$$\boldsymbol{u}(\boldsymbol{x},t) = \boldsymbol{u}(\boldsymbol{x},t_0) + (t-t_0)\,\partial_t \boldsymbol{u}|_{t_0} + \dots \qquad \text{with} \;\; \partial_t \boldsymbol{u}|_{t_0} = -\,\boldsymbol{u}\cdot\nabla\boldsymbol{u}|_{t_0}$$

As an illustration, one gets for u_1

$$\begin{aligned} u_1\,(x_1,x_2,t) &= A\cos(k_1x_1)\sin(k_2x_2) \\ &\quad + (t-t_0)\,\frac{k_1A^2}{2}\left[\cos(2k_1x_1)\sin^2(k_2x_2) + \sin(2k_1x_1)\cos^2(k_2x_2)\right] + \dots \end{aligned}$$

It can be noted the production of higher harmonics $(2k_1, 2k_2, k_1+k_2)$, that is of larger wavenumbers corresponding to smaller structures, and also of smaller harmonics (k_1-k_2)

What is a turbulent structure of wavenumber k ?

What is the smallest structure that can survive in the flow, before destruction by viscosity ?

Representation in spectral space

Model of a turbulent structure of wavenumber k : energy is contained in a narrow band around $k = 2\pi/l$, where l is a characteristic length scale, see figure on the right

A real turbulent structure (vortex or eddy) can be decomposed into waves of different wavelengths, with their amplitude and phase, using Fourier transform

Various other decompositions can also be used (wavelets for instance)

A structure of wavenumber k (of size $\sim 1/k$) can be seen as an elementary component of the previous decomposition

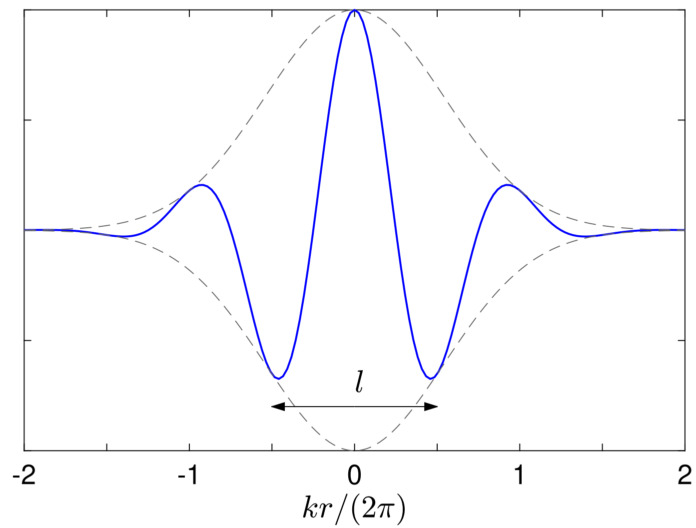

$f(r) = \cos(kr)\exp(-\log(2)(r/r0)^2)$
with $r_0 = 4/k$ here

The Fourier transform of f is centered around k

Viscous scales

The energy transfer induced by the convective acceleration $\boldsymbol{u}\cdot\nabla\boldsymbol{u}$ is stopped by the molecular viscosity (impossible to preserve small structures with too large velocity gradient)

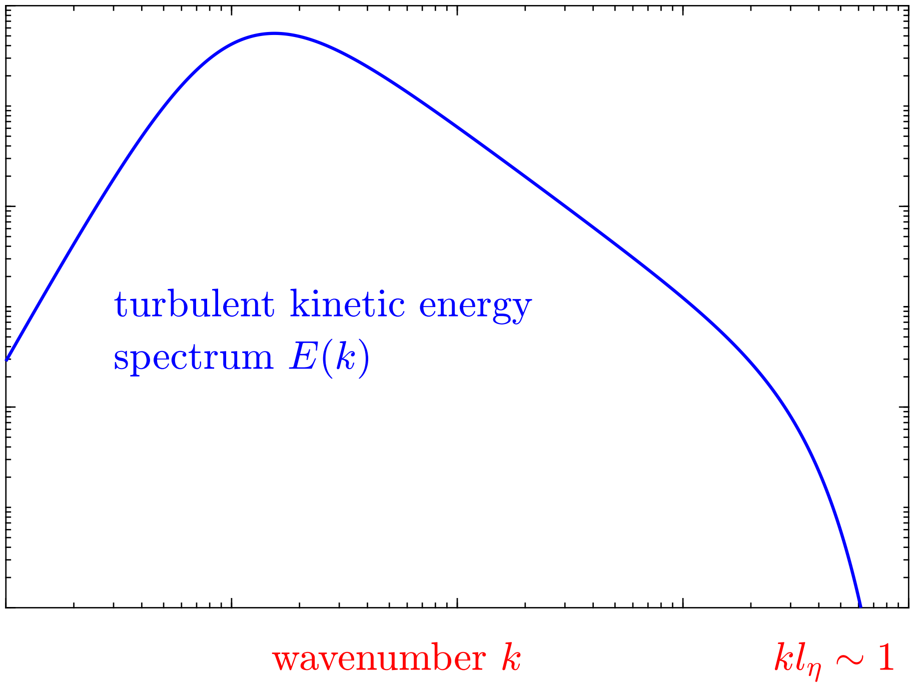

Smallest structures u_η $k_\eta \sim 1/l_\eta$

$$\frac{\partial \boldsymbol{u}}{\partial t} \simeq \nu \nabla^2 \boldsymbol{u} \quad \text{(Stokes)}$$

The balance between the two terms

$$\frac{\partial \boldsymbol{u}}{\partial t} \sim \frac{u_\eta^2}{l_\eta} \qquad \nu\nabla^2\boldsymbol{u} \sim \nu \frac{u_\eta}{l_\eta^2}$$

leads to

$$\mathrm{Re}_\eta = \frac{l_\eta u_\eta}{\nu} \sim 1$$

These viscous scales (u_η, l_η), also called Kolmogorov's scales, are the smallest scales of the flow allowed by viscosity. They impose the spatial resolution necessary for measurement or simulation

- **Turbulence is part of continuum mechanics**
  Viscous scale l_η wrt the free mean path λ_l of molecules

Knudsen number $$\mathrm{Kn} = \frac{\lambda_l}{l_\eta} \ll 1$$

- **Sensitivity to initial conditions**

  The nonlinearity of the Navier-Stokes equations does not allow the time evolution of turbulent fields to be predicted over a long period. The reason for this is that a small difference in the initial conditions introduces significant differences as time goes, linked to the largest Lyapunov exponent for chaotic systems.

  An initial separation of 1 cm between two fluid particles in the atmosphere results in a 10 km separation within just a day, the butterfly effect in chaos theory !

  Ruelle, D. and Takens, F., 1971, On the nature of turbulence, *Commun. Math. Phys.*, **20**, 167–192

- **Mean and fluctuating quantities**

The statistical mean $\bar{F}(\boldsymbol{x},t)$ of a variable $f(\boldsymbol{x},t)$ is defined as

$$\bar{F}(\boldsymbol{x},t) = \lim_{N\to\infty} \frac{1}{N} \sum_{i=1}^{N} f^{(i)}(\boldsymbol{x},t)$$

where $f^{(i)}$ is the i-th realization : convenient when manipulating equations but difficult to implement in practice, or even impossible for geophysical flows !

Can we approximate the ensemble mean $\bar{F}$ of $f = \bar{F} + f'$ by a sufficiently long time average F_T of one realization only ?

$$F_T = \frac{1}{T}\int_0^T f(t)dt$$

Time average

Time average makes sense only if turbulence is stationary, that is statistics are independent of time. The autocorrelation coefficient $\mathcal{R}$ is then only an even function of the time separation τ

$$\mathcal{R}(\tau) = \frac{\overline{f'(t)f'(t+\tau)}}{\overline{f'^2}}$$

We can estimate the difference between F_T obtained by a finite integration time and the true (ensemble) mean value $\bar{F}$ by considering

$$F_T - \bar{F} = \frac{1}{T}\int_0^T \left[f(t) - \bar{F}\right] dt = \frac{1}{T}\int_0^T f'(t)\,dt$$

The mean square value is

$$(F_T - \bar{F})^2 = \frac{1}{T}\int_0^T f'(t_1)\,dt_1 \times \frac{1}{T}\int_0^T f'(t_2)\,dt_2$$

Time average (cont.)

By taking the statistical average, that is $\overline{(F_T - \bar{F})^2}$, one has

$$\overline{(F_T - \bar{F})^2} = \frac{\overline{f'^2}}{T^2} \iint_{\mathcal{D}} \mathcal{R}(t_2 - t_1)\, dt_1\, dt_2 = \frac{\overline{f'^2}}{T^2} \iint_{\mathcal{D}'} \mathcal{R}(\tau)\, dt_1\, d\tau \qquad \tau = t_2 - t_1$$

The integration over t_1 can be achieved by splitting the domain $\mathcal{D}'$ as follows,

$$\iint_{\mathcal{D}'} \mathcal{R}(\tau) dt_1 d\tau$$
$$= \int_0^T (T-\tau)\mathcal{R}(\tau) d\tau + \int_{-T}^0 (T+\tau)\mathcal{R}(\tau) d\tau$$
$$= 2\int_0^T (T-\tau)\mathcal{R}(\tau) d\tau$$

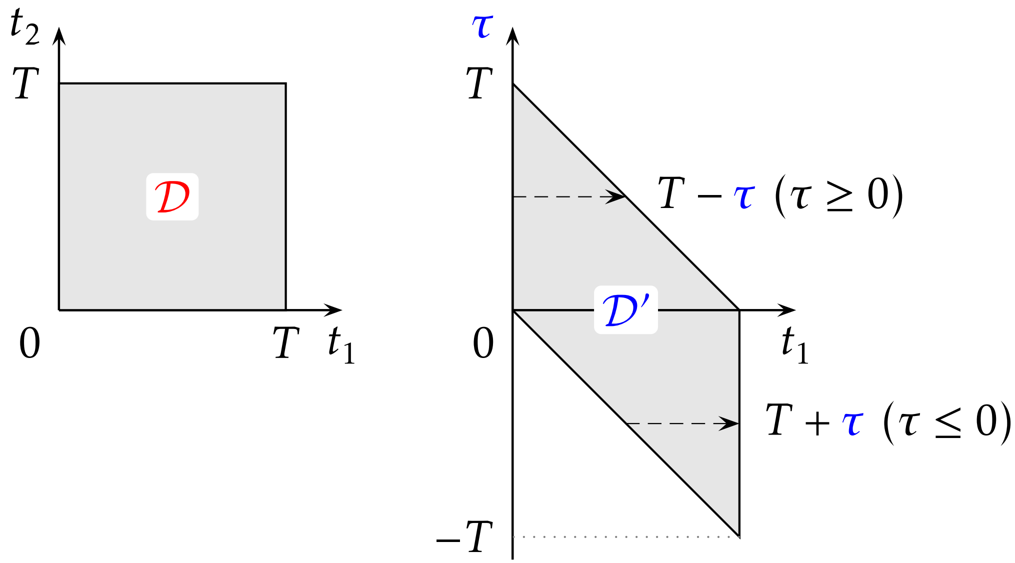

Time average (cont.)

The mean square error between F_T and the true mean value $\bar{F}$ can thus be estimated as

$$\overline{(F_T - \bar{F})^2} = 2\,\frac{\overline{f'^2}}{T}\int_0^T \left(1 - \frac{\tau}{T}\right)\mathcal{R}(\tau)\,d\tau \simeq 2\,\frac{\overline{f'^2}}{T}\int_0^T \mathcal{R}(\tau)\,d\tau \simeq 2\overline{f'^2}\,\frac{\Theta}{T}$$

if the time integration T is much longer than the integral time scale Θ, defined by

$$\Theta = \int_0^{\tau^\star} \mathcal{R}(\tau)d\tau$$

where $\tau^\star = \infty$ or the first zero crossing of $\mathcal{R}(\tau)$ in practice

The term τ/T is then small in the range of τ where $\mathcal{R}(\tau)$ is non-zero, and the time average value $F_T \to \bar{F}$ as $T \to \infty$

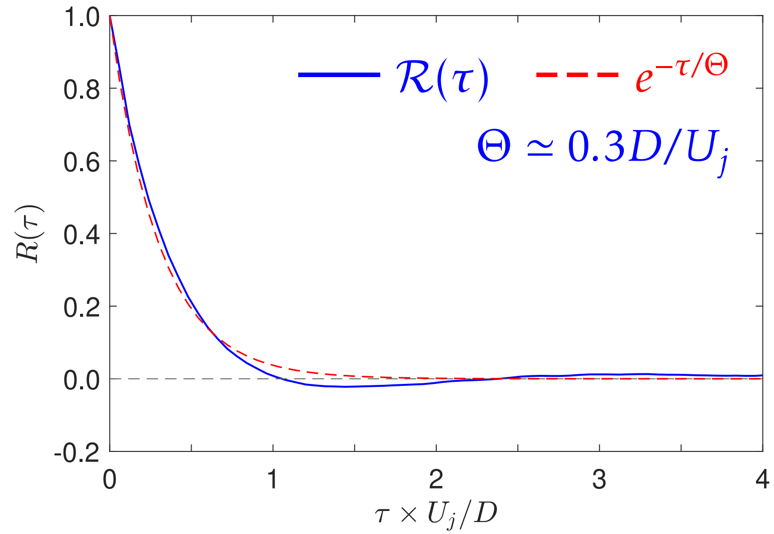

Subsonic jet at $\mathrm{Re}_D = 10^5$
$x_1 = 0$, $x_2 = 2D$

- **Ergodicity**

  By considering the time average in signal processing to approximate the ensemble mean, we assume that turbulence is an ergodic process.

  Ergodicity expresses the idea that a trajectory of a dynamical system (of a stochastic process signal) will eventually visit all parts of the phase space in which the system moves, in a uniform and random direction. Statistical properties can thus be deduced from a single (sufficiently long) realization.

Textbooks

Batchelor, G.K., 1967, An introduction to fluid dynamics, *Cambridge University Press*, Cambridge.

Bailly C. & **Comte Bellot** G., 2003 Turbulence, *CNRS éditions*, Paris (out of print).
———, 2015, *Turbulence* (in english), Springer, Heidelberg.
(360 pages, 147 illustrations, Foreword by Charles Meneveau)

Bailly C. & Comte Bellot G., 2003, *Turbulence* (in french), CNRS éditions, Paris.
———, 2015, *Turbulence* (in english), Springer, Heidelberg.

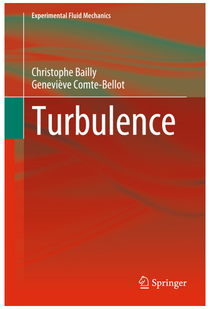

Springer, ISBN 978-3-319-16159-4,
360 pages, 147 illustrations.

Candel S., 1995, Mécanique des fluides, *Dunod Université*, 2nd édition, Paris.

Davidson P.A., 2004, *Turbulence. An introduction for scientists and engineers*, Oxford University Press, Oxford.

Davidson, P.A., **Kaneda**, Y., **Moffatt**, H.K. & **Sreenivasan**, K.R., Edts, 2011, *A voyage through Turbulence*, Cambridge University Press, Cambridge.

Guyon E., **Hulin** J.P. & **Petit** L., 2001, Physical hydrodynamics, *EDP Sciences / Editions du CNRS*, première édition 1991, Paris - Meudon.

Textbooks (cont.)

Hinze J.O., 1975, Turbulence, *McGraw-Hill International Book Company*, New York, 1ère édition en 1959.

Landau L. & **Lifchitz** E., 1971, Mécanique des fluides, *Editions MIR, Moscou*.
Also *Pergamon Press*, 2nd edition, 1987.

Lesieur M., 2008, Turbulence in fluids : stochastic and numerical modelling, *Kluwer Academic Publishers, 4th revised and enlarged ed.*, Springer.

Pope S.B., 2000, Turbulent flows, *Cambridge University Press*.

Tennekes H. & **Lumley** J.L., 1972, A first course in turbulence, *MIT Press*, Cambridge, Massachussetts.

Van Dyke M., 1982, An album of fluid motion, *The Parabolic Press*, Stanford, California.

White F., 2005, Viscous fluid flow, 3ed Ed., *McGraw-Hill, Inc.*, New-York (1st Ed. 1974).

Outline

The main objectives are the mastery of basic concepts (turbulence production, turbulence boundary layer, role of vorticity, homogeneous and isotropic turbulence, Kolmogorov theory), the development of skills in turbulence modeling, the critical analysis of results, and the acquisition of a global vision of experimental approaches.

- Introduction
- Statistical description of turbulent flows
- Wall-bounded turbulent flows
- Dynamics of vorticity
- Homogeneous and isotropic turbulence
- Dynamics of isotropic turbulence – Kolmogorov's theory
- Introduction to experimental techniques

Outline (cont.)

- **Practical work**

  Lab-session Numerical simulation of the mean flow in a channel
  BE1 – Small class of 4 hours - exercices
  BE2 – Small class of 4 hours to solve a complete problem

  Auditors : you are invited to follow these practical activities
  (Let us know about it !)

- **Teaching team** Christophe Bailly
  Christophe Bogey

Assessment for this course

- There are one practical lab session, and two small classes of 4h (so-called ‘BE’, may involve signal processing, coding of simple models using Matlab and analytical developments). **For 3rd year students,** the grade is obtained with BE 60% and lab work 40%.

- Absence : it is possible to exceptionally modify a lab session, only by exchanging your session with that of another student.

- **Master student**, additional final exam (closed book and open notes), wednesday 20 december 2023. The final mark will be the max between – the final exam mark – and (50% final exam + 30% BE + 20% lab work).

- **Course slides** can be downloaded by following this link https://acoustique.ec-lyon.fr/christophe.bailly.php#turbulence

airfoil	profil
bluff body	corps non profilé
boundary layer	couche limite
bulk velocity	vitesse de débit
buoyancy	flottabilité
curl	rotationnel
chord	corde
conservative force	force qui dérive d'un potentiel (gravité par exemple)
creeping flow	écoulement rampant
Darcy friction coefficient	coefficient de pertes de charge
drag	traînée
density (mass per unit volume)	masse volumique
efficiency	rendement
energy head	charge
friction velocity	vitesse de frottement
head loss	perte de charge
inviscid flow	écoulement non visqueux
leading edge	bord d'attaque (d'un profil)
lift	portance
lift-to-drag ratio	finesse
mass fraction	fraction massique
mixture	mélange
point vortex	tourbillon ponctuel

relative density	densité
shaft work	travail de l'arbre (d'une machine tournante)
skin-friction coefficient	coefficient de frottement
slip boundary condition	condition aux limite glissante
stall	décrochage
strain (deformation) tensor	tenseur des déformations
stream function	fonction de courant
streamlined body	corps profilé
stress tensor	tenseur des contraintes
thrust	poussée
torque (angular momentum)	couple
trailing edge	bord de fuite (d'un profil)
vortex shedding frequency	fréquence du lâcher tourbillonnaire
vortex sheet	nappe (infiniment mince) de vorticité
wake	sillage
wall shear stress	contrainte pariétale

aka	also known as
wrt	with respect to

- **Both indicial and boldface notations are used to indicate vectors**

  vector $\boldsymbol{U} \equiv \overrightarrow{U}$, i-th component U_i, norm U, $U^2 = \boldsymbol{U} \cdot \boldsymbol{U}$
  gravity $\boldsymbol{g}$, $g_i = -g\delta_{3i}$, $\boldsymbol{g} = (g_1, g_2, g_3) = (0, 0, -g)$, $g = 9.81$ m.s^{-2}
  density ρ (kg.m^{-3})
  δ_{ij} Kronecker delta

  Einstein summation convention
  When an index variable appears twice in a single term (dummy index), it implies summation of that term over all the values of the index.

  Scalar product between two vectors $\boldsymbol{a}$ and $\boldsymbol{b}$

$$\boldsymbol{a} \cdot \boldsymbol{b} = \sum_{i=1}^{3} a_i b_i = a_i b_i \quad \text{(dummy index } i \text{ repeated)}$$

  Short quiz $\quad \delta_{ij} a_j = ? \quad \delta_{ij}\delta_{ij} = ?$

- **Differential operators (expressed in Cartesian coordinates here)**
  The dot symbol · is never decorative : scalar product

Gradient

$$\boldsymbol{b} = \nabla f \equiv \overrightarrow{\text{grad}}\, f \qquad b_i = \frac{\partial f}{\partial x_i}$$

Divergence

$$\nabla \cdot \boldsymbol{U} = \text{div}(\boldsymbol{U}) = \sum_{i=1}^{3} \frac{\partial U_i}{\partial x_i} = \frac{\partial U_i}{\partial x_i}$$

Laplacian

$$\nabla^2 f = \Delta f = \sum_{i=1}^{3} \frac{\partial^2 f}{\partial x_i \partial x_i} = \frac{\partial^2 f}{\partial x_i \partial x_i}$$

Curl

$$\nabla \times \boldsymbol{U} = \overrightarrow{\text{rot}}\, \boldsymbol{U}$$

Differential operators (cont.)

Explicit expression of the velocity gradient tensor $\nabla \boldsymbol{U}$

$$\nabla \boldsymbol{U}\Big|_{ij} = \frac{\partial \boldsymbol{U}}{\partial \boldsymbol{x}}\Big|_{ij} = \begin{pmatrix} \dfrac{\partial U_1}{\partial x_1} & \dfrac{\partial U_1}{\partial x_2} & \dfrac{\partial U_1}{\partial x_3} \\ \dfrac{\partial U_2}{\partial x_1} & \dfrac{\partial U_2}{\partial x_2} & \dfrac{\partial U_2}{\partial x_3} \\ \dfrac{\partial U_3}{\partial x_1} & \dfrac{\partial U_3}{\partial x_2} & \dfrac{\partial U_3}{\partial x_3} \end{pmatrix}$$

Differential operators (cont.)

Divergence theorem : the involved surface is a closed surface (domain $\mathcal{D}$ bounded by the surface $\mathcal{S}$ and $\boldsymbol{n}$ unit outward normal vector)

$$\int_{\mathcal{D}} \nabla \cdot \overline{\overline{\boldsymbol{A}}} \, dv = \int_{\mathcal{S}} \overline{\overline{\boldsymbol{A}}} \cdot \boldsymbol{n} \, ds$$

for any given tensor $\overline{\overline{\boldsymbol{A}}}$.

As an illustration, one has for the pressure term :

$$\int_{\mathcal{D}} \nabla p \, dv = \int_{\mathcal{D}} \nabla \cdot (p\overline{\overline{\boldsymbol{I}}}) \, dv = \int_{\mathcal{S}} p\overline{\overline{\boldsymbol{I}}} \cdot \boldsymbol{n} \, ds = \int_{\mathcal{S}} p\boldsymbol{n} \, ds$$

Statistical description of turbulent flow

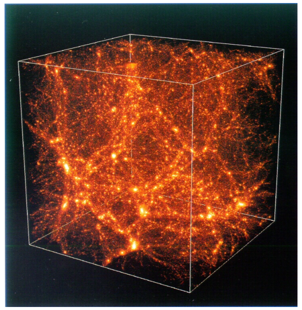
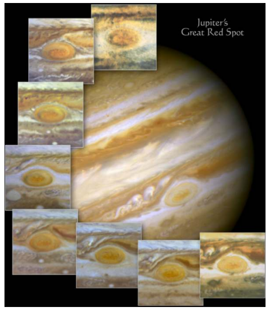

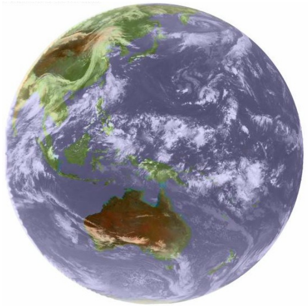

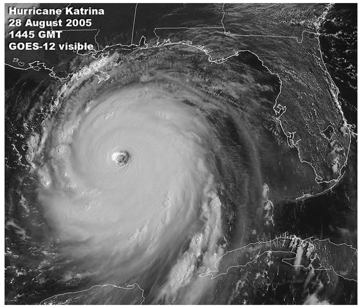

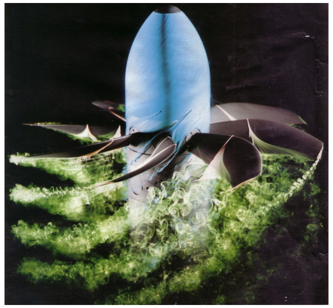

Introduction

The objective of this chapter is to establish the equations governing the mean flow field, and then to provide some hints on the closure of these equations.

For a given variable f, the Reynolds decomposition into mean and fluctuating components is introduced, $f = \bar{F} + f'$. For a stationary turbulence, $\bar{F}(\boldsymbol{x}, t) = \bar{F}(\boldsymbol{x})$, and the mean average can be well estimated by the time average of one realization, as discussed in the previous chapter.

A dual configuration is often considered for homogeneous turbulence. Statistics are independent of space, in particular $\bar{F}(\boldsymbol{x}, t) = \bar{F}(t)$. The ensemble mean is then usually approximated by spatial average,

$$\bar{F}(t) = \frac{1}{V} \int_V f(\boldsymbol{x}', t) d\boldsymbol{x}'$$

Properties of Reynolds decomposition

The statistical mean is a linear operator, which commutes with time and space derivative operators (the so-called rules of Reynolds)

- Centered fluctuating field

  $f \equiv \bar{F} + f' \quad \text{with} \quad \overline{f'} = 0 \qquad (f' = f - \bar{F}, \text{ and } \overline{f'} = \bar{F} - \bar{F} = 0)$

- Product of two variables f and g

  $fg \equiv (\bar{F} + f')(\bar{G} + g') = \bar{F}\bar{G} + \bar{F}g' + f'\bar{G} + f'g'$

  and thus,

  $$\overline{fg} = \bar{F}\,\bar{G} + \bar{F}\,\overline{g'} + \overline{f'}\,\bar{G} + \overline{f'g'} = \bar{F}\,\bar{G} + \overline{f'g'}$$

  $\overline{f'g'}$ is a new second-moment unknown variable

- Philosophy of the Reynolds decomposition, $u_i \equiv \bar{U}_i + u_i'$ with $\overline{u_i'} = 0$

  $\bar{U}_i$ part which can be reasonably calculated

  u_i' part which must be modelled (turbulent fluctuations)

The Reynolds Averaged Navier-Stokes (RANS) equations

For an incompressible flow $\nabla \cdot \boldsymbol{u} = 0$ with constant density $\rho = \text{cst}$ to simplify, the Navier-Stokes equations are given by

$$\frac{\partial u_i}{\partial x_i} = 0$$

$$\frac{\partial (\rho u_i)}{\partial t} + \frac{\partial}{\partial x_j}\left(\rho u_i u_j\right) = -\frac{\partial p}{\partial x_i} + \frac{\partial \tau_{ij}}{\partial x_j} \qquad \tau_{ij} = 2\mu s_{ij} \quad s_{ij} = \frac{1}{2}\left(\frac{\partial u_i}{\partial x_j} + \frac{\partial u_j}{\partial x_i}\right)$$

By introducing the Reynolds decomposition, and taking the average

$u_i \equiv \bar{U}_i + u_i' \qquad p \equiv \bar{P} + p' \qquad \tau_{ij} \equiv \bar{\tau}_{ij} + \tau_{ij}'$

$$\frac{\partial \bar{U}_i}{\partial x_i} = 0 \qquad \Longrightarrow \qquad \frac{\partial u_i'}{\partial x_i} = 0$$

$$\frac{\partial(\rho \bar{U}_i)}{\partial t} + \frac{\partial(\rho \bar{U}_i \bar{U}_j)}{\partial x_j} = -\frac{\partial \bar{P}}{\partial x_i} + \frac{\partial}{\partial x_j}\left(\bar{\tau}_{ij} - \rho \overline{u_i' u_j'}\right)$$

Reynolds Averaged Navier-Stokes (RANS) equations

$-\rho\overline{u_i'u_j'}$ Reynolds stress tensor (new unknown)

Generally this term is larger than the mean viscous stress tensor except for wall bounded flows, where viscosity effects become preponderant close to the wall.

Total stress seen by the fluid, $\tau_t = \bar{\tau}_{ij} - \rho\overline{u_i'u_j'}$

closure problem for $-\rho\overline{u_i'u_j'}$

- by writting a transport equation for $-\rho\overline{u_i'u_j'}$
- by directly modelling the Reynolds stress tensor

The study of the turbulent kinetic energy balance gives a global view on the energy exchange between the mean field and the turbulent field, and allows to identify the term(s) responsible of the production of this turbulent kinetic energy.

- **Kinetic energy budget of the mean flow**

$$\bar{U}_i \times \left\{ \frac{\partial(\rho \bar{U}_i)}{\partial t} + \frac{\partial(\rho \bar{U}_i \bar{U}_j)}{\partial x_j} = -\frac{\partial \bar{P}}{\partial x_i} + \frac{\partial}{\partial x_j}\left(\bar{\tau}_{ij} - \rho \overline{u_i' u_j'}\right) \right\} \quad \text{and} \quad \frac{\partial \bar{U}_i}{\partial x_i} = 0$$

The final result can be recast as

$$\rho \frac{\bar{D}}{Dt}\left(\frac{\bar{U}_i^2}{2}\right) = \rho \overline{u_i' u_j'} \frac{\partial \bar{U}_i}{\partial x_j} - \bar{\tau}_{ij} \frac{\partial \bar{U}_i}{\partial x_j} \underbrace{- \frac{\partial(\bar{U}_i \bar{P})}{\partial x_i} + \frac{\partial}{\partial x_j}(\bar{U}_i \bar{\tau}_{ij}) - \frac{\partial}{\partial x_j}(\bar{U}_i \rho \overline{u_i' u_j'})}_{\text{transport terms}}$$

where $\bar{D}/Dt \equiv \partial/\partial t + \bar{\boldsymbol{U}} \cdot \nabla = \partial/\partial t + \bar{U}_j \partial/\partial x_j$ is the material derivative along the mean flow. We recall that

$$\rho \frac{\bar{D}\varphi}{Dt} = \rho\left(\frac{\partial \varphi}{\partial t} + \bar{\boldsymbol{U}} \cdot \nabla \varphi\right) = \frac{\partial(\rho\varphi)}{\partial t} + \nabla \cdot (\rho \varphi \bar{\boldsymbol{U}})$$

Kinetic energy budget of the mean flow (cont.)

Transport terms are terms of the form $\nabla \cdot \overline{\boldsymbol{F}}$, with $\bar{F}_j = \bar{U}_i \rho \overline{u_i' u_j'}$ for instance. From the divergence theorem,

$$\int_{\mathcal{V}} \nabla \cdot \overline{\boldsymbol{F}} \, dv = \int_{\mathcal{S}} \overline{\boldsymbol{F}} \cdot \boldsymbol{n} \, ds \rightarrow 0$$

if $\bar{F}$ tends to zero on the control surface $\mathcal{S}$. In general, these terms act to homogenise $\overline{\boldsymbol{F}}$ inside the volume $\mathcal{V}$.

By integration over a control volume including the turbulent region of the flow, the kinetic energy budget is reduced to

$$\int_{\mathcal{V}} \rho \frac{\bar{D}}{Dt}\left(\frac{\bar{U}_i^2}{2}\right) ds \quad = \quad \int_{\mathcal{V}} \rho \overline{u_i' u_j'} \frac{\partial \bar{U}_i}{\partial x_j} \, ds \quad - \quad \int_{\mathcal{V}} \bar{\tau}_{ij} \frac{\partial \bar{U}_i}{\partial x_j} \, ds$$

variation of the kinetic energy inside $\mathcal{V}$	in general, transfer to the turbulent field	dissipation of the kinetic energy by viscous effects

Kinetic energy budget of the fluctuating field

To derive the transport equation on $\rho\overline{u_i'^2}/2$, we first consider the equation for the fluctuating velocity u_i', obtained by substraction between

$$\text{and} \qquad \begin{cases} \dfrac{\partial(\rho u_i)}{\partial t} + \dfrac{\partial}{\partial x_j}(\rho u_i u_j) = -\dfrac{\partial p}{\partial x_i} + \dfrac{\partial \tau_{ij}}{\partial x_j} \\ \dfrac{\partial(\rho \bar{U}_i)}{\partial t} + \dfrac{\partial(\rho \bar{U}_i\, \bar{U}_j)}{\partial x_j} = -\dfrac{\partial \bar{P}}{\partial x_i} + \dfrac{\partial}{\partial x_j}(\bar{\tau}_{ij} - \rho\overline{u_i' u_j'}) \end{cases}$$

which provides

$$\frac{\partial(\rho u_i')}{\partial t} + \frac{\partial}{\partial x_k}\left[\rho(u_i'\bar{U}_k + \bar{U}_i u_k' + u_i' u_k')\right] = -\frac{\partial p'}{\partial x_i} + \frac{\partial}{\partial x_k}\left(\rho\overline{u_i' u_k'} + \tau_{ik}'\right)$$

That equation is then multiplied by u_i' and statistically averaged, by remembering that $\partial u_i'/\partial x_i = 0$. One obtains,

- **Kinetic energy budget of the fluctuating field (cont.)**

$$\rho\frac{\bar{D}k_t}{Dt} = -\rho\overline{u_i'u_k'}\frac{\partial \bar{U}_i}{\partial x_k} - \overline{\tau_{ik}'\frac{\partial u_i'}{\partial x_k}} \underbrace{-\frac{1}{2}\frac{\partial}{\partial x_k}\overline{\rho u_i'u_i'u_k'} - \overline{u_i'\frac{\partial p'}{\partial x_i}} + \frac{\partial}{\partial x_k}\overline{u_i'\tau_{ik}'}}_{\text{transport terms}}$$

$$k_t \equiv \frac{1}{2}\overline{u_i'u_i'} = \frac{\overline{u_1'^2}+\overline{u_2'^2}+\overline{u_3'^2}}{2} \quad \text{(mean) turbulent kinetic energy} \quad (\mathrm{m}^2.\mathrm{s}^{-2})$$

Homogeneous turbulence case : statistical properties of turbulence are independent of the observer position $\boldsymbol{x}$, leading to

$$\rho\frac{\bar{D}k_t}{Dt} = -\rho\overline{u_i'u_j'}\frac{\partial \bar{U}_i}{\partial x_j} - \overline{\tau_{ik}'\frac{\partial u_i'}{\partial x_k}}$$

variation of the kinetic energy along the mean flow	energy transfer between the mean and turbulent fields	dissipation of the turbulent kinetic energy by viscous effects

Kinetic energy budget of the fluctuating field (cont.)

Dissipation rate of k_t

$$\rho\epsilon \equiv \overline{\tau'_{ik}\frac{\partial u'_i}{\partial x_k}} = 2\mu\,\overline{s'^2_{ij}} = \frac{1}{2}\mu\overline{\left(\frac{\partial u'_i}{\partial x_j}+\frac{\partial u'_j}{\partial x_i}\right)^2} \geq 0 \qquad (\epsilon \sim \mathrm{m}^2.\mathrm{s}^{-3})$$

Homogeneous turbulence case

$$\rho\frac{\bar{D}k_t}{Dt} = -\rho\overline{u'_i u'_k}\,\frac{\partial\bar{U}_i}{\partial x_k} - \overline{\tau'_{ik}\frac{\partial u'_i}{\partial x_k}}$$

$$= \underbrace{-\rho\overline{u'_i u'_k}\,\frac{\partial\bar{U}_i}{\partial x_k}}_{?} - \rho\epsilon \qquad\qquad \mathcal{P} \equiv -\rho\overline{u'_i u'_j}\,\frac{\partial\bar{U}_i}{\partial x_j}$$

Heuristic interpretation of the term $\mathcal{P}$

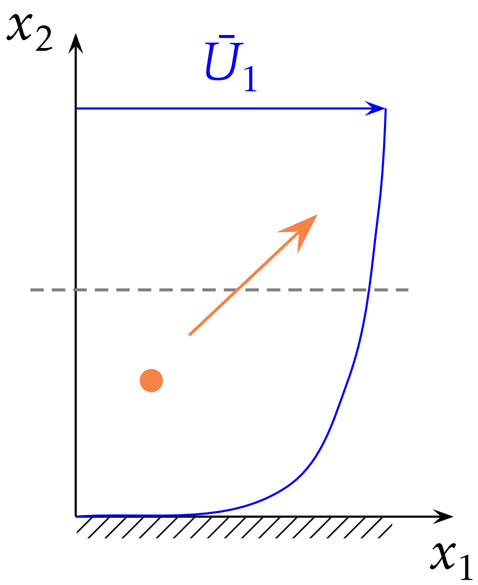

$$\begin{cases} u_2' > 0 \\ u_1' < 0 \end{cases} \qquad \overline{u_1' u_2'} < 0$$

$$\begin{cases} u_2' < 0 \\ u_1' > 0 \end{cases} \qquad \overline{u_1' u_2'} < 0$$

Therefore, a positive production term is expected

$$\mathcal{P} \simeq -\rho \overline{u_1' u_2'} \frac{d\bar{U}_1}{dx_2} > 0$$

The term $\mathcal{P}$ is generally a production term for the turbulent kinetic energy k_t.

- **Transfers between the mean flow and the turbulent field**

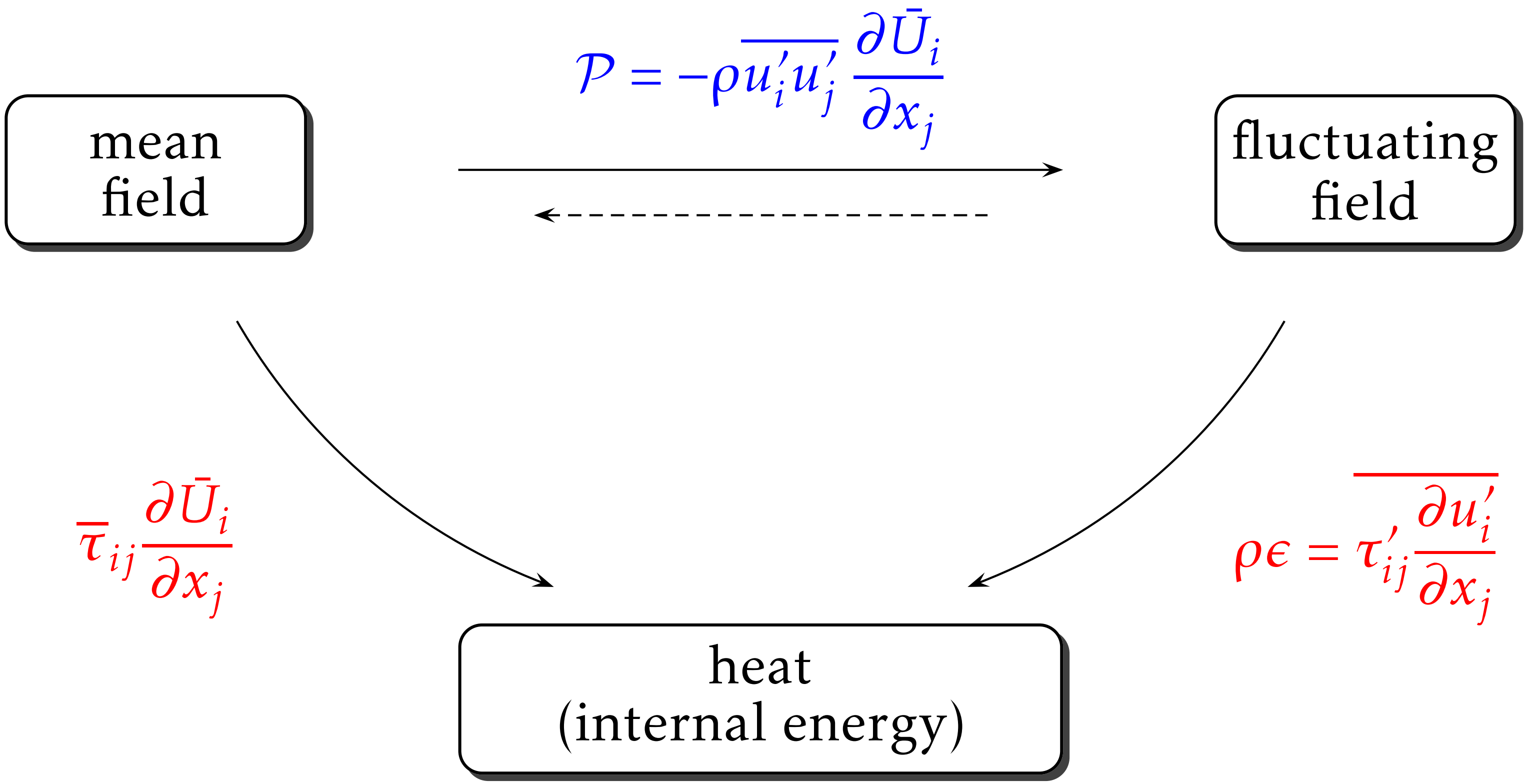

$$T = \bar{T} + \theta' \qquad a = \lambda/(\rho c_p)$$

$$\frac{\partial \bar{T}}{\partial t} + \frac{\partial(\bar{U}_j\bar{T})}{\partial x_j} = -\frac{\partial}{\partial x_j}\left(-a\frac{\partial \bar{T}}{\partial x_j} + \overline{\theta u_j'}\right) + \frac{1}{\rho c_p}\left(\bar{\tau}_{ij}\frac{\partial \bar{U}_i}{\partial x_j} + \overline{\tau_{ij}'\frac{\partial u_i'}{\partial x_j}}\right)$$

Small exercise : fluctuating irrotational field

The necessary rotational feature of a turbulent velocity field has been emphasized by Corrsin & Kistler (1954)

1. Remind the definition of an irrotational flow
2. By considering the following quantity

$$\overline{u_i'\left(\frac{\partial u_i'}{\partial x_j}-\frac{\partial u_j'}{\partial x_i}\right)}$$

   demonstrate that

$$\frac{\partial}{\partial x_i}\overline{u_i'u_j'}=\frac{\partial k_t}{\partial x_j}$$

3. Deduce the form of the RANS Equation for the case of a fluctuating irrotational velocity field, and comment carefully your result.
4. Is the Reynolds tensor diagonal for an irrotational flow ?

Turbulent viscosity concept for the Reynolds tensor Boussinesq model (1877)

- By analogy with the definition of the viscous tensor $\overline{\overline{\boldsymbol{\tau}}}$, the Reynolds stress tensor $-\rho\overline{u_i'u_j'}$ is modelled by

$$-\rho\overline{u_i'u_j'} = 2\mu_t\bar{S}_{ij} - \frac{2}{3}\rho k_t\delta_{ij} = \mu_t\left(\frac{\partial \bar{U}_i}{\partial x_j} + \frac{\partial \bar{U}_j}{\partial x_i}\right) - \frac{2}{3}\rho k_t\delta_{ij}$$

turbulent viscosity $\mu_t = \mu_t(\boldsymbol{x}, t)$: intrinsic property of the turbulent flow, and not of the fluid as the molecular viscosity.

- There is still a closure problem since the expression of μ_t is not defined (6 unknowns $\overline{u_i'u_j'} \rightarrow$ 1 unknown μ_t).

- A consequence of the turbulent-viscosity hypothesis is that $\mathcal{P} = 2\mu_t\overline{S}_{ij}^2 \geq 0$ by construction : always a positive energy transfer towards the turbulent field.

Application to free shear flows (jet, wake, mixing layer)

Mean velocity field $(\bar{U}_1, \bar{U}_2)$, and slowly variable flow along the x_1 direction, that is $\partial/\partial x_1 \ll \partial/\partial x_2$: quasi-homogeneous flow in the x_1 direction

Averaged Navier-Stokes equation along the x_1 axis

$$\frac{\partial(\bar{U}_1\bar{U}_1)}{\partial x_1} + \frac{\partial(\bar{U}_1\bar{U}_2)}{\partial x_2} = -\frac{\partial \bar{P}}{\partial x_1} + \frac{\partial}{\partial x_1}(\bar{\tau}_{11} - \rho\overline{u_1' u_1'}) + \frac{\partial}{\partial x_2}\left(\bar{\tau}_{12} - \rho\overline{u_1' u_2'}\right)$$

The total stress τ_t acting on the fluid reads

$$\tau_t = \bar{\tau}_{12} - \rho\overline{u_1' u_2'} = \mu\frac{d\bar{U}_1}{dx_2} + \mu_t\frac{d\bar{U}_1}{dx_2} = (\mu + \mu_t)\frac{d\bar{U}_1}{dx_2}$$

The total stress τ_t is therefore null when the mean velocity profile $\bar{U}_1$ reaches a local extremum. Furthermore, it is also expected that $\mu \ll \mu_t$

Illustration for a subsonic round jet

M = 0.16 and $\mathrm{Re}_D = 9.5 \times 10^4$ (from Hussein, Capp & George, 1994)

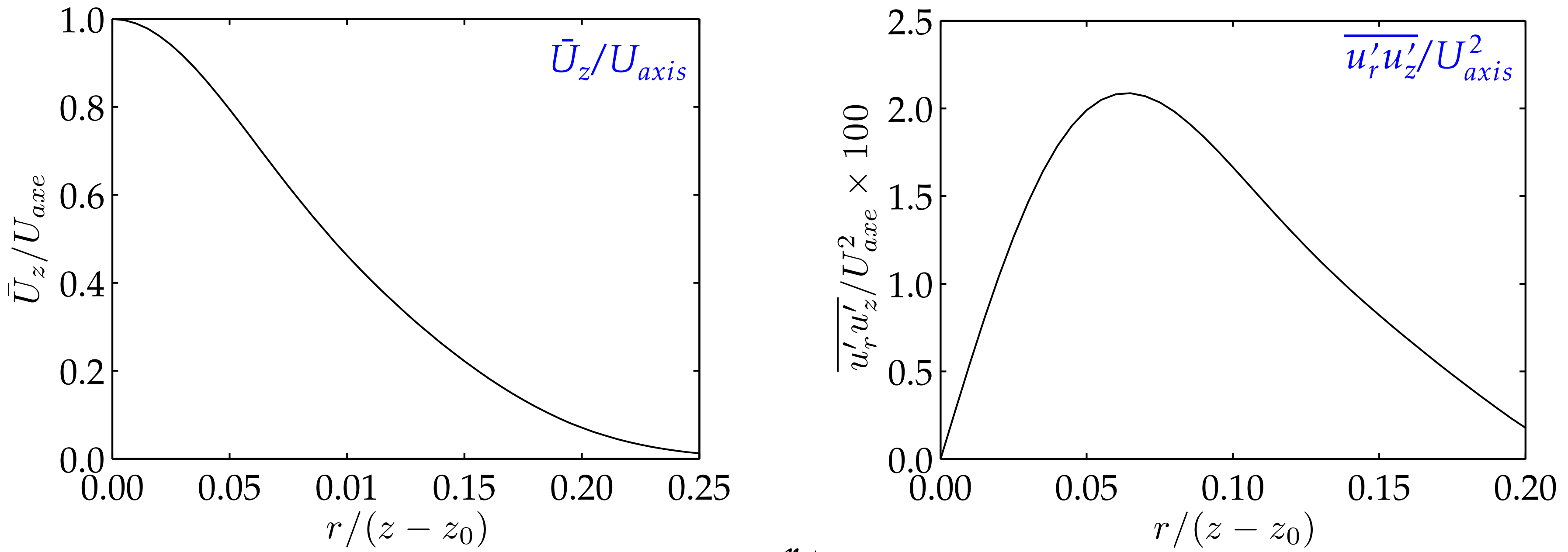

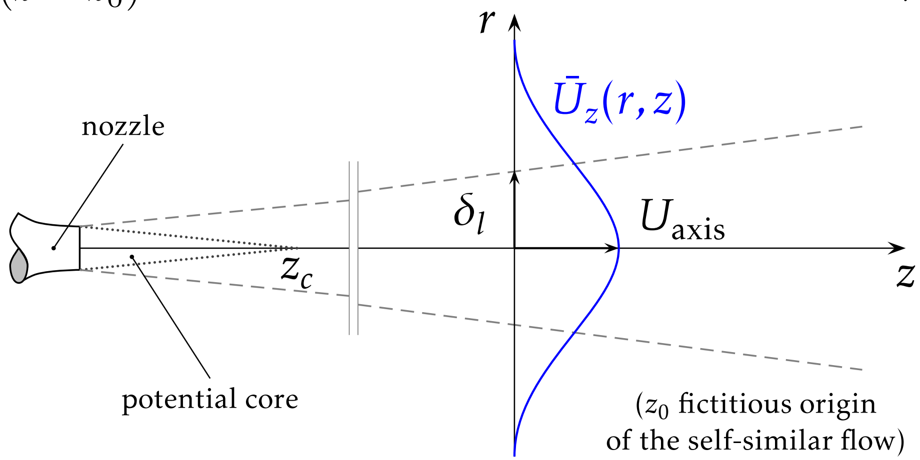

- **Two famous counter-examples (asymmetrical mean flow)**
  - channel flow with smooth and rough surfaces (Hanjalić & Launder, 1972)
  - plane wall jet (Mathieu, 1967)

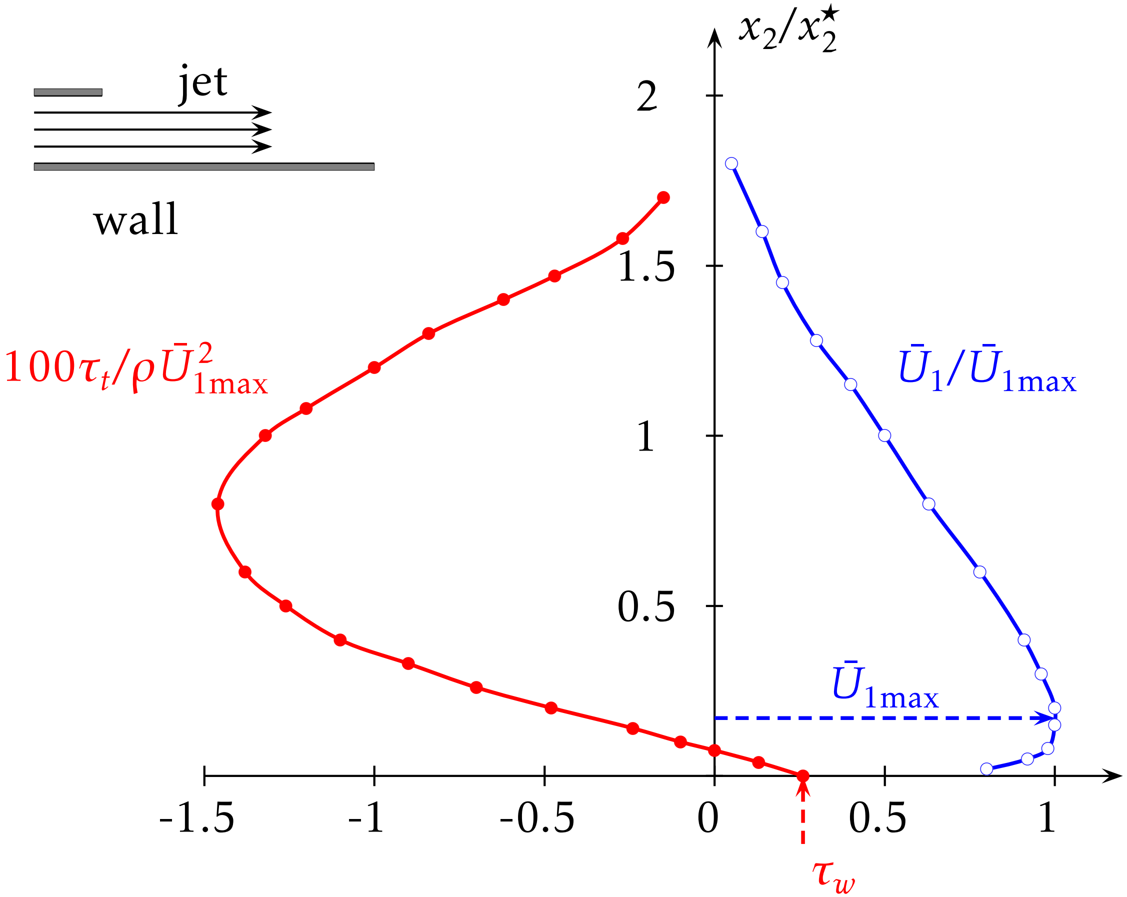

Plane wall jet (nozzle exit)

$\mathrm{Re} \simeq 2 \times 10^4$

$$\tau_t = \mu \frac{d\bar{U}_1}{dx_2} - \rho\overline{u_1' u_2'}$$

Some practical consequences

The total shear is usually much higher in turbulent régime :

- Reattachment of a turbulent boundary layer after detachment (and possible relaminarisation)
- Reduction of flow separation regions : the drag crisis phenomenon. The boundary layer separation point is moved downstream along a bluff body, with a reduction of the total drag with respect to the laminar regime : the increase in friction induced by turbulence is compensated by the reduction of the pressure drag, induced by the turbulent wake.

Flow past a sphere

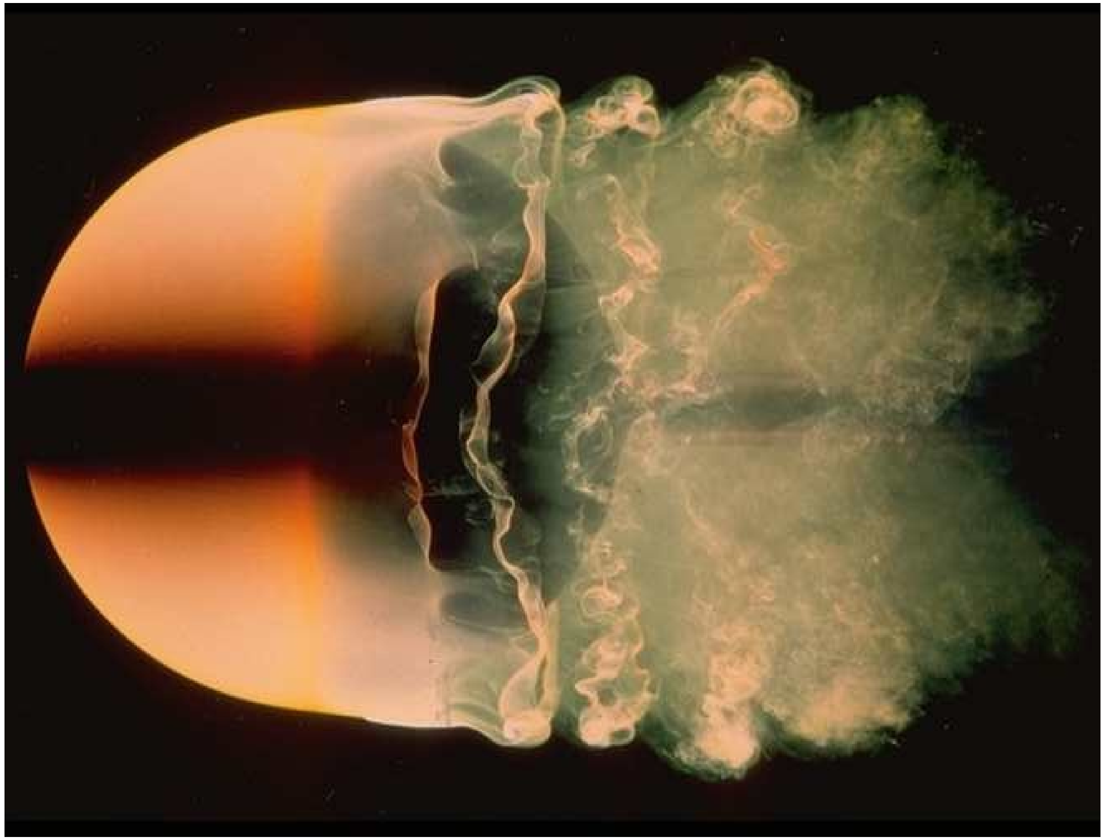

ONERA / DAFE, water tunnel, $\mathrm{Re}_D = 10^3$

Flow past a sphere

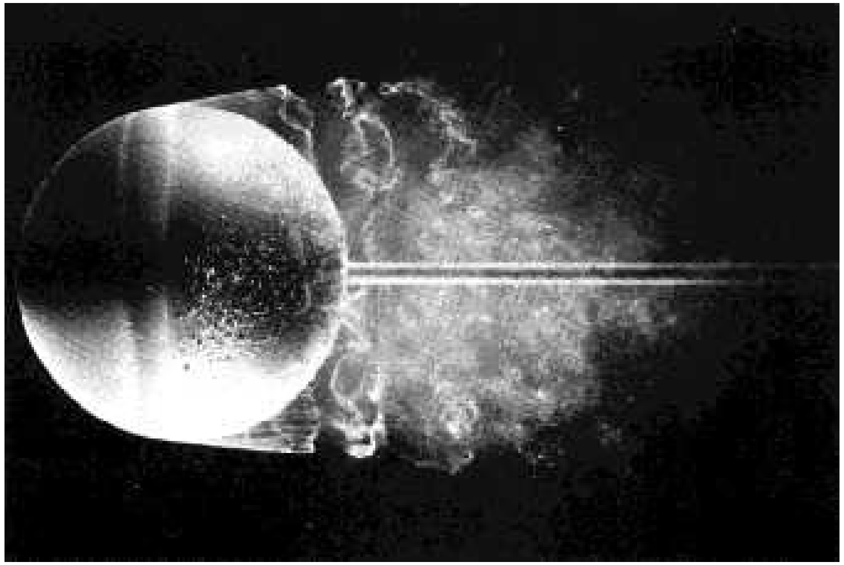

$\mathrm{Re}_D = 1.5 \times 10^4$

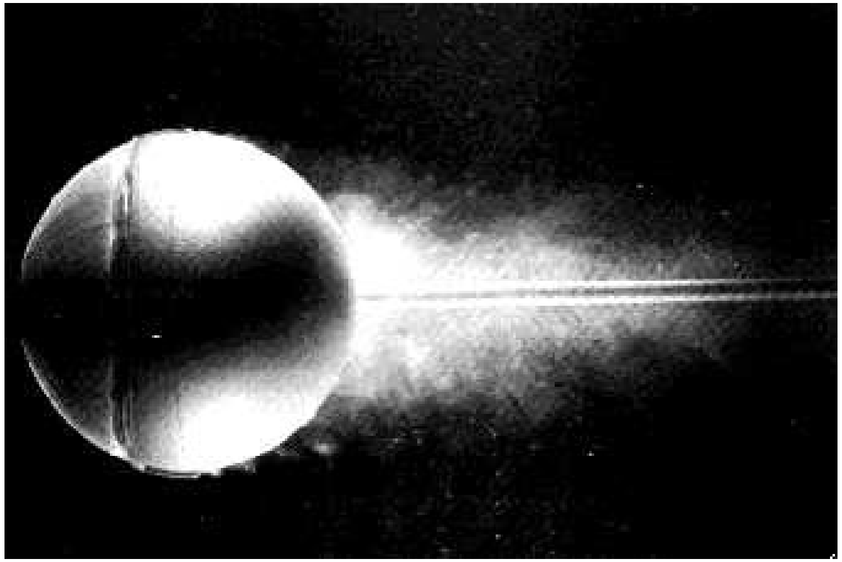

$\mathrm{Re}_D = 3.0 \times 10^4$ with a trip wire

ONERA, Werle (1980) in *An album of fluid motion*, Van Dyke (1982)

Sphere : critical Reynolds number $\mathrm{Re}_D^c \simeq 3 \times 10^5$

Flow around a bluff body

Drag crisis – critical Reynolds number for which the flow pattern changes, leaving a narrower turbulent wake : the boundary layer on the front surface becomes turbulent

RANS equation

$$\rho\left(\frac{\partial \bar{\boldsymbol{U}}}{\partial t} + \bar{\boldsymbol{U}} \cdot \nabla \bar{\boldsymbol{U}}\right) = -\nabla \bar{P} + \nabla \cdot (\overline{\overline{\boldsymbol{R}}} + \overline{\overline{\boldsymbol{\tau}}})$$

$\overline{\overline{\boldsymbol{R}}}$ Reynolds stress tensor

$R_{ij} \equiv -\rho \overline{u_i' u_j'}$

$$\boldsymbol{F}_{\text{flow} \rightarrow \text{body}} \equiv \overline{\boldsymbol{F}} = \int_{\mathcal{S}_w} -\bar{P} \boldsymbol{n} \, ds + \int_{\mathcal{S}_w} \overline{\overline{\boldsymbol{\tau}}} \cdot \boldsymbol{n} \, ds \qquad (\text{remembering that } \overline{\overline{\boldsymbol{R}}} = 0 \text{ on } \mathcal{S}_w)$$

Mean drag force $F_D = \boldsymbol{F} \cdot \boldsymbol{e}_\infty =$ pressure drag (form drag) + skin friction drag

A streamlined body looks like an airfoil at small angles of attack (narrow wake), whereas a bluff body looks like a sphere, or an airfoil at large angles of attack. For streamlined bodies, frictional drag is the dominant term. For a bluff body, drag is dominated by the pressure term

Drag coefficient for a smooth sphere

(adapted from Clift, Grace, & Weber, 1978)

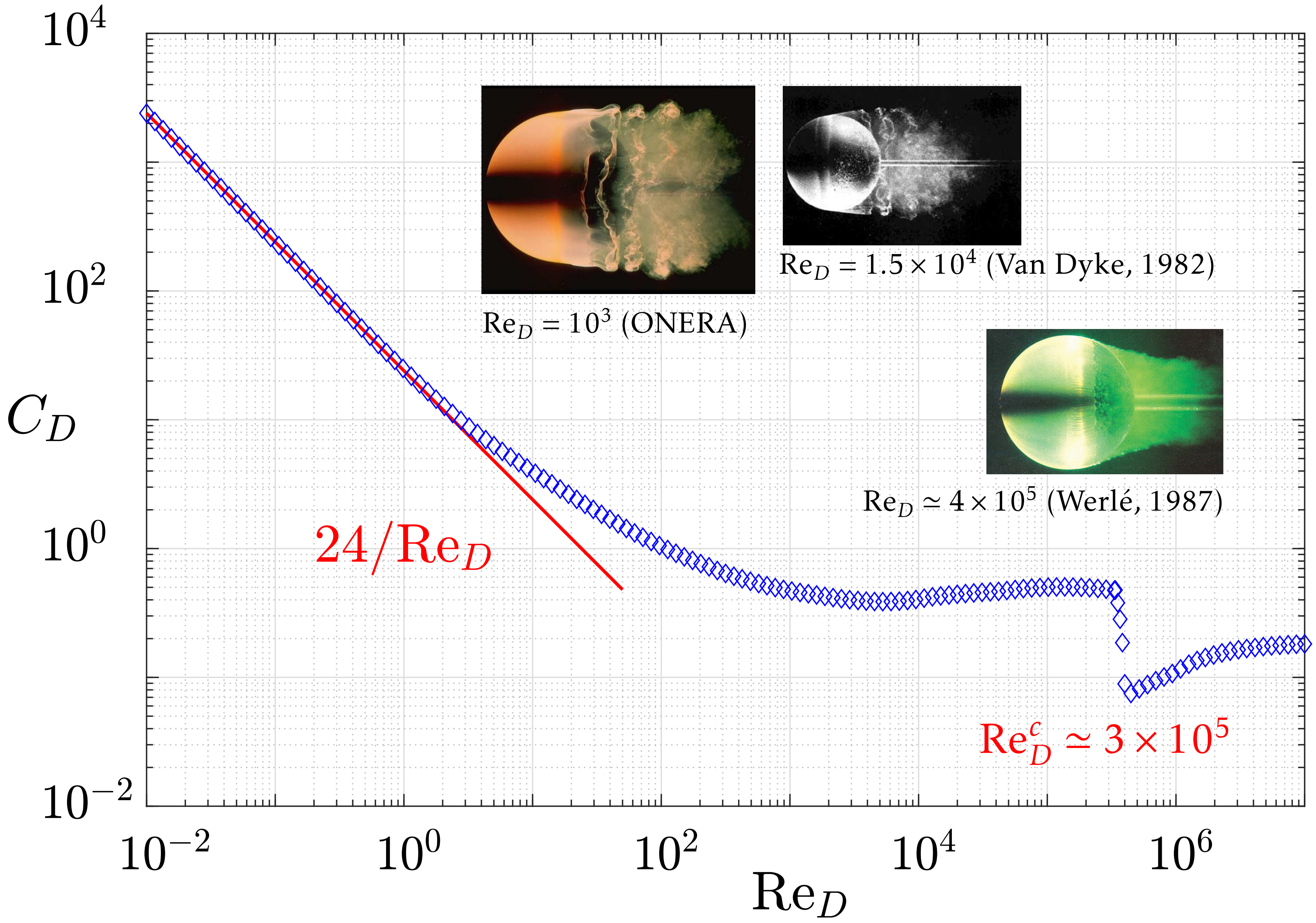

Why golf balls have dimples?

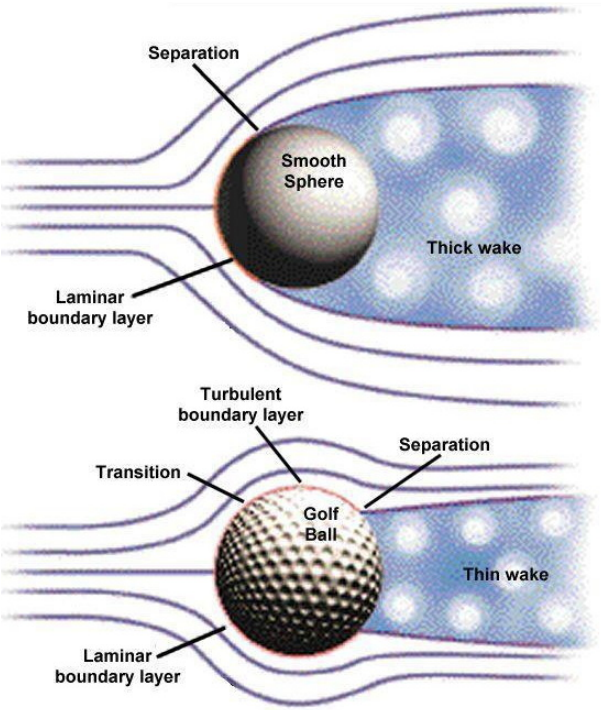

Moin & Kim, 1997, *Scientific American*

Drag coefficient of spheres with varying surface roughness. The drag crisis or sudden drop in drag as Reynolds number increases occurs when the boundary layer transitions to turbulence upstream of separation

$D = 4.3$ cm, $U \simeq 67$ m.s^{-1}, $\mathrm{Re} \simeq 1.9 \times 10^5$ (professional golfer)

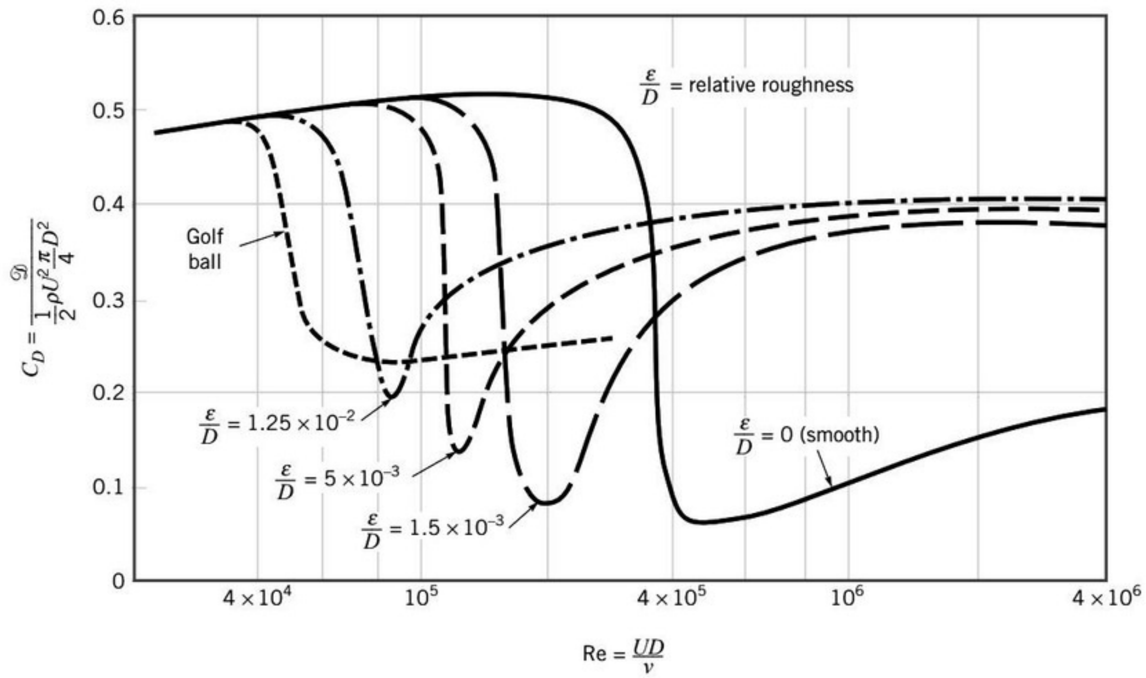

Munson *et al.*, 2014, *Fundamentals of fluid mechanics*

- **Vortex generators for delaying boundary layer separation**

Beechcraft Baron
(twin-engined piston aircraft)

Boeing-777-3ZG-ER
http://www.airliners.net/

Boundary layer separation

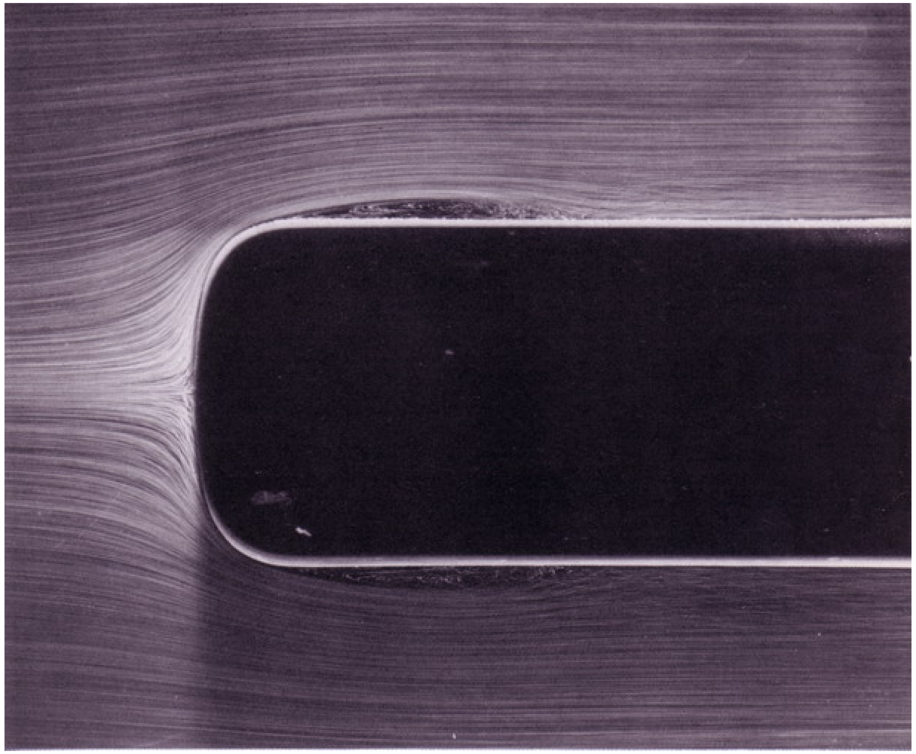

Separation of the laminar boundary layer on a body of revolution (Rankine ogive, $\mathrm{Re}_D = 6000$). The boundary layer becomes quickly turbulent and then reattaches to the surface, enclosing a short thin region of recirculation flow (visualization by air bubbles in water)

Werlé (ONERA) in Van Dyke (1982, fig. 33)

Elite cyclist : reduction of drag ...

(Blocken & Toparlar, *J. Wing. Eng. Ind. Aerodyn.*, 2015)

... when a cyclist is followed by a car

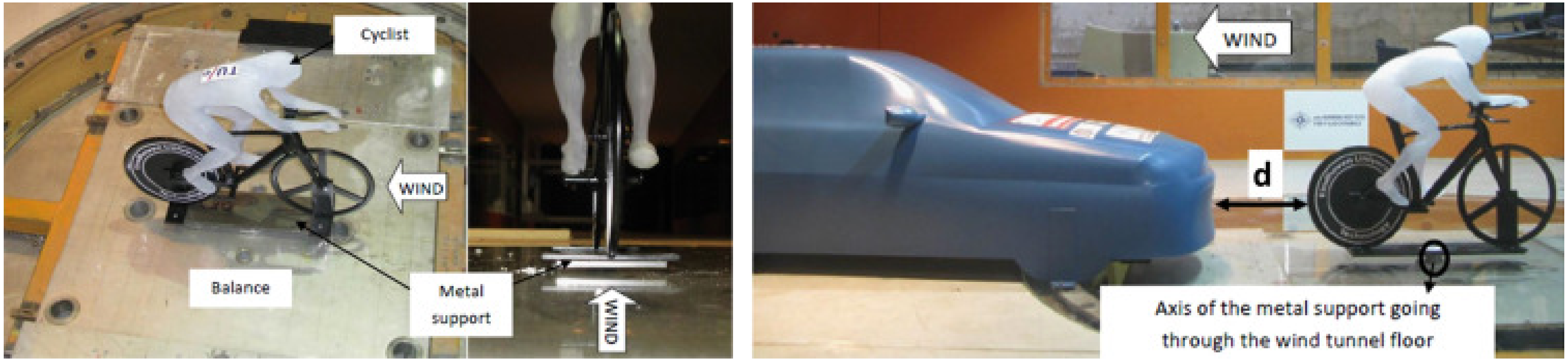

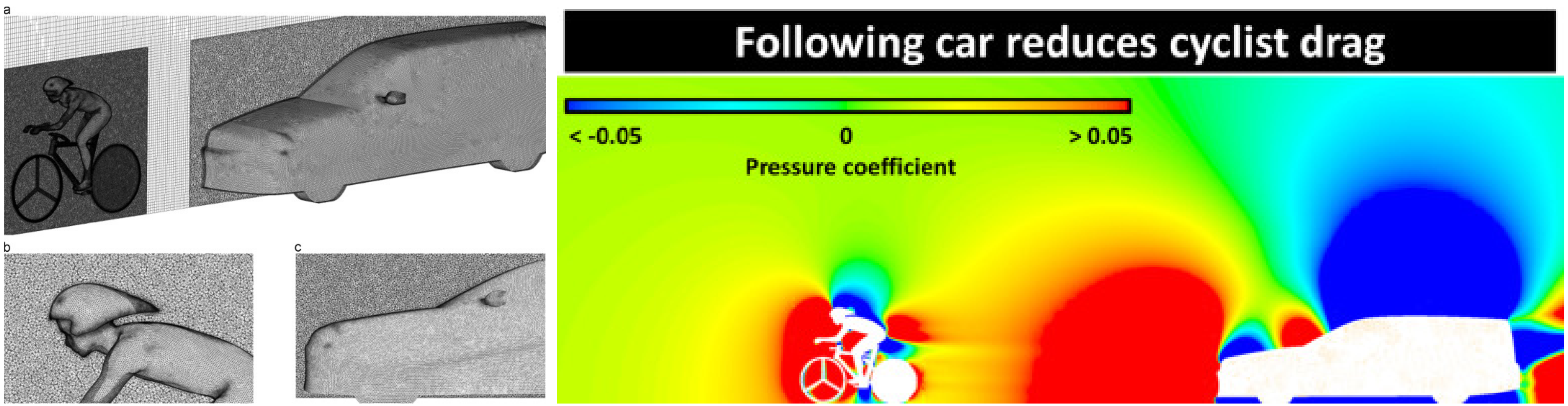

For a 50 km individual time trial : $3 \leq d \leq 10$ m $\Longrightarrow$ 1 mm $\rightarrow$ 4 s time reduction !
Recommendation for UCI, $d \geq 30$ m

Run a new marathon record in under two hours

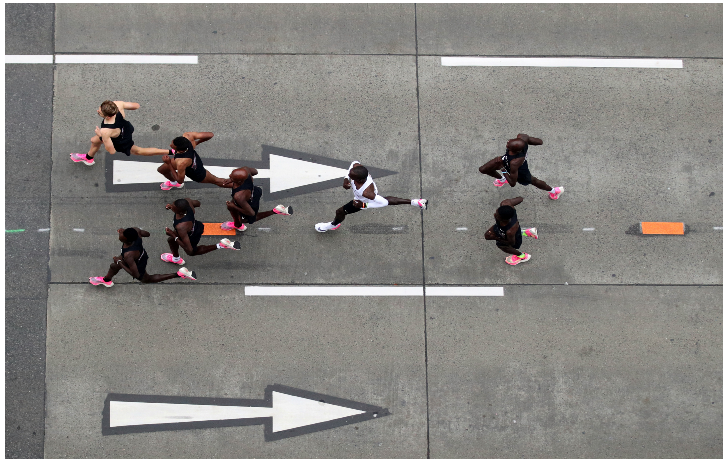

Drafting formation used to reduce air resistance by positioning other pacers around the top runner

Mannequins mounted around the main runner (fixed on the load cell support) in wind tunnel to replicate the formation used by Eliud Kipchoge (drag reduced by 50%)

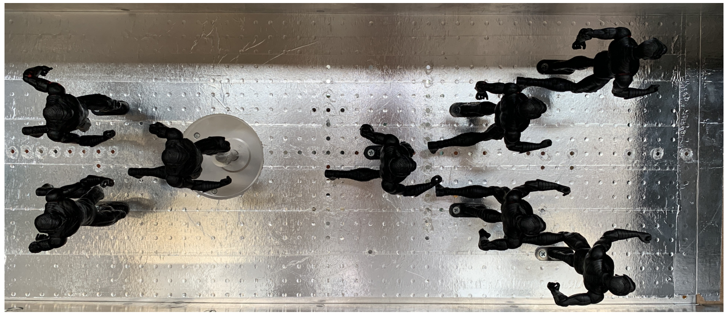

Elite runner Eliud Kipchoge became the first person to run a marathon in under two hours in Vienna (INEOS 1 :59 Challenge on 12th Oct. 2019, unofficial race in 1 :59 :40). He is assisted by seven pacers, five forming an inverted arrow in front of him and two others behind him

Swordfish-shaped arrangement of seven pacers that lowered the air resistance on the top runner by about 60% compared with a solo runner

The identified swordfish-shaped configuration, a skinny diamond in front of the top runner and two pacers in the back, would save roughly four minutes off of a marathon time. Eliud Kipchoge could reduced his time by an additional 40 seconds

Massimo Marro, Jack Leckert, Ethan Rollier, Pietro Salizzoni and Christophe Bailly
Wind tunnel evaluation of novel drafting formations for an elite marathon runner,
Proc. Roy Soc. A, **479**, 2023

Wall-bounded turbulent flow

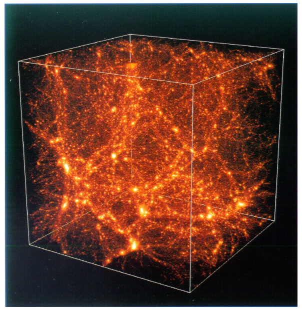
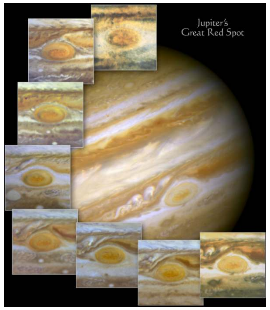

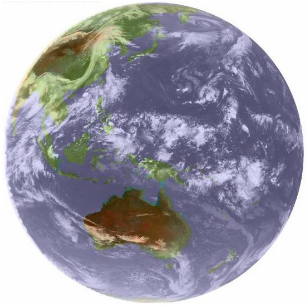

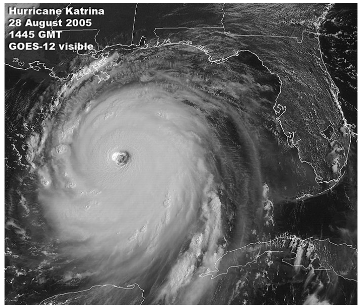

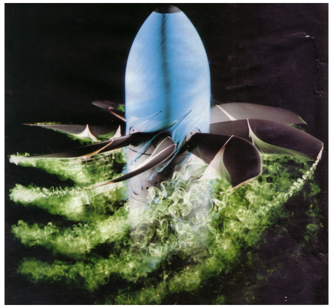

- **Two main classes of wall flows : confined flows & external flows**

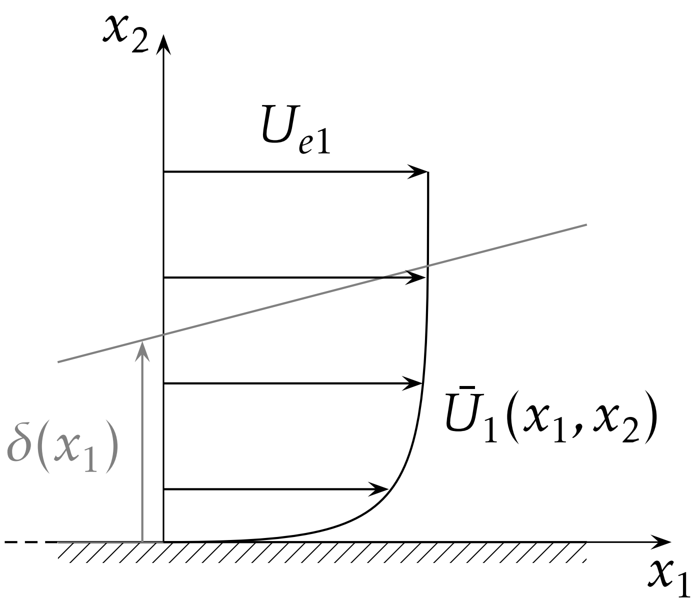

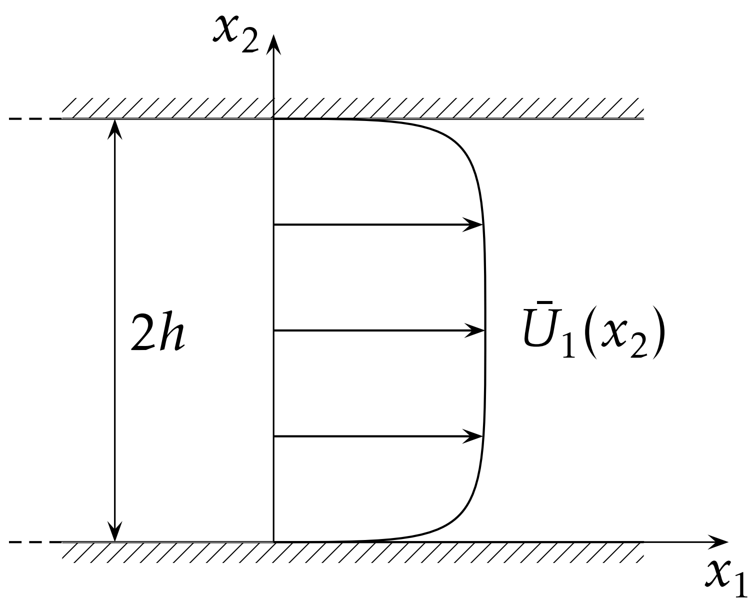

flat-plate boundary layer

$$\mathrm{Re}_\delta = \frac{U_{e1}\delta}{\nu}$$

fully turbulent for $\mathrm{Re}_\delta \geq 2800$

channel flow

$$\mathrm{Re}_{2h} = \frac{U_d 2h}{\nu} \qquad (U_d \text{ bulk velocity})$$

fully turbulent for $\mathrm{Re}_{2h} \geq 1800$

homogeneous flow along x_1

Fully developed channel flow

Reynolds-Averaged Navier-Stokes equations : $\bar{U}_1 = \bar{U}_1(x_2)$ and $\bar{U}_2 = \bar{U}_3 = 0$.
In addition, the flow is homogenous along x_1

$$\begin{cases} 0 = -\dfrac{\partial \bar{P}}{\partial x_1} - \dfrac{d}{dx_1}(\rho \overline{u_1'^2}) + \dfrac{d}{dx_2}\left(\mu \dfrac{d\bar{U}_1}{dx_2} - \rho \overline{u_1' u_2'}\right) & \text{(i)} \\ 0 = -\dfrac{\partial \bar{P}}{\partial x_2} - \dfrac{d}{dx_1}(\rho \overline{u_1' u_2'}) - \dfrac{d}{dx_2}\left(\rho \overline{u_2' u_2'}\right) & \text{(ii)} \end{cases}$$

By integration of Eq. (ii) from the wall ($x_2 = 0$) to a current point x_2, one obtains

$$\bar{P}(x_1, x_2) = \bar{P}_w - \rho \overline{u_2' u_2'}$$

where $\bar{P}_w = \bar{P}(x_1, x_2 = 0)$ is the mean wall pressure (measurable quantity)

Fully developed channel flow

The Navier-Stokes equation (i) can now be rewritten as

$$0 = -\frac{d\bar{P}_w}{dx_1} + \frac{d}{dx_2}\underbrace{\left(-\rho\overline{u_1'u_2'} + \mu\frac{d\bar{U}_1}{dx_2}\right)}_{\bar{\tau}_t(x_2)}$$

$\bar{\tau}_t$ mean total stress applied to the fluid

By integration along the transverse direction again, up to a current point x_2

$$\frac{d\bar{P}_w}{dx_1}x_2 = -\rho\overline{u_1'u_2'} + \mu\frac{d\bar{U}_1}{dx_2} - \bar{\tau}_w \qquad \text{where} \qquad \bar{\tau}_w \equiv \mu\frac{d\bar{U}_1}{dx_2}\bigg|_{x_2=0}$$

where $\bar{\tau}_w$ is the mean shear stress at the wall.

Fully developed channel flow

Introduction of the friction velocity

$$u_\tau \equiv \sqrt{\bar{\tau}_w/\rho}$$

The friction velocity is the characteristic turbulent velocity scale for the turbulent boundary layer near the wall. In particular, $|\overline{u_i'u_j'}| \sim u_\tau^2$

There is a direct link between this friction velocity and the pressure drop. For $x_2 = h$, that is on the symmetry plane of the channel, one has

$$\frac{d\bar{P}_w}{dx_1} h = -\bar{\tau}_w \qquad \Longrightarrow \qquad u_\tau^2 = -\frac{1}{\rho}\frac{d\bar{P}_w}{dx_1} h = \text{ cst for a pipe flow}$$

In the end, the mean velocity $\bar{U}_1$ is governed by

$$u_\tau^2\left(\frac{x_2}{h} - 1\right) - \overline{u_1'u_2'} + \nu\frac{d\bar{U}_1}{dx_2} = 0 \quad \text{or equivalently} \quad \bar{\tau}_t = \bar{\tau}_w\left(1 - \frac{x_2}{h}\right) \qquad (1)$$

Fully developed channel flow

Plane channel of width $2h \equiv 2D$ (Comte-Bellot, 1965)

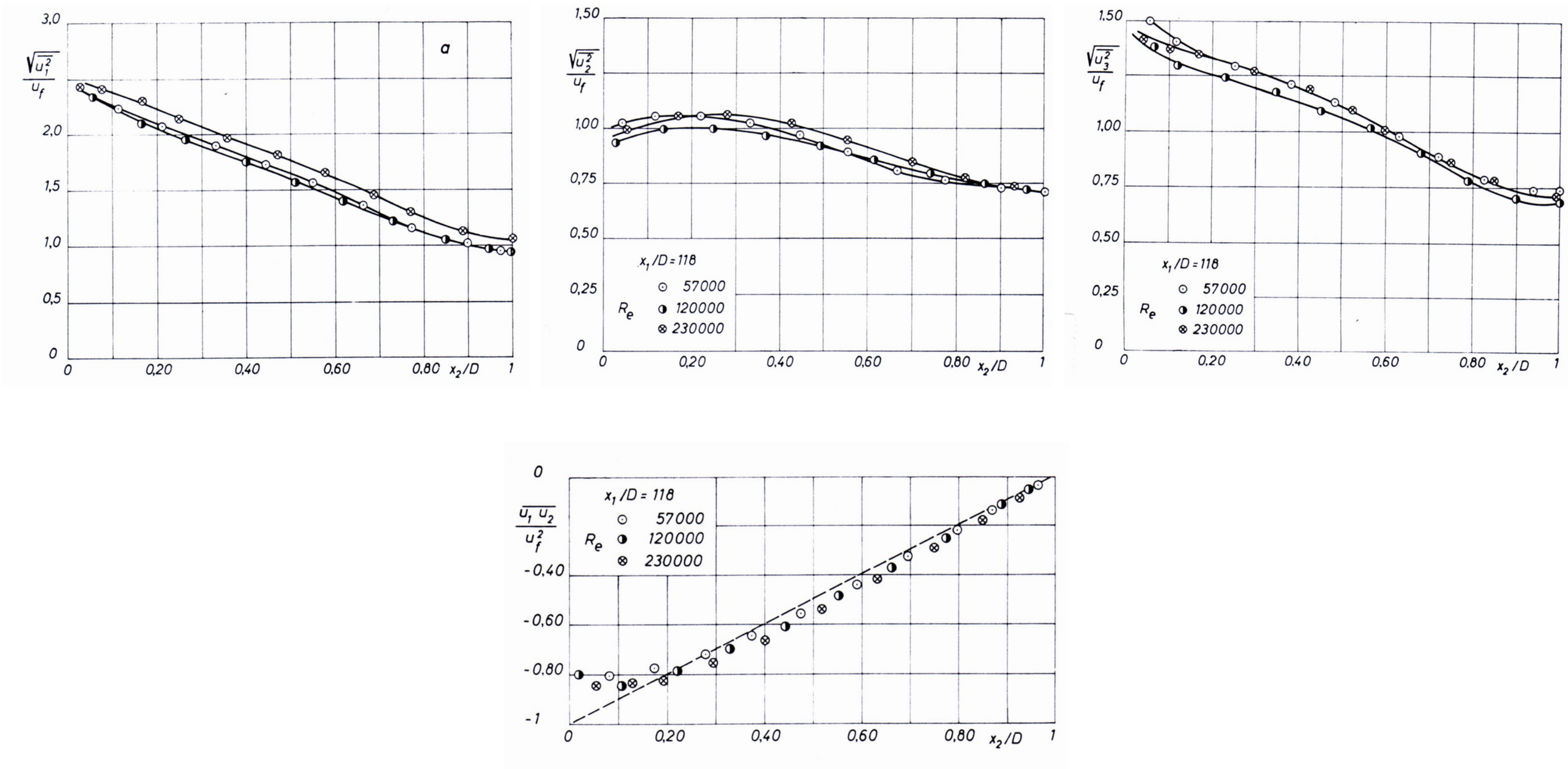

(wall) (axis)

$$5.7 \times 10^4 \leq \mathrm{Re}_h \leq 2.3 \times 10^5 \qquad \mathrm{Re}_\tau = 178, 392, 587$$

- **Fully developed channel flow**
  Geneviève Comte-Bellot (PhD thesis, Grenoble in 1963)

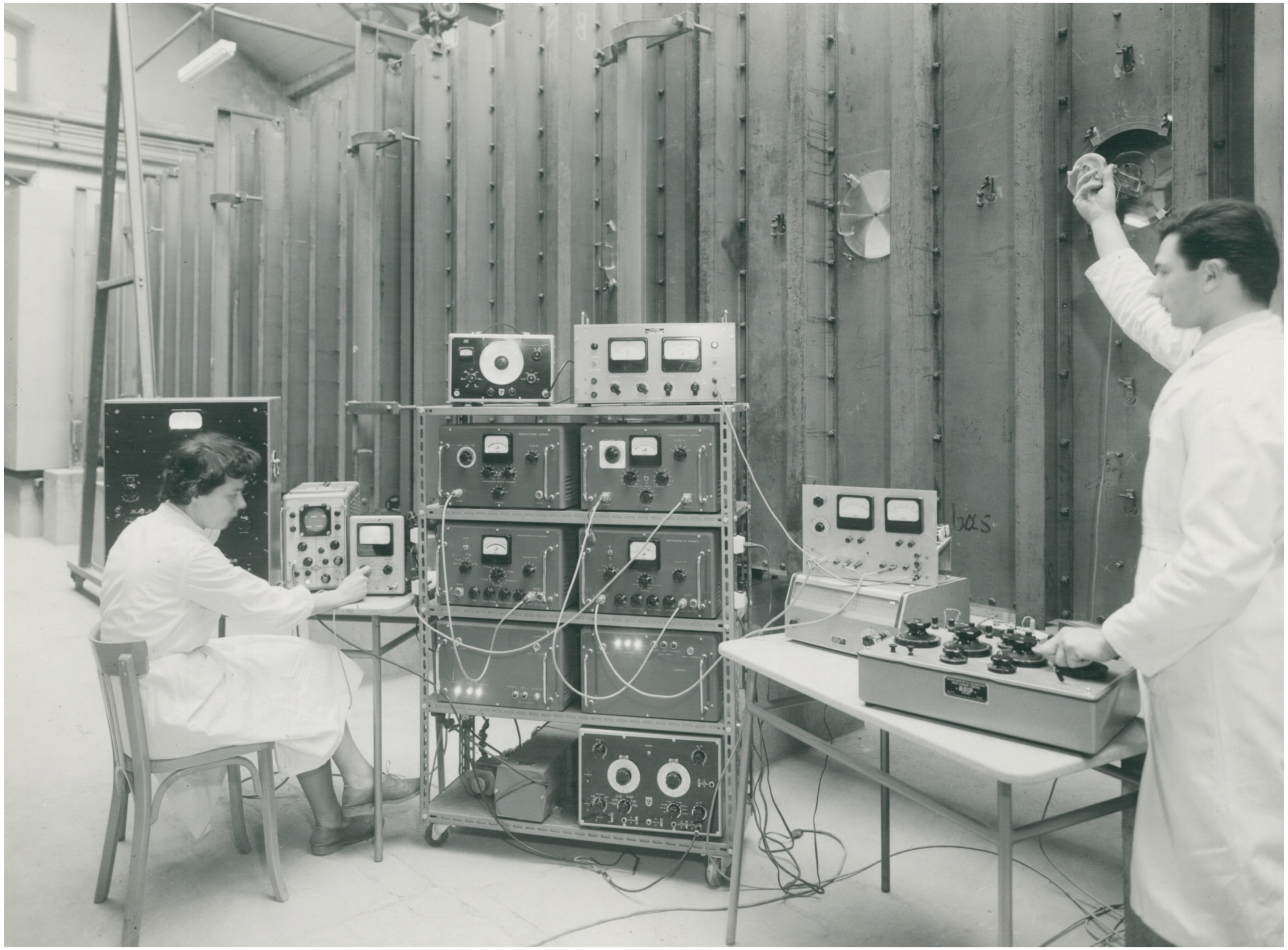

Small exercise : skin-friction coefficient for a circular pipe

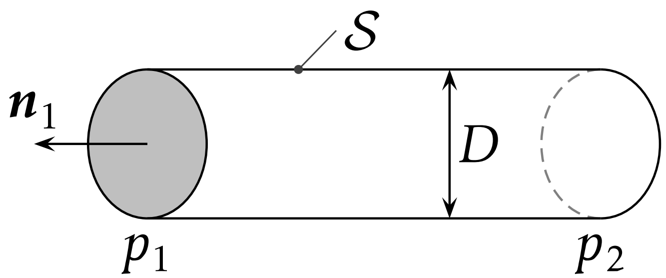

1. Identify the following equation,

$$\rho \frac{D\boldsymbol{u}}{Dt} = \nabla \cdot \overline{\overline{\boldsymbol{\sigma}}}$$

2. For a pipe of diameter D and length L, write the integral momentum conservation.
3. By introducing the wall shear stress τ_w, and the skin-friction coefficient $C_f = \tau_w/(\rho U_d^2/2)$ where U_d is the bulk velocity, show that the head pressure lost $\Delta p = p_1 - p_2$ can be recast as

$$\Delta p = 4C_f \frac{L}{D}\frac{1}{2}\rho U_d^2$$

4. Now consider in the above Reynolds' decomposition : what should be changed ?

Small exercise : skin-friction coefficient for a circular pipe

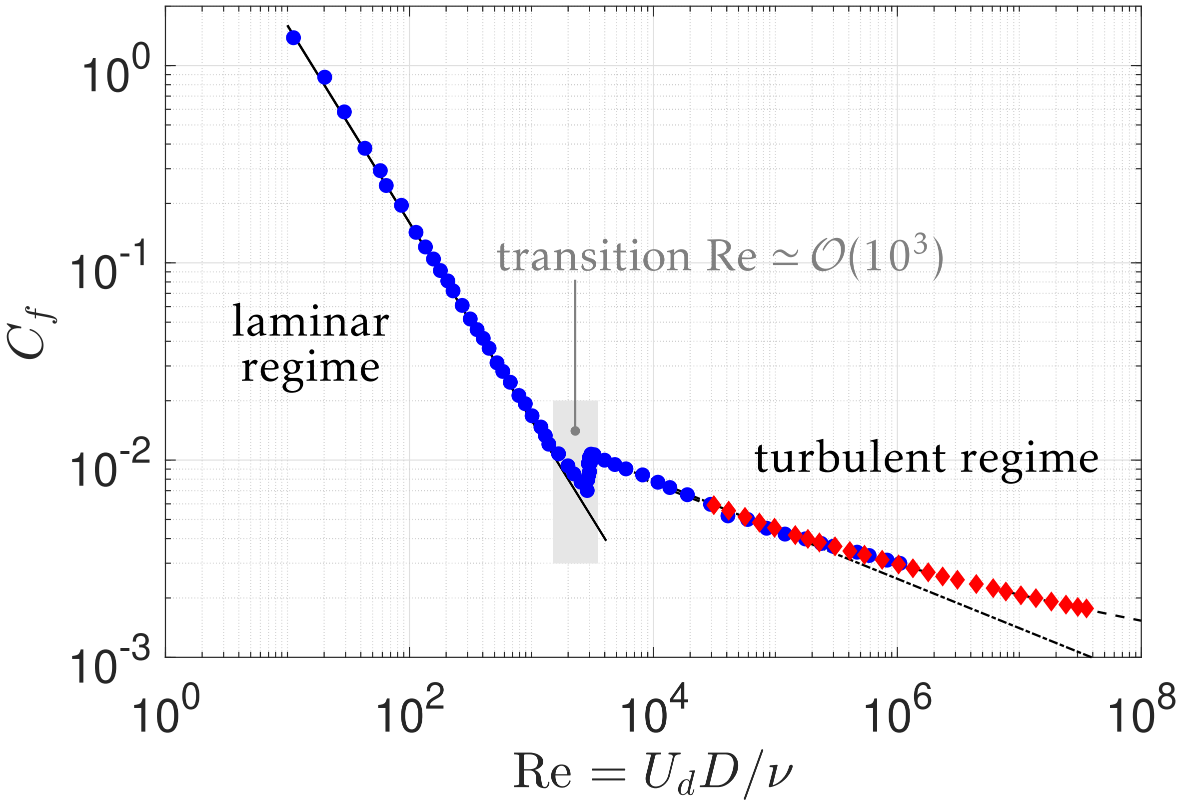

— laminar regime $C_f = 16/\mathrm{Re}$

-·-·- Blasius' relationship, $C_f \simeq 0.0791\,\mathrm{Re}^{-1/4}$

- - - $1/C_f^{1/2} \simeq 3.860 \log_{10}(\mathrm{Re}\, C_f^{1/2}) - 0.088$

● Oregon facility

♦ Princeton *Superpipe*

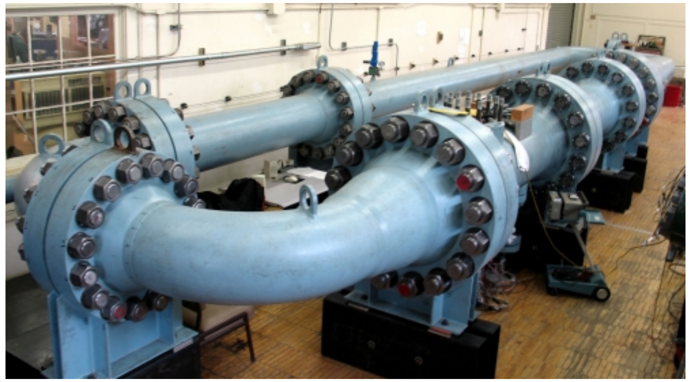

McKeon *et al.* (2004) - *Superpipe*, the Reynolds number is increased through the pressure

Laminar versus turbulent regime

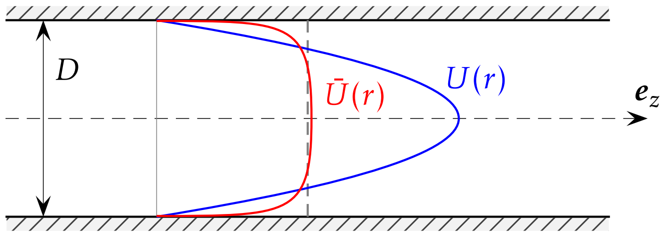

Turbulent boundary layer equations

Prandtl's approximations ($\delta \ll L$) for the RANS equations
Conservation of mass

$$\frac{\partial \bar{U}_1}{\partial x_1} + \frac{\partial \bar{U}_2}{\partial x_2} = 0 \qquad \Longrightarrow \qquad V \sim \frac{\delta}{L} U$$

Averaged Navier-Stokes equation along x_1 ($\neq$ laminar case)

$$\begin{cases} \bar{U}_1 \dfrac{\partial \bar{U}_1}{\partial x_1} + \bar{U}_2 \dfrac{\partial \bar{U}_1}{\partial x_2} = -\dfrac{1}{\rho}\dfrac{\partial \bar{P}}{\partial x_1} - \dfrac{\partial \overline{u_1'^2}}{\partial x_1} - \dfrac{\partial \overline{u_1' u_2'}}{\partial x_2} + \nu \left(\dfrac{\partial^2}{\partial x_1^2} + \dfrac{\partial^2}{\partial x_2^2} \right) \bar{U}_1 \\ \sim \dfrac{U^2}{L} \qquad \sim \dfrac{U^2}{L} \qquad\qquad\qquad \sim \dfrac{u^2}{L} \qquad \sim \dfrac{u^2}{\delta} \qquad \sim \nu \left(\dfrac{U}{L^2} ; \dfrac{U}{\delta^2} \right) \end{cases}$$

We impose the balance between the convection along x_1 and the turbulent diffusion along x_2 : a turbulent flow can only be observed if $u \sim \sqrt{\delta / L}\, U$

Turbulent boundary layer equations (cont.)

Averaged Navier-Stokes equation along x_2

$$\begin{cases} \bar{U}_1 \dfrac{\partial \bar{U}_2}{\partial x_1} + \bar{U}_2 \dfrac{\partial \bar{U}_2}{\partial x_2} = -\dfrac{1}{\rho}\dfrac{\partial \bar{P}}{\partial x_2} - \dfrac{\partial \overline{u_1' u_2'}}{\partial x_1} - \dfrac{\partial \overline{u_2'^2}}{\partial x_2} + \nu \left(\dfrac{\partial^2}{\partial x_1^2} + \dfrac{\partial^2}{\partial x_2^2} \right) \bar{U}_2 \\ \sim \dfrac{\delta}{L}\dfrac{U^2}{L} \quad \sim \dfrac{\delta}{L}\dfrac{U^2}{L} \quad\quad \sim \dfrac{\delta}{L}\dfrac{U^2}{L} \quad \sim \dfrac{\delta}{L}\dfrac{U^2}{\delta} \quad \sim \nu \dfrac{\delta}{L}\dfrac{U}{\delta^2} \sim \dfrac{1}{\mathrm{Re}_\delta}\dfrac{\delta}{L}\dfrac{U^2}{\delta} \end{cases}$$

All the terms are smaller by a factor δ/L (refer also to the laminar boundary layer). In addition, the pressure term must balance the dominant red term. By integration in the transverse direction x_2, one gets $\bar{P} + \rho\overline{u_2'^2} = \mathrm{cst}$ across the boundary layer.

Turbulent boundary layer equations (cont.)

The mean pressure gradient is imposed by the external flow (through wall curvature for instance)

$$\bar{P} + \rho\overline{u_2'^2} = P_e = \bar{P}_w$$

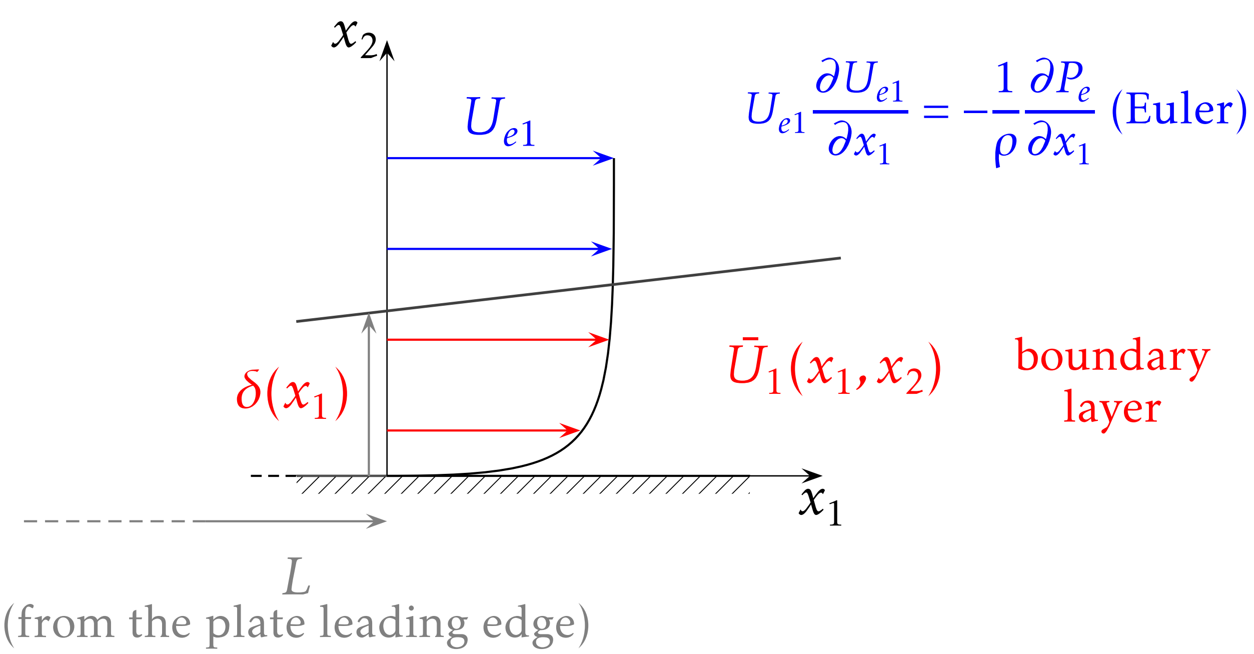

- **Turbulent boundary layer equations (cont.)**

$$\begin{cases} \bar{U}_1 \dfrac{\partial \bar{U}_1}{\partial x_1} + \bar{U}_2 \dfrac{\partial \bar{U}_1}{\partial x_2} = -\dfrac{1}{\rho}\dfrac{dP_e}{dx_1} + \dfrac{\partial}{\partial x_2}\left(\nu \dfrac{\partial \bar{U}_1}{\partial x_2} - \overline{u_1' u_2'}\right) & \text{(i)} \\ \bar{P}(x_1, x_2) = P_e - \rho \overline{u_2'^2} & \text{(ii)} \end{cases}$$

Compared with pipe and channel flows, there is a continuous growth of the boundary layer, and the flow is thus never homogeneous along the x_1 direction (but slowly variable). In addition, the mean pressure gradient is imposed by the external flow.

In what follows, a zero-pressure-gradient (ZPG) boundary layer is assumed,

$$\frac{dP_e}{dx_1} = 0 \qquad \text{(uniform external mean flow, } U_{e1} = \text{cst)}$$

Turbulent boundary layer equations : Ludwig Prandtl (1875-1953)

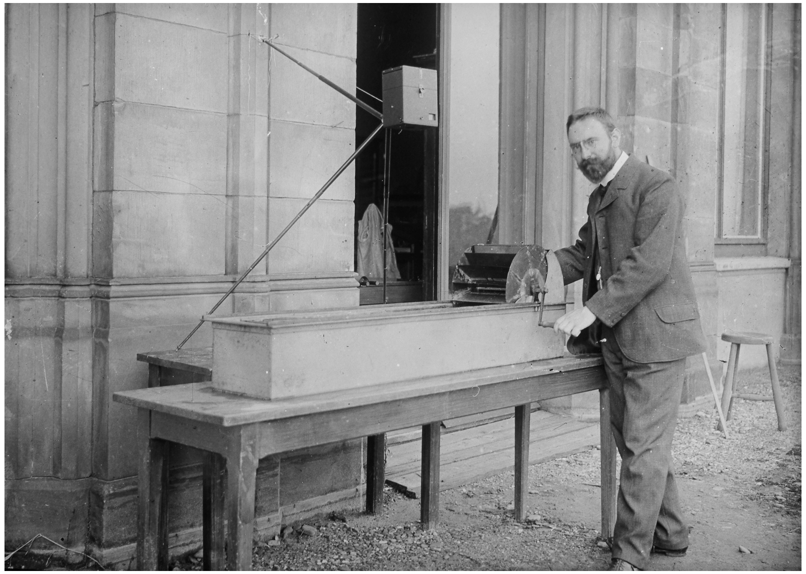

Ludwig Prandtl with his water tunnel in 1903
(for flow visualization of large structures
using particle tracers)

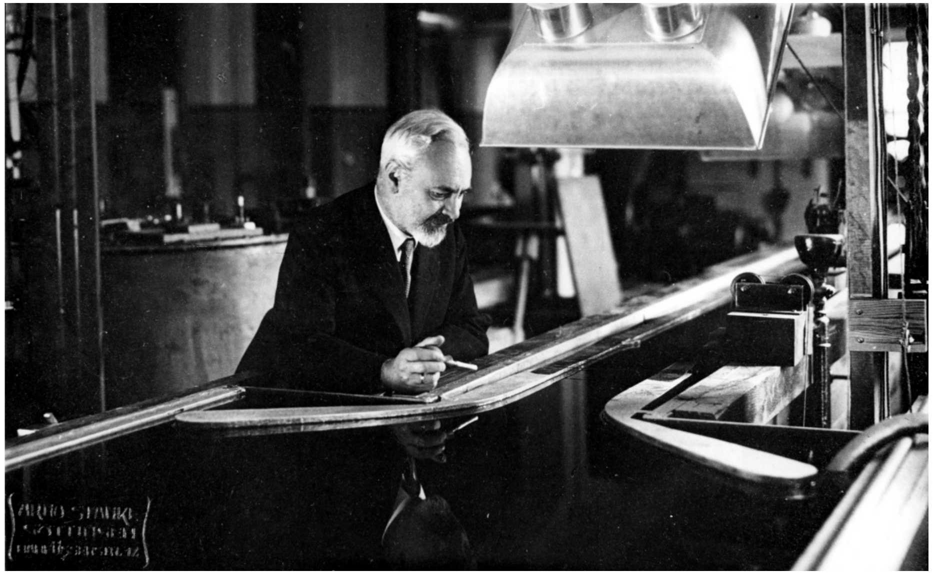

and in the mid to late 1930s

A voyage through Turbulence
edited by, P. A. Davidson, Y Kaneda, H.K. Moffatt & K.R. Sreenivasan
(Cambridge University Press, 2011)

Anderson Jr, D.J., 2005, *Physics Today*, **58**(12), 42–48.

Small exercise : unsteady free stream velocity

The following unsteady external velocity U_{e1} is imposed for a flow past a flat plate, $U_{e1} = u_\infty(1 - a\tilde{x}_1) + u_\infty a\tilde{x}_1 \sin(\omega t)$ where $0 \leq \tilde{x}_1 \leq 1$ is a normalized distance, and $a > 0$ a dimensionless control parameter.

1. Discuss briefly the expression of U_{e1}
2. Calculate the pressure gradient dp_e/dx_1 associated with the unsteady free stream, and its mean value $d\bar{P}_e/dx_1$ over one oscillation period
3. Examine the two cases $f = 0$ and $f \neq 0$

Zero-pressure-gradient boundary layer

For a boundary layer (as also for wake flows), a velocity defect $U_{e1} - \bar{U}_1$ is usually introduced : this quantity is bounded in $x_2 = 0$ and in $x_2 \to \infty$(δ in practice).
The rearrangement of the mass conservation equation leads to,

$$\frac{\partial}{\partial x_1}(\bar{U}_1 U_{e1}) + \frac{\partial}{\partial x_2}(\bar{U}_2 U_{e1}) = 0 \qquad \text{(iii)}$$

By integration in the transverse direction of the Navier-Stokes Eqs. (i) + (iii)

$$\int_0^\infty \frac{\partial}{\partial x_1}\bar{U}_1(\bar{U}_1 - U_{e1})dx_2 + \left[\bar{U}_2(\bar{U}_1 - U_{e1})\right]_0^\infty = \left[-\overline{u_1' u_2'} + \nu\frac{\partial \bar{U}_1}{\partial x_2}\right]_0^\infty$$

$$U_{e1}^2 \frac{\partial}{\partial x_1}\int_0^\infty \frac{\bar{U}_1}{U_{e1}}\left(\frac{\bar{U}_1}{U_{e1}} - 1\right)dx_2 + 0 = 0 - u_\tau^2$$

$$u_\tau^2 = U_{e1}^2 \frac{d\delta_\theta}{dx_1} \qquad \text{with} \qquad \delta_\theta \equiv \int_0^\infty \frac{\bar{U}_1}{U_{e1}}\left(1 - \frac{\bar{U}_1}{U_{e1}}\right)dx_2$$

δ_θ is the momentum thickness of the boundary layer

Zero-pressure-gradient boundary layer

Friction velocity u_τ and local skin-friction coefficient C_f

$$u_\tau^2 = U_{e1}^2 \frac{d\delta_\theta}{dx_1} \qquad\qquad C_f \equiv \frac{\rho u_\tau^2}{\frac{1}{2}\rho U_{e1}^2} = 2\,\frac{d\delta_\theta}{dx_1}$$

The friction velocity u_τ is a function of x_1 (but slow variable) in a boundary layer (≠ established flow in pipe)

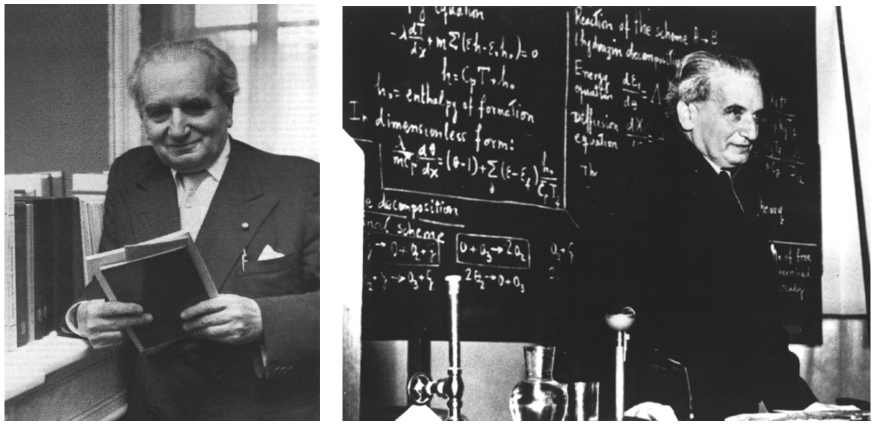

Theodore von Kármán (1881-1963)

General expression for the momentum-integral equation (Gruschwitz, 1931)

$$u_\tau^2 = \frac{d(U_{e1}^2\delta_\theta)}{dx_1} + \delta^\star \underbrace{U_{e1}\frac{dU_{e1}}{dx_1}}_{=-(1/\rho)\partial_{x_1}P_e}$$

Zero-pressure-gradient boundary layer : interpretation of δ_θ ?

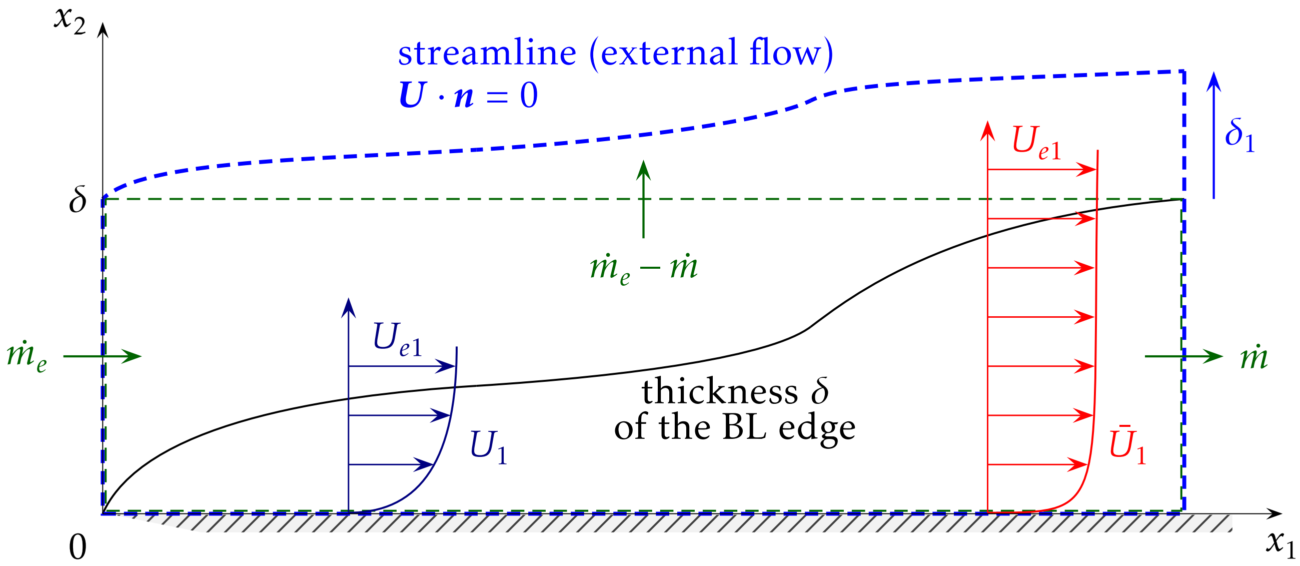

Using the green control volume,

$$\dot{m}_e-\dot{m}=\int_0^\delta(\rho U_{e1}-\rho\bar{U}_1)dx_2$$
$$=\rho U_{e1}\delta_1$$

Using the blue control volume,

$$\rho U_{e1}^2\delta-\int_0^\delta\rho\bar{U}_1^2dx_2-\rho U_{e1}^2\delta_1$$
$$=\rho U_{e1}^2\int_0^\delta\frac{\bar{U}_1}{U_{e1}}\left(1-\frac{\bar{U}_1}{U_{e1}}\right)dx_2$$
$$=\rho U_{e1}^2\delta_\theta$$

Integral momentum conservation (cst pressure)

$$\frac{d}{dt}\int_{\mathcal{V}}\rho\boldsymbol{u}=\boldsymbol{0}=\int_{\mathcal{V}}\rho\frac{D\boldsymbol{u}}{Dt}-\int_{\mathcal{S}}\rho\boldsymbol{u}(\boldsymbol{u}\cdot\boldsymbol{n})\,ds=\int_{\mathcal{S}}\overline{\overline{\boldsymbol{\tau}}}\cdot\boldsymbol{n}\,ds-\int_{\mathcal{S}}\rho\boldsymbol{u}(\boldsymbol{u}\cdot\boldsymbol{n})\,ds$$

Wall force acting on the wall, $\boldsymbol{F}_{f\to w}=\rho U_{e1}^2\delta_\theta\boldsymbol{e}_1$

Mean velocity of a zero-pressure-gradient boundary layer

From the Navier-Stokes Eq. (i), by integration in the normal direction to the wall up to a given point x_2

$$\int_0^{x_2} \rho\left(\bar{U}_1\frac{\partial \bar{U}_1}{\partial x_1} + \bar{U}_2\frac{\partial \bar{U}_1}{\partial x_2}\right)dx_2 = \bar{\tau}_t(x_2) - \bar{\tau}_w \qquad \bar{\tau}_t(x_2) \equiv -\rho\overline{u_1'u_2'} + \mu\frac{\partial \bar{U}_1}{\partial x_2} \tag{2}$$

Simplistic assumption : the left-hand side is approximated by a linear term as follows,

$$\int_0^{x_2} \rho\left(\bar{U}_1\frac{\partial \bar{U}_1}{\partial x_1} + \bar{U}_2\frac{\partial \bar{U}_1}{\partial x_2}\right)dx_2 \simeq -\frac{x_2}{\delta}\tau_w \qquad \boxed{\bar{\tau}_t(x_2) \simeq \tau_w\left(1 - \frac{x_2}{\delta}\right)}$$

As a result, the mean velocity $\bar{U}_1$ is governed by the same equation than for the channel/pipe (by noting $\delta \equiv h$) except that the friction velocity is now a function of x_1, $u_\tau = u_\tau(x_1)$.

(refer to the exercises for further discussion)

Mean velocity profile : the viscous sublayer

Very close to the wall, $x_2/\delta \ll 1$, turbulence cannot develop and the viscous stress dominates the total stress $\bar{\tau}_t$ (at the wall $u_i' = 0$),

$$\bar{\tau}_t \simeq \mu \frac{\partial \bar{U}_1}{\partial x_2} \qquad \text{and} \qquad \bar{\tau}_w = \rho u_\tau^2 \qquad \text{in the viscous sublayer}$$

Consequently, a linear evolution of the mean velocity $\bar{U}_1$ is predicted, as in the case of the Couette flow,

$$\frac{\bar{U}_1}{u_\tau} = \frac{x_2 u_\tau}{\nu}$$

Introduction of wall units to form dimensionless variables

$$\bar{U}_1^+ \equiv \frac{\bar{U}_1}{u_\tau} \qquad x_2^+ \equiv \frac{x_2 u_\tau}{\nu} = \frac{x_2}{l_v} \qquad \text{with} \qquad l_v = \frac{\nu}{u_\tau} \equiv \text{ wall unit length}$$

In the viscous sublayer, $\boxed{\bar{U}_1^+ = x_2^+}$

Mean velocity profile : the viscous sublayer (cont.)

- The viscous length scale l_v and the friction velocity u_τ are the two appropriate scales for describing flow in the near-wall region : inner scales of the boundary layer

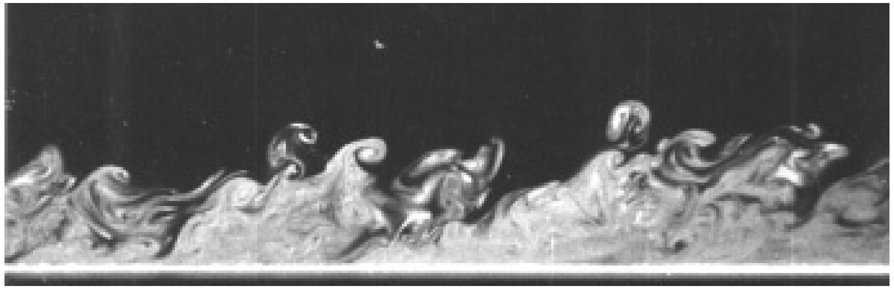

F. Laadhari (LMFA)

$$\mathrm{Re}_\theta \simeq 1000 \quad U_{e1} = 2.1 \text{ m.s}^{-1}$$
$$\delta \simeq 7 \text{ cm} \quad u_\tau \simeq 0.1 \text{ m.s}^{-1}$$
$$x_1 \simeq 3 \text{ m} \quad \text{(air flow)}$$

$$x_2^+ = \frac{u_\tau x_2}{\nu} = 1 \quad \Longrightarrow \quad x_2 = l_v = 0.15 \text{ mm}$$

Mean velocity profile : the viscous sublayer (cont.)

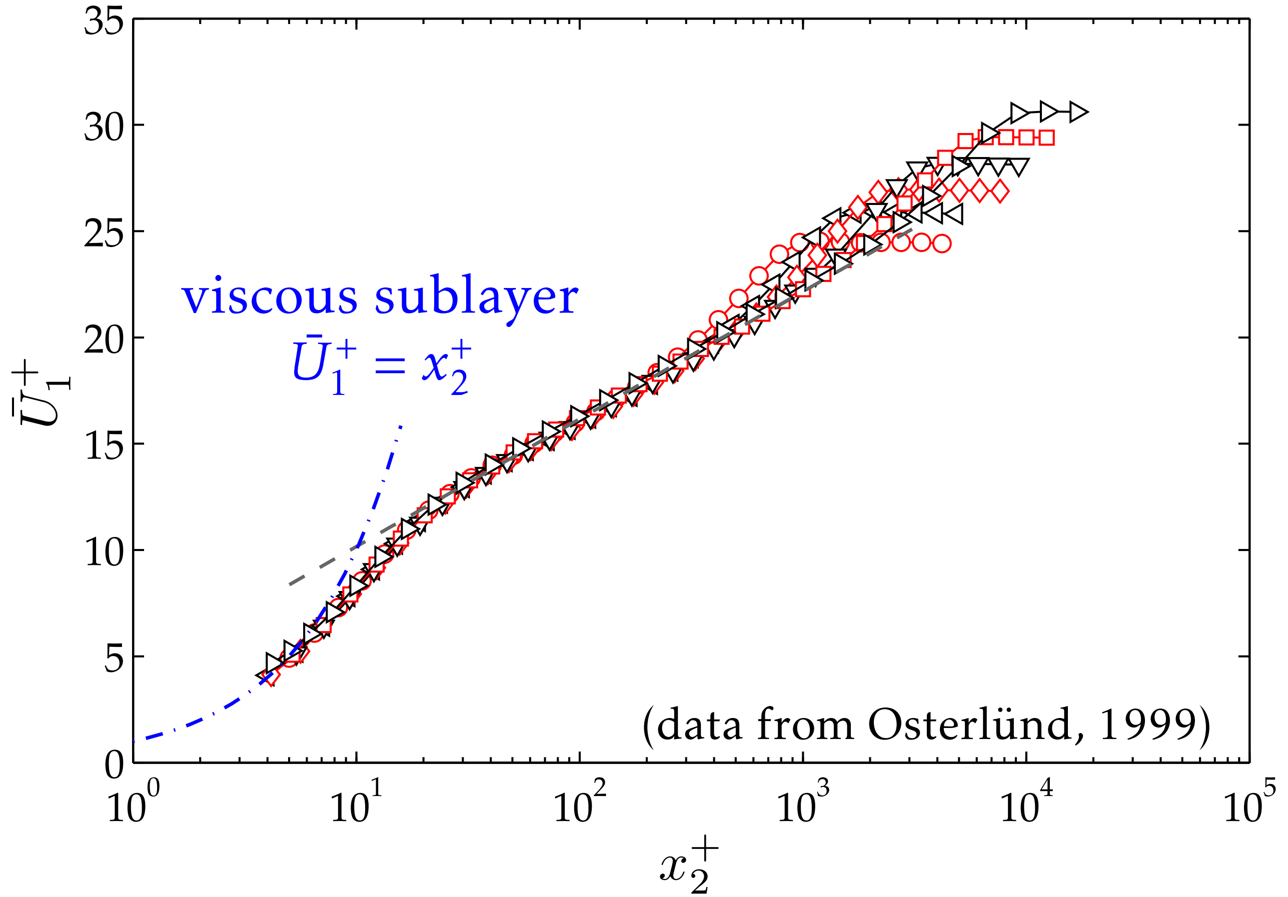

$Re_{\delta_{0.95}}$	1.7×10^4	2.8×10^4	4.3×10^4	6.9×10^4	1.1×10^5	1.9×10^5
$Re^+_{\delta_{0.95}}$	684	1092	1594	2462	3944	6147
	○	◁	◊	▽	□	▷

Two illustrations of the disparity in scales

Turbulent boundary layer along a flat plate : particle tracing in water, hydrogen bubble method, $U_\infty = 20.4$ cm.s^{-1}, $\mathrm{Re}_{\delta_\theta} = 990$
from *Visualized flow*, Japan Soc. Mech. Eng. (1988)

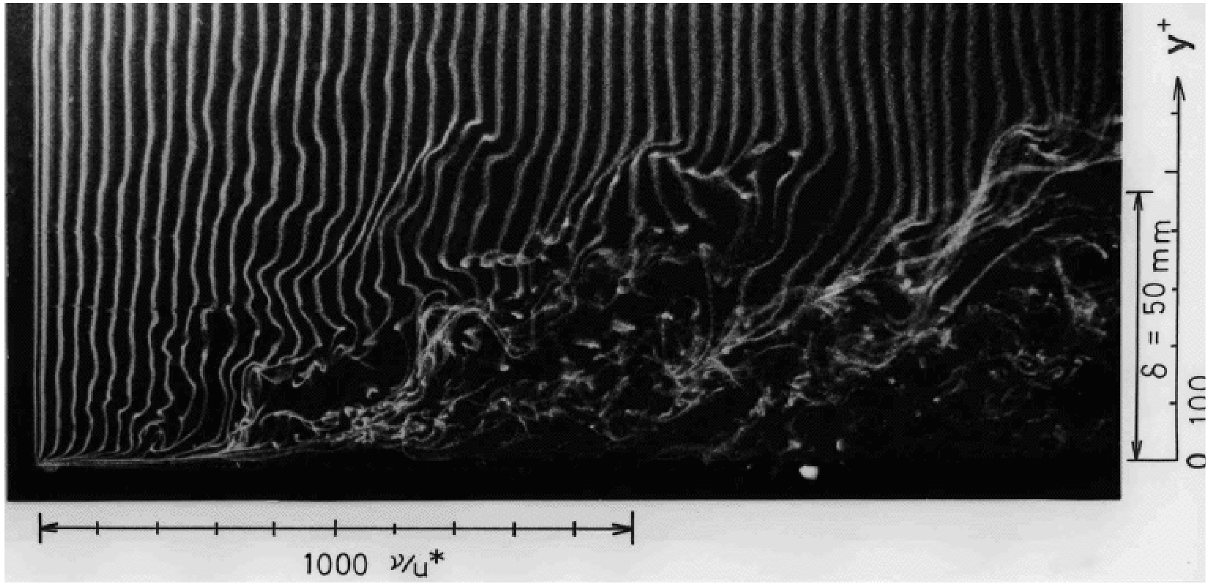

Spatially developing turbulent boundary layer on a flat plate
from Lee, Kwon, Hutchins & Monty (University of Melbourne)

Mean velocity profile : the logarithmic law

We have two characteristic length scales in a boundary layer : δ and $l_v = \nu/u_\tau$,

$$x_2^+ = \frac{x_2 u_\tau}{\nu} = \mathrm{Re}^+ \times \frac{x_2}{\delta} \qquad \boxed{\mathrm{Re}^+ \equiv \frac{u_\tau \delta}{\nu} = \delta^+} \quad \text{Karman number}$$

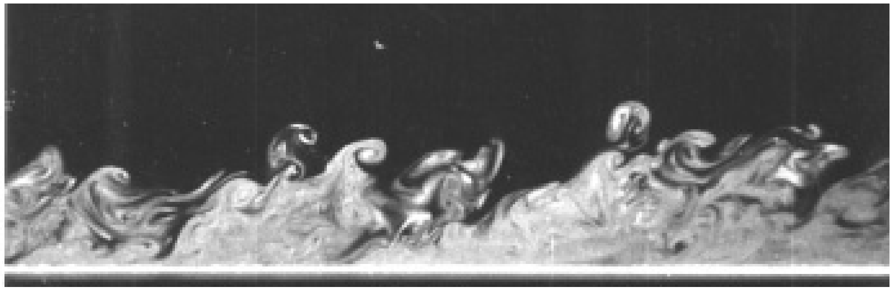

F. Laadhari (LMFA)

$$\mathrm{Re}_\theta \simeq 1000 \quad U_{e1} = 2.1 \text{ m.s}^{-1}$$
$$\delta \simeq 7 \text{ cm} \quad u_\tau \simeq 0.1 \text{ m.s}^{-1}$$
$$x_1 \simeq 3 \text{ m} \quad \text{(air flow)}$$
$$l_v = 0.15 \text{ mm } (x_2^+ = 1) \qquad \mathrm{Re}^+ \simeq 467$$

It is thus possible to satisfy $x_2^+ \gg 1$, $\mathrm{Re}^+ \gg 1$, but also $x_2/\delta \ll 1$

As an illustration, one has for this flow,

$$x_2^+ = 30 \qquad \frac{x_2}{\delta} = \frac{x_2^+}{\mathrm{Re}^+} \simeq 6 \times 10^{-2} \ll 1$$

- **Mean velocity profile : the logarithmic law (cont.)**

Dimensional analysis

$$\frac{\bar{U}_1}{u_\tau} = f\left(\frac{x_2 u_\tau}{\nu}, \frac{x_2}{\delta}\right) \quad \Longrightarrow \quad \begin{cases} \dfrac{\bar{U}_1}{u_\tau} = f_1\left(\dfrac{u_\tau x_2}{\nu}\right) & \text{in the inner layer} \\[2ex] \dfrac{U_{e1} - \bar{U}_1}{u_\tau} = f_2\left(\dfrac{x_2}{\delta}\right) & \text{in the outer layer} \end{cases}$$

By imposing the continuity of the velocity $\bar{U}_1$ and of its derivative $\partial \bar{U}_1 / \partial x_2$

$$\begin{cases} \dfrac{\bar{U}_1}{u_\tau} = \dfrac{1}{\kappa} \ln\left(\dfrac{u_\tau x_2}{\nu}\right) + B \\[2ex] \dfrac{U_{e1} - \bar{U}_1}{u_\tau} = -\dfrac{1}{\kappa} \ln\left(\dfrac{x_2}{\delta}\right) + A \end{cases} \qquad \text{with} \quad \frac{U_{e1}}{u_\tau} = \ln(\mathrm{Re}^+) + A + B$$

where κ is the von Kármán constant : does not seem to be a universal constant, even for canonical flows ! $\quad 0.38 \leq \kappa \leq 0.41$

Mean velocity profile : the logarithmic law (inner scales)

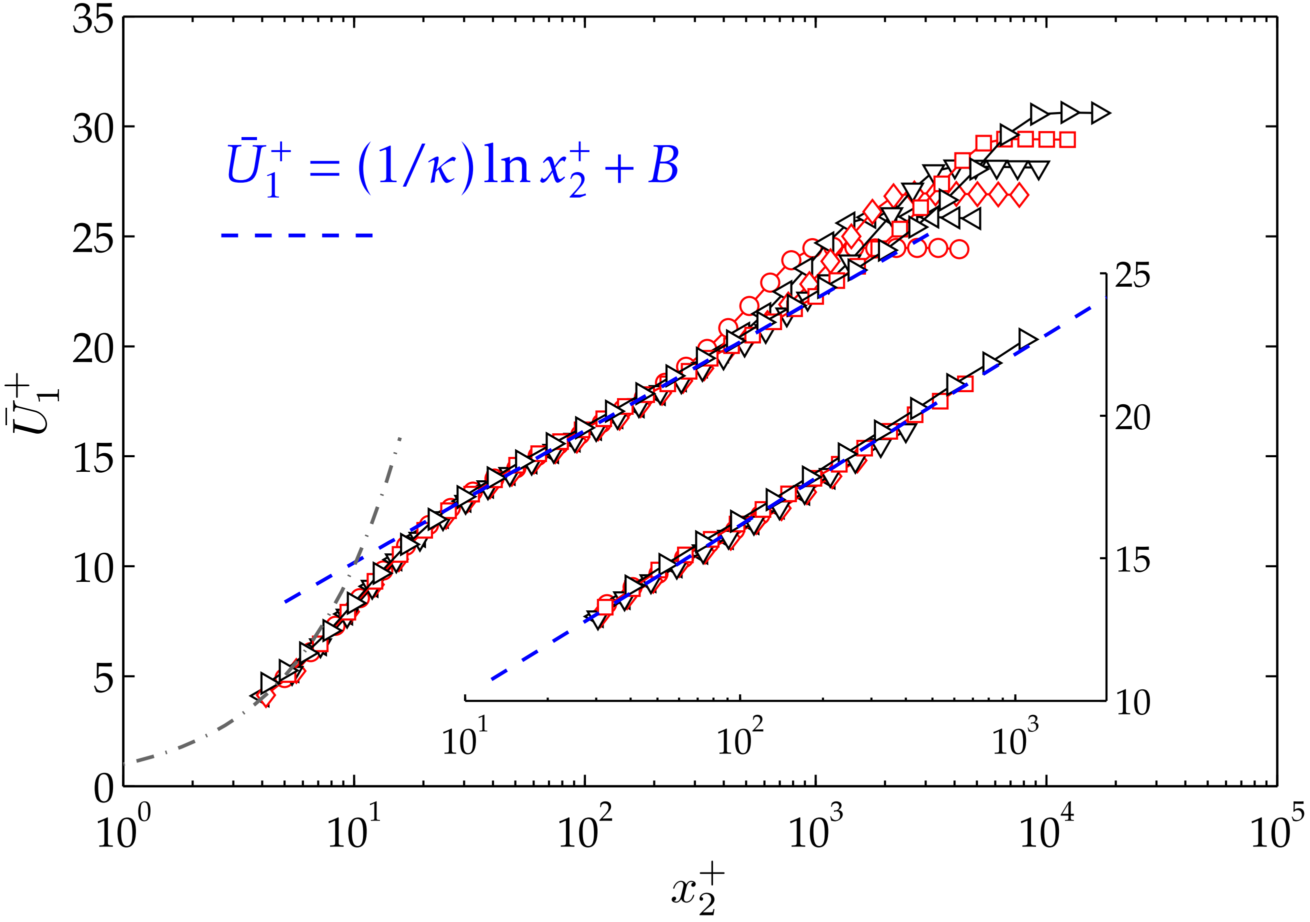

For a zero-pressure-gradient boundary layer,

$\kappa \simeq 0.384 \quad B \simeq 4.17$

log-law $\quad x_2^+ \geq 30$ & $x_2/\delta \leq 0.20$

(data from Osterlünd, 1999)

Mean velocity profile : the logarithmic law (outer scales, wake law)

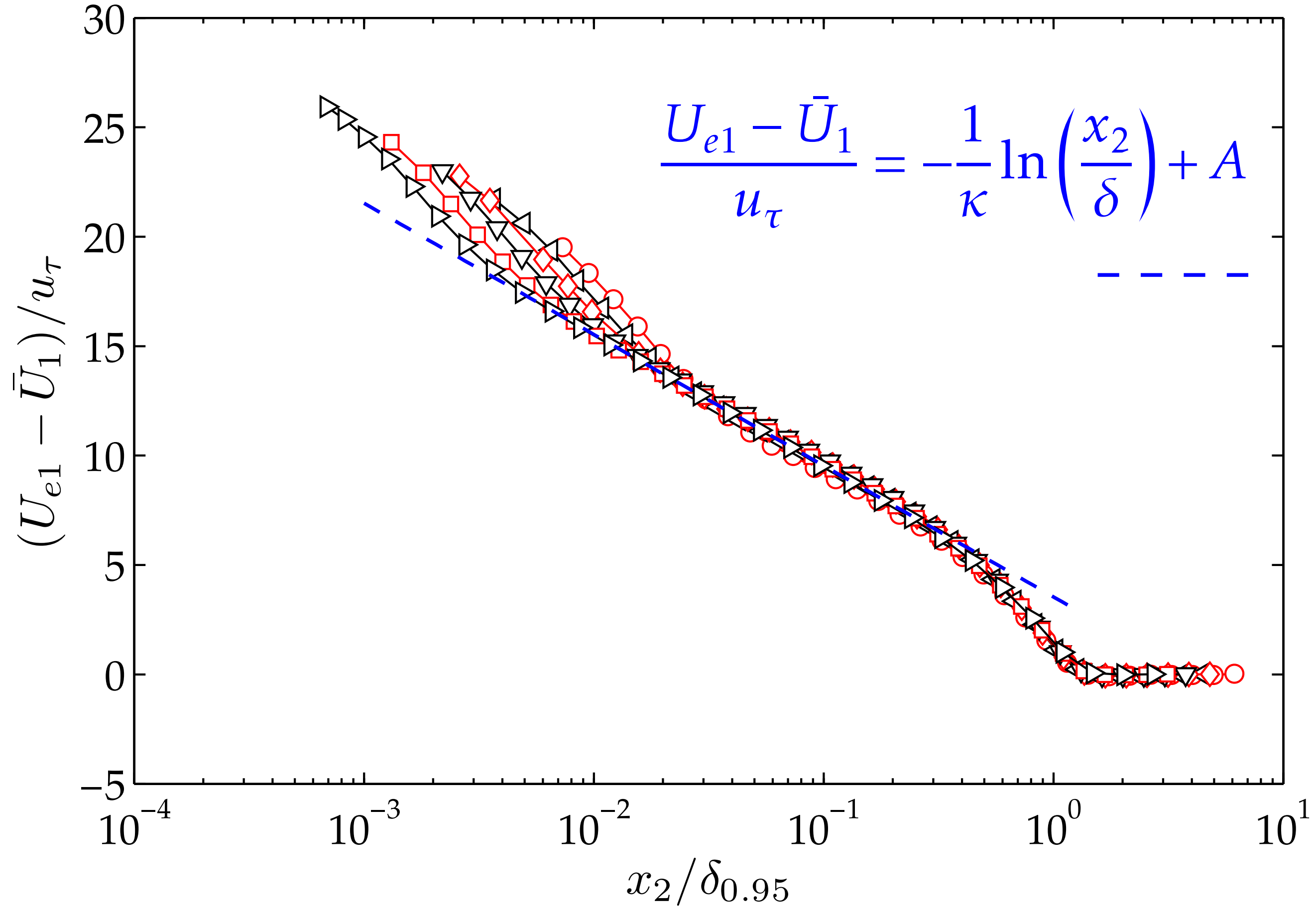

(data from Osterlünd, 1999)

For a zero-pressure-gradient boundary layer,

$\kappa \simeq 0.384 \quad A \simeq 3.54$

- **Mean velocity profiles in a turbulent pipe flow**
  Zagarola & Smits (1998, Princeton *Superpipe* facility)

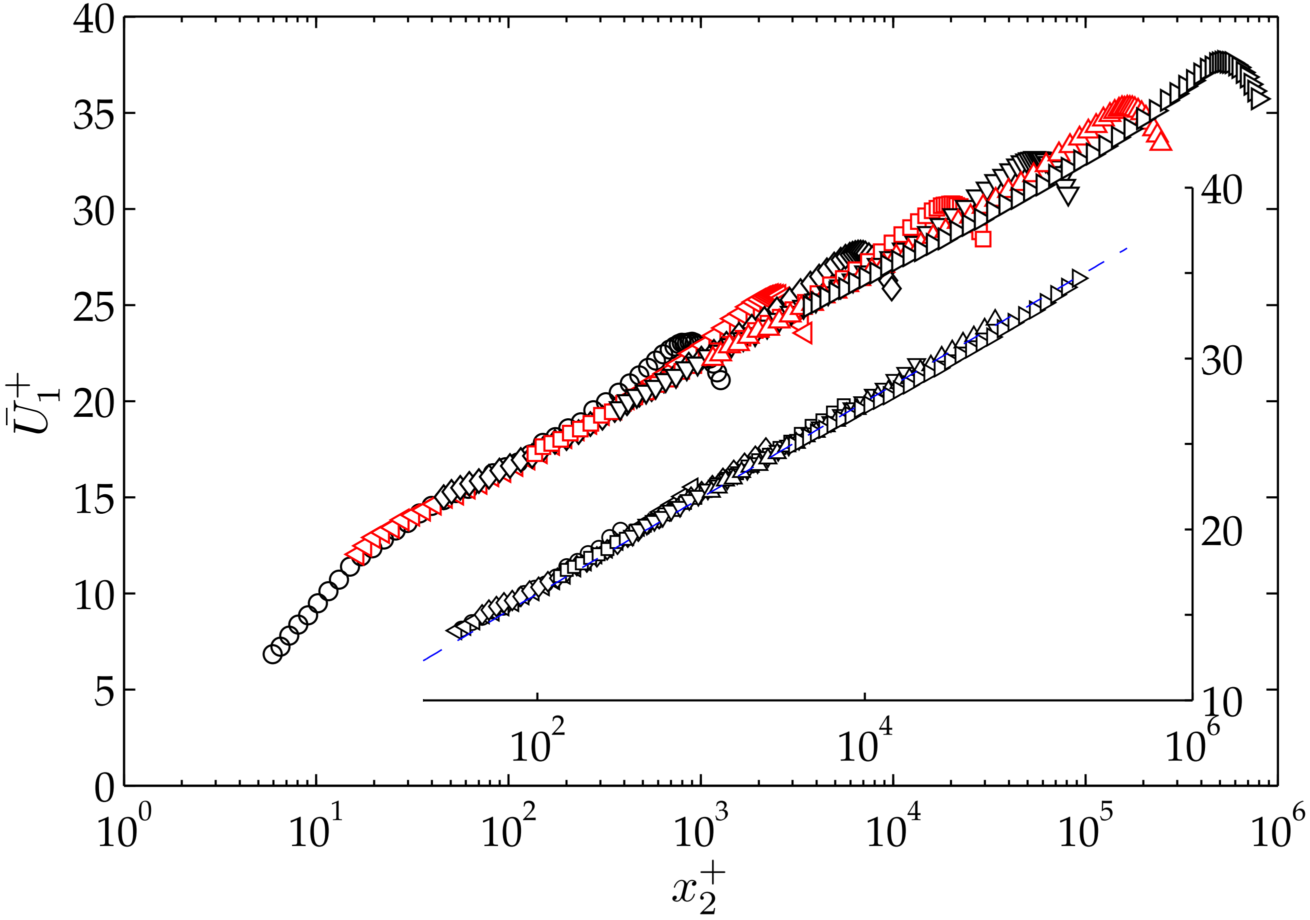

$\mathrm{Re}_D = 3.2 \times 10^3$ ○
9.9×10^4 ◁
3.1×10^5 ◇
1.0×10^6 □
3.1×10^6 ▽
1.0×10^7 △
3.5×10^7 ▷

log-law
$\kappa \simeq 0.41$ $B \simeq 5.0$

Fully developed channel flow : experiments

Comte-Bellot, G. (1965)

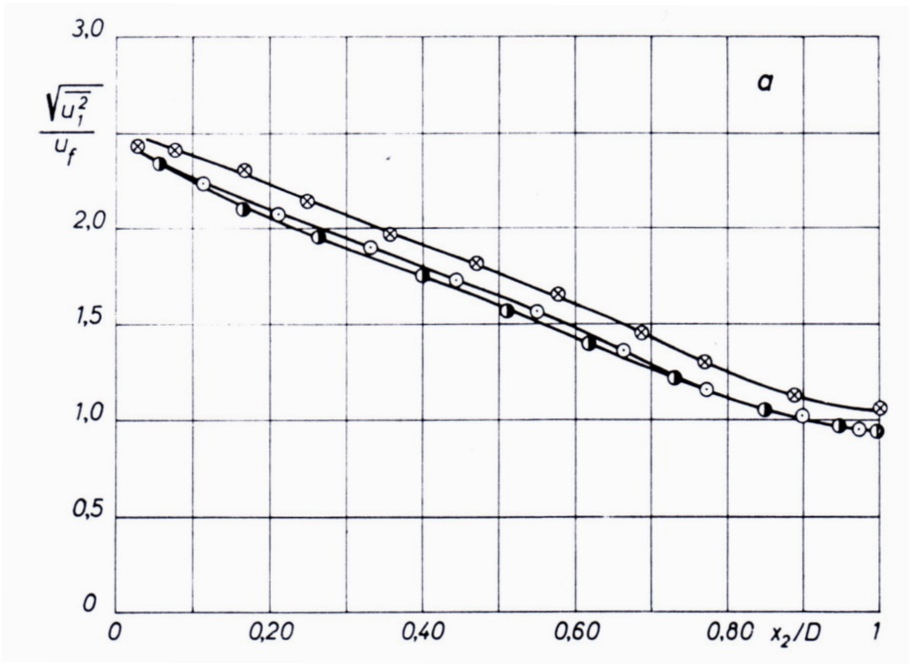

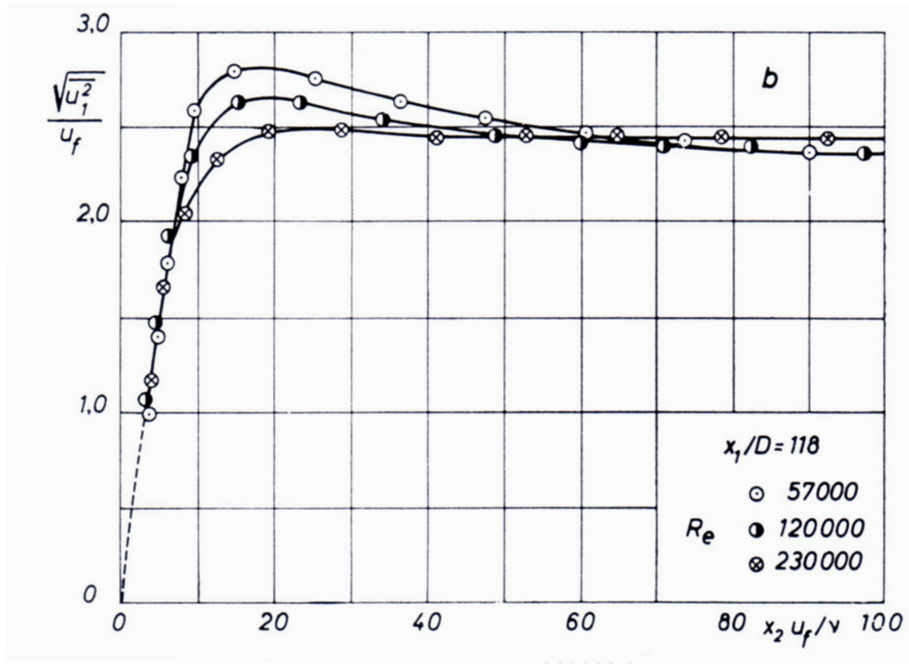

Plane channel of width $2h \equiv 2D$ $\quad 5.7\times10^4 \le \mathrm{Re}_h \le 2.3\times10^5$

Fully developed channel flow : Direct Numerical Simulation (DNS)

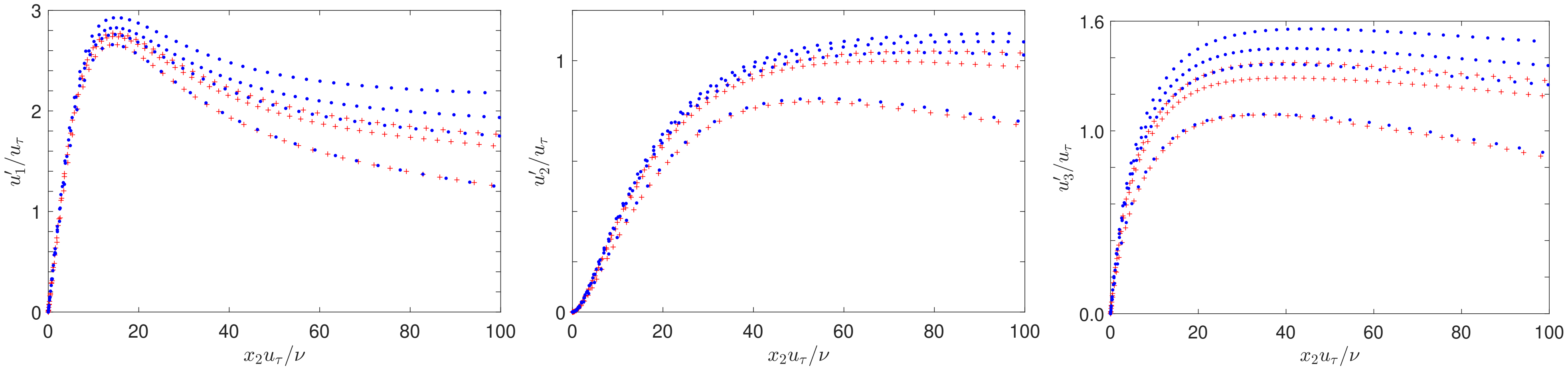

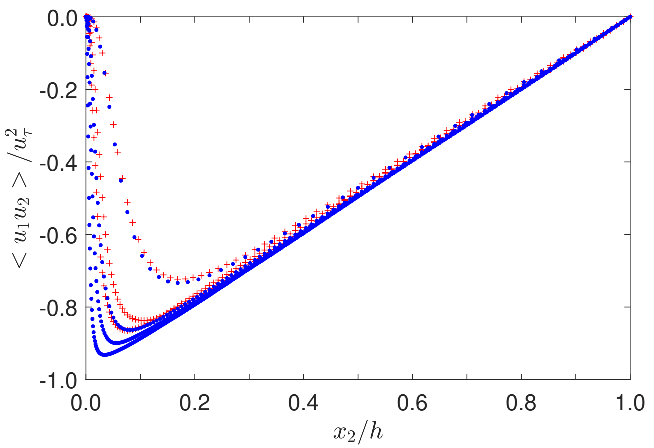

Moser, Kim & Mansour (1999)

\+ $Re^+ = 180$, $Re^+ = 395$, $Re^+ = 590$

Hoyas & Jiménez (2006)

• $Re^+ = 180$, $Re^+ = 550$, $Re^+ = 950$, $Re^+ = 2000$

...

Balance between production and dissipation in the log-law

For an observer located in the log-law region of a boundary layer, an almost perfect balance is found between **production and dissipation** of the turbulent kinetic energy k_t, that is

$$\boxed{\mathcal{P} \equiv -\rho \overline{u_1' u_2'} \frac{d\bar{U}_1}{dx_2} \quad \simeq \quad \rho\epsilon} \qquad \text{inside the log-law}$$

This result is the starting point of various developments for turbulence models, even if there is no formal demonstration.

Turbulent kinetic energy budget in a channel flow

Ratio of $\mathcal{P}/(\rho\epsilon^h)$ for $\mathrm{Re}^+ = 180, 550, 950, 2000$ (DNS by Hoyas & Jiménez, 2006)

We can observe the increase of the equilibrium region with the increase of the Reynolds number

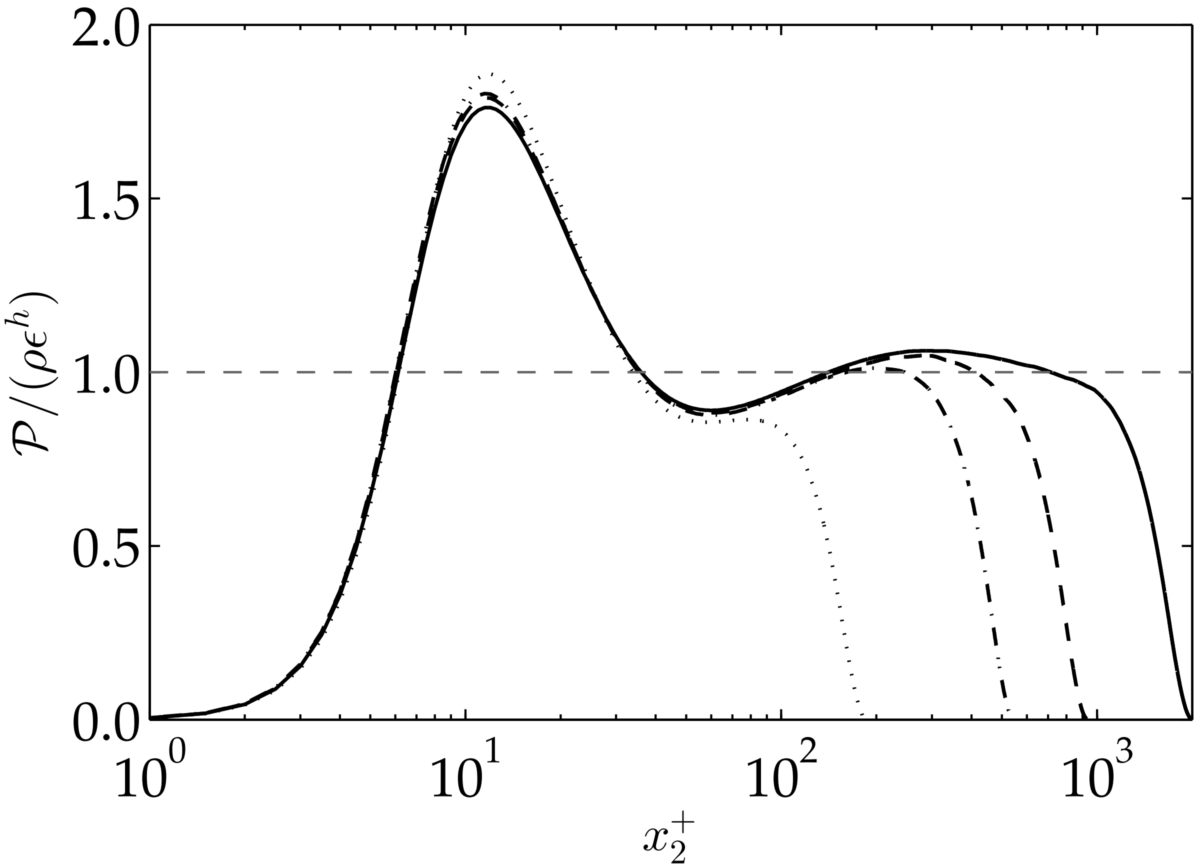

A first example of turbulence model : mixing length model

We first investigate the near wall region, in assuming that $x_2/\delta \ll 1$, to derive the mixing length model by Prandtl (1925), and the governing equation for the mean velocity $\bar{U}_1$ (also valid for a channel flow with $h = \delta$)

$$\bar{\tau}_t(x_2) = -\rho\overline{u_1'u_2'} + \mu\frac{d\bar{U}_1}{dx_2} \simeq \bar{\tau}_w \qquad \text{or also} \qquad -\overline{u_1'u_2'}^+ + \frac{d\bar{U}_1^+}{dx_2^+} \simeq 1$$

The turbulent viscosity concept (introduced in Chapter 2) leads to

$$-\overline{u_1'u_2'}^+ = -\frac{\overline{u_1'u_2'}}{u_\tau^2} = \nu_t^+\frac{d\bar{U}_1^+}{dx_2^+} \qquad \nu_t^+ \equiv \frac{\nu_t}{\nu}$$

where the turbulent viscosity is dimensionally the product of a velocity scale u' by a length scale l_m, that is $\nu_t \sim u' \times l_m$.

(by analogy with the molecular motion for a perfect gas : ν is roughly the product of the speed of sound by the free mean path)

Mixing length model (cont.)

In an algebraic model (*aka* a zero-equation model), the evolution of the mixing length l_m is imposed by the user. For a boundary layer, a linear evolution in the normal direction to the wall is assumed, that is $l_m^+ = \alpha x_2^+$

The velocity scale u' is then obtained by assuming that the frequency of the mean flow is imposed to the turbulent motion (through the production term). This frequency matching leads to

$$\frac{u'^+}{l_m^+} = \frac{d\bar{U}_1^+}{dx_2^+}$$

As a result, the turbulent viscosity and the Reynolds stress component are given in wall unit by

$$\nu_t^+ = (l_m^+)^2 \left| \frac{d\bar{U}_1^+}{dx_2^+} \right| \qquad \text{and} \qquad -\overline{u_1' u_2'}^+ = \underbrace{(l_m^+)^2 \left| \frac{d\bar{U}_1^+}{dx_2^+} \right|}_{\nu_t^+} \frac{d\bar{U}_1^+}{dx_2^+}$$

Mixing length model (cont.)

The governing equation for the mean velocity can thus be recast as follows with our assumptions

$$(\alpha x_2^+)^2 \left(\frac{d\bar{U}_1^+}{dx_2^+} \right)^2 + \frac{d\bar{U}_1^+}{dx_2^+} - 1 = 0$$

The mean velocity gradient $d\bar{U}_1^+/dx_2^+$ satisfies a quadratic equation. The relevant solution is given by

$$\frac{d\bar{U}_1^+}{dx_2^+} = \frac{-1 + \sqrt{1 + 4\,(\alpha x_2^+)^2}}{2\,(\alpha x_2^+)^2} \geq 0$$

For $x_2^+ \to 0, \quad \dfrac{d\bar{U}_1^+}{dx_2^+} \to 1$

One finds $\bar{U}_1^+ = x_2^+$, that is the velocity law expected in the viscous sublayer

For $x_2^+ \to \infty, \quad \dfrac{d\bar{U}_1^+}{dx_2^+} \to \dfrac{1}{\alpha x_2^+}$

A log-law is found for $\bar{U}_1^+$, and by identification, $\alpha = \kappa$ $(x_2/\delta \ll 1)$

Mixing length model (cont.)

However, the previous model has one flaw, and thus requires a correction proposed by Van Driest (see next small classe)

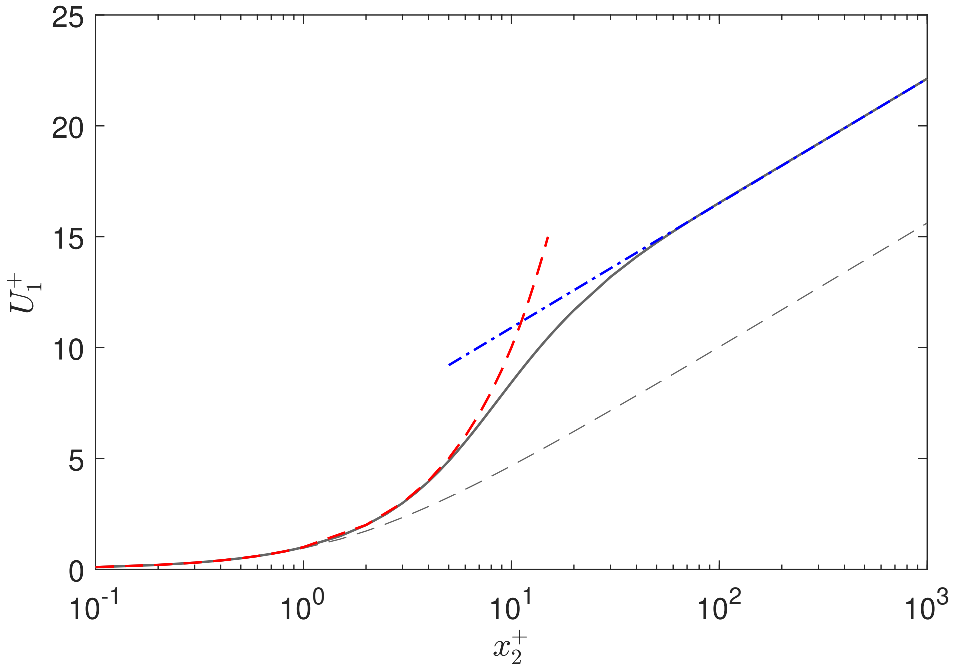

$l_m^+ = \kappa x_2^+$

$l_m^+ = \kappa x_2^+(1 - e^{-x_2^+/A_0^+}) \quad A_0^+ = 26$

$U_1^+ = x_2^+$ viscous sublayer

$U_1^+ = (1/\kappa)\ln(x_2^+) + B$

Using Van Driest damping function, $-\overline{u_1' u_2'}^+ \sim x_2^{+4}$ as $x_2^+ \to 0$, rather than $-\overline{u_1' u_2'}^+ \sim x_2^{+2}$ using $l_m^+ = \kappa x_2^+$.

However,from the governing equations, it can be shown that $-\overline{u_1' u_2'}^+ \sim x_2^{+3}$!

The buffer layer : streaks and harpin (horseshoe) vortices

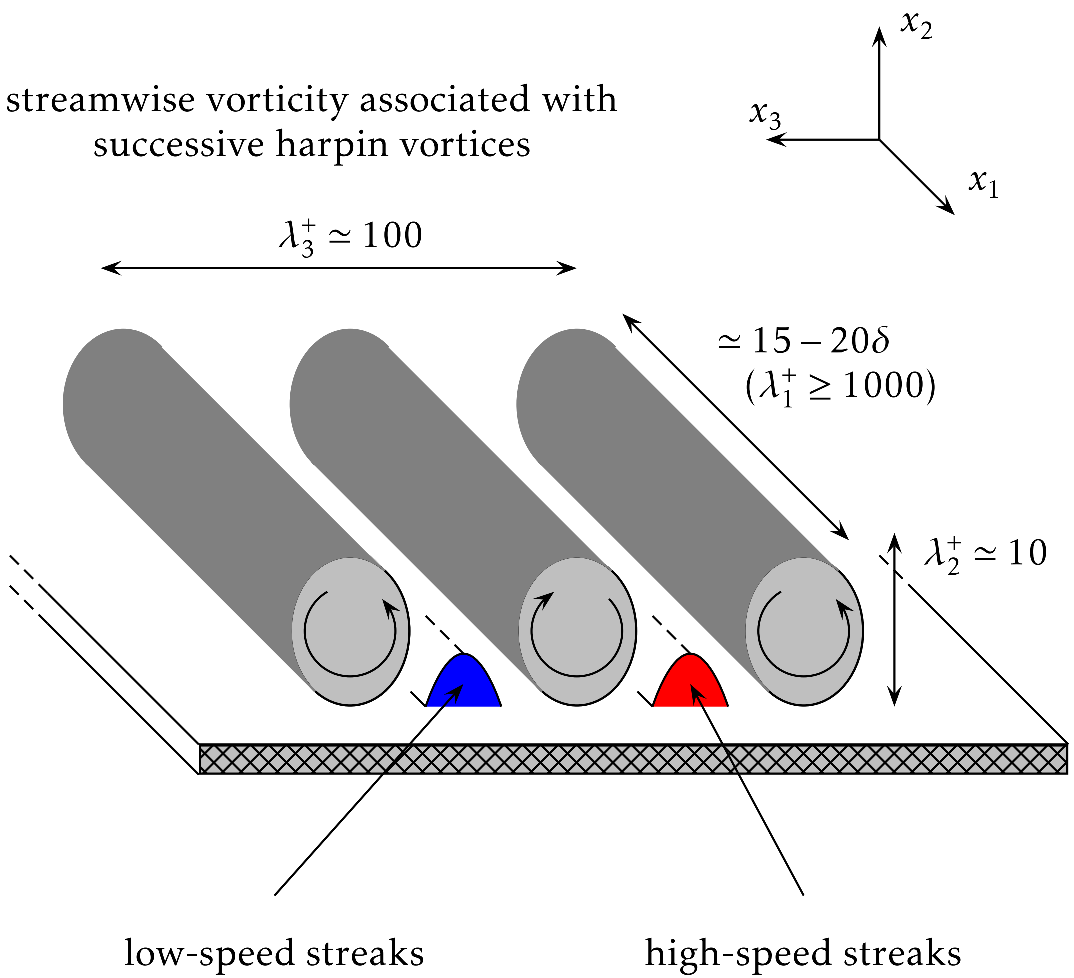

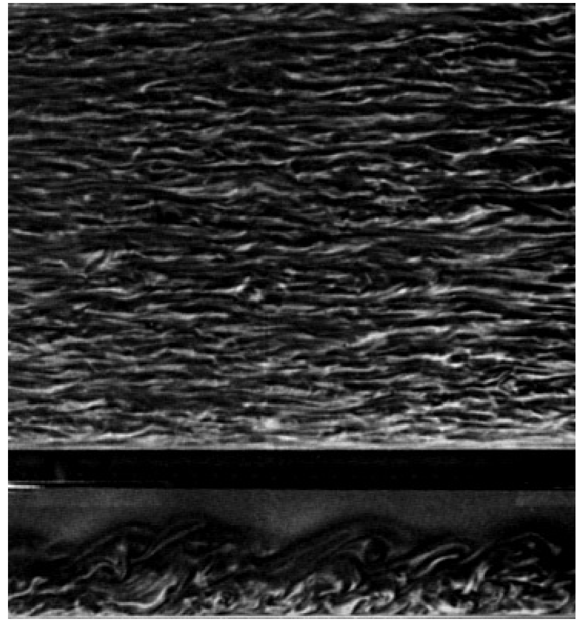

Cantwell, Coles & Dimotakis (1978)

Visualization of sublayer streaks from a suspension of aluminium particules (water, $U_\infty = 15$ cm.s^{-1})

- **The buffer layer : streaks and harpin (horseshoe) vortices**
  Conceptual view from Adrian, Meinhart & Tomkins (2000)

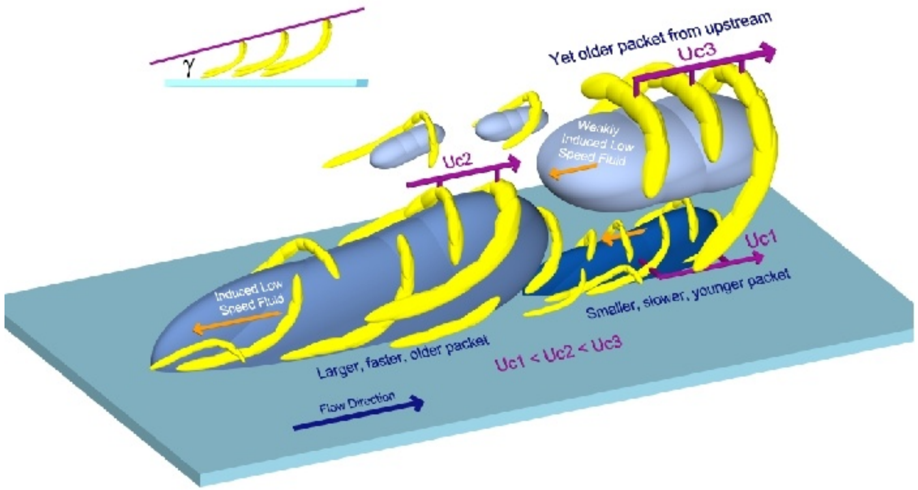

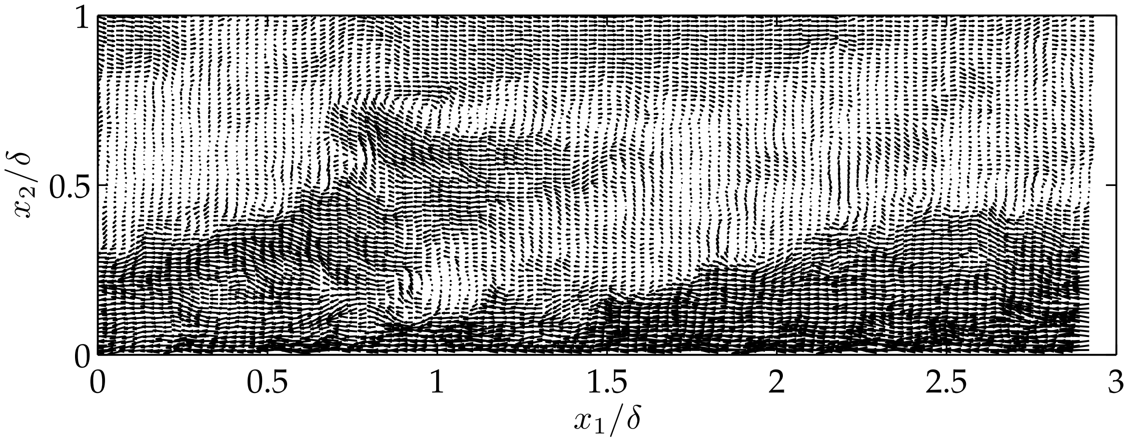

PIV measurements
$\mathrm{Re}_{\delta_\theta} = 7705$
plot of $\boldsymbol{u} - 0.87\boldsymbol{U}_{e1}$

- **The buffer layer : streaks and harpin (horseshoe) vortices**

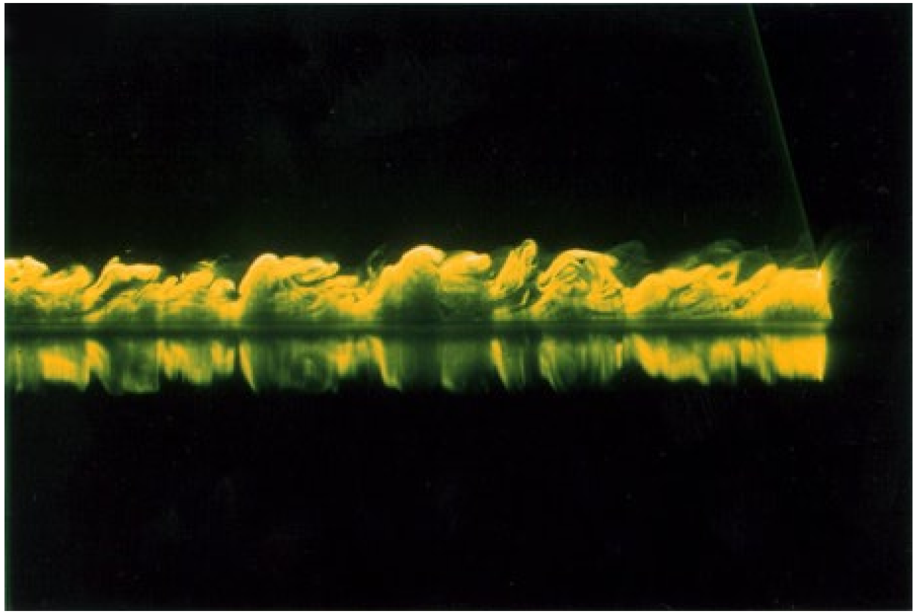

Side view of large eddies in a turbulent boundary layer
by laser-induced fluorescence

Gad-el-Hak, University of Notre-Dame, USA

http://www.efluids.com

The buffer layer

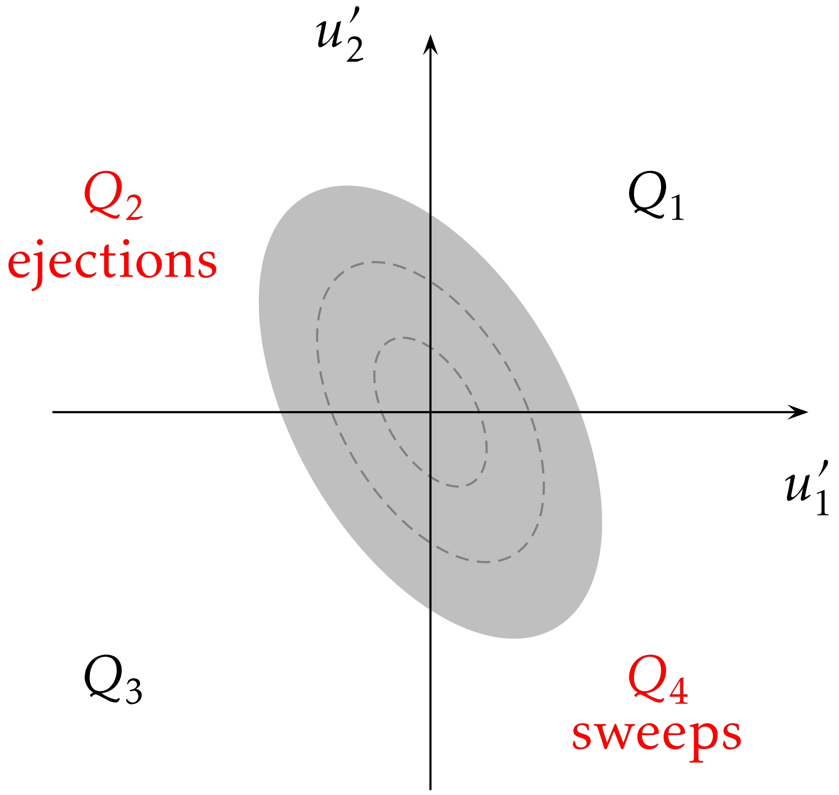

- Drag generating events fall in the second and fourth quadrant, positive turbulent production

$$\mathcal{P} \simeq -\rho \overline{u'_1 u'_2} \frac{\partial \bar{U}_1}{\partial x_2}$$

DNS of a plane channel flow

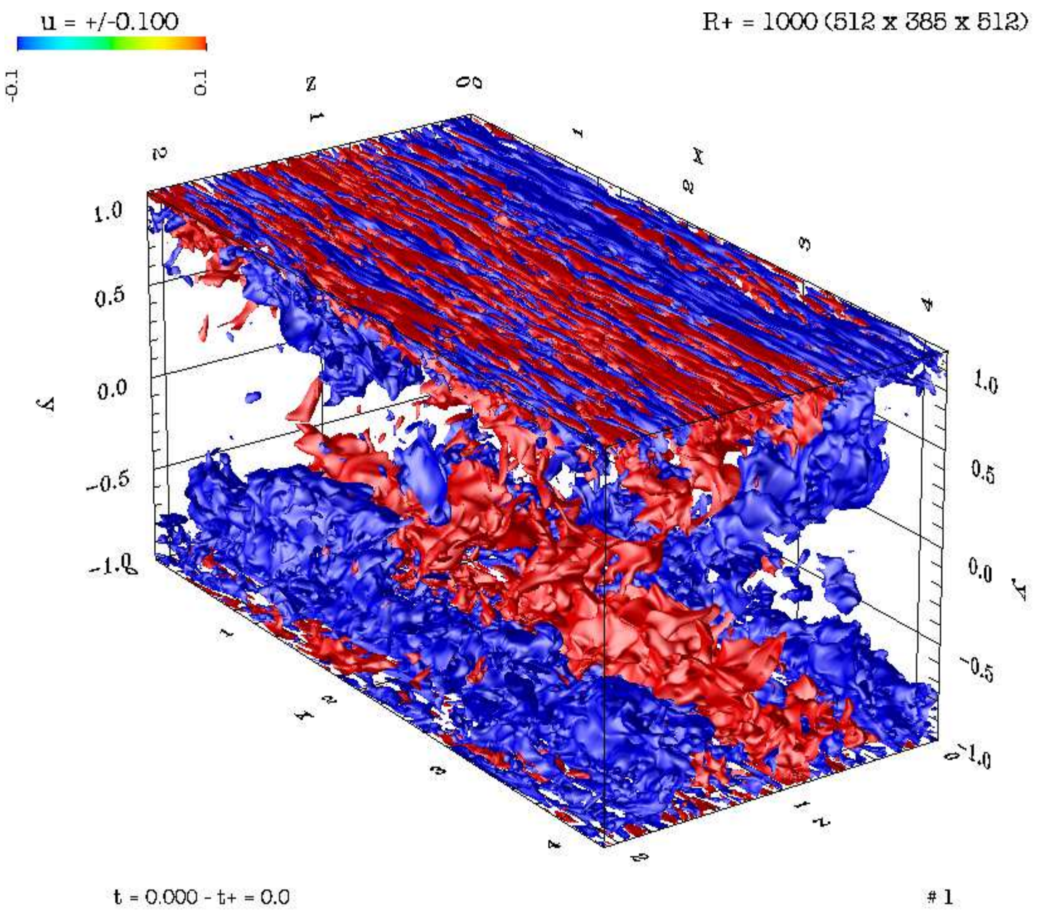

Iso-surfaces of the streamwise fluctating velocity
(red $u'/U_c = 0.12$, blue $u'/U_c = -0.12$)

- Laadhari, *Phys. Fluids* (2007)
  $n_{\text{dof}} = 512 \times 385 \times 512 \simeq 101 \times 10^6$
  $\text{Re}_h = 20100$, $\text{Re}^+ = 1000$
  $(\text{Re}^+)^{3/4}/n_y \simeq 0.46$
  cost$\sim$ $\text{Re}^{+3} \sim 10^9$
  IBM SP4 / CINES

- **DNS of a boundary layer over a flate plate**

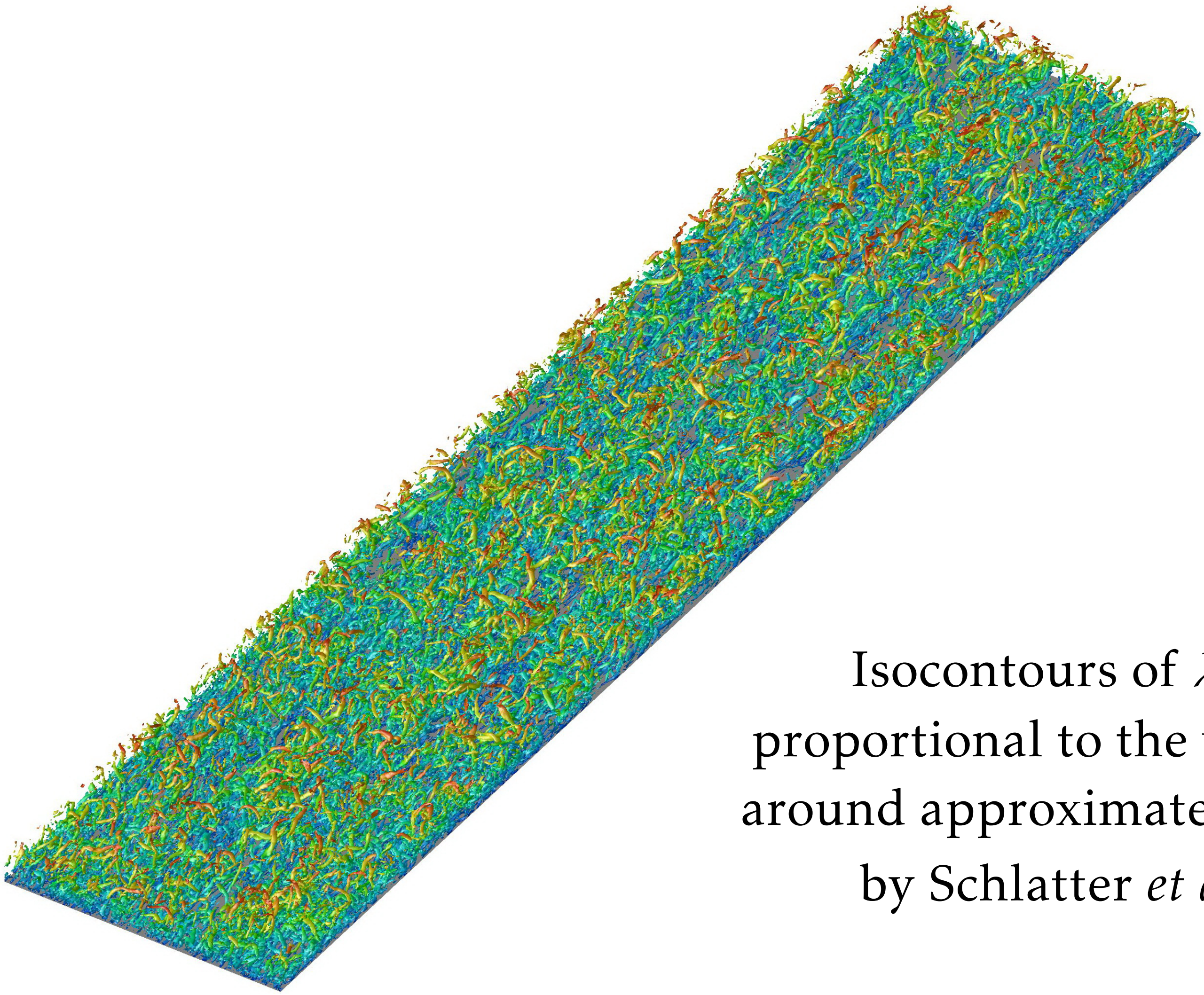

Isocontours of λ_2 (colour proportional to the wall distance) around approximately $Re_{\delta_\theta} = 1400$ by Schlatter *et al.* (2009)

http://www.mech.kth.se/~pschlatt/DATA/

Turbulent boundary layer with pressure gradient

Dimensionless parameter β

$$\beta = \frac{\delta_1}{\rho u_\tau^2}\frac{dP_e}{dx_1} = -\frac{\delta_c}{u_\tau}\frac{dU_{e1}}{dx_1} \sim \frac{\tau_{\mathrm{bl}}}{\tau_e} \qquad \delta_c = \int_0^\infty \frac{U_{e1}-U_1}{u_\tau}dx_2 = \delta_1\frac{U_{e1}}{u_\tau}$$

- time scale of the boundary layer $\tau_{\mathrm{bl}} \sim \delta_c/u_\tau$
- time scale of the external flow $\tau_e \sim (dU_{e1}/dx_1)^{-1}$

Coles (1956)

$$f_2 = A\cos^2\left(\frac{\pi x_2}{2\delta}\right) - \frac{1}{\kappa}\ln\left(\frac{x_2}{\delta}\right) \qquad \frac{U_{e1}}{u_\tau} = \frac{1}{\kappa}\ln(\mathrm{Re}^+) + A + B$$

$A \simeq 2.5$ zero pressure gradient
$A < 2.5$ favorable gradient
$A > 2.5$ adverse gradient

Small exercise : key scales for the log-law of a boundary layer

1. Determine the general expression of the Kolmogorov length scale l_η by considering the dissipation ϵ and the Reynolds number for viscous scales.
2. Show that in the logarithmic region of the mean velocity profile of a turbulent boundary layer, the Kolmogorov scale is approximated by the expression
   $l_\eta^+ \simeq (\kappa x_2^+)1/4$
3. Recall also the expression of the mixing length l_m^+ and of the turbulent viscosity ν_t^+ ?

Dynamics of vorticity

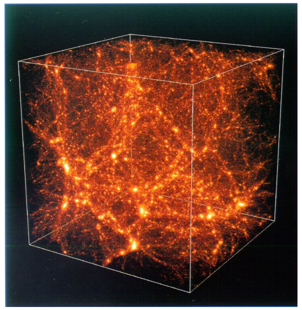

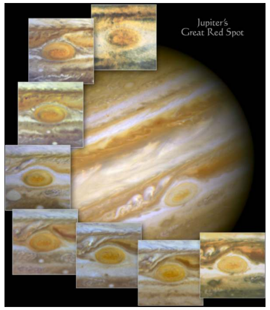

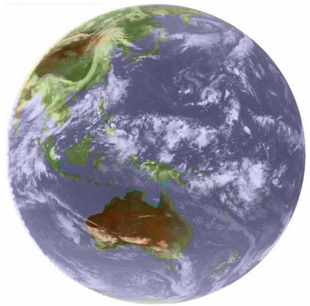

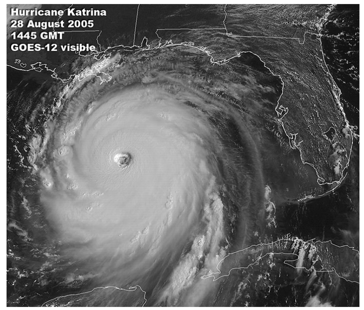

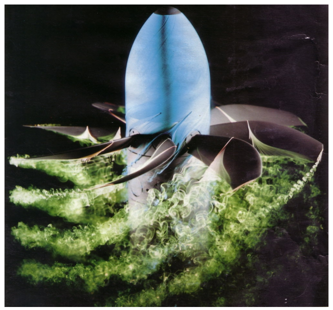

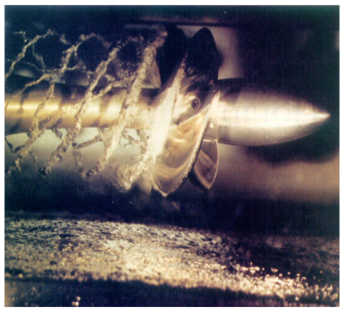

Vorticity vector ω

$$\boldsymbol{\omega} = \nabla \times \boldsymbol{u} \qquad \omega_i = \epsilon_{ijk} \frac{\partial u_k}{\partial x_j} \qquad \underbrace{\epsilon_{ijk} = \frac{1}{2}(i-j)(j-k)(k-i)}_{\text{permutation tensor}}$$

The vorticity is always assumed to be a concentrated (localized) quantity in space, vortex tube or sheet.

The Biot & Savart law allows to express the velocity field induced by a given vorticity distribution.

- For an incompressible velocity field, $\nabla \cdot \boldsymbol{u} = 0$. A vector potential defined by $\boldsymbol{u} = \nabla \times \boldsymbol{A}$ can thus be introduced, associated with the condition $\nabla \cdot \boldsymbol{A} = 0$ (uniqueness)

- This vector potential $\boldsymbol{A}$ satisfies a Poisson equation whose source term is the vorticity vector,

$$\boldsymbol{\omega} = \nabla \times \boldsymbol{u} = \nabla \times (\nabla \times \boldsymbol{A}) = \nabla (\nabla \cdot \boldsymbol{A}) - \nabla^2 \boldsymbol{A} = -\nabla^2 \boldsymbol{A}$$

Biot & Savart's law (1820)

From the knowledge of the free-space Green's function, the integral solution is given by

$$\boldsymbol{A}(\boldsymbol{x}) = \frac{1}{4\pi}\int_{\mathcal{V}} \frac{\boldsymbol{\omega}(\boldsymbol{y})}{|\boldsymbol{x}-\boldsymbol{y}|}\, d\boldsymbol{y}$$

The velocity field is then obtained by taking the curl of $\boldsymbol{A}$

$$\boldsymbol{u}(\boldsymbol{x}) = \nabla_x \times \boldsymbol{A} = \frac{1}{4\pi}\nabla_x \times \int_{\mathcal{V}} \frac{\boldsymbol{\omega}(\boldsymbol{y})}{|\boldsymbol{x}-\boldsymbol{y}|}\, d\boldsymbol{y} = \frac{1}{4\pi}\int_{\mathcal{V}} \frac{\boldsymbol{\omega}(\boldsymbol{y})\times(\boldsymbol{x}-\boldsymbol{y})}{|\boldsymbol{x}-\boldsymbol{y}|^3}\, d\boldsymbol{y}$$

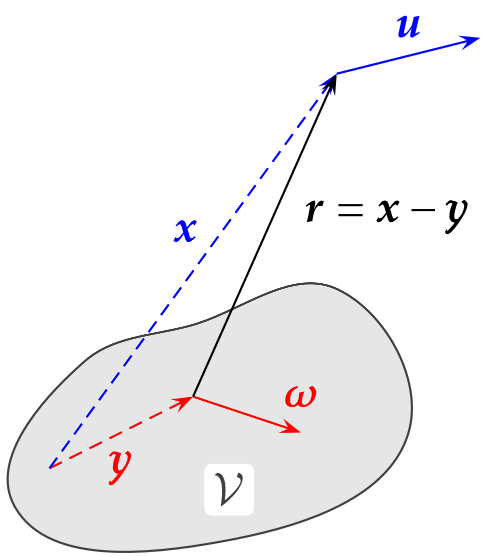

$$\boxed{\boldsymbol{u}(\boldsymbol{x}) = \frac{1}{4\pi}\int_{\mathcal{V}} \frac{\boldsymbol{\omega}(\boldsymbol{y})\times\boldsymbol{r}}{r^3}\, d\boldsymbol{y}}$$

► Nonlocal relationship between the vorticity field $\boldsymbol{\omega}$ and the velocity field $\boldsymbol{u}$

Example of the Rankine vortex (1858)

Rankine (1820-1872)

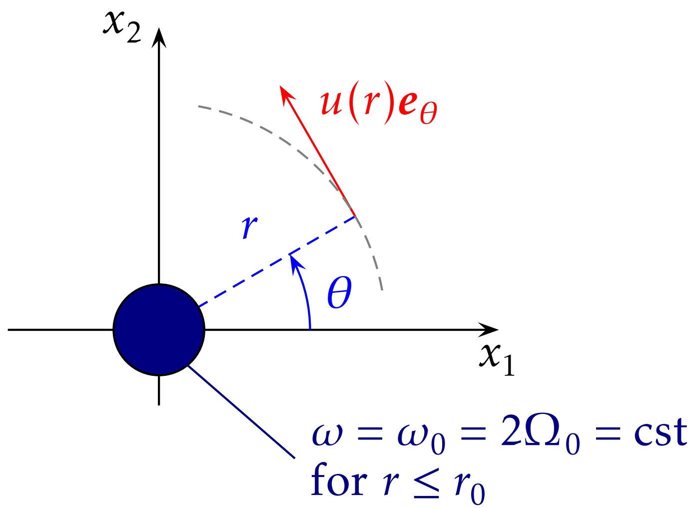

$$\begin{cases} u(r) = v_0 \dfrac{r}{r_0} = \Omega_0 r & r \leq r_0 \\ u(r) = v_0 \dfrac{r_0}{r} = \Omega_0 r_0 \dfrac{r_0}{r} & r > r_0 \end{cases}$$

$(v_0 = \Omega_0 r_0 = \omega_0 r_0/2)$

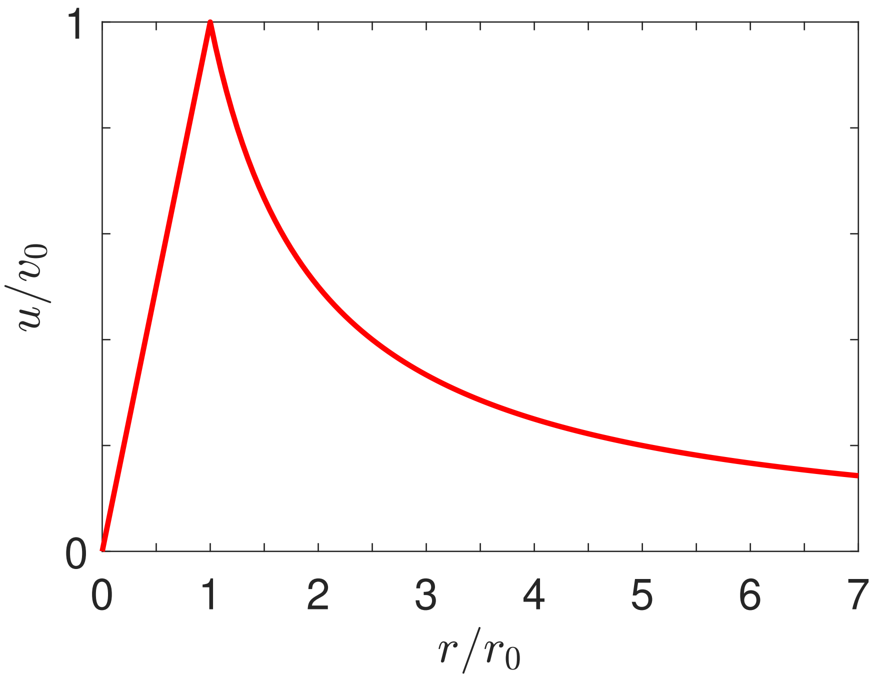

Solid body motion inside the vortex itself, *i.e.* for $r \leq r_0$ in the vortical region

Irrotational flow outside, for $r > r_0$: the localized circular patch of vorticity produces a velocity field away from the vortical region

Vorticity distribution in a turbulence box

in a slab of $1024^2 \times 128$

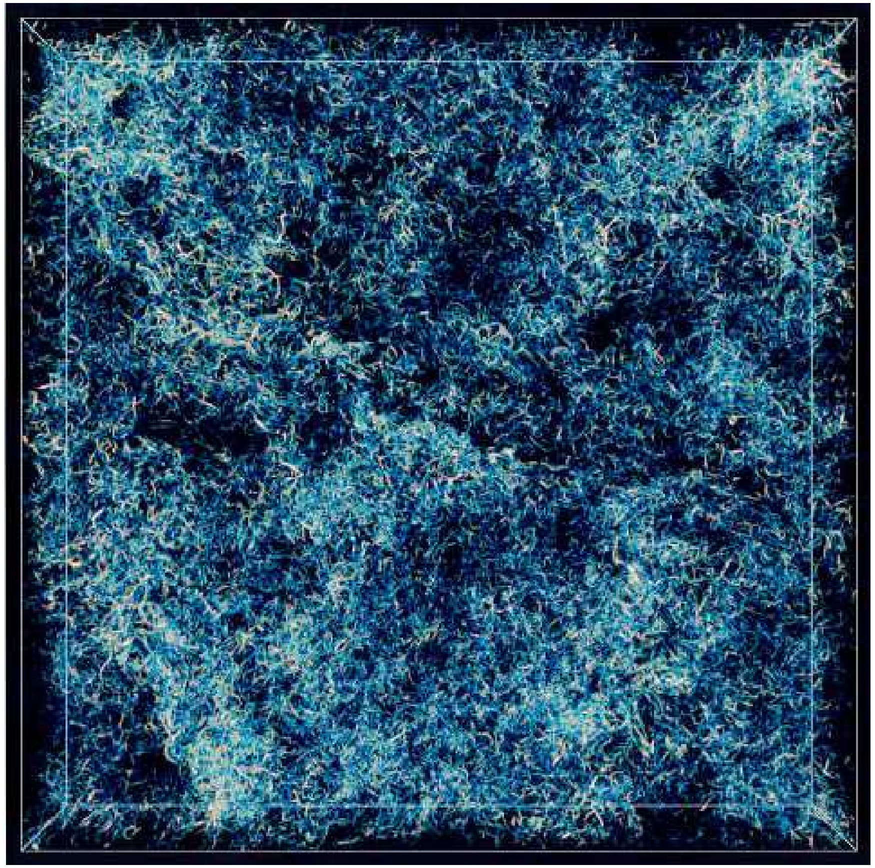

in the inertial range

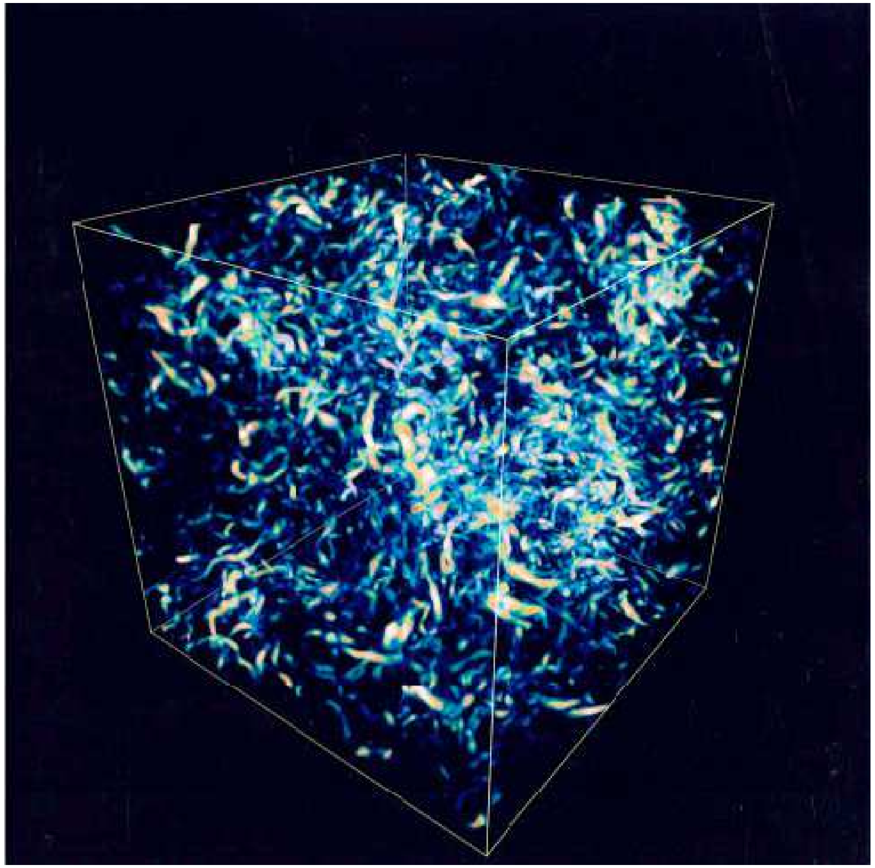

Porter, Woodward & Pouquet, *Phys. Fluids*, 1998

Kelvin's circulation theorem (1869)

For an inviscid flow submitted to conservative body forces, the circulation around a material closed curve $\mathcal{C}$ is governed by

$$\frac{D\Gamma_{\mathcal{C}}}{Dt} = \frac{D}{Dt}\oint \boldsymbol{U}\cdot d\boldsymbol{l} = \int_{\mathcal{S}} \frac{1}{\rho^2}\nabla\rho\times\nabla p\cdot\boldsymbol{n}\, d\mathcal{S} = 0 \qquad \text{for barotropic flows, } \rho = \rho(p)$$

Note that constant density, isothermal, and isentropic flows are barotropic. As a result, the material circulation $\Gamma_{\mathcal{C}}$ is preserved,

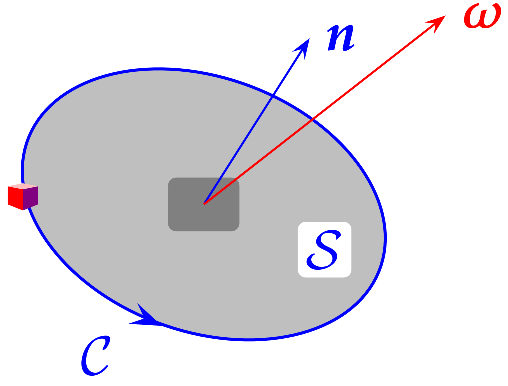

$$\frac{D\Gamma_{\mathcal{C}}}{Dt} = 0$$

$$\Gamma_c = \oint_{\mathcal{C}} \boldsymbol{U}\cdot d\boldsymbol{l} = \int_{\mathcal{S}} \boldsymbol{\omega}\cdot\boldsymbol{n}\, d\mathcal{S} = \text{cst}$$

Introduction to vortex stretching

A consequence of Kelvin's circulation theorem

$$\frac{d\Gamma}{dt} = \frac{d}{dt}\left[\oint_{\mathcal{C}} \boldsymbol{u}\cdot d\boldsymbol{l}\right] = \frac{d}{dt}\int_{\mathcal{S}} (\nabla\times\boldsymbol{u})\cdot\boldsymbol{n}\, d\mathcal{S} = \frac{d}{dt}\int_{\mathcal{S}} \boldsymbol{\omega}\cdot\boldsymbol{n}\, d\mathcal{S} = 0$$

is that the vorticity flux crossing the material surface $\mathcal{S}$ is also an invariant.

Consider an elementary homogeneous vortex tube of length L, radius R and vorticity ω,

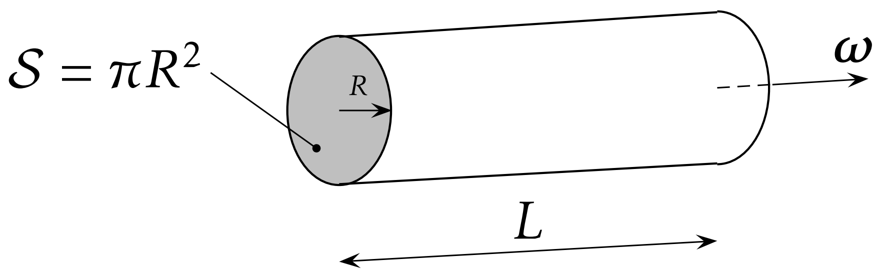

$$\Gamma = \oint_{\mathcal{C}} \boldsymbol{u}\cdot d\boldsymbol{l} = \int_{\mathcal{S}} \boldsymbol{\omega}\cdot d\boldsymbol{x} = \pi R^2 \omega$$

Introduction to vortex strechting (cont.)

For this elementary vortex,

- conservation of circulation Γ, $R^2\omega = \text{cst}$
- conservation of mass, $\rho\pi R^2 L \sim R^2 L = \text{cst}$

and an estimate of the kinetic energy $\mathcal{E}_c$ is given by

$$\mathcal{E}_c = \rho\pi R^2 L \frac{R^2\omega^2}{2} \sim \underbrace{R^2 L\, R^2\omega}_{\text{cst}}\ \omega \quad \Longrightarrow \quad \mathcal{E}_c \sim \omega \sim \frac{1}{R^2} \sim L$$

The kinetic energy is directly proportional to the vortex length. The increase in kinetic energy for the vortex - and consequently for the turbulent velocity field, is associated with vortex stretching. It's an important basic mechanism to interprete the behaviour of turbulent flow.

In other words, during the stretching process in one direction, the kinetic energy in the perpendicular plane increases whereas the length scales decrease.

Introduction to vortex strechting (cont.)

Principal axes of the deformation tensor for shear flow
$\bar{U}_1 = S x_2$ et $\bar{U}_2 = \bar{U}_3 = 0$

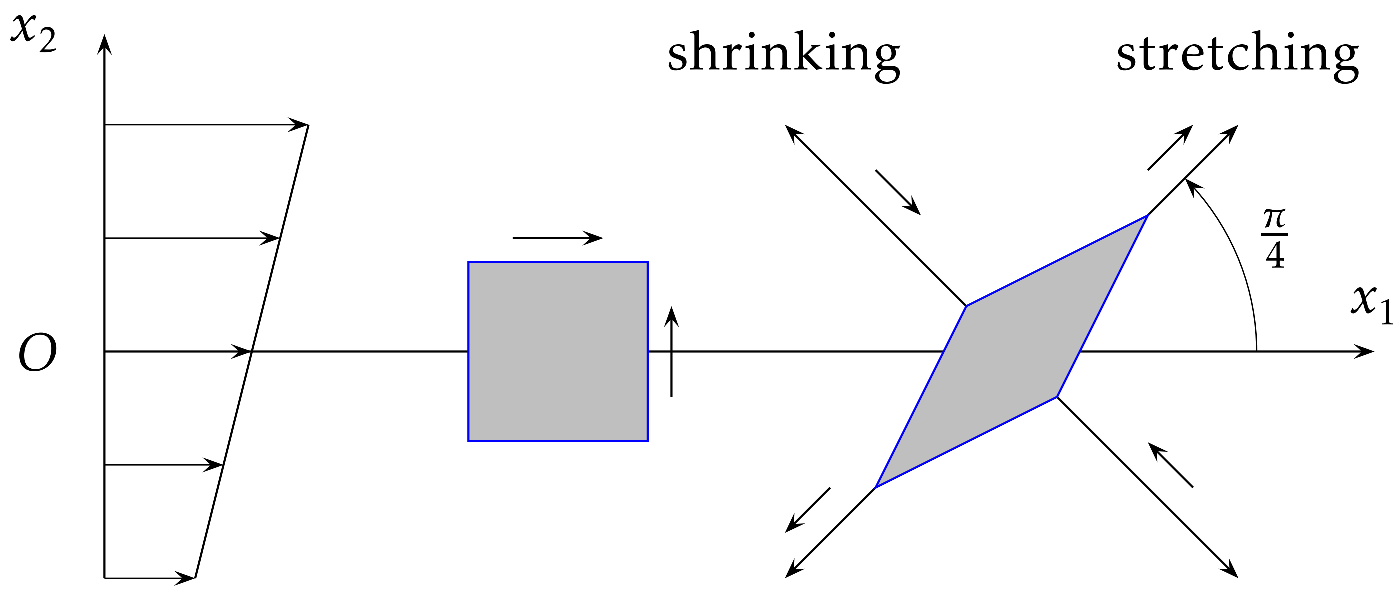

$$\bar{S}_{ij} = \frac{1}{2}\left(\frac{\partial \bar{U}_i}{\partial x_j} + \frac{\partial \bar{U}_j}{\partial x_i}\right) = \frac{\overline{S}}{2}\begin{pmatrix} 0 & 1 \\ 1 & 0 \end{pmatrix} \qquad \bar{S}^d_{ij} = \frac{\overline{S}}{2}\begin{pmatrix} 1 & 0 \\ 0 & -1 \end{pmatrix}$$

Helmholtz's equation

The Helmholtz equation is the transport equation for the vorticity vector, obtained by taking the curl of the Navier-Stokes equation

$$\nabla\times\left\{\frac{\partial \boldsymbol{u}}{\partial t}+\boldsymbol{u}\cdot\nabla\boldsymbol{u}=-\frac{1}{\rho}\nabla p+\nu\nabla^2\boldsymbol{u}\right\}$$

Using the following vectorial identities

$$\nabla\times(\boldsymbol{u}\cdot\nabla\boldsymbol{u})=\nabla\times\left[\nabla\left(\frac{\boldsymbol{u}^2}{2}\right)+\boldsymbol{\omega}\times\boldsymbol{u}\right]=\nabla\times(\boldsymbol{\omega}\times\boldsymbol{u})$$

and moreover $\nabla\times(\boldsymbol{\omega}\times\boldsymbol{u})=\boldsymbol{u}\cdot\nabla\boldsymbol{\omega}-\boldsymbol{u}\nabla\cdot\omega-\boldsymbol{\omega}\cdot\nabla\boldsymbol{u}+\boldsymbol{\omega}\nabla\cdot u$
since $\nabla\cdot\boldsymbol{\omega}\equiv 0$ (solenoidal vorticity field) and $\nabla\cdot\boldsymbol{u}=0$ (incompressible flow)

$$\frac{\partial\omega}{\partial t}+\boldsymbol{u}\cdot\nabla\omega=\omega\cdot\nabla\boldsymbol{u}-\nabla\times\left(\frac{1}{\rho}\nabla p\right)+\nu\nabla^2\omega$$

Helmholtz's equation (cont.)

Assuming a barotropic flow, that is a flow whose pressure is a function of density only $p = p(\rho)$, one has for the pressure term

$$\nabla \times \left(\frac{1}{\rho}\nabla p\right) = \nabla\left(\frac{1}{\rho}\right) \times \nabla p + \frac{1}{\rho}\nabla \times (\nabla p) = -\frac{1}{\rho^2}\nabla\rho \times \nabla p = 0$$

The transport equation for vorticity reads

$$\frac{\partial \boldsymbol{\omega}}{\partial t} + \boldsymbol{u} \cdot \nabla\boldsymbol{\omega} = \boldsymbol{\omega} \cdot \nabla\boldsymbol{u} + \nu\nabla^2\boldsymbol{\omega}$$

$$\left\{\begin{array}{c}\text{convection}\\ \text{of } \boldsymbol{\omega}\end{array}\right\} = \left\{\begin{array}{c}\text{3-D effect}\\ \text{(source term)}\end{array}\right\} + \left\{\begin{array}{c}\text{viscous}\\ \text{diffusion}\end{array}\right\}$$

Hermann von Helmholtz
(1821 - 1894)

The evolution of vorticity is directly linked to the term associated with 3-D effect : this term is zero for a two-dimensional flow, $\boldsymbol{\omega} \cdot \nabla\boldsymbol{u} \equiv 0$

► 2-D flow represents a specific/particular configuration ...

Interpretation of Helmholtz's equation

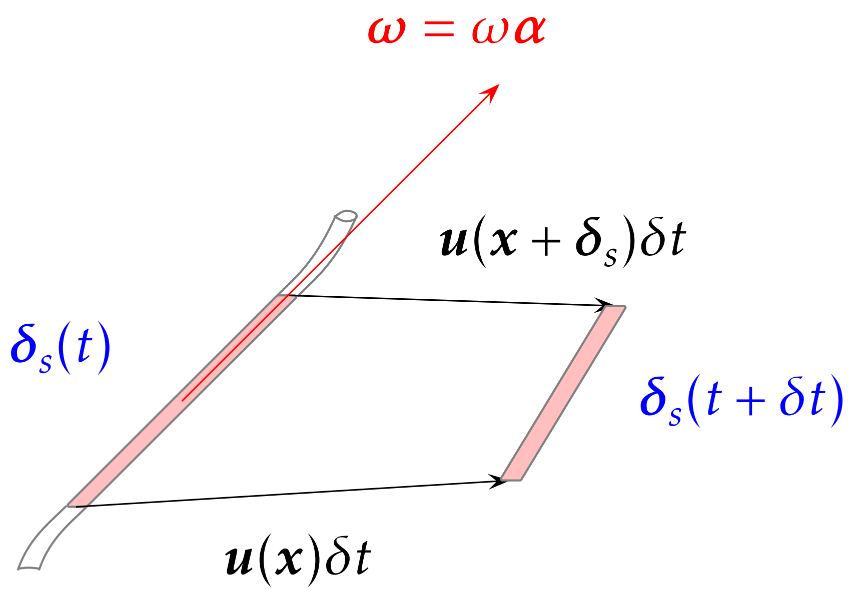

Deformation of an elementary tube (filament) of vorticity

$$\frac{\boldsymbol{\delta}_s(t+dt)-\boldsymbol{\delta}_s(t)}{\delta t} = \boldsymbol{u}(\boldsymbol{x}+\boldsymbol{\delta}_s) - \boldsymbol{u}(\boldsymbol{x})$$

$$\frac{d\boldsymbol{\delta}_s(t)}{dt} = \boldsymbol{\delta}_s \cdot \nabla \boldsymbol{u}$$

Length of the elementary tube

$\tilde{\delta}_s = \|\boldsymbol{\delta}_s\| = \boldsymbol{\delta}_s \cdot \boldsymbol{\alpha} \qquad \boldsymbol{\alpha}^2 = 1$

$$\frac{D\tilde{\delta}_s}{Dt} = \boldsymbol{\alpha} \cdot \left(\boldsymbol{\delta}_s \cdot \nabla \boldsymbol{u}\right)$$

$$= \frac{\omega_i}{\omega}\left(\tilde{\delta}_s \frac{\omega_j}{\omega} \frac{\partial u_i}{\partial x_j}\right)$$

$$= \frac{\omega_i \omega_j}{\omega^2} \frac{\partial u_i}{\partial x_j} \tilde{\delta}_s$$

Interpretation of Helmholtz's equation (cont.)

Furthermore, by neglecting the viscous term in Helmholtz's 'equation and taking the scalar product with $\boldsymbol{\omega}$, we obtain

$$\boldsymbol{\omega}\cdot\frac{D\boldsymbol{\omega}}{Dt} = \boldsymbol{\omega}\cdot(\boldsymbol{\omega}\cdot\nabla\boldsymbol{u}) \quad \text{that is} \quad \frac{D}{Dt}\left(\frac{\omega^2}{2}\right) = \omega_i\omega_j\frac{\partial u_i}{\partial x_j}$$

By identification with the previous equation, it can be deduced that

$$\frac{1}{\omega^2}\frac{D}{Dt}\left(\frac{\omega^2}{2}\right) = \frac{1}{\tilde{\delta}_s}\frac{D\tilde{\delta}_s}{Dt} \quad \text{and by integration,} \quad \frac{\omega}{\tilde{\delta}_s} = \text{cst}$$

The length of an elementary tube vortex is thus proportional to vorticity ω. We find the conclusion already obtained with the dimensional analysis, to highlight vortex stretching mechanism and the increase in turbulent fluctuations. In addition, the term associated with the lengthening of vortex tubes corresponds to the term of 3-D effect in the transport equation of vorticity.

Interpretation of Helmholtz's equation (cont.)

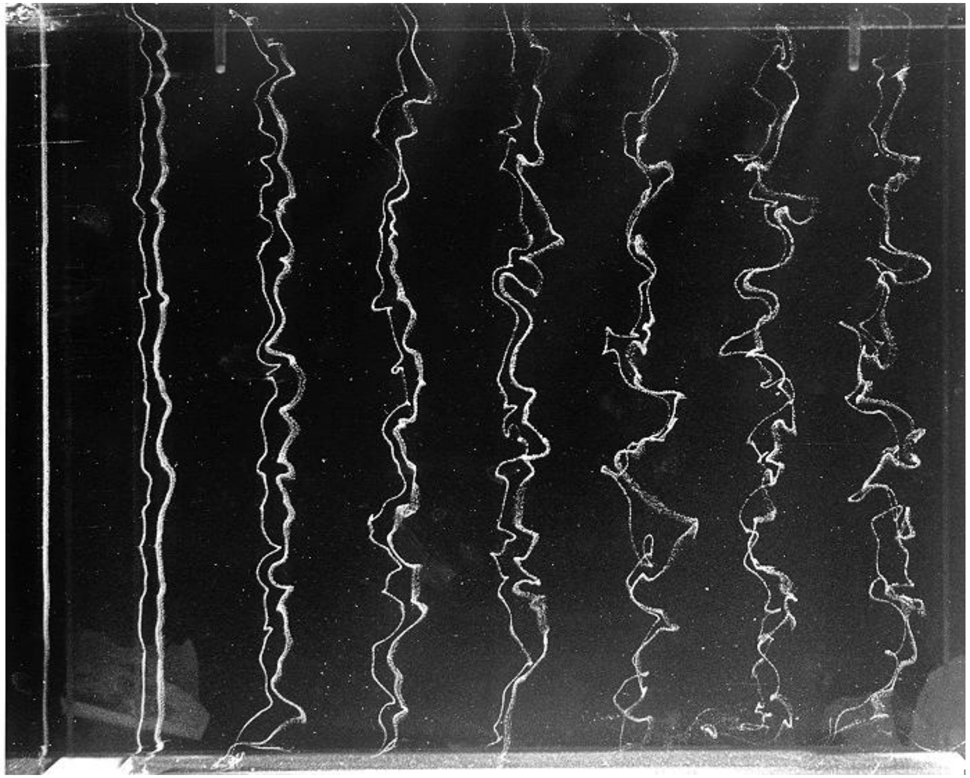

Growth of material lines in isotropic turbulence $Re_D = 1360$ (based on the grid rod diameter)

Corrsin & Karweit, 1969, *J. Fluid Mech.*, **39**(1)

The increase in vortex intensity, and thus in turbulent fluctuations, is accompanied by stretching of vorticity filaments, and by the increase of distance between fluid particles : the origin of sensitivity to initial conditions ...

- **An illustration of the lengthening of vortex filament**
  (from Tennekes & Lumley, 1972, chap. 8)

  Mean flow for which gradients are aligned with the frame axes

$$\frac{\partial \bar{U}_i}{\partial x_j} = \begin{pmatrix} \overline{S} & 0 \\ 0 & -\overline{S} \end{pmatrix}$$

$$\bar{U}_1 = \overline{S} x_1 \qquad \bar{U}_2 = -\overline{S} x_2 \qquad \bar{\Omega}_i \equiv 0$$

pure strain flow

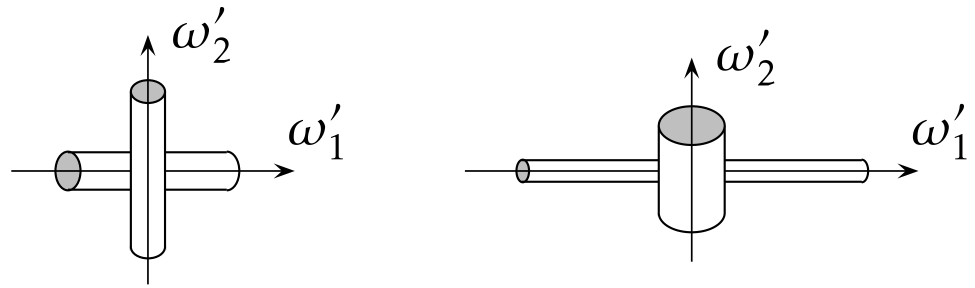

Helmholtz's Eq. linearized around this mean flow (inviscid flow to simplify algebra, not an issue because the viscous terms are linear)

$$\frac{\partial \boldsymbol{\omega}'}{\partial t} + \bar{\boldsymbol{U}} \cdot \nabla \boldsymbol{\omega}' = \boldsymbol{\omega}' \cdot \nabla \bar{\boldsymbol{U}}$$

$$\frac{\bar{D}\omega_1'}{\bar{D}t} = +\overline{S}\omega_1' \qquad \frac{\bar{D}\omega_2'}{\bar{D}t} = -\overline{S}\omega_2' \qquad \frac{\bar{D}}{\bar{D}t} \equiv \frac{\partial}{\partial t} + \bar{U}_j \frac{\partial}{\partial x_j}$$

An illustration of the lengthening of vortex filament (cont.)

By integration along the mean flow, or with the following formal change of variables $\xi_1 = x_1 e^{-\overline{S}t}$, $\xi_2 = x_2 e^{\overline{S}t}$ and $\tau = t$, one gets

$$\omega_1' = \omega_0 e^{\overline{S}t} \qquad \omega_2' = \omega_0 e^{-\overline{S}t}$$

The vorticity component ω_1' is thus stretched faster than the component ω_2' through a nonlinear processus, and finally vorticity fluctuations increase as

$$\omega_1'^2 + \omega_2'^2 = 2\omega_0^2 \cosh(2\overline{S}t)$$

- **Bradshaw's tree diagram (1971) illustrating of the concept of energy cascade** originally introduced by Richardson (1926)

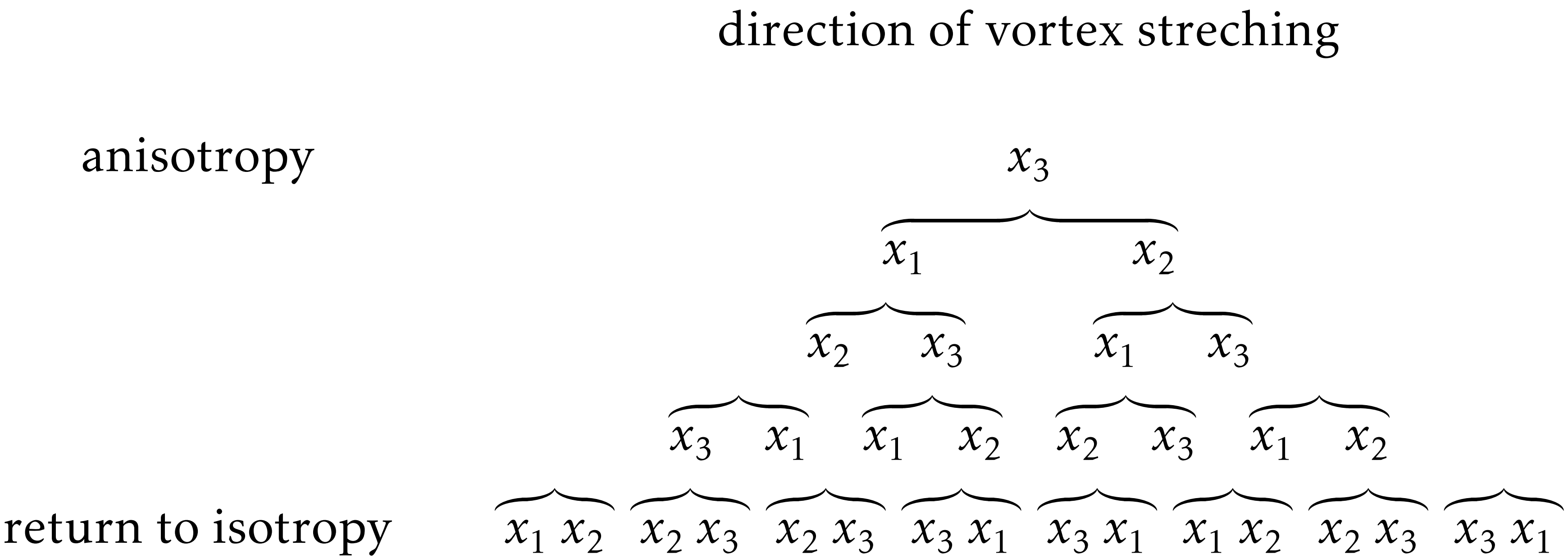

- **Plane mixing layer – an example of inverse energy cascade**
  Identification of vortex pairing

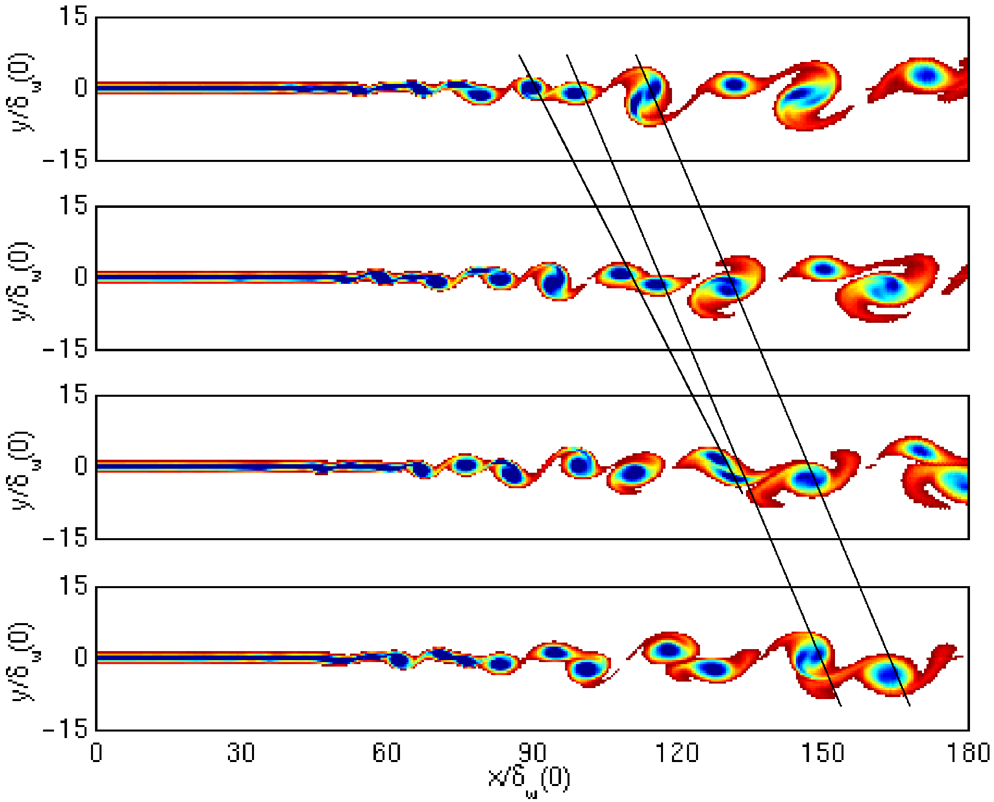

Simulation of a plane mixing layer ($M_1 = 0.12$, $M_2 = 0.48$, $\mathrm{Re}_{\delta_\omega} = 1.28 \times 10^4$), snaphots of the vorticity field at 4 consecutive times separated by $17\delta_\omega/U_c$, where U_c is the convection velocity. (Bogey, Bailly & Juvé, *AIAA Journal*, 2000)

- **Plane mixing layer forced at f_0**
  (f_0 fundamental frequency corresponding to most amplified perturbations)

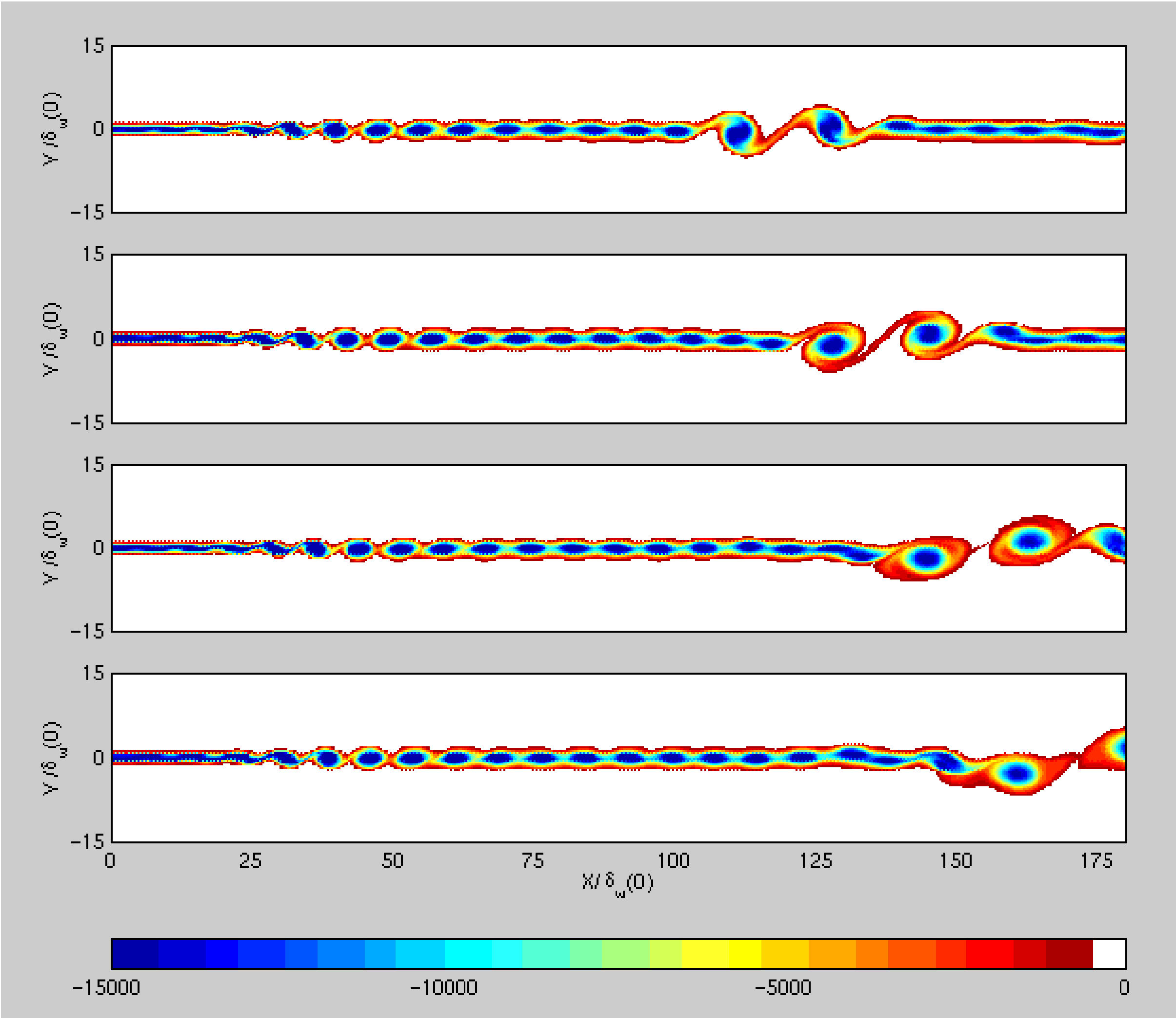

- **Plane mixing layer forced at f_1**
  ($f_1 = f_0/2$, first subharmonic frequency)

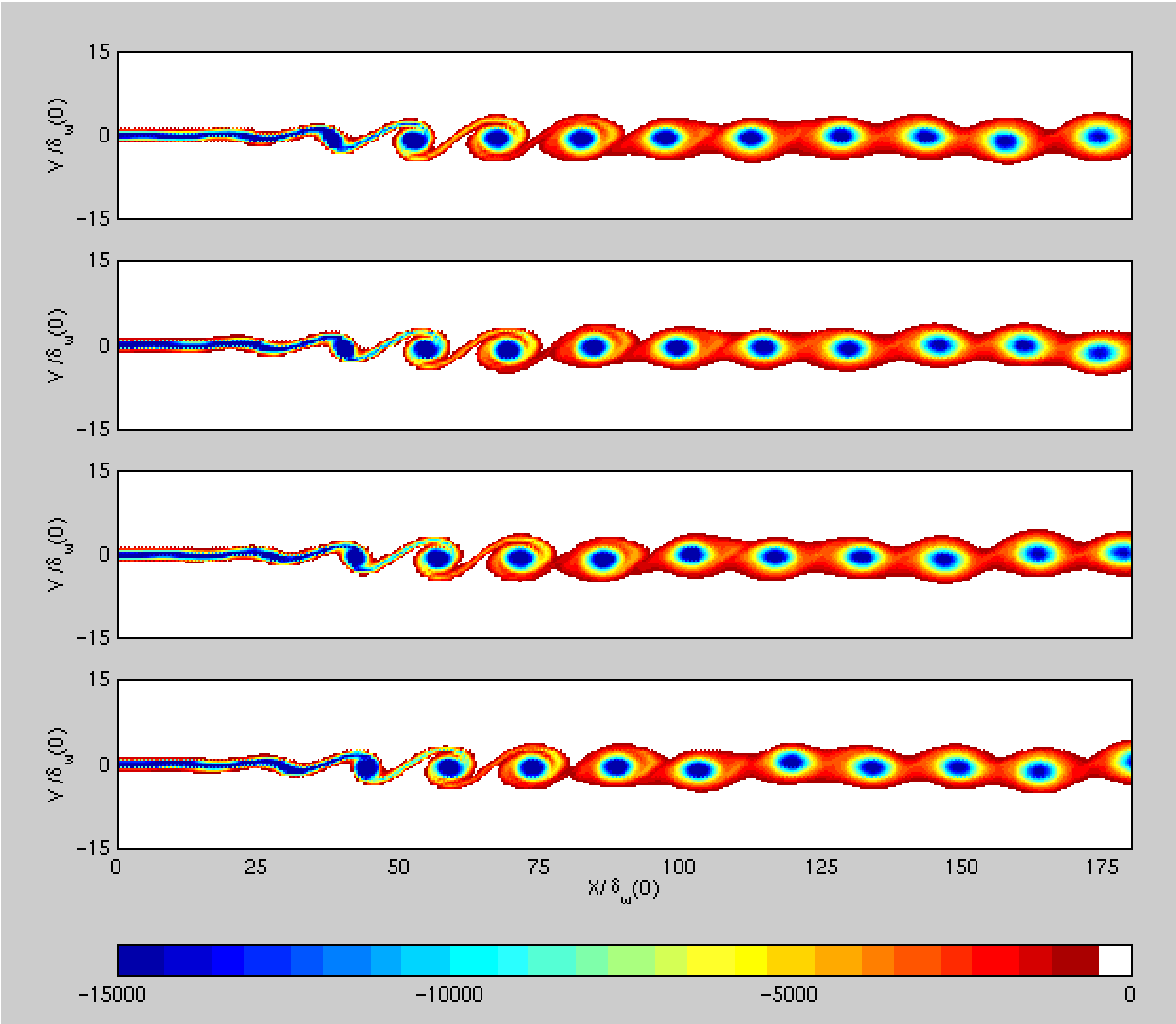

- **Plane mixing layer forced at f_0 and f_1**
  Vortex pairings occurred at fixed streamwise locations

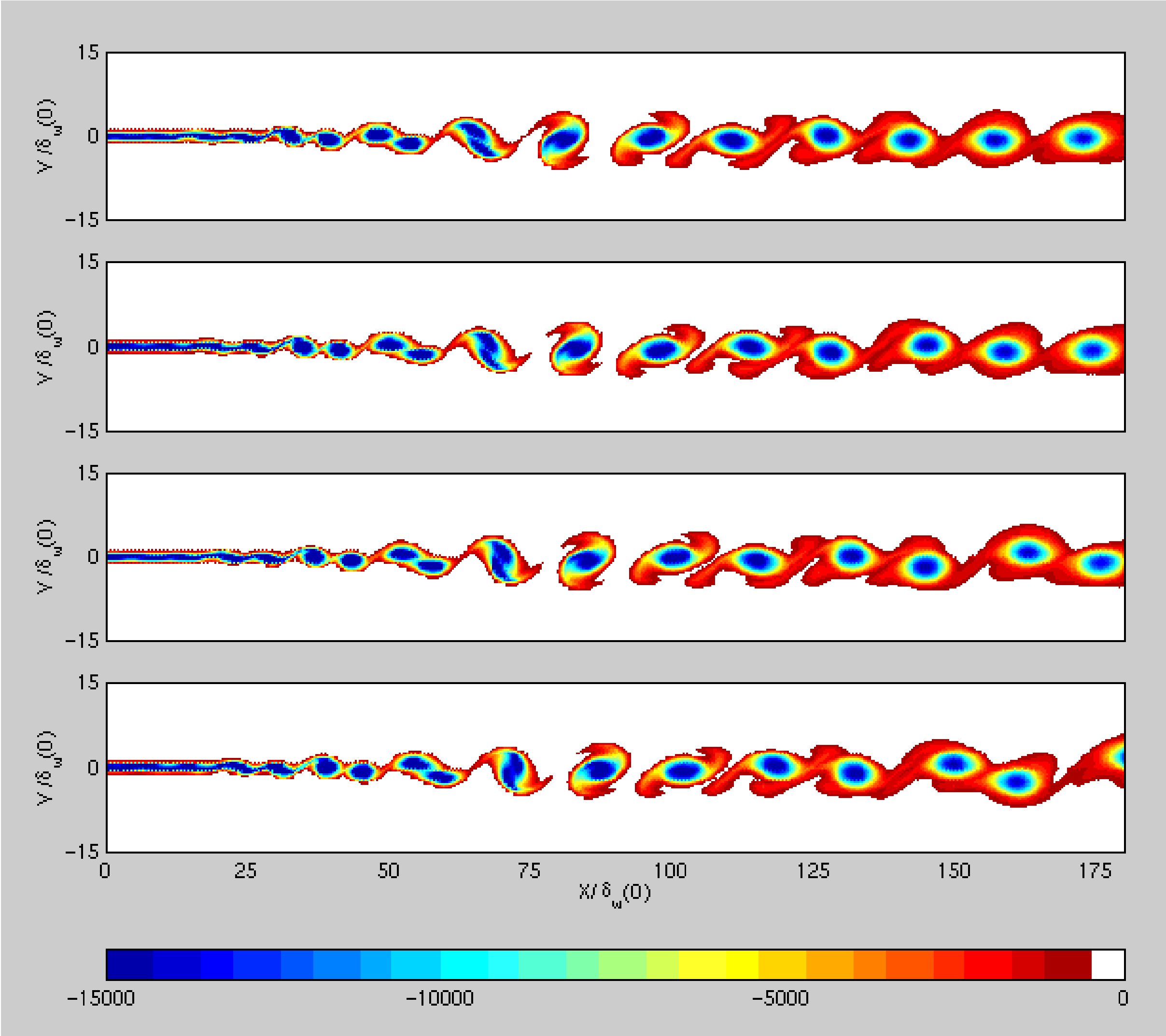

Vortex pairing in a plane mixing layer

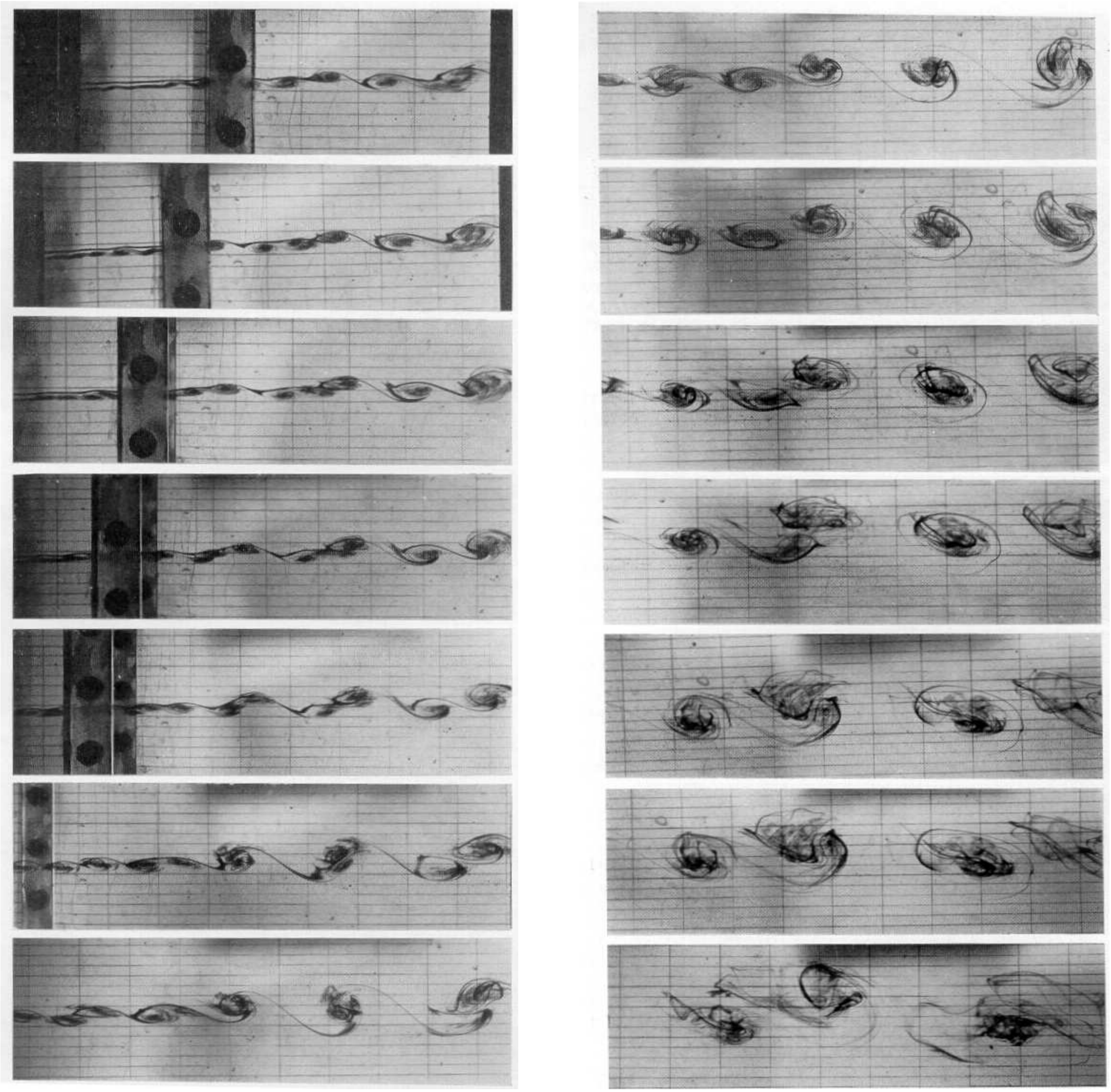

Winant & Browand

J. Fluid Mech. (1974)

- **2-D simulations must be proscribed : no energy cascade**

Flow separation behind a rounded leading edge (3-D versus 2-D !)

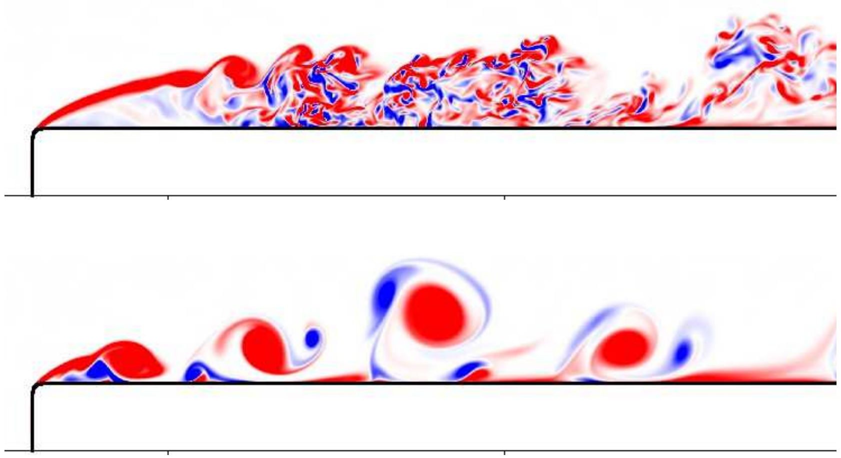

Spanwise vorticity ω_z, from red to blue with $\omega_z = \pm 5U_\infty/H$, DNS with inflow perturbations $u'_{\text{inflow}} = 0.1\% U_\infty$ ($\eta = 0.125$)

Courtesy of Lamballais, Sylvestrini & Laizet
Int. Journal Heat Fluid Flow, **31**, 2010

2-D free jet, vorticity field

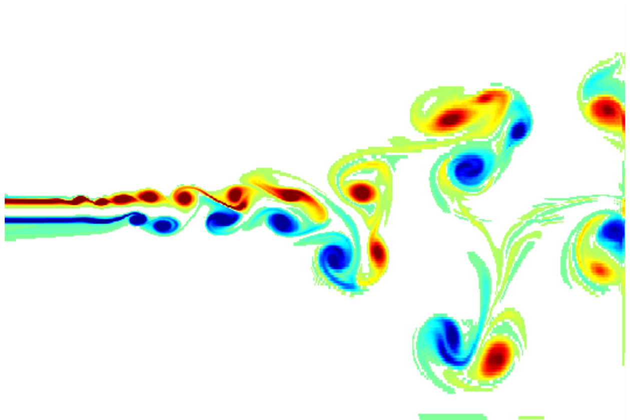

Bogey (Ph.D. EC-Lyon, 1999)

- **Transport equation for the mean vorticity** $\omega_i = \bar{\Omega}_i + \omega'_i$

$$\frac{\partial \bar{\Omega}_i}{\partial t} + \bar{U}_j \frac{\partial \bar{\Omega}_i}{\partial x_j} = \bar{\Omega}_j \frac{\partial \bar{U}_i}{\partial x_j} + \underbrace{\frac{\partial}{\partial x_j}\left(\overline{\omega'_j u'_i} - \overline{\omega'_i u'_j}\right)}_{(a)} + \underbrace{\nu \frac{\partial^2 \bar{\Omega}_i}{\partial x_j \partial x_j}}_{(b)}$$

(a) $\sim$ correlation term involving turbulence fluctuations only, must be closed to solve this equation

(b) $\sim$ viscous diffusion

In practice, this equation is rarely (if ever !) solved to obtain the mean flow field : turbulence models are based on the resolution of the mean velocity field (RANS Eqs.). This equation is theoretically used to study enstrophy.

Enstrophy

Similar to the kinetic energy for velocity, that is

$$\frac{\overline{\omega_i'\omega_i'}}{2} \equiv \frac{\overline{\omega_1'^2} + \overline{\omega_2'^2} + \overline{\omega_3'^2}}{2}$$

To quickly derive its transport equation, we assume that there is no mean flow, that is $\bar{U}_i \equiv 0$ et $\bar{\Omega}_i \equiv 0$

$$\frac{\partial}{\partial t}\left(\frac{\overline{\omega_i'\omega_i'}}{2}\right) + \frac{\partial}{\partial x_j}\left(\overline{u_j'\frac{\omega_i'\omega_i'}{2}}\right) = \overline{\omega_i'\omega_j'\frac{\partial u_i'}{\partial x_j}} - \nu\overline{\frac{\partial \omega_i'}{\partial x_j}\frac{\partial \omega_i'}{\partial x_j}} + \nu\frac{\partial^2}{\partial x_j^2}\left(\frac{\overline{\omega_i'\omega_i'}}{2}\right)$$

As usual, this Eq. can be greatly simplified for homogeneous turbulence, in order to isolate basic physical mechanisms

$$\frac{\partial}{\partial t}\left(\frac{\overline{\omega_i'\omega_i'}}{2}\right) = \underbrace{\overline{\omega_i'\omega_j'\frac{\partial u_i'}{\partial x_j}}}_{(a)} - \underbrace{\nu\overline{\frac{\partial \omega_i'}{\partial x_j}\frac{\partial \omega_i'}{\partial x_j}}}_{(b)} \tag{3}$$

Enstrophy (cont.)

The term (a) is linked to the stretching of vortices, and the term (b) to viscous dissipation.

Historically, the term (a) was assumed to be zero by von Kármán (1937), but Taylor (1938) demonstrated later that this term is not zero and furthermore, must be positive. It expresses that two fluid particles initially close one from the other will be later separated by turbulence in average.

Singular behaviour of two-dimensional turbulent flow again,
enstrophy can only decrease

$$\frac{\partial}{\partial t}\left(\frac{\overline{\omega_i'\omega_i'}}{2}\right) = -\nu \overline{\frac{\partial \omega_i'}{\partial x_j}\frac{\partial \omega_i'}{\partial x_j}}$$

Enstrophy (cont.)

In order to solve Eq. (3), the nonlinear term can be modeled with an acceptable dimensional expression. For instance,

$$\overline{\omega_i'\omega_j'\frac{\partial u_i'}{\partial x_j}} \simeq A(\overline{\omega^2})^{3/2} \qquad A = \text{cst} \qquad \omega^2 \equiv \omega_i'\omega_i'$$

Neglecting viscous effects to simplify calculations, the integration leads to the following time evolution.

$$\frac{\overline{\omega^2}}{\omega_0^2} = \frac{1}{\left[1 - A\sqrt{\omega_0^2}\,(t_0 - t)\right]^2}$$

A singularity is thus obtained for a finite time ... refer to Leray (1934), Moffatt (2000) : artefact induced by the model itself and the incompressibility condition. Not so easy to derive an acceptable model for physics !

- **Helicity**
  Quantity widely studied by Moffatt (1969)

$$\mathcal{H} \equiv \int_V \boldsymbol{u} \cdot \boldsymbol{\omega} \, d\boldsymbol{x}$$

This quantity is an invariant of the flow motion, under the same assumptions introduced for Kelvin's circulation theorem.

For a two-dimensional flow, $\mathcal{H} = 0$.

Interpretation ?

Helicity (cont.)

Sketch of two linked vortex tubes T_1 and T_2

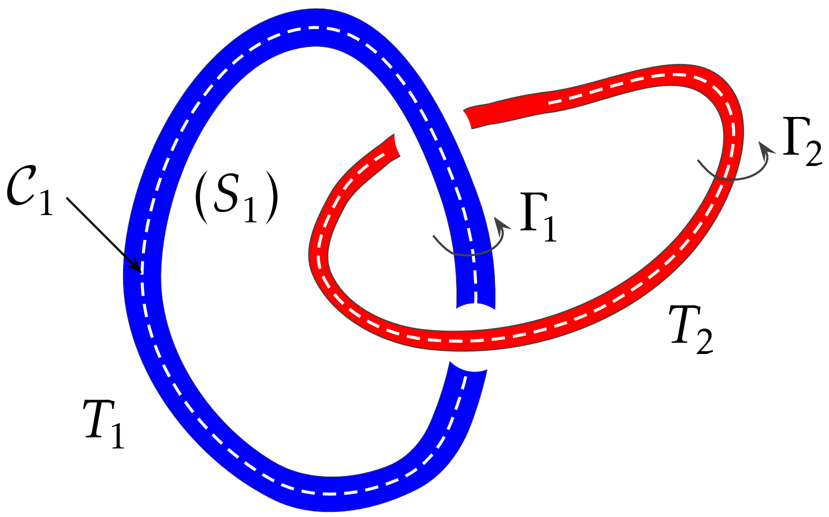

$$\mathcal{H} = \int_{\mathcal{V}} \boldsymbol{u}\cdot\boldsymbol{\omega}\, d\boldsymbol{x} = \int_{T_1} \boldsymbol{u}\cdot\boldsymbol{\omega}\, d\boldsymbol{x} + \int_{T_2} \boldsymbol{u}\cdot\boldsymbol{\omega}\, d\boldsymbol{x}$$

Consider the integral over the vortex T_1

$$\int_{T_1} \boldsymbol{u}\cdot\boldsymbol{\omega}\, d\boldsymbol{x} \simeq \Gamma_1 \oint_{\mathcal{C}_1} \boldsymbol{u}\cdot d\boldsymbol{l} = \Gamma_1 \int_{\mathcal{S}_1} (\nabla\times\boldsymbol{u})\cdot\boldsymbol{n}\, d\mathcal{S}$$

$$= \begin{cases} \Gamma_1\Gamma_2 & \text{if } \mathcal{C}_1 \text{ and } \mathcal{C}_2 \text{ are linked,} \\ 0 & \text{otherwise} \end{cases}$$

$\mathcal{H} = \pm 2n\Gamma_1\Gamma_2$ $\quad$ n linking number

Homogeneous and isotropic turbulence

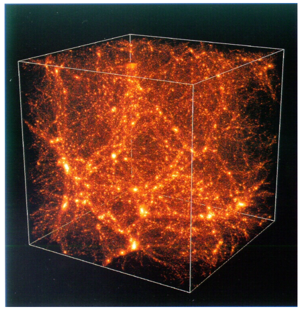
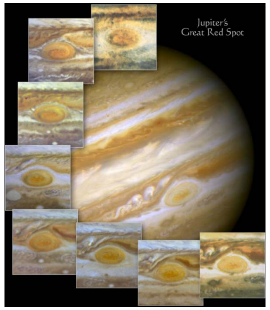

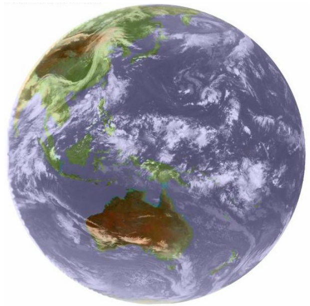

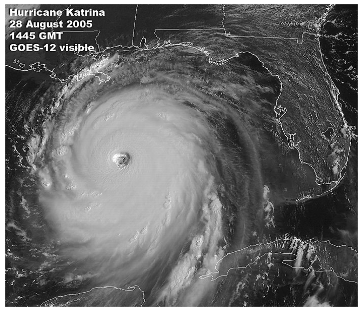

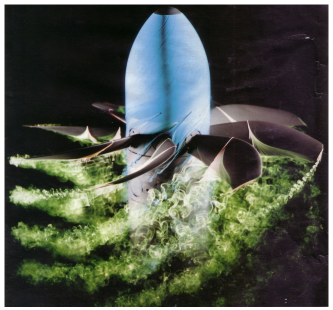
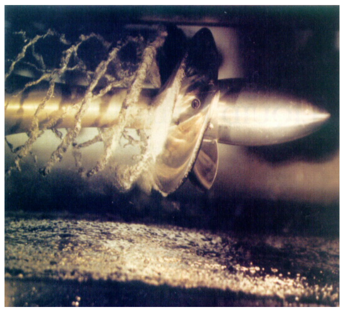


Homogeneous turbulence

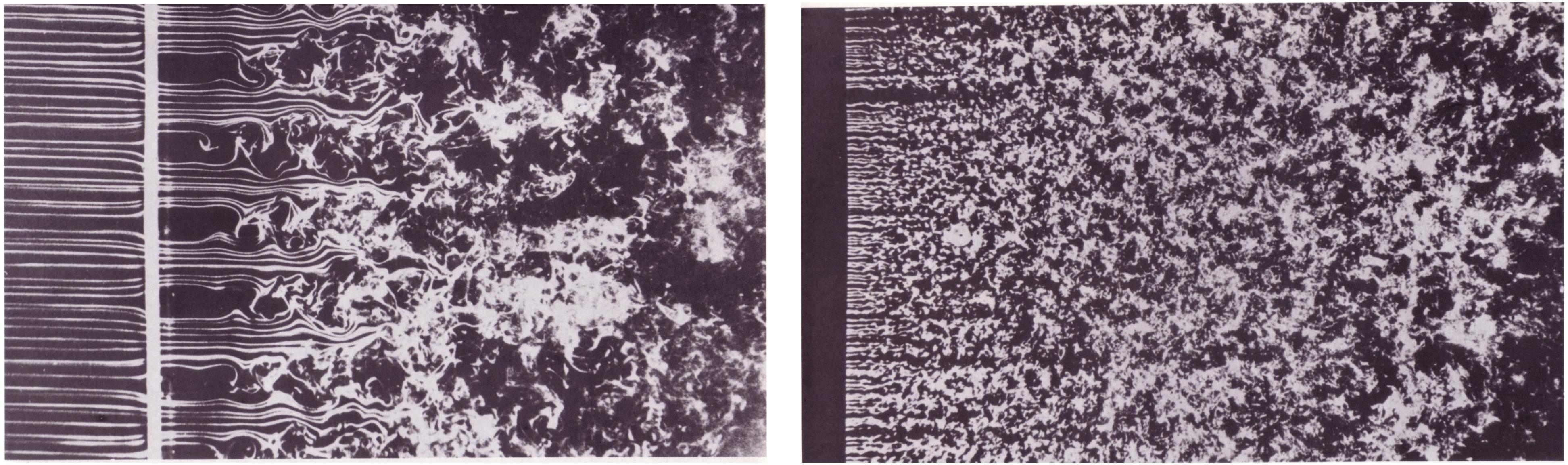

Generation of turbulence behind a grid, $\mathrm{Re}_M = 1500$ & $M = 2.54$ cm
Corke & Nagib, in *Van Dyke*, figs. 152 & 152 (1982)

Statistics are independants of space coordinates in homogeneous directions. In the present case, the turbulent flow is homogeneous in the x_2 and x_3 directions (transverse plane), *e.g.* the Reynolds tensor $-\overline{u_i' u_j'}$ is only a function of x_1 (and t).

The objective is to obtain simple configurations, without transport term

Homogeneous turbulence

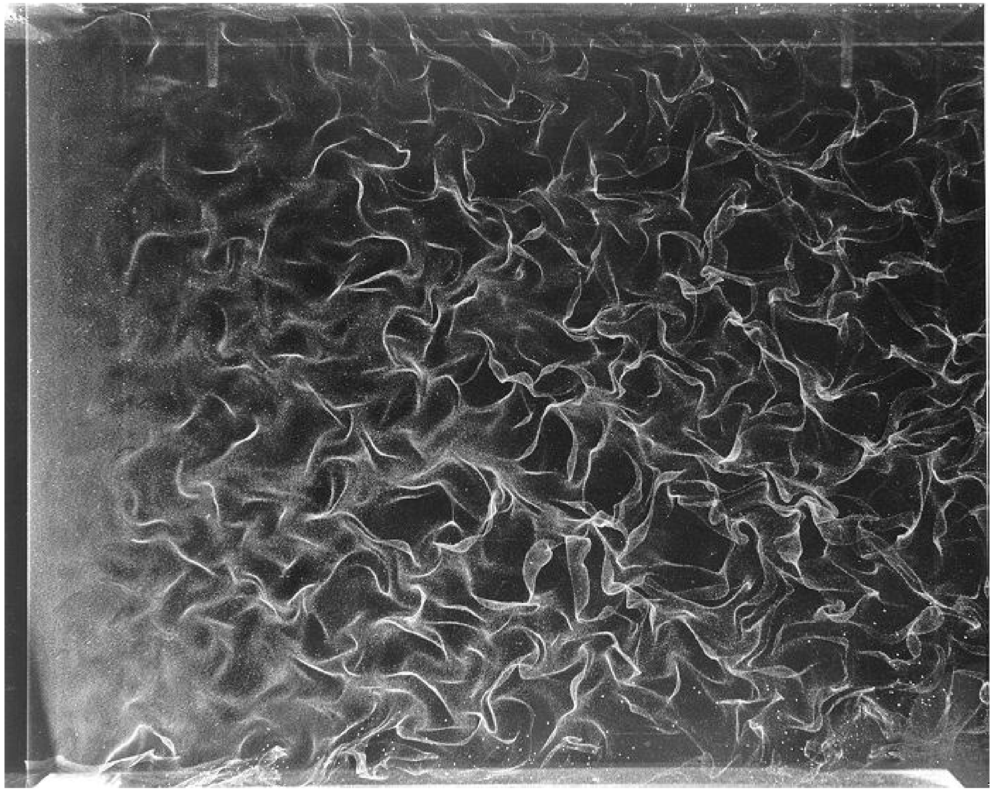

Wrinkling of a fluid surface in isotropic turbulence
Karweit in *Van Dyke*, fig. 155 (1982)

A platinum wire generates a continuous sheet of hydrogen bubbles, which is then deformed by the nearly isotropic turbulence behind the grid.

Velocity correlation tensor

Definition :

$$R_{ij}(\boldsymbol{x},\boldsymbol{r},t) \equiv \overline{u_i'(\boldsymbol{x},t)\, u_j'(\boldsymbol{x}+\boldsymbol{r},t)} = R_{ij}(\boldsymbol{r},t)$$

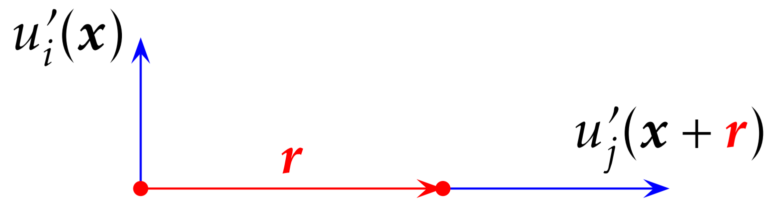

The function R_{ij} is only a function of the separation vector $\boldsymbol{r}$, between the two measurement points $\boldsymbol{x}$ and $\boldsymbol{x}' = \boldsymbol{x} + \boldsymbol{r}$: invariance by translation of the observer location $\boldsymbol{x}$.

Correlation coefficient $\mathcal{R}_{ij}$ (normalized correlation function R_{ij})

$$-1 \leq \mathcal{R}_{ij}(\boldsymbol{r}) \equiv \frac{\overline{u_i'(\boldsymbol{x})\, u_j'(\boldsymbol{x}')}}{\sqrt{\overline{u_i'^2}(\boldsymbol{x})}\sqrt{\overline{u_j'^2}(\boldsymbol{x}')}} \leq +1$$

Velocity correlation tensor (cont.)

A few remarks

- Autocorrelation
  $R_{11}(r,0,0) = \overline{u_1'^2}\mathcal{R}_{11}(r,0,0)$ with $\boldsymbol{r} = (r,0,0)$
  $R_{11}(\boldsymbol{r}) = R_{11}(-\boldsymbol{r})$, the autocorrelation function is an even function

- $R_{ij}(\boldsymbol{r}) = R_{ji}(-\boldsymbol{r})$

- Incompressibility of the turbulent field

$$\frac{\partial u_j'}{\partial x_j} = 0 \quad \Longrightarrow \quad \frac{\partial}{\partial r_j} R_{ij}(\boldsymbol{r}) = 0 \qquad \frac{\partial}{\partial r_i} R_{ij}(\boldsymbol{r}) = 0$$

- $R_{ii}(0) = \overline{u_1'^2} + \overline{u_2'^2} + \overline{u_2'^2} = 2k_t$

- **Turbulent kinetic energy budget k_t** (refer to this slide)

General case of homogeneous turbulence

$$\frac{\partial(\rho k_t)}{\partial t} = -\rho\overline{u_i'u_j'}\frac{\partial \bar{U}_i}{\partial x_j} - \overline{\tau_{ij}'\frac{\partial u_i'}{\partial x_j}} \quad (= \mathcal{P} - \rho\epsilon)$$

with $\partial\bar{U}_i/\partial x_j = \text{cst}$ to preserve homogeneous turbulence (Craya, 1958)

Decaying turbulence generated behind a grid,

Stationary turbulence, homogeneous in the plane (x_2, x_3) only

$$\bar{U}_1\frac{\partial k_t}{\partial x_1} = -\epsilon$$

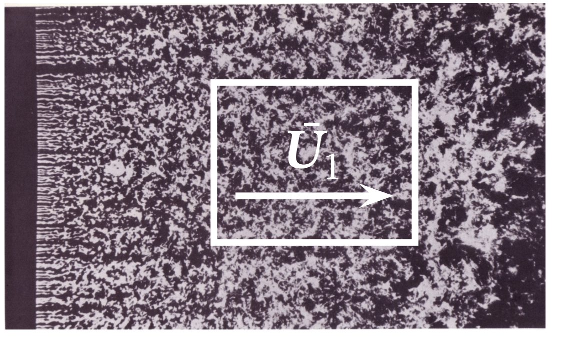

In a frame moving with the mean velocity $\bar{U}_1$,

$$\frac{\partial k_t}{\partial t} = -\epsilon$$

Integral length scales

Longitudinal integral length scale : an estimate of the size of the most energetic turbulent structures, given by the integration of the correlation coefficient of the velocity component u_1' between two points in the x_1 direction

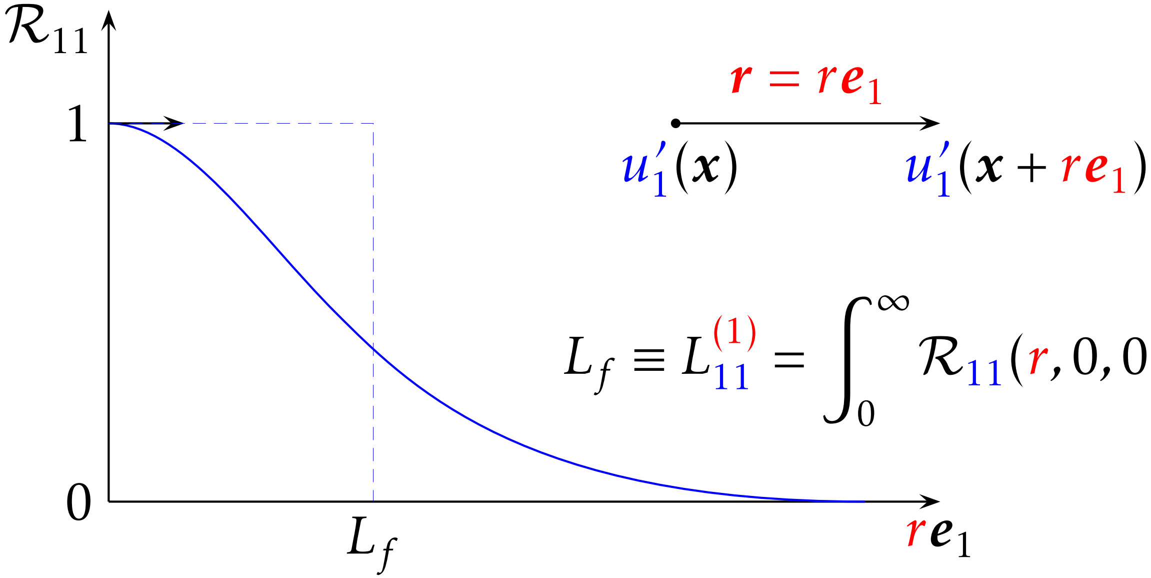

$$L_f \equiv L_{11}^{(1)} = \int_0^\infty \mathcal{R}_{11}(r,0,0)\,dr$$

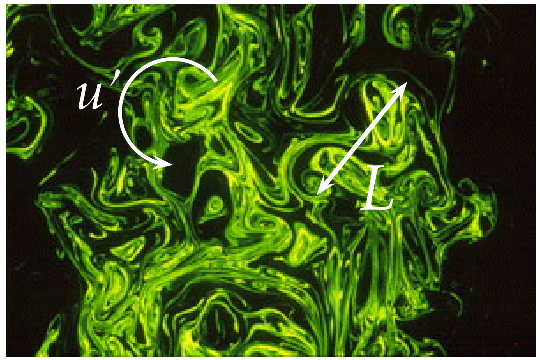

Tavoularis (2003), passive scalar mixing, Sc $\simeq$ 2000

A transverse integral length scale $L_g \equiv L_{11}^{(2)}$ is also introduced

$$L_g \equiv L_{11}^{(2)} = \int_0^\infty \mathcal{R}_{11}(0,r,0)\,dr$$

Turbulence scales

- Large scales (u', L) associated with production of larger scales by the mean shear flow ; energy containing eddies : the peak of the turbulent kinetic energy spectrum is located arround $kL \sim 1$

- We need also to introduce Taylor microscales λ associated with large scales of the dissipation spectrum, and formally defined from the Taylor series of the velocity correlation coefficient at the origin,

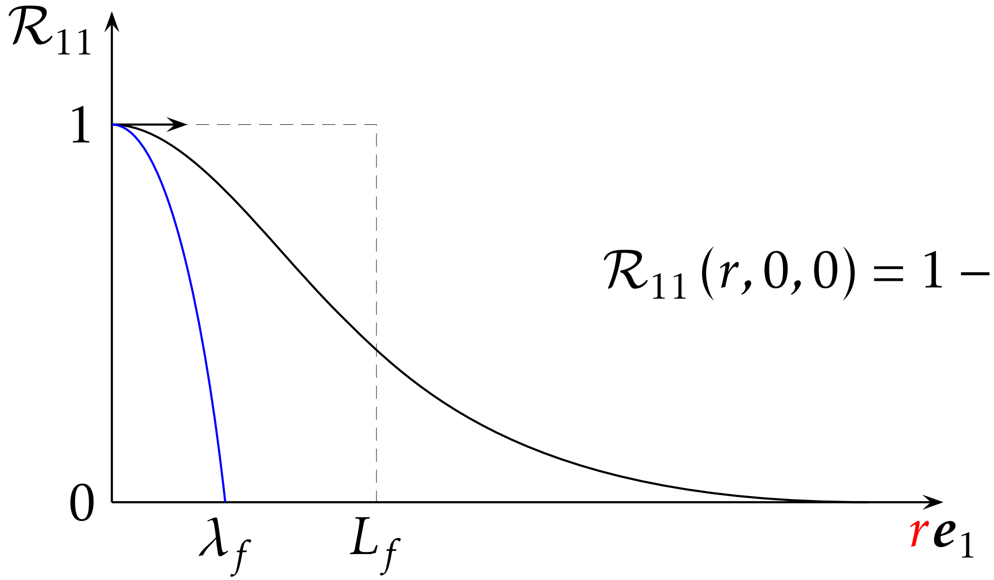

$$\mathcal{R}_{11}(r,0,0) = 1 - \frac{r^2}{{\lambda_f}^2} + \dots \qquad (\lambda_f \ll L_f)$$

Taylor microscales

Taylor series of $u_1'(r,0,0)$ as $r \to 0$,

$$u_1'(r,0,0) = u_1'(0,0,0) + r\left.\frac{\partial u_1'}{\partial x_1}\right|_{x=0} + \frac{r^2}{2}\left.\frac{\partial^2 u_1'}{\partial x_1^2}\right|_{x=0} + \dots$$

Hence,

$$R_{11}(r,0,0) = \overline{u_1'(0,0,0)\,u_1'(r,0,0)}$$

$$= \overline{u_1'^2} + r\,\overline{u_1'\frac{\partial u_1'}{\partial x_1}} + \frac{r^2}{2}\,\overline{u_1'\frac{\partial^2 u_1'}{\partial x_1^2}} + \dots$$

$$= \overline{u_1'^2} + r\,\frac{\partial}{\partial x_1}\left(\frac{\overline{u_1'^2}}{2}\right) + \frac{r^2}{2}\,\frac{\partial}{\partial x_1}\left(\overline{u_1'\frac{\partial u_1'}{\partial x_1}}\right) - \frac{r^2}{2}\,\overline{\left(\frac{\partial u_1'}{\partial x_1}\right)^2} + \dots$$

$$\mathcal{R}_{11}(r,0,0) = 1 - \frac{r^2}{2\overline{u_1'^2}}\,\overline{\left(\frac{\partial u_1'}{\partial x_1}\right)^2} \equiv 1 - \frac{r^2}{\lambda_f^2} + \dots$$

Taylor microscales (cont.)

Longitudinal Taylor microscale λ_f

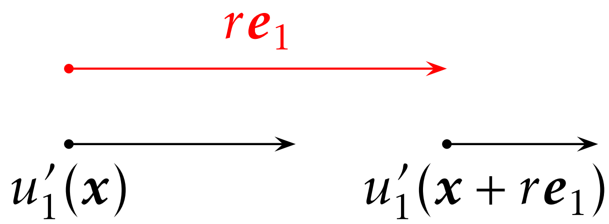

$$\frac{1}{\lambda_f^2} \equiv -\frac{1}{2}\frac{d^2\mathcal{R}_{11}}{dr_1^2}\bigg|_{r=0} = \frac{1}{2\overline{u_1'^2}}\overline{\left(\frac{\partial u_1'}{\partial x_1}\right)^2}$$

Transverse Taylor microscale λ_g

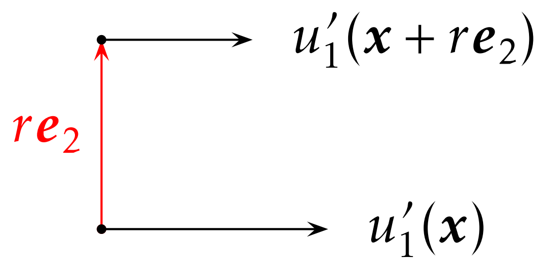

$$\frac{1}{\lambda_g^2} \equiv -\frac{1}{2}\frac{d^2\mathcal{R}_{11}}{dr_2^2}\bigg|_{r=0} = \frac{1}{2\overline{u_1'^2}}\overline{\left(\frac{\partial u_1'}{\partial x_2}\right)^2}$$

Dissipation rate ϵ of the turbulent kinetic energy

$$\rho\epsilon = \overline{\tau'_{ik}\frac{\partial u'_i}{\partial x_k}} = 2\mu\overline{s'_{ij}s'_{ij}} = 2\mu\,\overline{\frac{1}{4}\left(\frac{\partial u'_i}{\partial x_j}+\frac{\partial u'_j}{\partial x_i}\right)^2} = \underbrace{\mu\overline{\frac{\partial u'_i}{\partial x_j}\frac{\partial u'_i}{\partial x_j}}}_{(a)} + \underbrace{\mu\overline{\frac{\partial u'_i}{\partial x_j}\frac{\partial u'_j}{\partial x_i}}}_{(b)}$$

$$(a) \equiv \epsilon^h = \nu\overline{\frac{\partial u'_i}{\partial x_j}\frac{\partial u'_i}{\partial x_j}} \sim \nu\frac{u'^2}{\lambda^2}$$

correlation of the turbulent velocity gradients, dominant term for the dissipation since $\lambda \ll L$

$$(b) = \nu\overline{\frac{\partial u'_i}{\partial x_j}\frac{\partial u'_j}{\partial x_i}} = \frac{\partial^2\overline{u'_i u'_j}}{\partial x_i \partial x_j} \sim \nu\frac{u'^2}{L^2}$$

derivative of the turbulent velocity correlation (using the incompressibility condition)

for homogeneous turbulence, (b) is identically zero and $\epsilon = \epsilon^h$

ϵ^h is an approximation of the dissipation ϵ when $\lambda \ll L$, that is for high Reynolds number turbulent flow (the ϵ^h equation is solved in the standard $k_t - \epsilon$ model)

Spectral tensor

The spectral tensor $\phi_{ij}(\boldsymbol{k})$ is defined as the Fourier transform of the velocity correlation tensor $R_{ij}(\boldsymbol{r})$

$$\begin{cases} \phi_{ij}(\boldsymbol{k}) = \dfrac{1}{(2\pi)^3} \displaystyle\int_{\mathrm{R}^3} R_{ij}(\boldsymbol{r})\, e^{-i\boldsymbol{k}\cdot\boldsymbol{r}} d\boldsymbol{r} \\ R_{ij}(\boldsymbol{r}) = \displaystyle\int_{\mathrm{R}^3} \phi_{ij}(\boldsymbol{k})\, e^{i\boldsymbol{k}\cdot\boldsymbol{r}} d\boldsymbol{k} \end{cases}$$

The incompressibility condition formulated in Fourier space reads,
$k_i\phi_{ij}(\boldsymbol{k}) = k_j\phi_{ij}(\boldsymbol{k}) = 0$

It is essential in practice to introduce one-dimensional spectra, which can be measured or computed numerically,

$$E_{ij}^{(1)}(k_1) = \iint_{\mathrm{R}^2} \phi_{ij}(\boldsymbol{k})\; dk_2 dk_3$$

One-dimensional spectrum

Let us consider the case $i = j = 1$ with a zero separation vector $\boldsymbol{r} = 0$,

$$\overline{u_1'^2} = R_{11}(\boldsymbol{r} = 0) = \int_{\mathbb{R}^3} \phi_{11}(\boldsymbol{k}) d\boldsymbol{k} = \int_{-\infty}^{+\infty} E_{11}^{(1)}(k_1)\ dk_1$$

The relation between the autocorrelation $R_{11}(\boldsymbol{r})$ with $\boldsymbol{r} = (r_1, 0, 0)$, and the one-dimensional spectrum $E_{11}^{(1)}(k_1)$ is found to be

$$R_{11}(r_1, 0, 0) = \int_{\mathbb{R}^3} \phi_{11}(\boldsymbol{k})\ e^{ik_1 r_1} d\boldsymbol{k} = \int_{-\infty}^{+\infty} E_{11}^{(1)}(k_1)\ e^{ik_1 r_1} dk_1$$

and conversely by Fourier transform, one has

$$E_{11}^{(1)}(k_1) = \frac{1}{2\pi} \int_{-\infty}^{+\infty} R_{11}(r_1, 0, 0)\ e^{-ik_1 r_1} dr_1$$

For $k_1 = 0$, $\quad E_{11}^{(1)}(0) = \frac{1}{2\pi} \int_{-\infty}^{+\infty} R_{11}(r_1, 0, 0)\ dr_1 = \frac{1}{2\pi} 2\overline{u_1'^2} L_f$

$$L_f = \pi \frac{E_{11}^{(1)}(0)}{\overline{u_1'^2}}$$

- **Frozen turbulence approximation or Taylor's hypothesis (1938)**

The velocity spectral tensor and the corresponding one-dimensional spectra cannot be directly measured from the Fourier transform of velocity correlation functions in general. Only the time evolution of the velocity in one given point is known, that is $u_1'(t)$.

In order to estimate these spectral functions, it is usually assumed that the turbulent flow is frozen during the measurement, meaning that the observed quantity is simply convected by the local mean flow $\bar{U}_1$, which leads to

$$\frac{\partial}{\partial t} = -\bar{U}_1 \frac{\partial}{\partial x_1} \qquad k_1 = 2\pi f / \bar{U}_1 \qquad \text{Taylor's hypothesis}$$

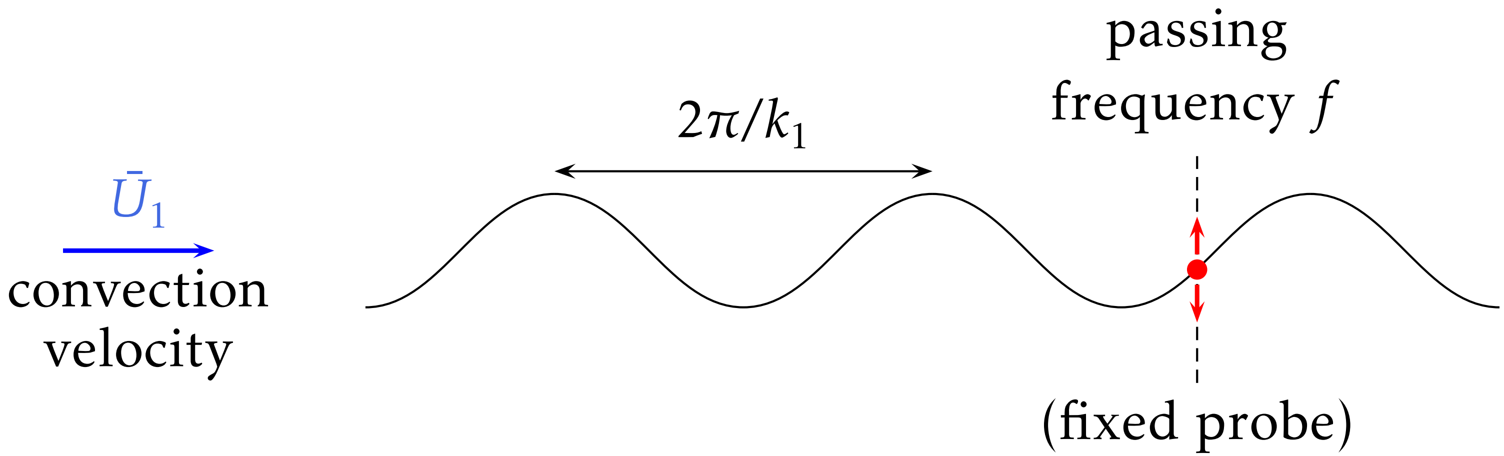

Frozen turbulence approximation or Taylor's hypothesis (1938)

Geoffrey Ingram Taylor (right) at age 69 (in 1956), in his laboratory with his assistant Walter Thompson *(Physics Today, May 2000)*

At Stanford (1968)

Application to the estimation of L_1, $u_1'(t) \rightarrow \Phi_{11}(f)$ $\overline{u_1'^2} \equiv \int_0^\infty \Phi_{11}(f)df$

$$\overline{u_1'^2} = \int_{-\infty}^{+\infty} E_{11}^{(1)}(k_1)\ dk_1 \equiv \int_0^\infty \frac{\bar{U}_1}{2\pi}\Phi_{11}\left(f = k_1\bar{U}_1/2\pi\right)dk_1$$

$$L_{11}^{(1)} = \pi\frac{E_{11}^{(1)}(k_1=0)}{\overline{u_1'^2}} = \frac{1}{4}\ \bar{U}_1\frac{\Phi_{11}(f=0)}{\overline{u_1'^2}}$$

Frozen turbulence approximation or Taylor's hypothesis (1938)

Spectrum of longitudinal velocity fluctuations
free round jet, $\mathrm{Re}_D \simeq 10^5$, hot-wire located at $x_1 = 2D$ and $x_2 = D/2$
(see also the time correlation function, $\Theta \simeq L_f/\bar{U}_1$)

$\Phi_{11}(f)$ for $f \geq 0$
--- to estimate L_f and $f^{-5/3}$ law

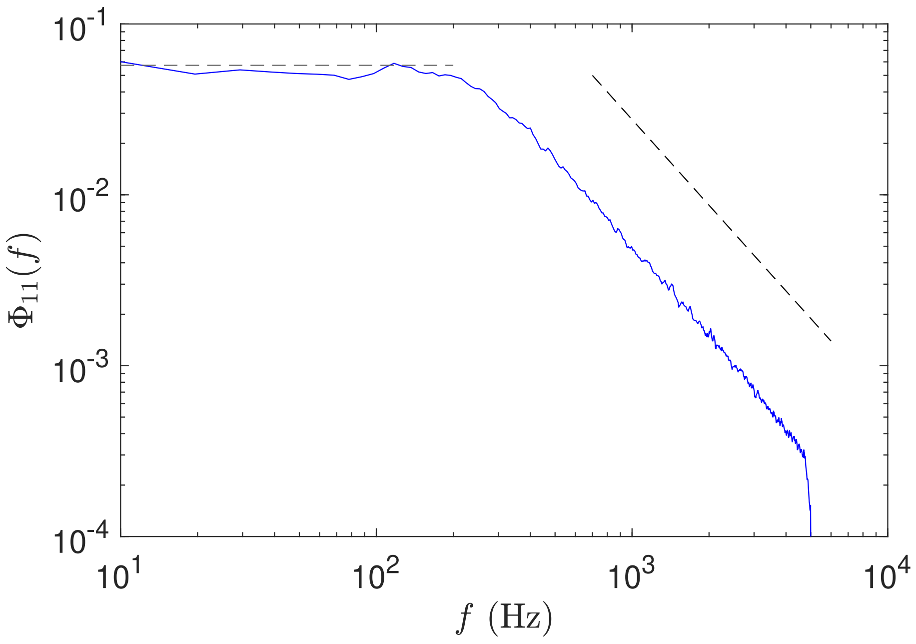

$E_{11}^{(1)}(k_1)$ for $-\infty \leq k_1 \leq \infty$
--- to estimate L_f and $k_1^{-5/3}$ law

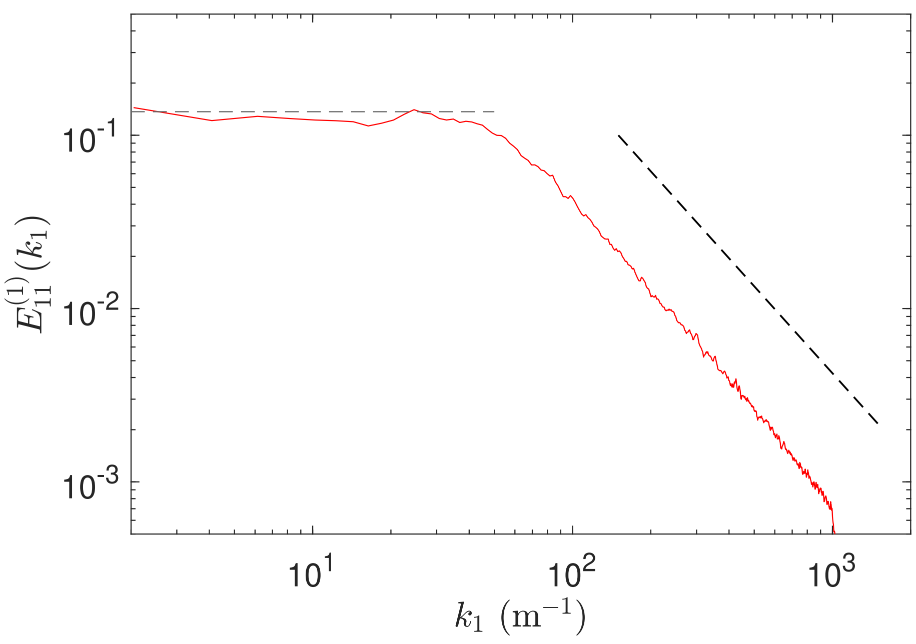

Turbulent kinetic energy and dissipation spectra

Turbulent kinetic energy spectrum

$$k_t = \frac{\overline{u_i' u_i'}}{2} = \frac{1}{2} R_{ii}(\boldsymbol{r} = 0) = \frac{1}{2} \int_{\mathbb{R}^3} \phi_{ii}(\boldsymbol{k})\, d\boldsymbol{k}$$

Dissipation spectrum

Usually, it is more convenient to first calculate the enstrophy spectrum from the Fourier transform of the vorticity vector, $\hat{\omega}(\boldsymbol{k}) = i\boldsymbol{k} \times \hat{\boldsymbol{u}}(\boldsymbol{k})$. It can be shown that,

$$\frac{\overline{\omega_i' \omega_i'}}{2} = \frac{1}{2} \int_{\mathbb{R}^3} k^2 \phi_{ii}(\boldsymbol{k})\, d\boldsymbol{k}$$

Then, by noting that $\epsilon = \nu \overline{\omega_i' \omega_i'}$, the following expression is obtained from the dissipation spectrum

$$\epsilon = \nu \overline{\omega_i' \omega_i'} = \nu \int_0^\infty k^2 \phi_{ii}(\boldsymbol{k}) d\boldsymbol{k}$$

Isotropic turbulence

An isotropic turbulent flow is a class of homogeneous turbulent flow whose statistics are invariant under rotation of the coordinate axes and under reflection in a plane.

Impossible to distinguish any privileged direction
a priori, the most simple configuration ! (ideal theoretical framework)

In order to characterize properties induced by homogeneous and isotropic turbulence, a virtual device is introduced to measure

– a fluctuating scalar quantity : temperature, pressure, ...

– a fluctuating vector quantity : projection on a given unit vector of the turbulent velocity, ...

- **Second-order correlation in one point : Reynolds tensor**

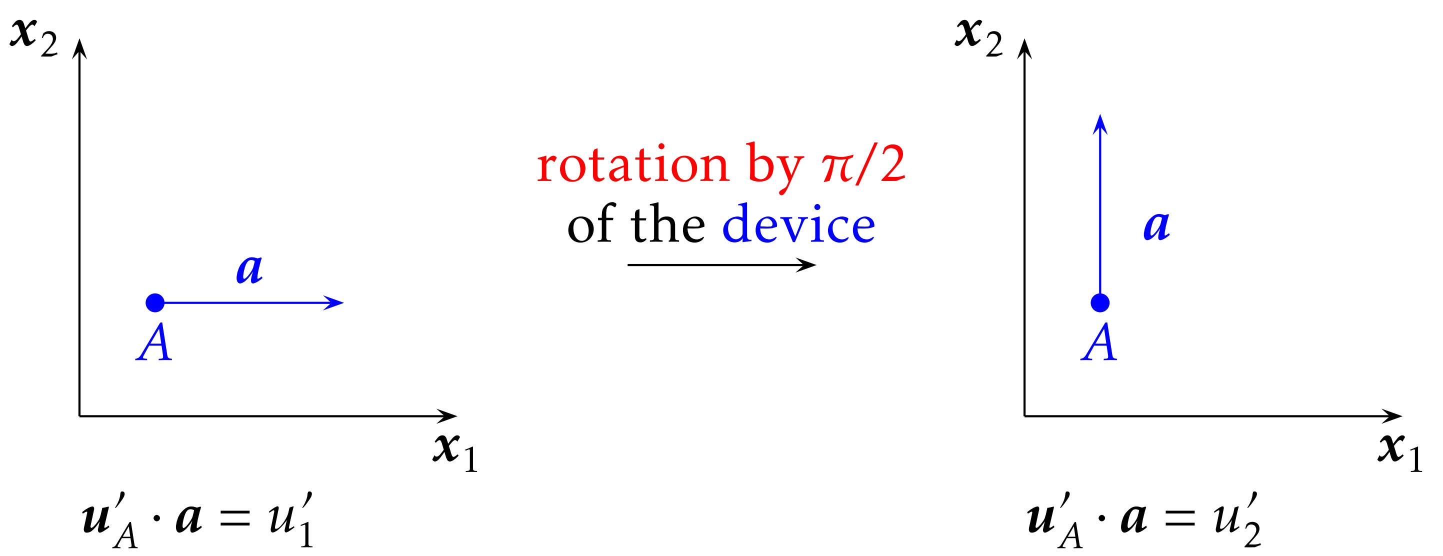

The two measurements must be equal for isotropic turbulence, and therefore $\overline{u_1'^2} = \overline{u_2'^2}$. More generally,

$$\overline{u_1'^2} = \overline{u_2'^2} = \overline{u_3'^2} = u'^2 \qquad \text{by noting } u' \equiv \left(\overline{u'^2}\right)^{1/2}$$

Second-order correlation in one point : Reynolds tensor

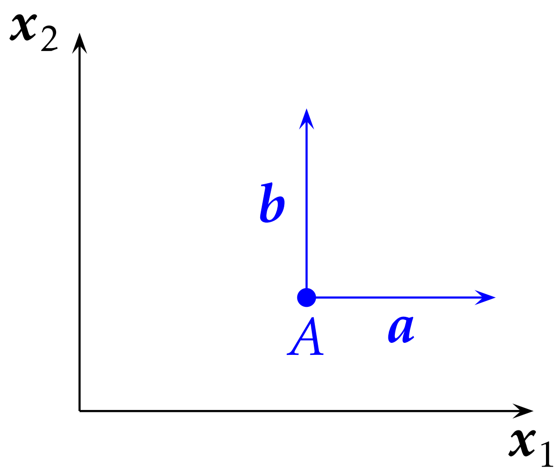

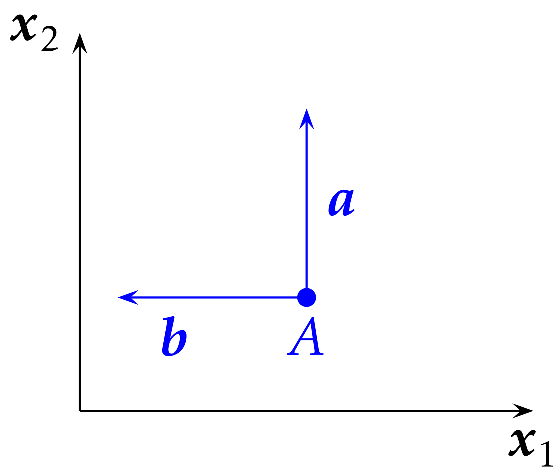

$$(\boldsymbol{u}'_A \cdot \boldsymbol{a})(\boldsymbol{u}'_A \cdot \boldsymbol{b}) = u'_1 u'_2 \qquad (\boldsymbol{u}'_A \cdot \boldsymbol{a})(\boldsymbol{u}'_A \cdot \boldsymbol{b}) = -u'_1 u'_2$$

Consequently, $\overline{u'_1 u'_2} = -\,\overline{u'_1 u'_2}$ and $\overline{u'_1 u'_2} = 0$

$$\boxed{\overline{u'_i u'_j} = u'^2\,\delta_{ij} = \frac{2}{3}k_t\,\delta_{ij}}$$

- **Second-order velocity correlation in two points**

A at $\boldsymbol{x}$ and B at $\boldsymbol{x}+\boldsymbol{r}$:

$$\mathcal{F} \equiv \frac{\overline{(\boldsymbol{u}'_A \cdot \boldsymbol{a})(\boldsymbol{u}'_B \cdot \boldsymbol{b})}}{\sqrt{\overline{\boldsymbol{u}'^2_A}}\sqrt{\overline{\boldsymbol{u}'^2_B}}} = \frac{\overline{u'_{iA}u'_{jB}}(\boldsymbol{r})}{u'^2} a_i b_j = \mathcal{R}_{ij}\, a_i b_j$$

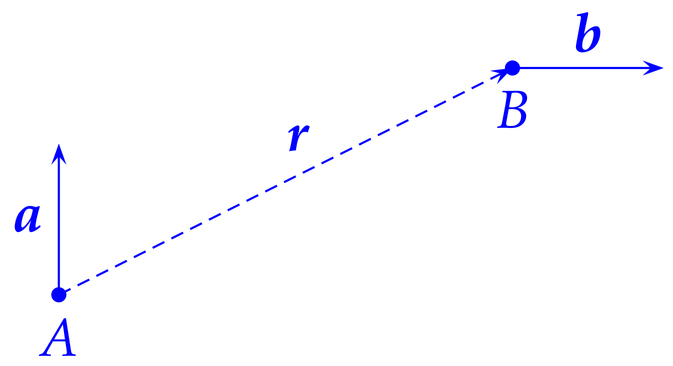

The bilinear function $\mathcal{F}$ can only be a function of the invariants associated with the measurement device, that is distances and angles :
$\boldsymbol{r}^2 = r_i r_i$, $\boldsymbol{a}\cdot\boldsymbol{r} = a_i r_i$, $\boldsymbol{b}\cdot\boldsymbol{r} = b_j r_j$, $\boldsymbol{a}\cdot\boldsymbol{b} = a_i b_i = a_i b_j \delta_{ij}$
and also the volume defined by $(\boldsymbol{r},\boldsymbol{a},\boldsymbol{b})$, given by the mixed product
$(\boldsymbol{a}\times\boldsymbol{b})\cdot\boldsymbol{r} = \epsilon_{ijk} a_i b_j r_k$

General expression of an isotropic second-order two-point tensor
(Robertson, 1940)

$$\mathcal{R}_{ij}(\boldsymbol{r}) = \alpha(r)\, r_i r_j + \beta(r)\,\delta_{ij}$$

where α and β are two scalar functions of r.

Second-order two-point velocity correlation (cont.)

It is generally found more convenient to introduce two functions $f(r)$ and $g(r)$ that can be measured in practice, rather than the two arbitrary functions $\alpha(r)$ and $\beta(r)$. Hence,

$$f(r) \equiv \mathcal{R}_{11}(r,0,0) \quad \text{longitudinal correlation function}$$
$$g(r) \equiv \mathcal{R}_{11}(0,r,0) \quad \text{transverse correlation function}$$

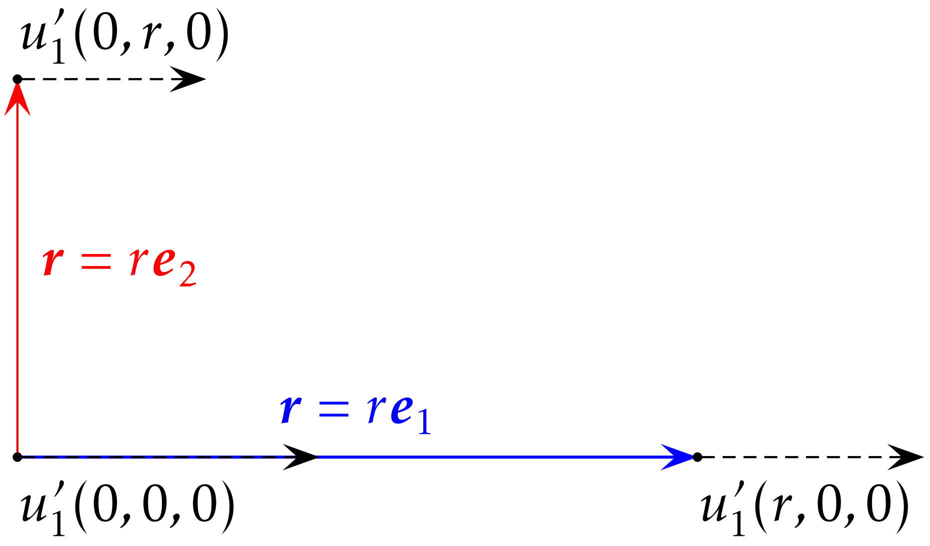

Kármán & Howarth (1938)

$$\mathcal{R}_{ij}(\boldsymbol{r}) = (f-g)\frac{r_i r_j}{r^2} + g\delta_{ij}$$

Take care of $R_{ij}(\boldsymbol{r}) = u'^2\mathcal{R}_{ij}(\boldsymbol{r})$

- **Compressibility condition** applied to the second-order two-point velocity correlation recast by Kármán & Howarth

$$\frac{\partial \mathcal{R}_{ij}(\boldsymbol{r})}{\partial r_i} = 0 \qquad \Longrightarrow \qquad \frac{\partial}{\partial r_i}\left[\frac{f-g}{r^2} r_i r_j + g\delta_{ij}\right] = 0$$

which leads for a 3-D turbulence to the following expression (the details are left as an exercise),

$$g = f + \frac{r}{2} f' = \frac{1}{r}\frac{d}{dr}\left(\frac{r^2}{2} f\right)$$

The correlation coefficient $\mathcal{R}_{ij}$ is determined by a single scalar function, the longitudinal autocorrelation in space $f(r)$, for incompressible isotropic turbulence.

Turbulent kinetic energy and dissipation spectra

Using a similar approach applied now to the spectral tensor $\phi_{ij}(\boldsymbol{k})$, and taking account for the incompressibility condition, it can be shown that only one scalar function $E(k)$ is required to specify $\phi_{ij}(\boldsymbol{k})$, that is

$$\phi_{ij}(\boldsymbol{k}) = \frac{E(k)}{4\pi k^2}\left(\delta_{ij} - \frac{k_i k_j}{k^2}\right) \qquad \text{with} \qquad k_t \equiv \int_0^\infty E(k)\,dk$$

The expression of the dissipation spectrum is then deduced from the relationship established for homogeneous turbulence, see here,

$$\epsilon = 2\nu \int_0^\infty k^2 E(k)\,dk$$

Isotropic turbulence

Many other remarkable results can be established for homogeneous and isotropic turbulence : refer to textbooks mentioned in the introduction of this course.

Three points must be however still considered to provide a first full overview of isotropic turbulence

- How to generate isotropic turbulence in laboratory ?
- What is the time evolution of isotropic turbulence ?
- Can we measure or derive analytically the expression of $E(k)$?

Isotropic turbulence in laboratory

Various configurations have been investigated to generate isotropic turbulence. One of the most famous is the so-called "Porcupine" by Betchov (1957)

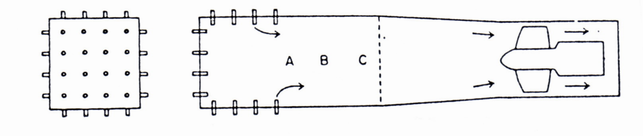

The ' Porcupine '. The mixing of 80 small jets produces a strong turbulence in the region marked A, B, C.

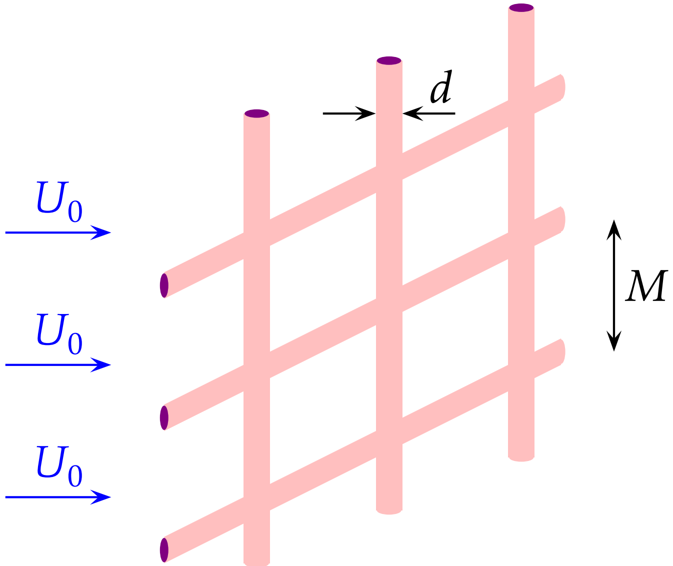

Turbulence behind a grid, homogeneous but not fully isotropic turbulent flow

$$\overline{u_1'^2} = 1.2\,\overline{u_2'^2} = 1.2\,\overline{u_3'^2}$$

and one typically gets for turbulence intensity

$$\frac{u'}{U_0} \simeq 2\% \qquad \mathrm{Re}_M = \frac{U_0 M}{\nu} \simeq 10^4 \text{ to } 10^5$$

Isotropic turbulence in laboratory (cont.)

Experiences by Comte-Bellot & Corrsin at Johns Hopkins University

J. Fluid Mech., 1966, **25**(4) & 1971 **48**(2)

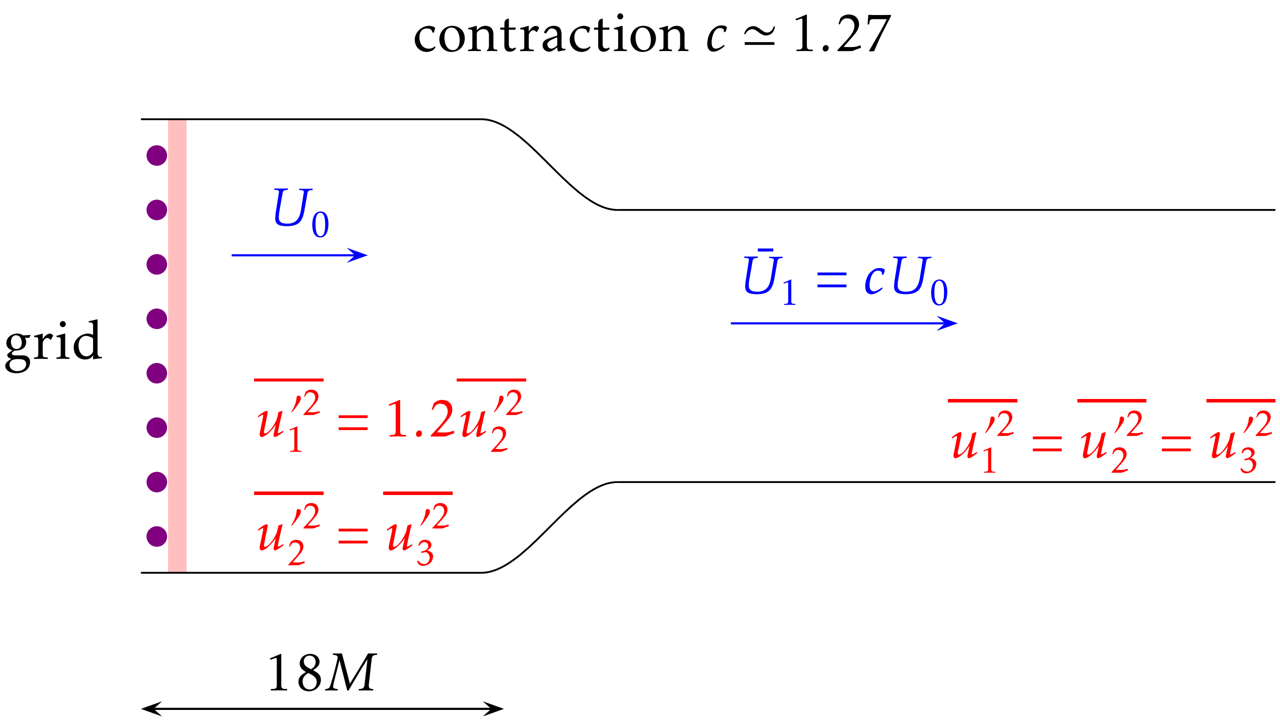

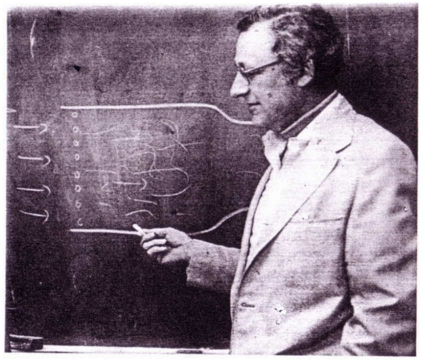

Stanley Corrsin

Hopkins researcher finds fascination in turbulence

By Albert Sehlstedt, Jr.

Stanley Corrsin is a specialist in turbulence, a very complex scientific problem subject that deals with airplanes flying through the clouds, curling cigarette smoke rising under a lampshade and blood flowing through human bodies.

Explaining these seemingly commonplace occurrences poses a problem that has puzzled scientists for decades.

"It is sufficiently difficult [a subject] that the problem is not likely to be solved in my lifetime," Dr. Corrsin observed in his Maryland Hall office on the Homewood campus of the Johns Hopkins University.

"That means I'm not in danger of being unemployed," the 62-year-old scientist added with a smile. "Also, I think it is aesthetically interesting. Turbulent flows make beautiful pictures."

Turbulent flows are movements of matter in which the velocity at a

"Stan is not only a person who himself has contributed [through research], but his discourses have been stimulating to other people."

— Lawrence Talbot Berkeley professor

Stanley Corrsin, winner of the American Physical Society's 1983 Fluid Dynamics Prize, is respected as both researcher and teacher.

critical review of fluid dynamics," which "have touched a legion of students and associates."

"Stan is not only a person who himself has contributed, but his discourses have been stimulating to other people," said Lawrence Talbot,

decision-making that he would rather not undertake.

Better to talk of airplanes, soaring albatrosses, flowing water — and swallowing.

There is a "swallowing center," a complex assembly of muscles and

called non-uniform surface tension may be the answer, he said.

There is also the question of why contact lenses stay attached to the surface of the eye. Dr. Corrsin and his colleagues examined this mystery, too, but he said, "We never did

who was helping to edit a monograph on jet propulsion at a place that has since become famous for guiding spacecraft to the planets — the Jet Propulsion Laboratory in Pasadena, Calif.

Dr. Corrsin said he chose Hopkins

Decaying isotropic turbulence

In a frame moving with the mean velocity,

- Decay of the normal stresses

$$\frac{\overline{u'^2}}{U_0^2} = \frac{1}{A}\left(\frac{tU_0}{M} - \frac{t_0U_0}{M}\right)^{-n} \qquad \text{with} \qquad n \simeq 1.3$$

Comte-Bellot & Corrsin (1966), Mohamed & Larue (1990)

- The dissipation rate of the turbulent kinetic energy is imposed by larger turbulent structures,

$$\boxed{\epsilon \simeq \frac{u'^3}{L_f}} \qquad \frac{\partial k_t}{\partial t} = -\epsilon \sim \frac{u'^2}{L_f/u'}$$

where L_f is the longitudinal integral length scale, $L_f = \int_0^\infty f(r)dr$

Decaying isotropic turbulence

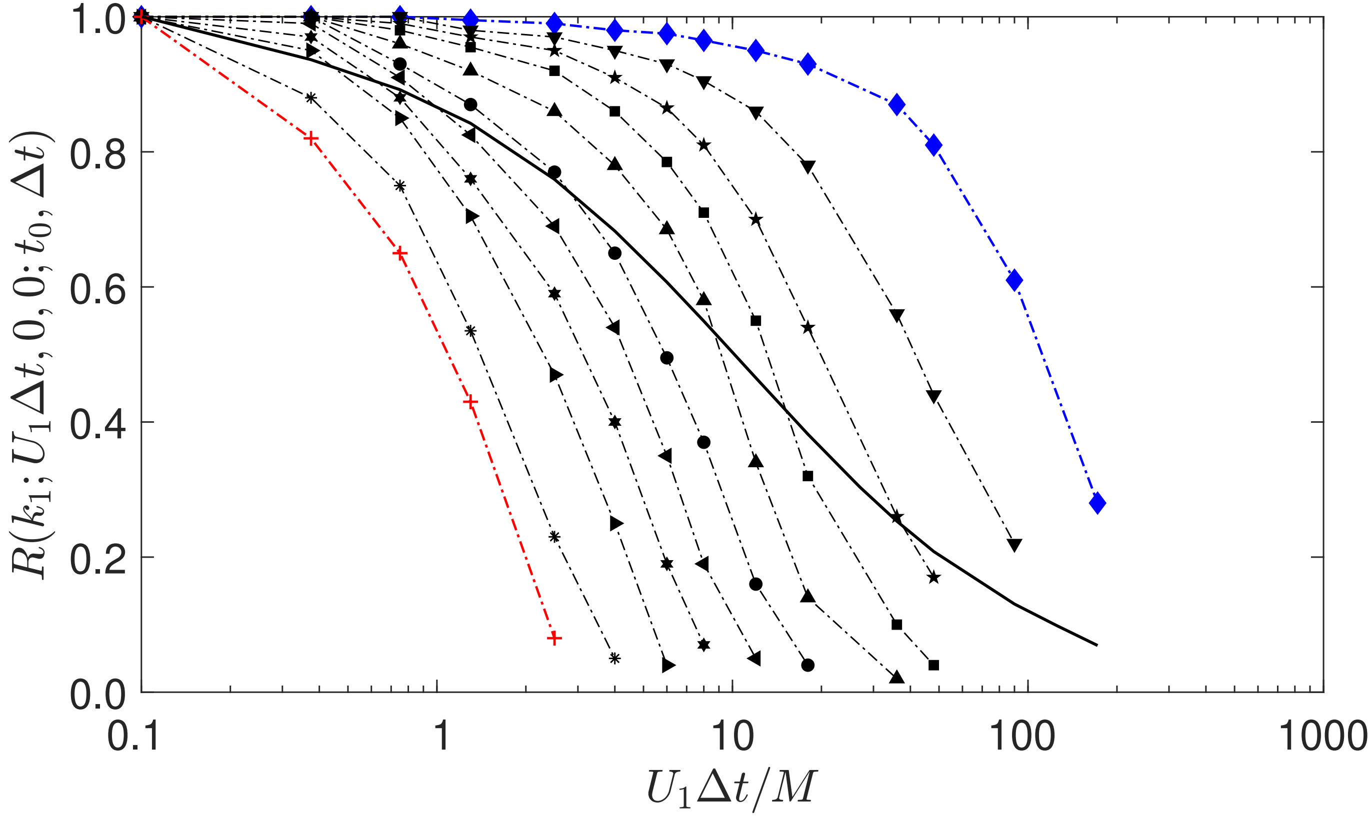

Time correlation in a frame travelling with the mean velocity $\bar{U}_1$ for different values of the wavenumber, from $k_1 = 0.25$ cm^{-1} (♦) to $k = 10.10$ cm^{-1} (+)

—— total signal (full-band case)

Space-time correlations

$$\mathcal{R}_{11}(\Delta x_1, 0, 0; \tau) = \overline{u_1'(\boldsymbol{x}, t) u_1'(\boldsymbol{x} + \Delta x_1 \boldsymbol{e}_1, t + \tau)} / \overline{u_1'^2}$$

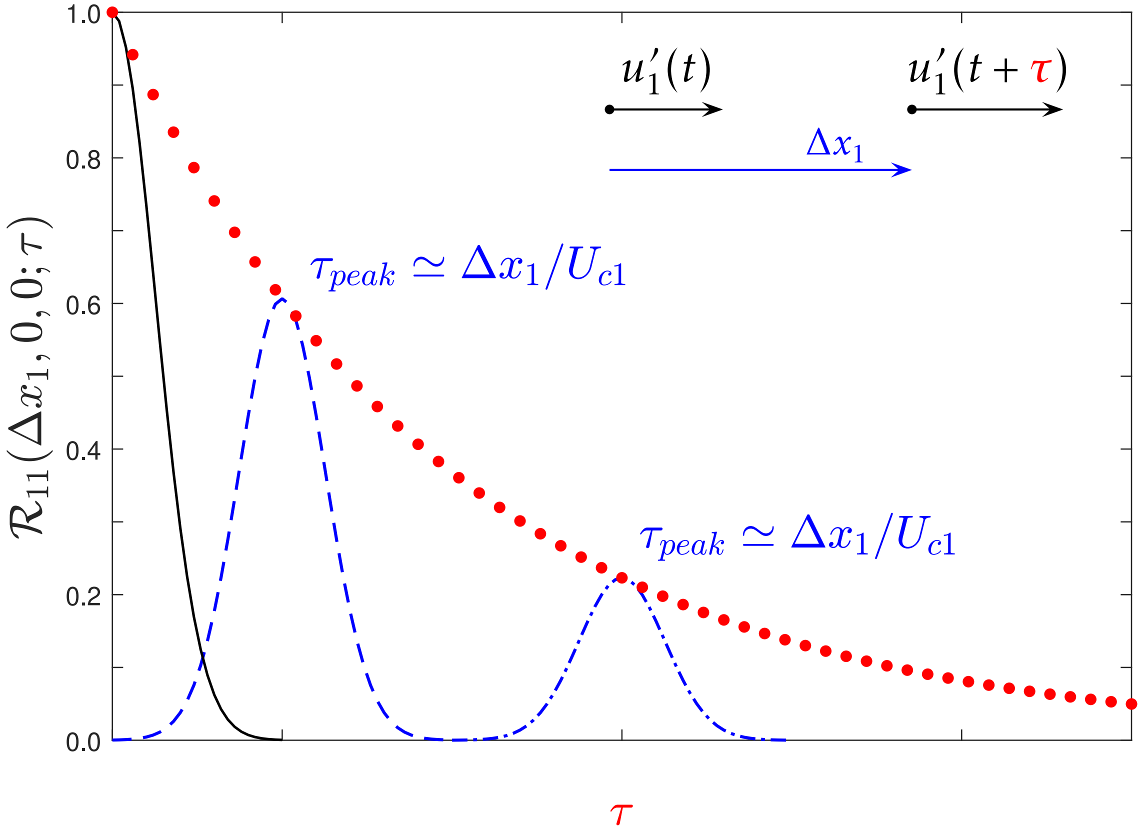

—— time autocorrelation function ($\Delta x_1 = 0$), which provides the integral time scale in the fixed frame $\Theta_1 \sim L_f / U_{c1}$ (Taylor)

- - - time correlation for a given separation Δx_1 of the two probes

—— time autocorrelation function in the convected frame

$$\Theta_{c1} = \int_0^\infty \mathcal{R}_{c11}(\tau) d\tau$$

$\Theta_{c1} \sim L_f / u_1'$ represents the time characterizing the loss of coherence or the memory time of turbulence

Isotropic turbulence submitted to ...

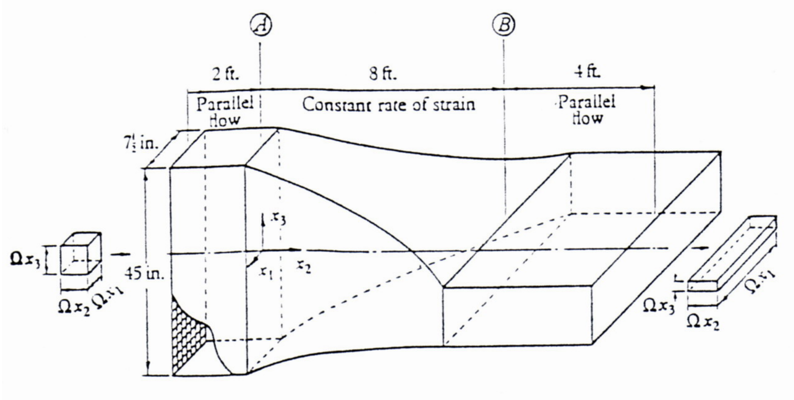

Tucker & Reynolds - Plane strain

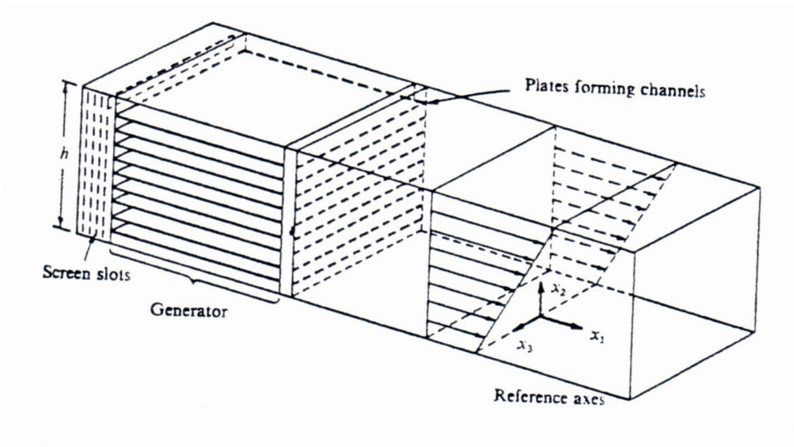

Champagne et al. - Sheared mean flow

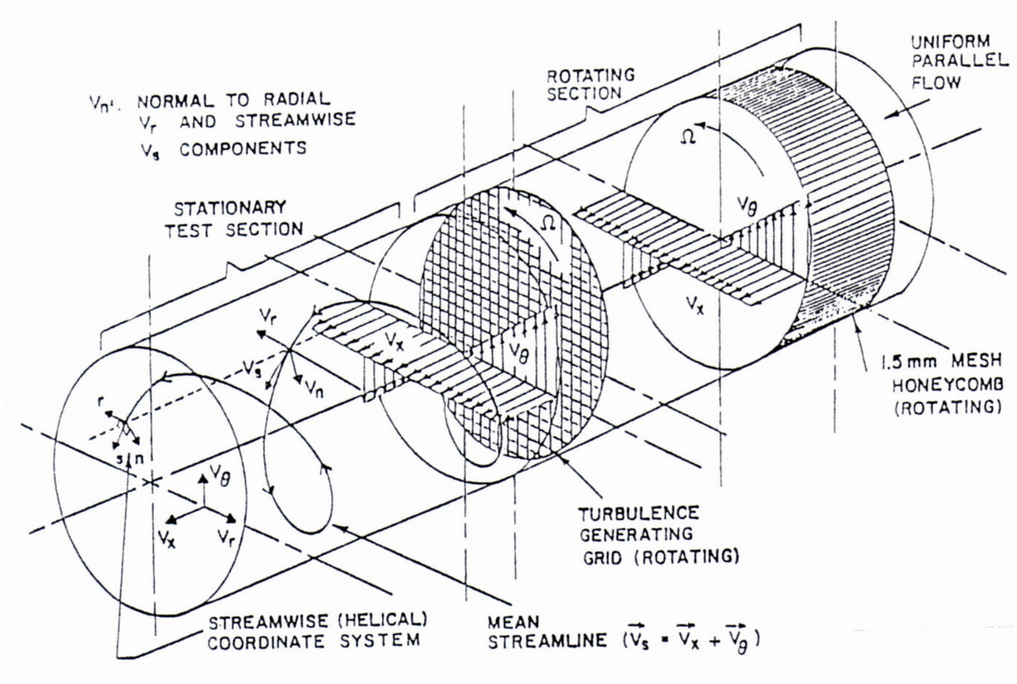

Wigeland & Nagib - Solid body rotation

Exercise #1

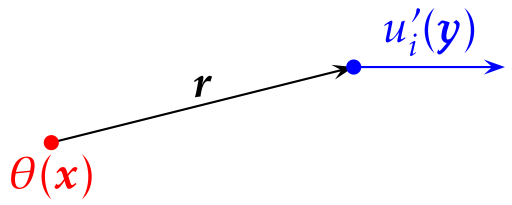

Correlation between temperature and a velocity component in two points $\boldsymbol{x}$ and $\boldsymbol{y} = \boldsymbol{x} + \boldsymbol{r}$ where $\boldsymbol{r} = \boldsymbol{y} - \boldsymbol{x}$ is the separation vector

1. Expression of the two-point correlation $\overline{\theta(\boldsymbol{x}) u_i'(\boldsymbol{y})}$ for isotropic turbulence ?
2. Can we generalize the previous result for any scalar quantity ? (temperature, pressure, concentration, ...)

Exercise #2

Scales

1. Show from Kármán & Howarth's relation, that for 3-D incompressible turbulence,

$$g = f + \frac{r}{2} f'$$

2. Deduce that $L_f = 2L_g$ and that $\lambda_f = \sqrt{2}\lambda_g$, by noting that

$$\frac{1}{\lambda_f^2} = -\frac{1}{2} f''(0) \qquad \frac{1}{\lambda_g^2} = -\frac{1}{2} g''(0)$$

3. Deduce the two followwing addtional expressions of dissipation,

$$\epsilon = \frac{15}{2} \nu \overline{\left(\frac{\partial u_1'}{\partial x_2}\right)^2} = 15 \nu \overline{\left(\frac{\partial u_1'}{\partial x_1}\right)^2}$$

Exercise #3

Cumulus clouds : the length scale of the large eddies is about 250 m and the fluctuating velocity is 1 $m.s^{-1}$

1. Estimate the energy dissipation rate in a cumulus cloud, both per unit mass and for the entire cloud (from Tennekes & Lumley, 1972). Compute the total dissipation rate in kilowatts. Also estimate the Kolmogorov scale. Compare with the power received at the surface of the Earth from the Sun.

Dynamics of isotropic turbulence – Kolmogorov’s theory

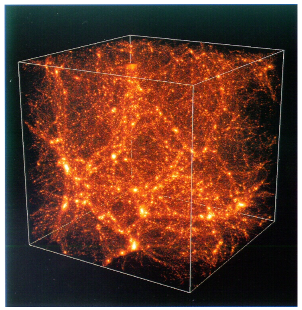

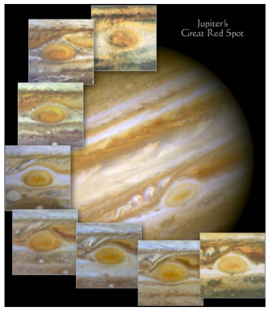

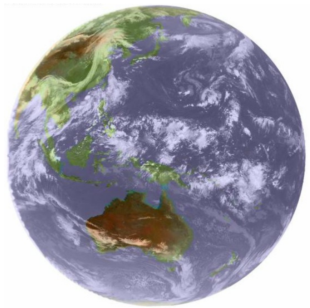

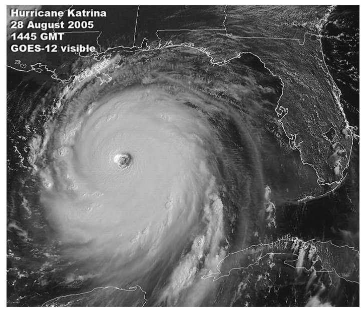

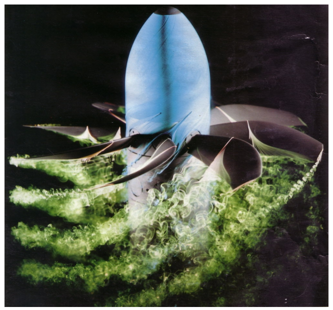

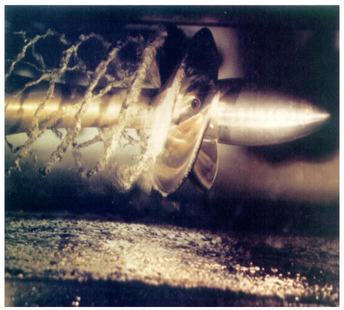

Introduction

The spectrum of turbulent kinetic energy is the key function for isotropic turbulence. Can we determine the form of $E(k)$ and its time evolution ?

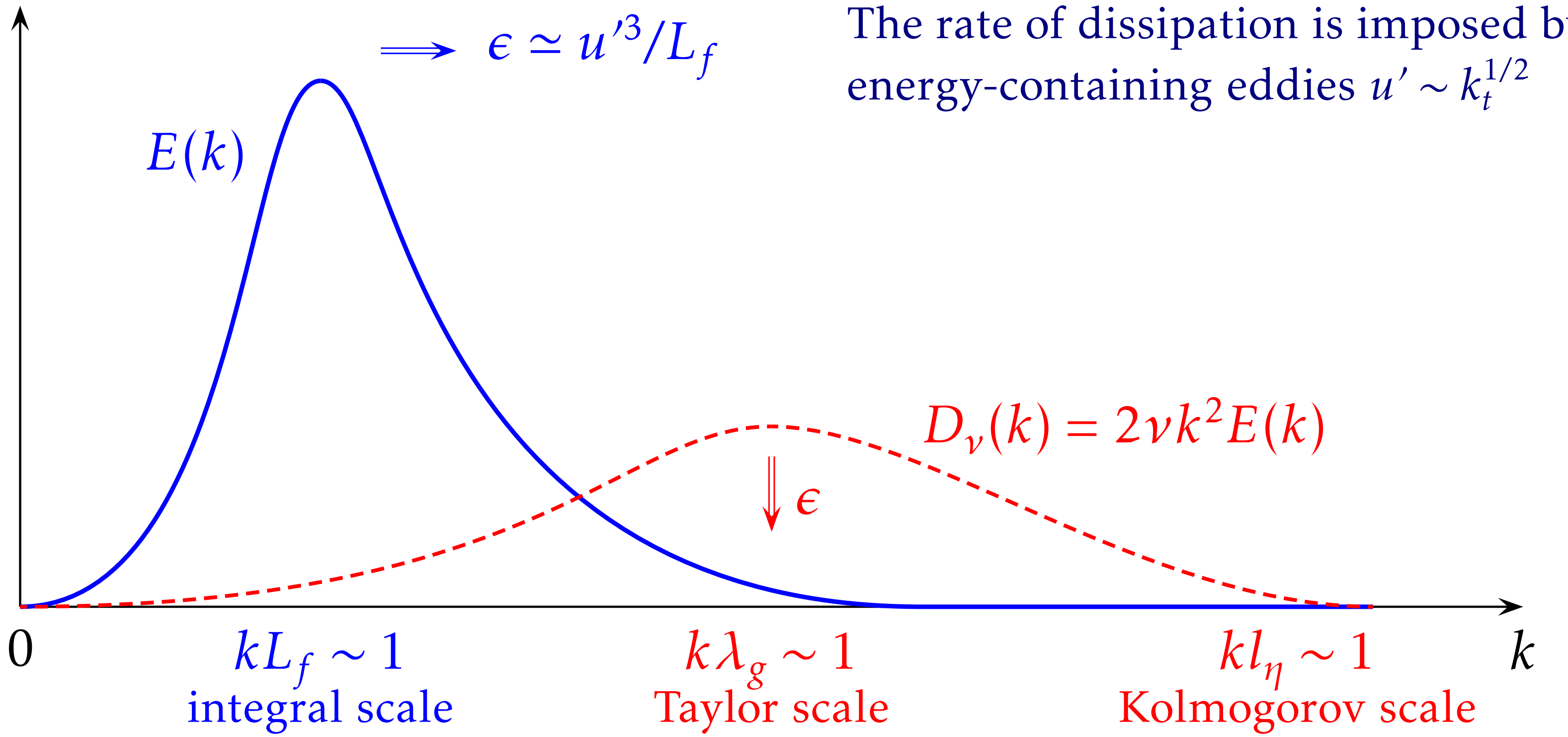

The rate of dissipation is imposed by larger structures, energy-containing eddies $u' \sim k_t^{1/2}$ time $\sim L_f/u'$

viscous scales ($\mathrm{Re}_\eta = 1$)

$l_\eta = \nu^{3/4}\epsilon^{-1/4}$ $u_\eta = \nu^{1/4}\epsilon^{1/4}$

Energy cascade

The higher the Reynolds number is, the more spectra of the kinetic energy and dissipation will be separated : fully developed turbulence.

$$\frac{L_f}{l_\eta} = \frac{L_f}{\nu^{3/4}\epsilon^{-1/4}} = \left(\frac{u' L_f}{\nu}\right)^{3/4} = \mathrm{Re}_{L_f}^{3/4} \qquad \mathrm{Re}_{L_f} \equiv \frac{u' L_f}{\nu}$$

Reynolds number of large structures

Kolmogorov (1941) – energy cascade

The dissipation rate ϵ is imposed by large eddies, but carries out by the smallest ones (at Kolmogorov scales), it can be argued as assumptions that

- the dissipation rate ϵ is finite, even when $\mathrm{Re} \to \infty$,
- there is a self-similar dynamics ; velocity scale of an eddy of size l varies as $u_l \sim l^p$ (that is a power law)

- **Representation in spectral space**

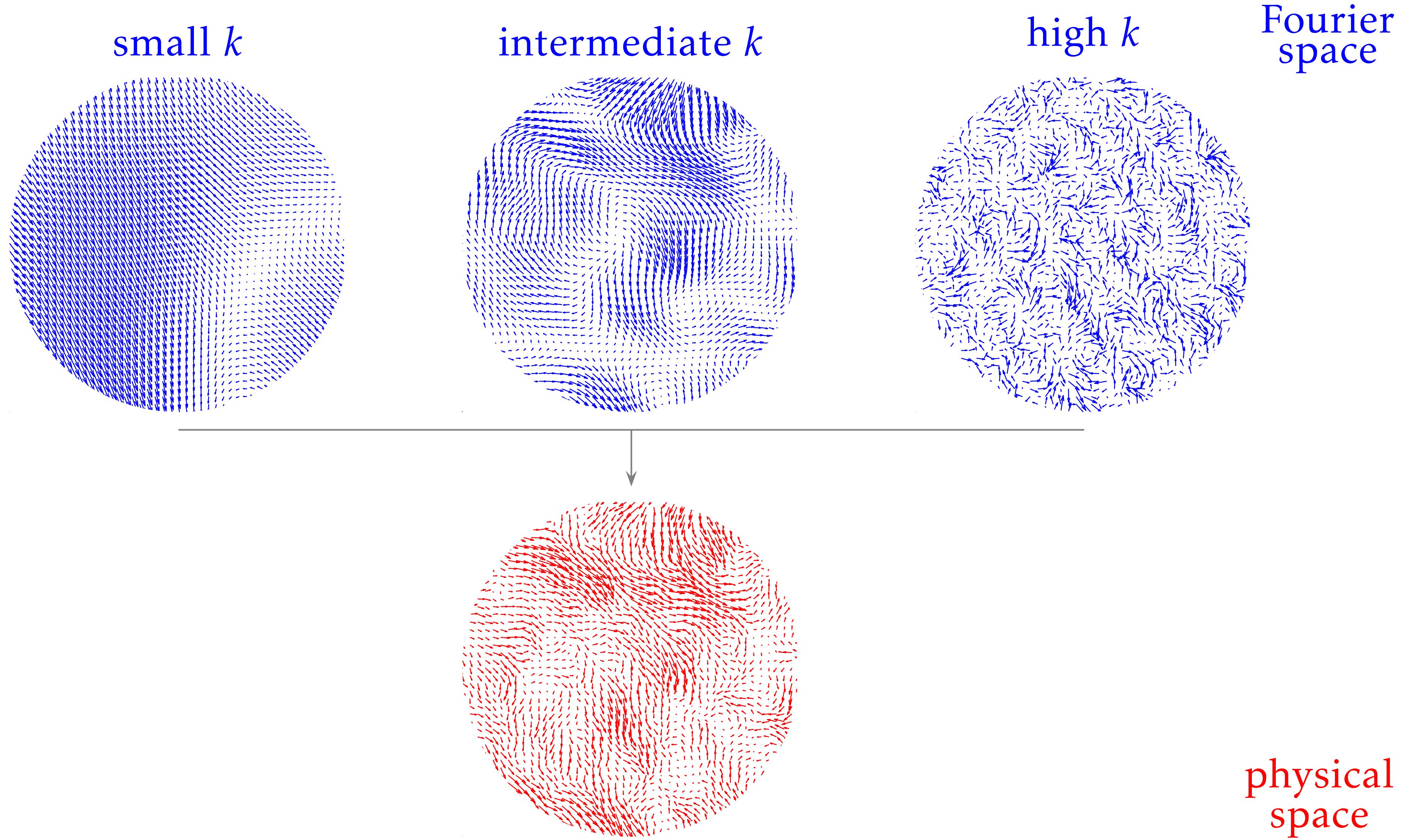

Representation in spectral space (cont.)

For isotropic turbulence, the turbulent kinetic energy spectrum $E(k)$ is decomposed over spheres of radius k, with elementary turbulent structures of wavenumber k as already discussed in the Introduction Chapter.

For exponential spectra, this will be the case for $E(k)$, it is interesting to introduce a linear representation in logarithmic scale. For a geometric sequence k_n,

$$\frac{k_n}{k_{n-1/2}} = a = \frac{k_{n+1/2}}{k_n} \qquad \Delta k_n = k_{n+1/2} - k_{n-1/2}$$

and it is always possible to choose the common ratio a such as $\Delta k_n / k_n = 1$.
With a constant bandwidth for $d \ln k = dk/k$,

$$\int_{k_{n-1/2}}^{k_{n+1/2}} E(k)\, dk = \int_{k_{n-1/2}}^{k_{n+1/2}} kE(k)\, d\ln k \sim k_n E(k_n)$$

In the same way, the importance of frequency weighted spectra or compensated spectra is underlined for exponential form.

Benefit of frequency weighted spectrum

equal areas = equal contributions using log-axes

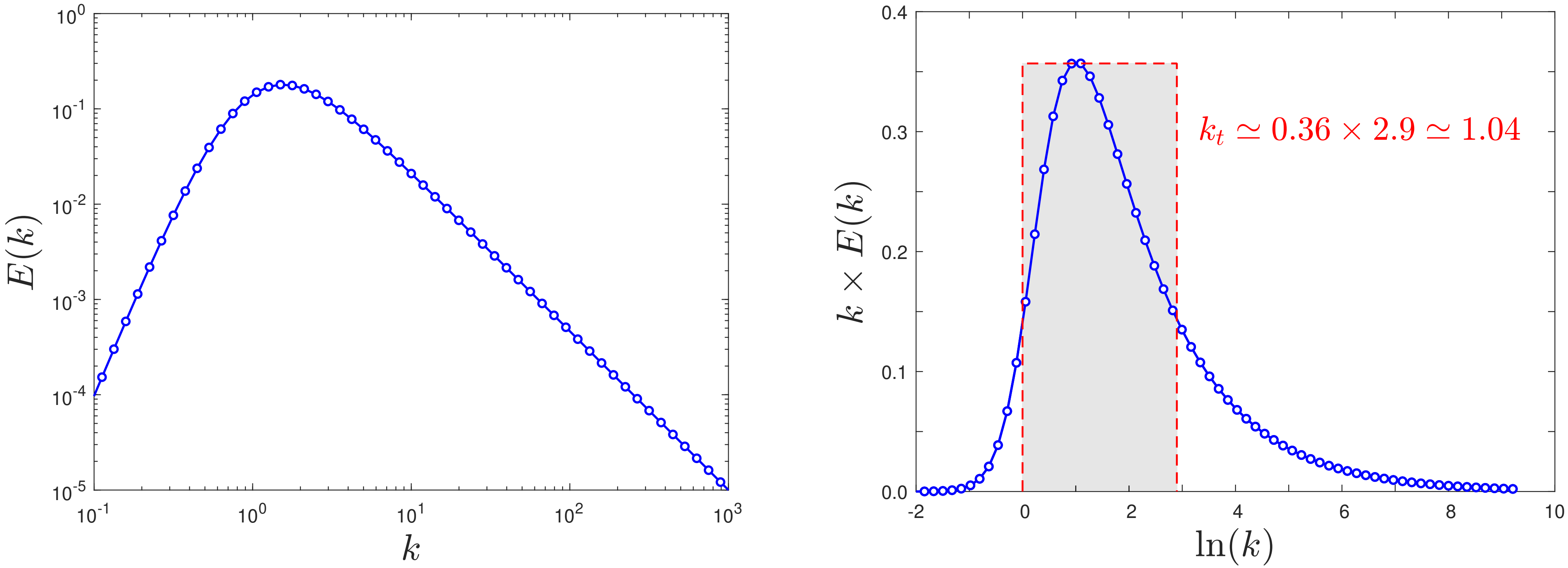

$$k_t = \int_0^\infty E(k)\, dk = \int_0^\infty kE(k)\, d\ln k$$

von Kármán spectrum model,

$$E(k) = \frac{k^4}{(1+k^2)^{17/6}} \qquad k_{t\,\text{exact}} \simeq 1.0325$$

Benefit of frequency weighted spectrum (cont.)

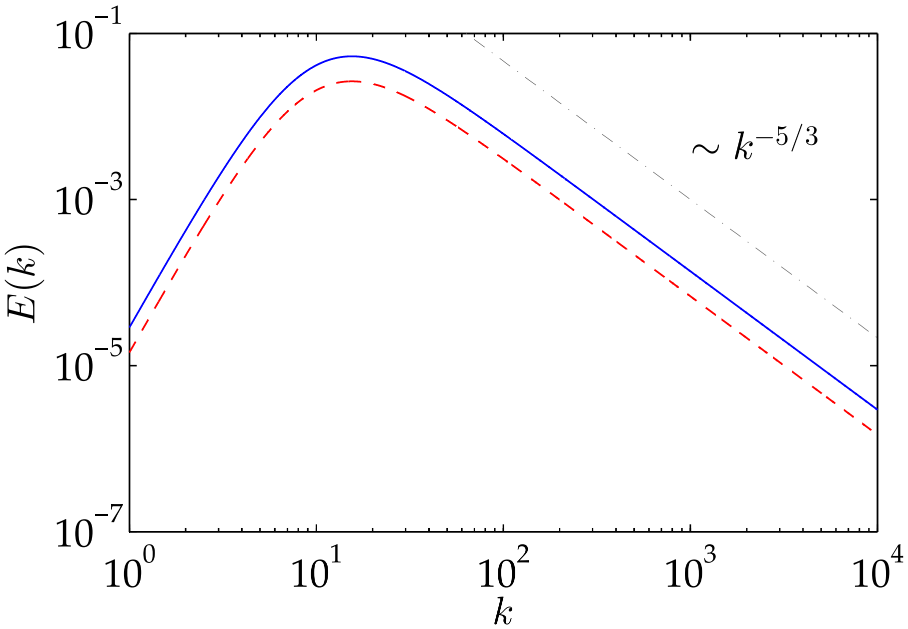

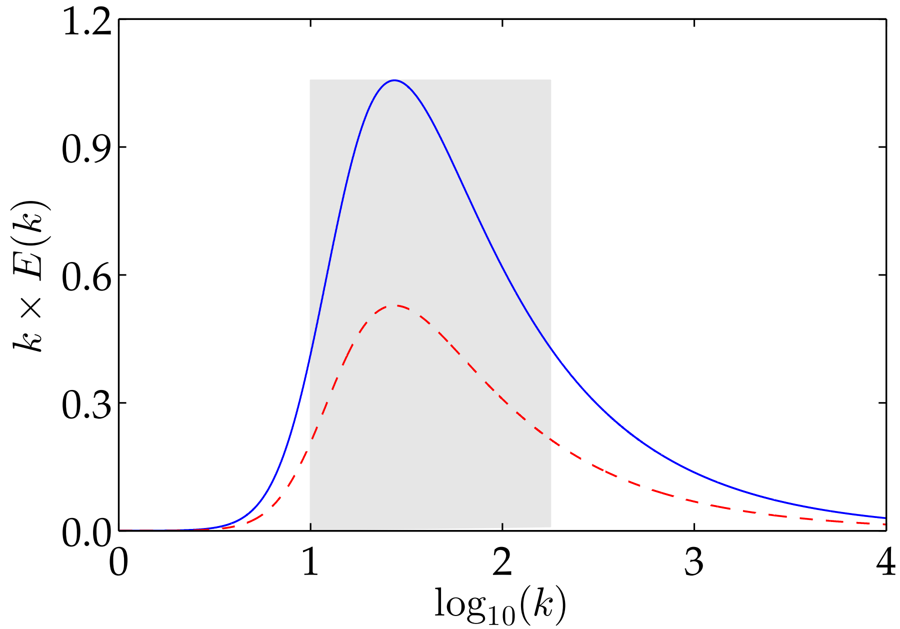

von Kármán spectrum (arbitrary units here)

—— for $k_t = 3$ - - - for $k_t = 1.5$

log-log scales (to observe the $-5/3$ law) versus $k \times E(k)$ on linear scales

On the right, area of the grey rectangle, $1.25 \times \ln(10) \times 1.05 \simeq 3$

(error detection is straightforward)

Theory of Kolmogorov – K41

- Eddy of size l and of velocity u_l,
  eddy-life time or turn-over time $t_l \sim l/u_l$

$$\frac{u_l^2}{l/u_l} = \text{cst} = \epsilon \qquad \Longrightarrow \qquad u_l \sim (\epsilon l)^{1/3}$$

- Kinematic energy $\mathcal{E}_l$ associated with eddies of size $l \sim 1/k_l$
  $\mathcal{E}_l \sim u_l'^2 \sim (\epsilon l)^{2/3}$

- Turbulent kinetic energy spectrum $\mathcal{E}_l \sim k_l E(k_l)$, and thus

$$E(k_l) \sim \frac{\epsilon^{2/3} k_l^{-2/3}}{k_l} \sim \epsilon^{2/3} k_l^{-5/3} \qquad \text{Kolmogorov's law}$$

Inertial subrange between kL_f and kl_η at high-Reynolds number,
where $E(k, \epsilon, \nu) = E(k, \epsilon)$

Theory of Kolmogorov – K41 (cont.)

In the inertial subrange (fine turbulence structures) of the turbulent kinetic energy spectrum, there is a universal spectrum shape

$$E(k) = C_K \epsilon^{2/3} k^{-5/3} \qquad C_K \simeq 1.5$$

where C_K is the Kolmogorov constant, and this region widens as the Reynolds number increases.

The original formulation by Kolmogorov (1941, 1962) is based on structure functions, see exercises. The theory is still debated, *e.g.* self-similarity at small scales, intermittence in the dissipation process.

The concept of energy cascade has been introduced by Richardson (1922), and first developed theoretically by Kolmogorov (1941) and also Obukhov (1941).

Arnold Kolmogorov (1903-1987)

Theory of Kolmogorov – Experimental evidence

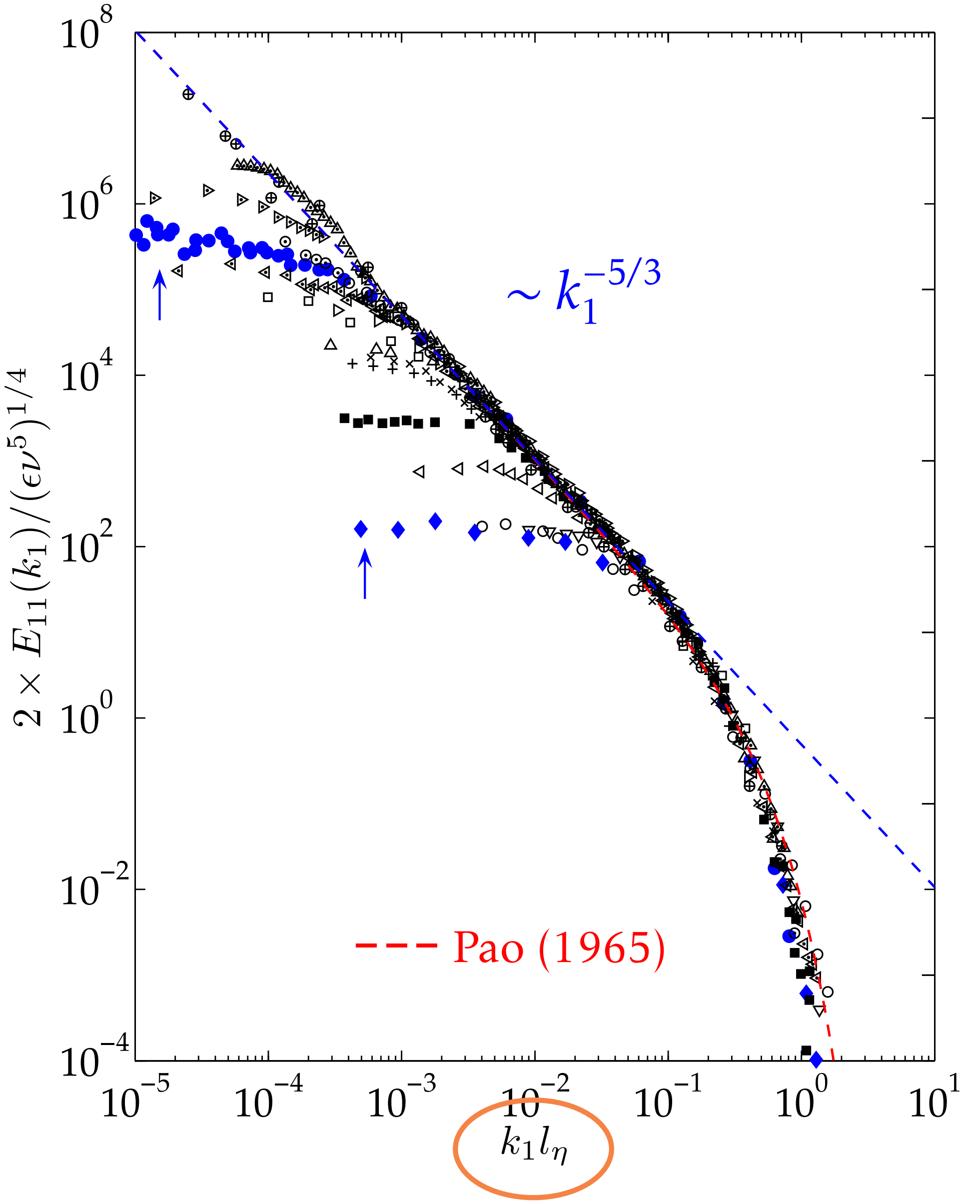

$$\overline{u_1'^2} = \int_{-\infty}^{+\infty} E_{11}^{(1)}(k_1)dk_1$$

Re_{λ_g}

○	23	boundary layer (Tielman, 1967)
♦	23	cylinder wake (Uberoi & Freymuth, 1969)
▽	37	grid turbulence (Comte Bellot & Corrsin, 1971)
◁	72	grid turbulence (Comte Bellot & Corrsin, 1971)
■	130	homogeneous shear flow (Champagne *et al.*, 1970)
+	170	pipe flow (Laufer, 1952)
×	282	boundary layer (Tielman, 1969)
□	308	cylinder wake (Uberoi & Freymuth, 1969)
△	401	boundary layer (Sanborn & Marshall, 1965)
▷	540	grid turbulence (Kistler & Vrebalovich, 1966)
◁	600	boundary layer (Saddoughi, 1994)
⊙	780	round jet (Gibson, 1963)
●	850	boundary layer (Coantic & Favre, 1974)
▷	1500	boundary layer (Saddoughi, 1994)
⊕	2000	tidal channel (Grant *et al.*, 1962)
△	3180	return channel (CAHI Moscou, 1991)

Theory of Kolmogorov – Experimental evidence

Measurements of Grant, Stewart & Moilliet (1962)

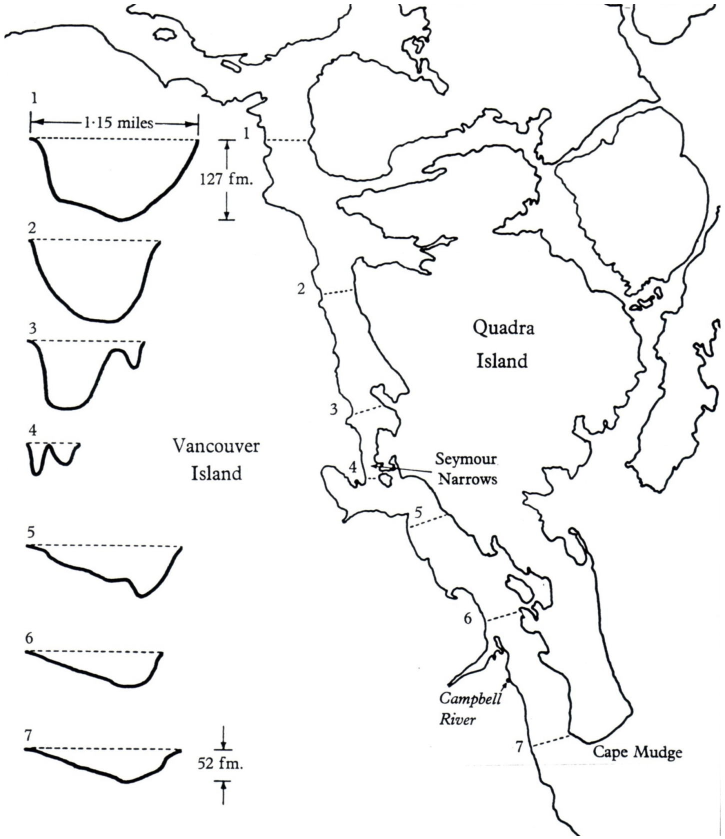

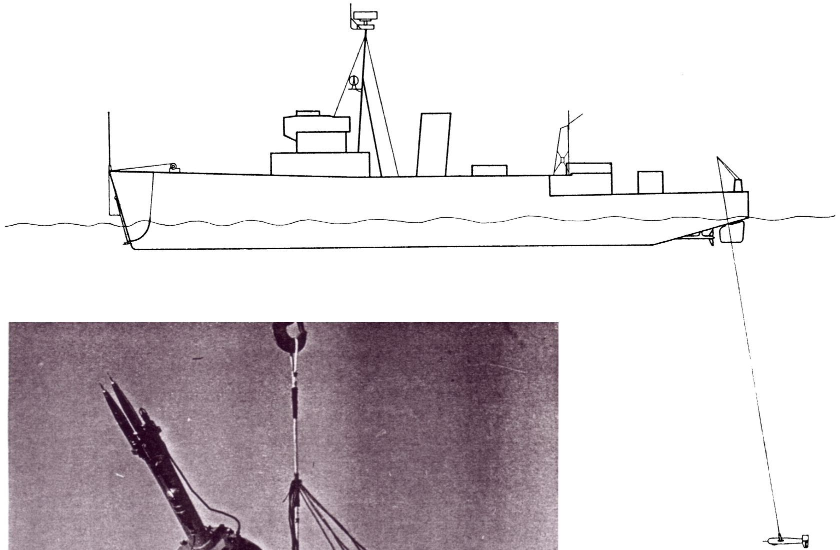

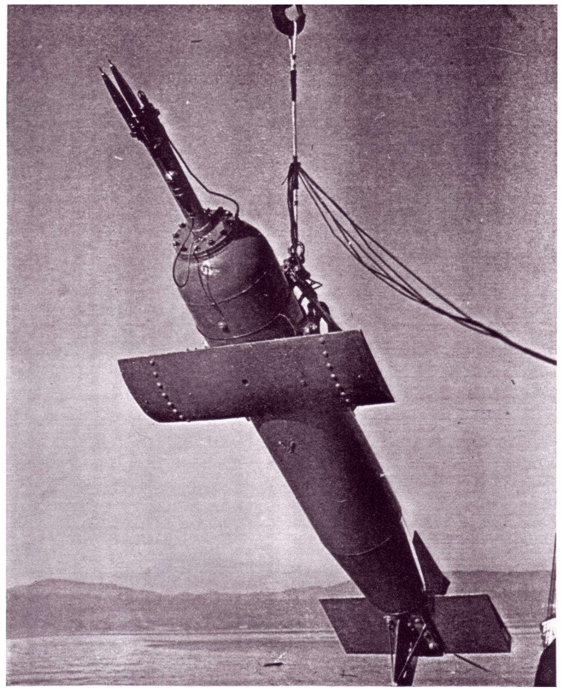

In summary

The rate of dissipation is imposed by larger structures, energy-containing eddies $u' \sim k_t^{1/2}$ time $\sim L_f/u'$

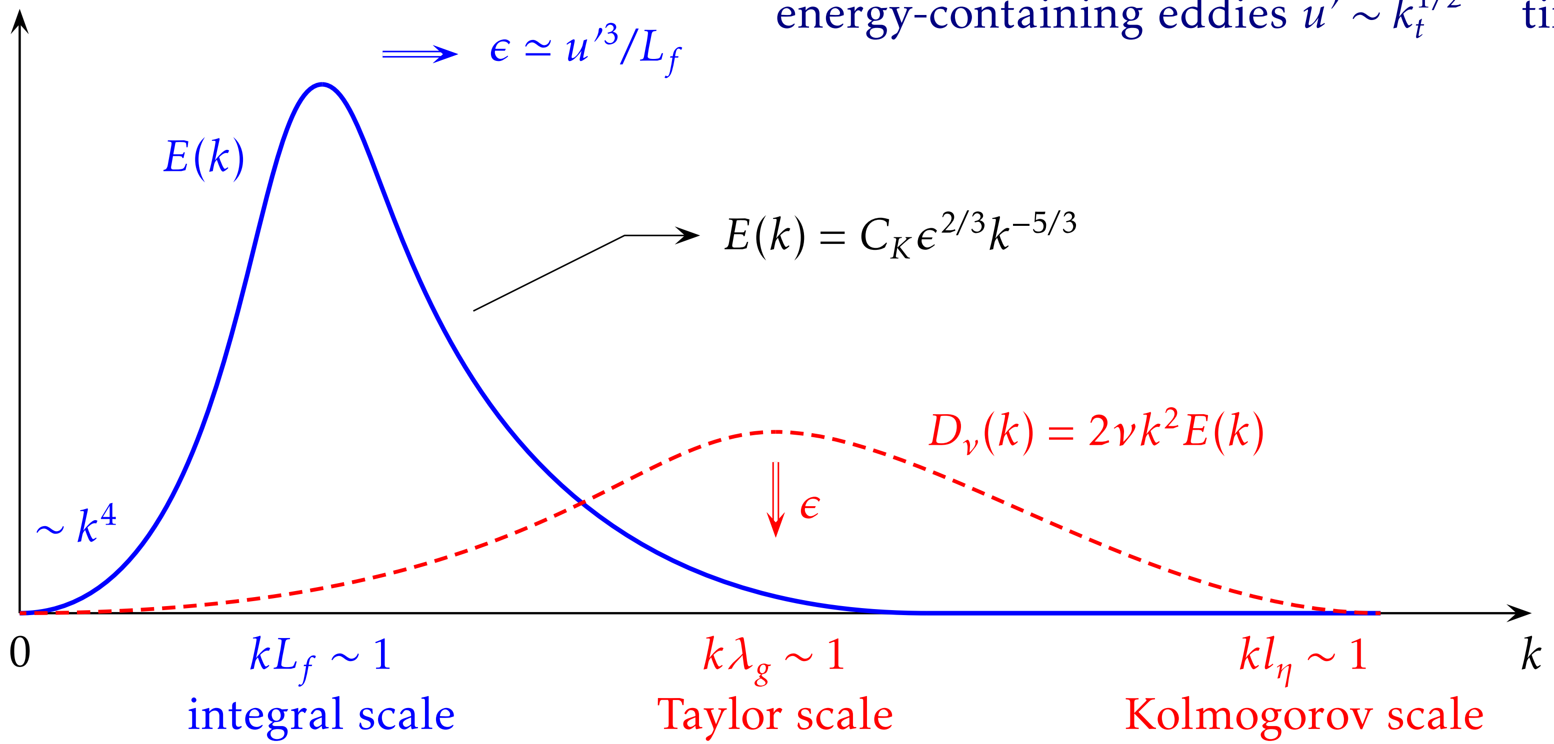

viscous scales ($\mathrm{Re}_\eta = 1$)

$l_\eta = \nu^{3/4}\epsilon^{-1/4}$ $\quad u_\eta = \nu^{1/4}\epsilon^{1/4}$

$L/l_\eta \sim \mathrm{Re}_{L_f}^{3/4}$

- **Energy cascade in a turbulent mixing layer (Brown & Roshko, 1974)**
  Shadowgraphs (spark source)

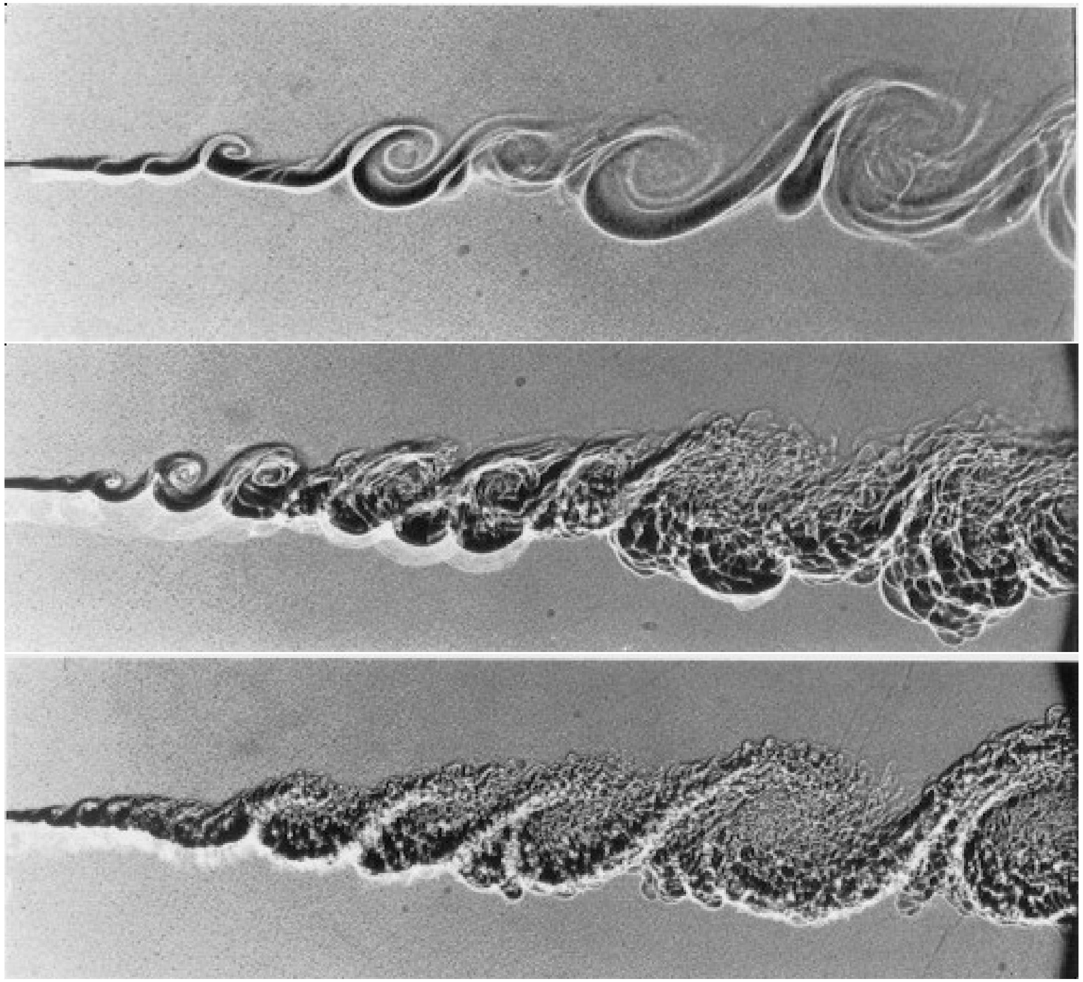

Energy cascade in a mixing layer by increasing the Reynolds number (through pressure and velocity, ×2 for each view)

More small-scale structures are produced without basically altering the large-scale ones

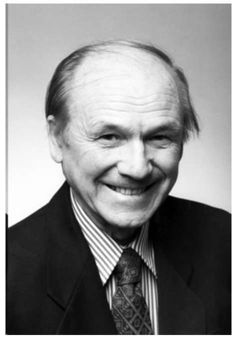

Anatol Roshko (1923-2017)

- **Lin's equation (1947)**

  Transport equation for the turbulent kinetic energy spectrum $E(k)$

  A way to derive this equation is

  to consider the transport equation for the Reynolds tensor $R_{ij} = \overline{u_i'(\boldsymbol{x})u_j'(\boldsymbol{x}+\boldsymbol{r})}$, known as the Kármán & Howarth equation

  to take its Fourier transform and to contract subscripts as follows $i = j$

  ... which gives

$$\boxed{\frac{\partial}{\partial t}E\,(k,t) = T\,(k,t) - 2\nu k^2 E\,(k,t)}$$

  where the nonlinear term $T(E)$ is linked to the third-order (triple) velocity correlation. This term can be directly associated with the energy transfer between turbulent structures of different size.

Lin's equation (cont.)

In order to illustrate this point, Lin's equation can be integrated over all the wavenumbers k

$$\underbrace{\frac{\partial}{\partial t}\int_0^\infty E(k,t)\,dk}_{=\partial k_t/\partial t} = \int_0^\infty T(k,t)\,dk - \underbrace{2\nu\int_0^\infty k^2 E(k,t)\,dk}_{=\epsilon}$$

For isotropic turbulence $\partial k_t/\partial t = -\epsilon$. Consequently, the transfer term integral must be zero

$$\int_0^\infty T(k,t)\,dk = 0$$

The term T corresponds to the rate of energy transferred to successively smaller and smaller scales of the turbulent field.

Note that this term T is difficult to measure, and it makes sense only for high Reynolds number turbulent flows, in order to ensure the presence of an inertial region in the spectrum $E(k)$.

Lin's equation (cont.)

Let us introduce the function $S(k,t)$ defined by

$$S(k,t) = -\int_0^k T(k',t)\,dk'$$

$S(k,t)$ represents the energy transferred from all the wavenumbers smaller than k (large structures) to wavenumbers larger than k (small structures)

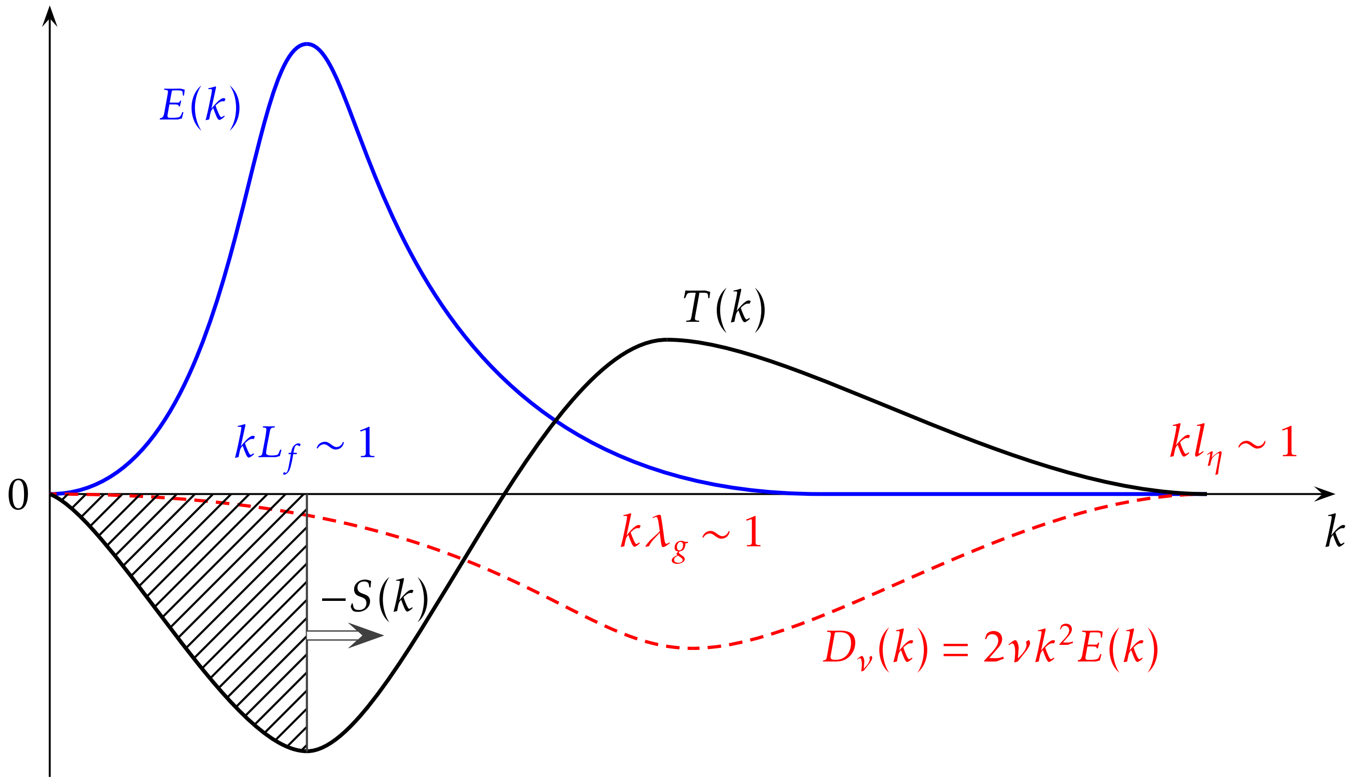

Introduction to experimental techniques

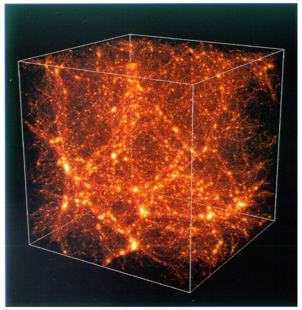

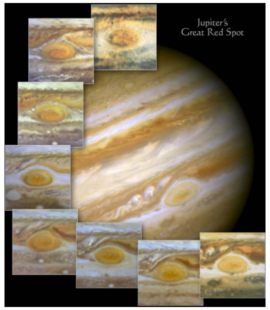

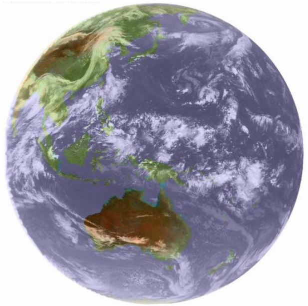

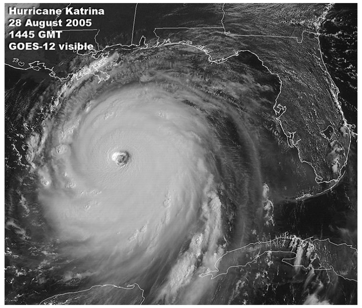

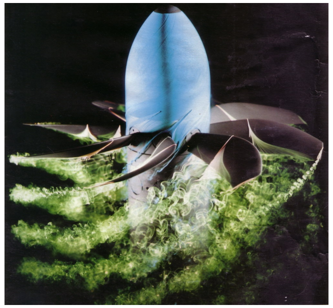

Flow field survey and visualization

Aerodynamics : loads (forces, moments) acting on a tested body, Pitot tube, pressure rack (flow distorsion), 5-hole pressure probe (flow direction), surface flow visualization (skin friction line pattern, separation), wall shear stress τ_w

Velocity field : hot wire anemometry (HWA), laser doppler velocimetry (LDV), particle image velocimetry (PIV), and also time-resolved 3D-particle tracking (PTV-4D)

Optical techniques for flow visualization : ombroscopy, Schlieren methods, laser-induced fluorescence (LIF)

Wall pressure field : pressure sensitive paint (PSP), MEMS microphone antenna

More advances methods : Rayleigh diffusion (velocity and temperature)

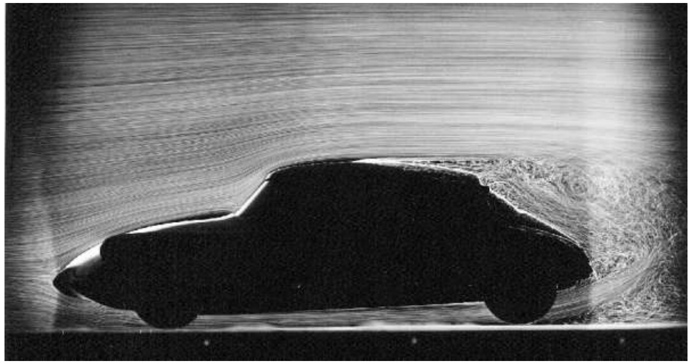

Water tunnel visualisation of the flow past the Citroën DS21 (H. Werlé, ONERA)

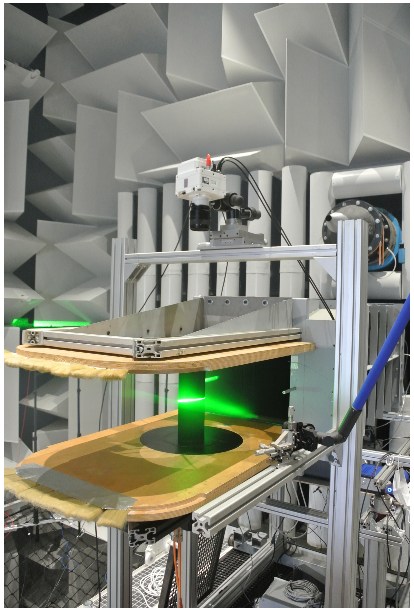

PIV on a wind turbine blade (E. Jondeau, LMFA)

Flow field survey and visualization (cont.)

All these measurement techniques are complementary : intrusive or not, global view of the field versus single point measurement, quantitative/qualitative technique, ease of implementation, space and time resolution, ...

There are many similarities between numerical simulation and experimental work : spatial and temporal resolutions, signal processing, processing on supercomputers (PIV for example)

Some introductory references to complement the textbook lists given in Introduction :

Délery, J., 2011, courses & conferences, https://www.onera.fr/fr/cours-exposes-conferences

Fernholz, H.H. *et al.*, 1996, New developments and applications of skin-friction measuring techniques *Meas. Sci. Technol.*, **7** 1396-1409.

Goldstein, R.J., 1996, *Fluid Mechanics Measurements* (2nd ed.), CRC Press.

Merzkirch, W., 1987, *Flow visualization* (2nd ed.), Academic Press, New-York.

Settles, G.S., 2001, *Schlieren and shadowgraph techniques : Visualizing phenomena in transparent media*, Springer-Verlag, Berlin.

Hot Wire Anemometry (HWA)

The fluid flow will cool the resistance proportionally to its velocity

Single wire set normal to the mean flow $\bar{U}_1$

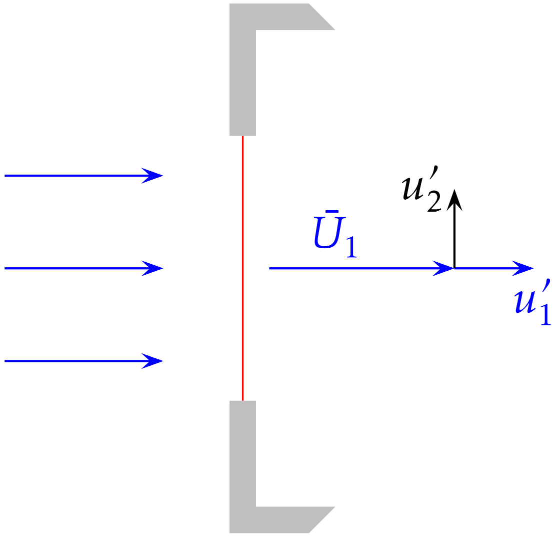

$$U_n \simeq \bar{U}_1 + u_1'$$

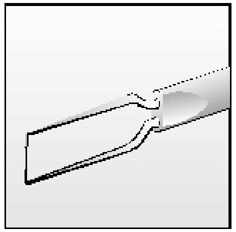

X hot-wire probe

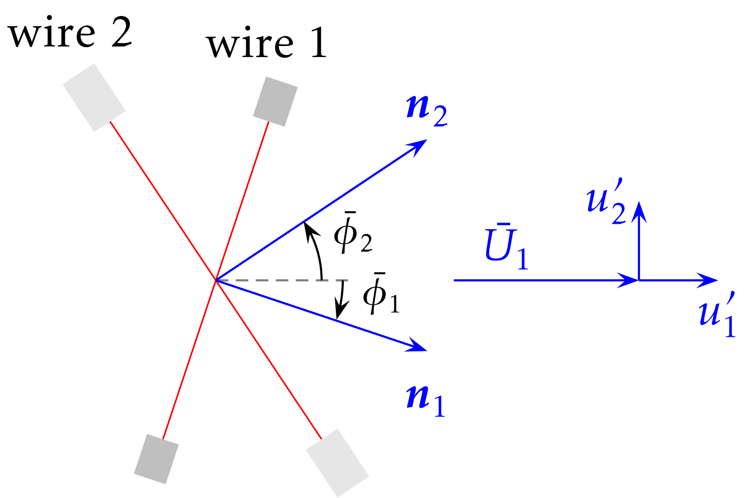

$$\begin{cases} U_{n_1} \simeq (\bar{U}_1 + u_1')\cos\bar{\phi}_1 - u_2'\sin\bar{\phi}_1 \\ U_{n_2} \simeq (\bar{U}_1 + u_1')\cos\bar{\phi}_2 + u_2'\sin\bar{\phi}_2 \end{cases}$$

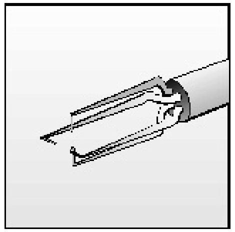

Hot Wire Anemometry (cont.)

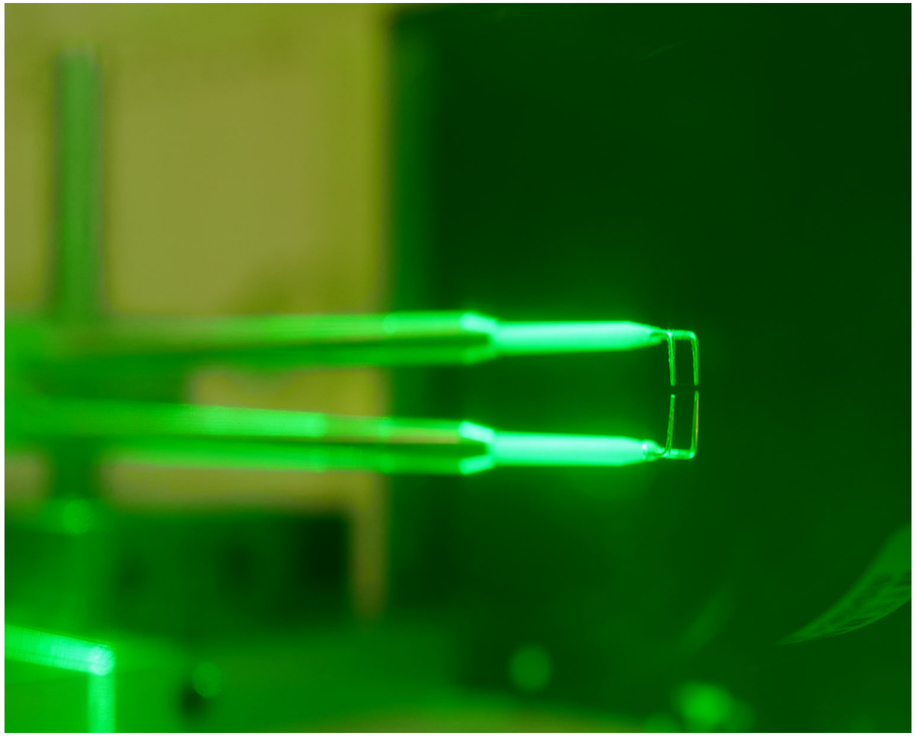

(image from LMFA UMR 5509)

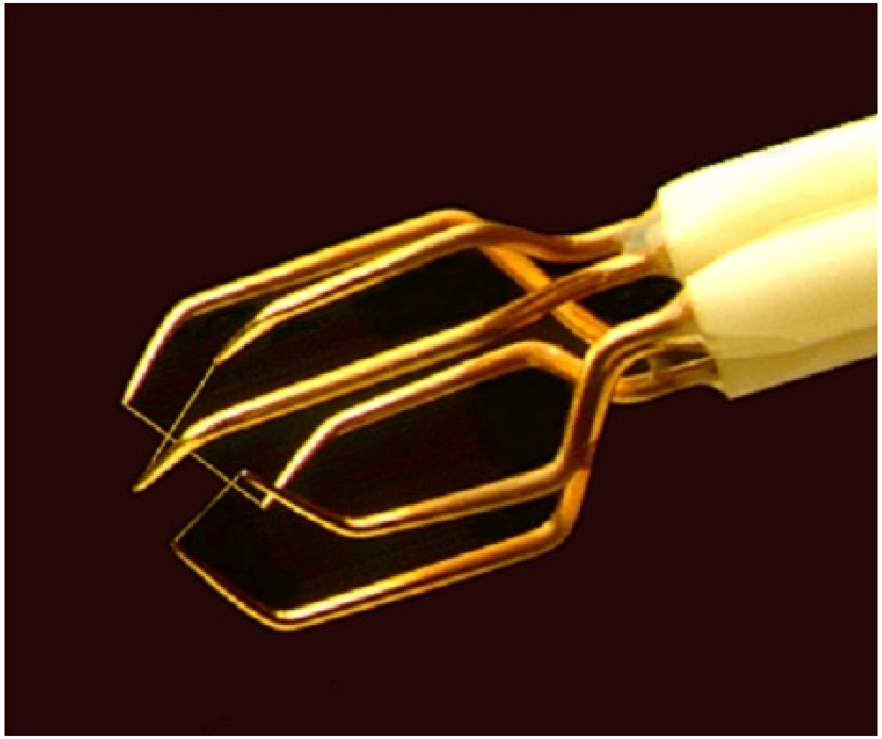

Tri-axial probes for 3-D flows : 3 sensors in an orthogonal system, measures within 70° cone
(image from Dantec)

Hot Wire Anemometry (cont.)

- usually wire made of platinum or tungsten, $d \simeq 2$ to $5\ \mu$m, $2l \simeq 0.5$ to 1 mm (which imposed the spatial resolution)

- wire cooling by forced convection, the heat balance was formulated by King's law (1914) : Joule energy brought to the wire corresponds to the heat loss by forced convection

Louis Vessot King (1886 - 1956)

$$\mathrm{Nu}_d = f(\mathrm{Re}_d, \mathrm{Pr}) = a\,\mathrm{Pr}^{1/5} + b\,\mathrm{Pr}^{1/3}\,\mathrm{Re}_d^{1/2}$$

with $\mathrm{Re}_d = \dfrac{U_n d}{\nu}$ and $\mathrm{Nu}_d = \dfrac{R_w I_w^2}{2\pi l \lambda (T_w - T)}$

3 possible modes : Constant Temperature Anemometer (CTA), Constant Current Anemometer (CCA) and more recently Constant Voltage Anemometer (CVA, velocity and temperature)

Hot Wire Anemometry (cont.)

Advantages

- u_i', $\overline{u_i' u_j'}$ and also θ, $\overline{u_i' \theta}$ with greater difficulty
- wall shear stress τ_w (hot film)
- continuous detection $f \sim 70$ kHz
- inexpensive

Drawbacks

- intrusive, point measurement
- tricky for free edges, recirculations zones... (no forced convection regime)
- no information about the sign of U_n
- calibration, nonlinear response for high-intensity turbulence (high levels)
- fragile

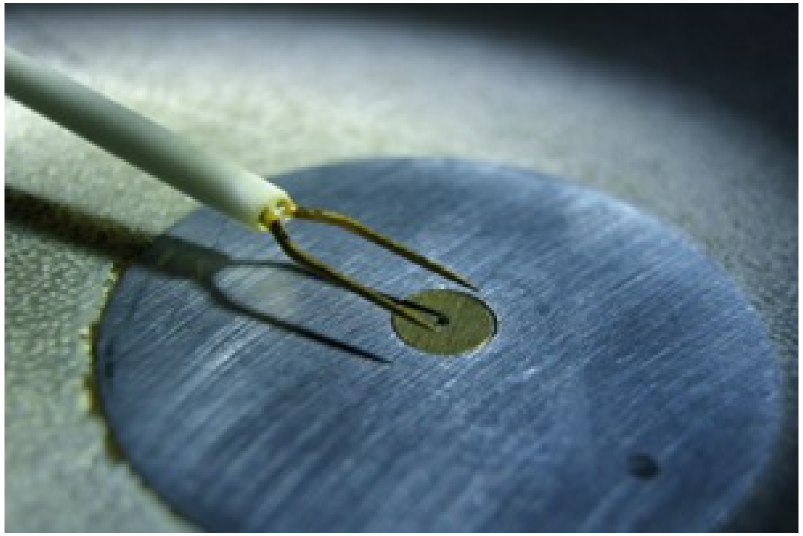

Hot-wire sensor and wall pressure pin-hole microphone to investigate a turbulent boundary layer (E. Salze, LMFA)

Hot Wire Anemometry (cont.)

HWA in mode CVA to mesure u_1' in a supersonic boundary layer

M = 2.3, $x_2 = 0.27\delta$, $\delta = 15 \times 10^{-3}$, $U_{e1} = 555$ m.s^{-1}, $T_e = 145$ K, $P_e = 0.492 \times 10^5$ Pa

Comte-Bellot & Sarma, 2001, *AIAA Journal*, **39**(2)

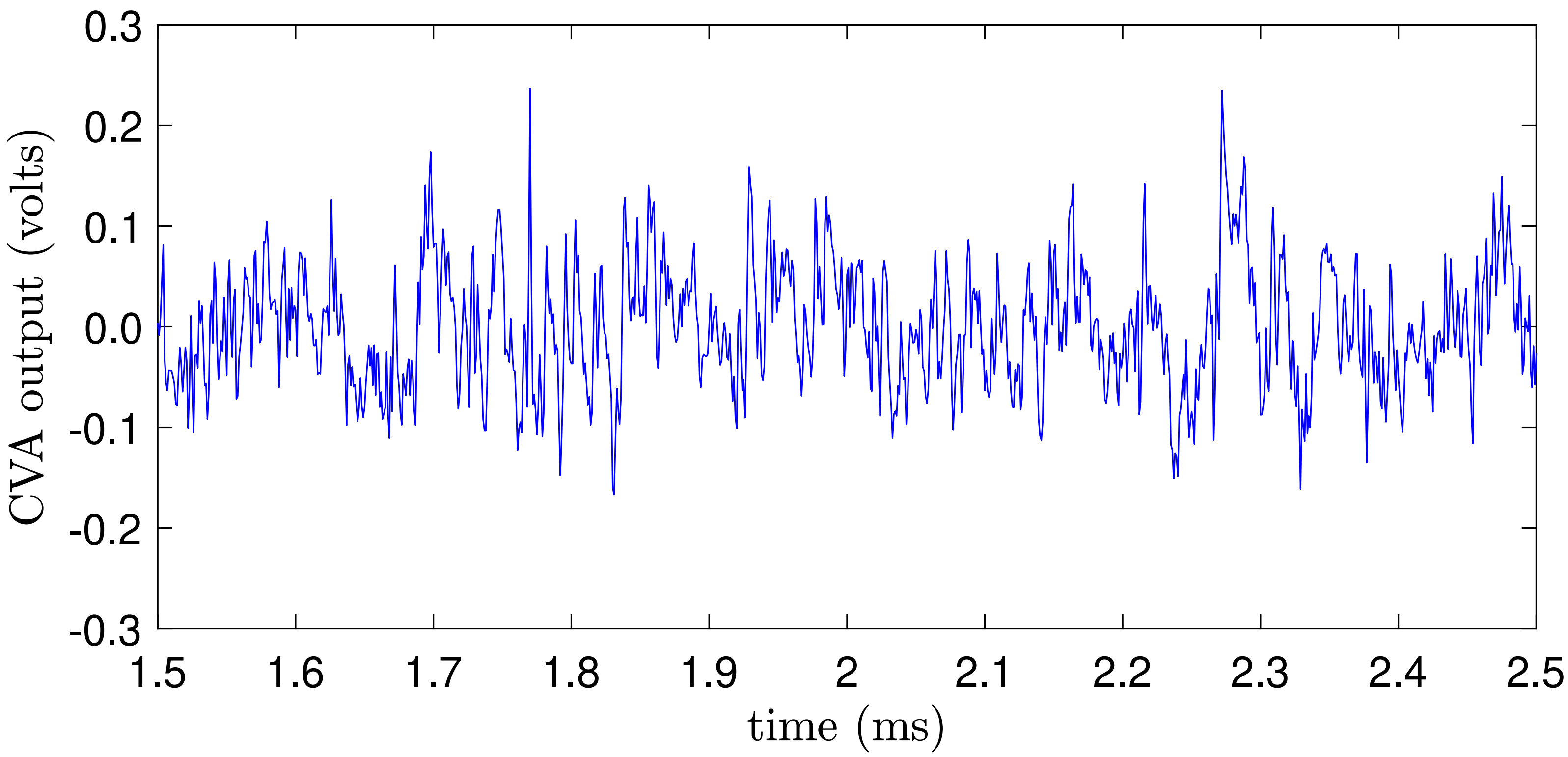

Laser Doppler Anemometry (LDA)

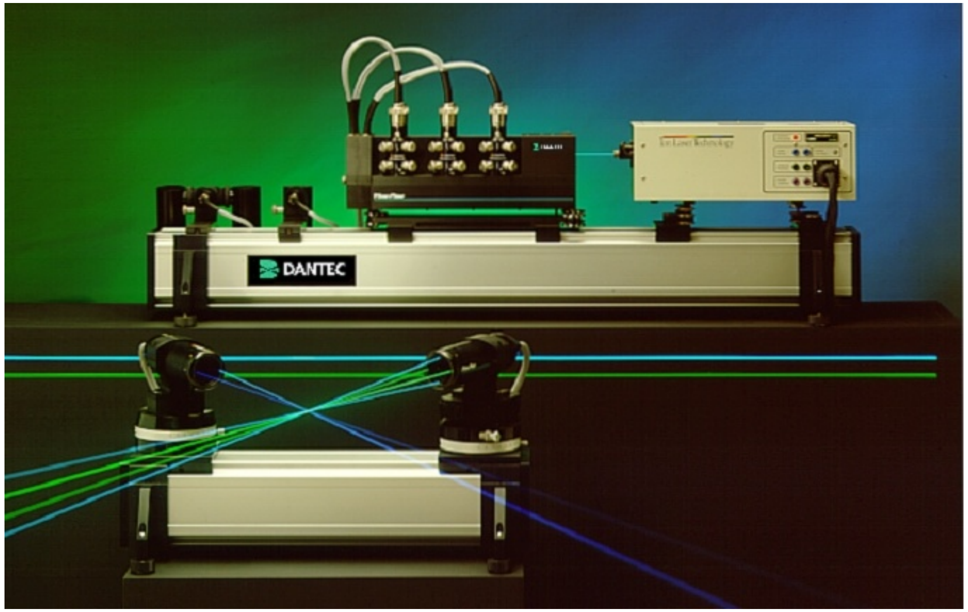

Set-up for 3-D velocity measurements (image from Dantec)

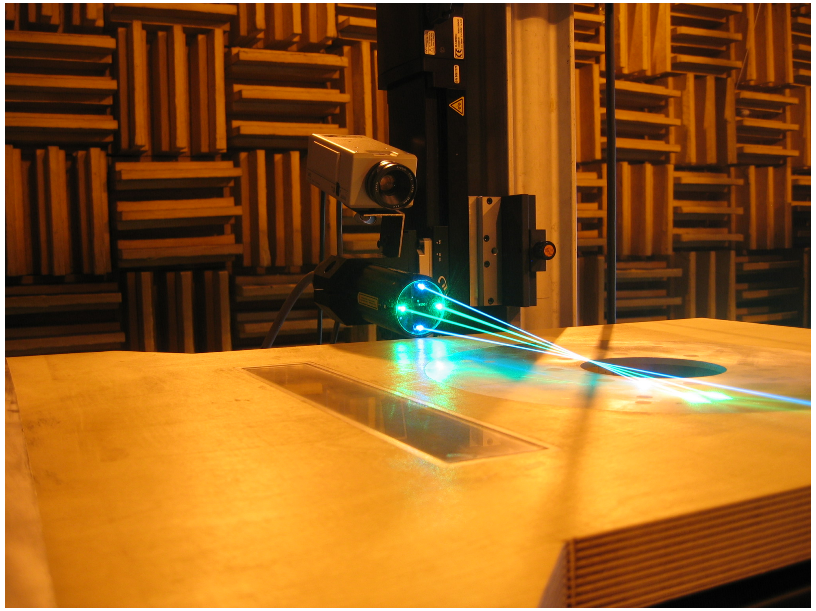

Measurement of the velocity in the shear layer developing above a round cavity (E. Jondeau, LMFA)

Doppler effect

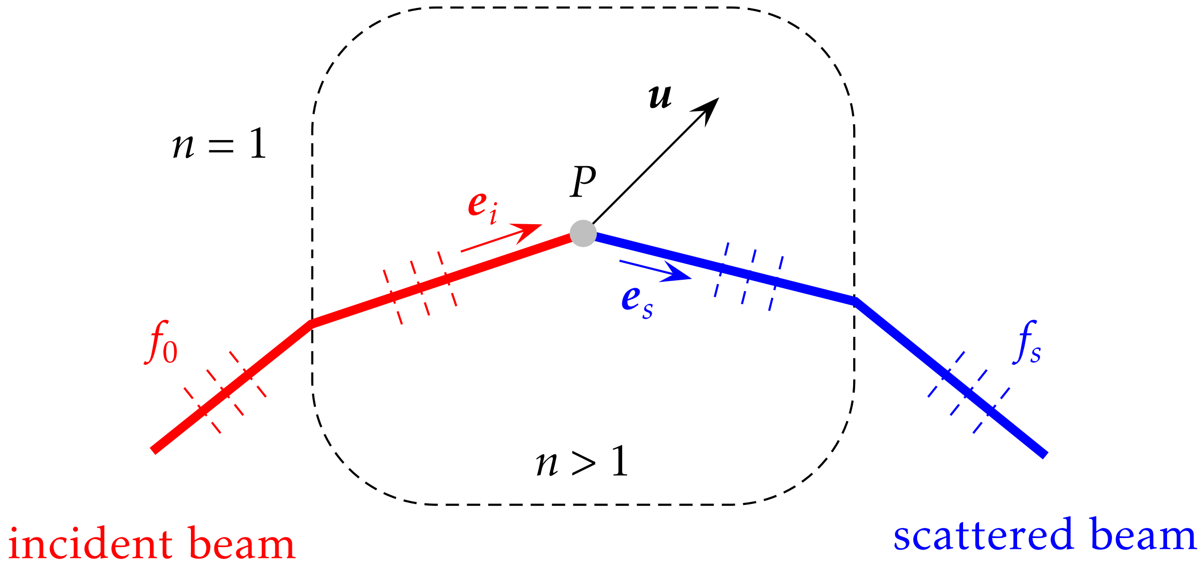

Doppler effect for a fluid particle P moving at velocity $\boldsymbol{u}$
in a medium of refractive index n

$$\Delta f = f_s - f_0 = \frac{1}{\lambda_b} \boldsymbol{u} \cdot (\boldsymbol{e}_s - \boldsymbol{e}_i)$$

Dual-beam Laser Doppler Anemometer

Scattered light collected in the backward direction (back scattering)

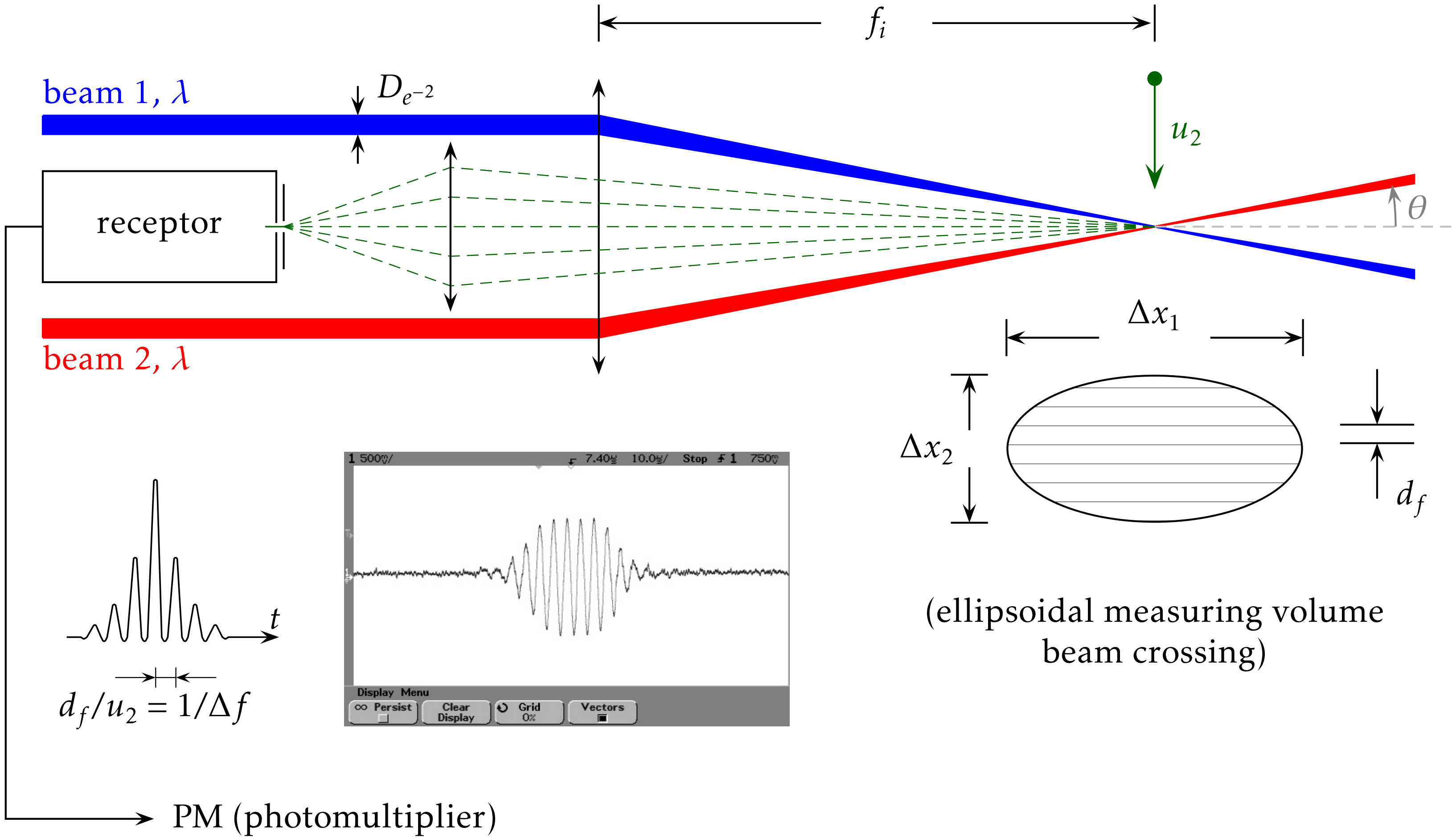

Laser Doppler Anemometry

Advantages

- non-intrusive method
- only the velocity is measured u_i', in $3-D$, and also two-point correlation $\overline{u_i'u_j'}$
- detached flows, recirculation zones, high levels of velocity fluctuations (linear response for the Doppler shift)

Drawbacks

- seeding of the flow with tracer particles (fluid which must be optically transparent)
- detection (random sampling)
- formally measurement of particle velocity : relaxation time $\tau_s = d_P^2\rho_P/(18\mu)$ from Stokes drag $\boldsymbol{u}_P = \boldsymbol{u}(1-e^{-t/\tau_s})$

LDV measurement in a free subsonic jet in the anechoic wind tunnel (V. Fleury & S. Barré, LMFA)

Argon-ion laser $W \simeq 1$ W ; two colors, green $\lambda_b = 514.5$ nm and blue $\lambda_b = 488.0$ nm ; continuous laser excitation

Particle Image Velocimetry (PIV)

Particles are illuminated in a plane of the flow twice within a short time interval $\Delta t \sim \mu$s

$u_1 \simeq \Delta x_1/\Delta t \quad u_2 \simeq \Delta x_2/\Delta t$
(How to match each particle between the two images ?)

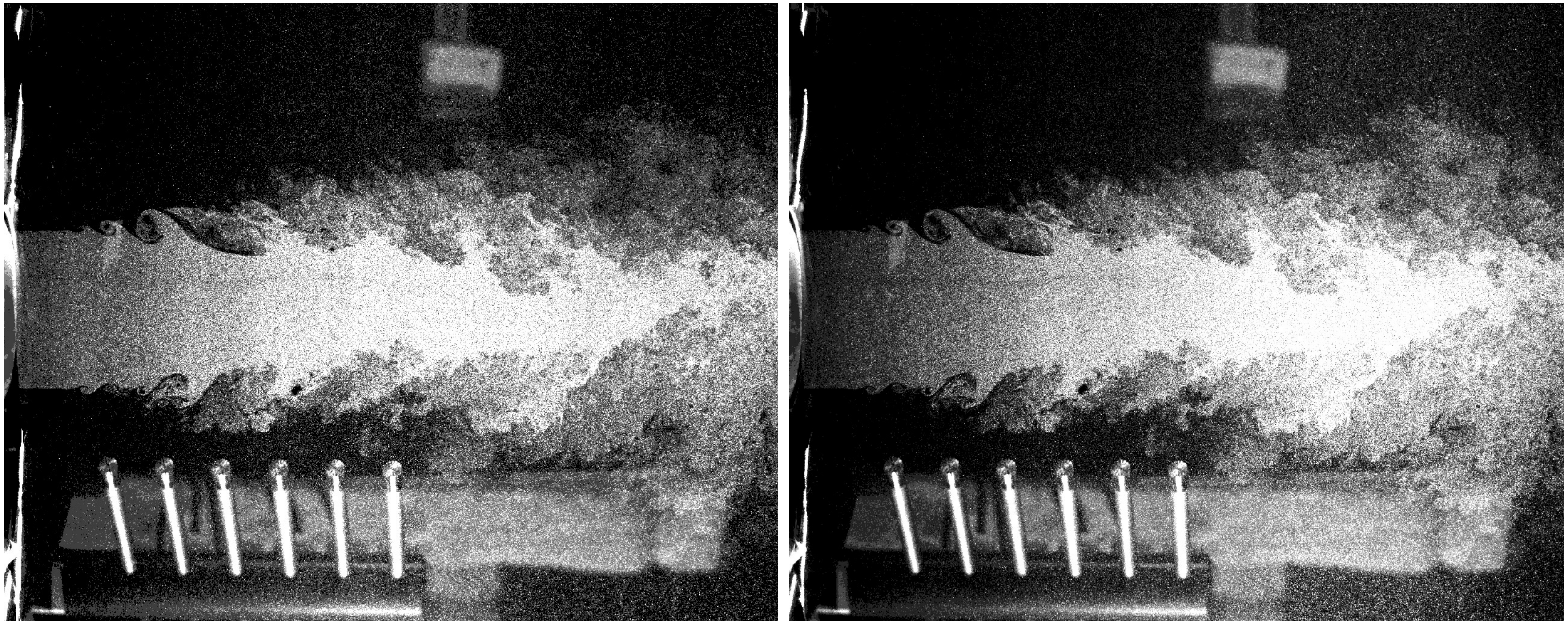

Two successive particle images of a free subsonic jet (V. Fleury, LMFA)

Particle Image Velocimetry (cont.)

Advantages

- non-intrusive method
- only the velocity is measured u_i', in $3-D$, and also two-point correlation $\overline{u_i' u_j'}$
- vue instantanée globale du champ de vitesse
- facile d'emploi

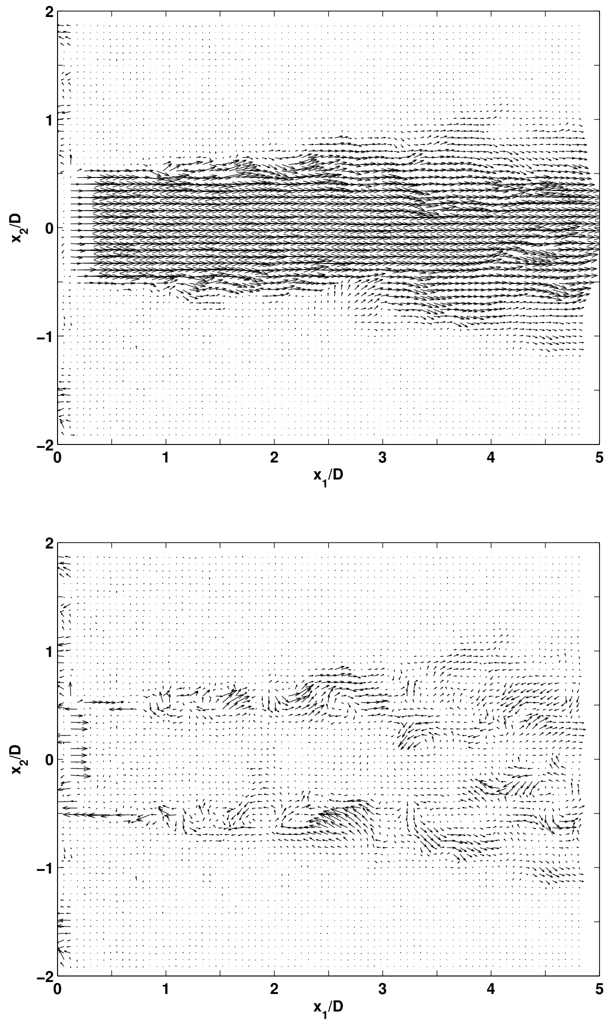

Subsonic jet, $Re_D = 6.3 \times 10^4$, $u_j = 18.8$ m.s^{-1}, $D = 5$ cm, (V. Fleury, LMFA)

Drawbacks

- ensemencement de l'écoulement (optiquement transparent)
- fréquence d'acquisition faible, $f \leq 100$ Hz
- mesure ponctuelle de vitesses de particules (cf. LDV)
- relativement coûteux

- **Space-time velocity correlations by dual-PIV** (Fleury *et al.*, *AIAA J.*, 2008)
  Subsonic jet flow

  $\mathrm{Re}_D = 7.5\times10^5$, $\mathrm{M}=0.9$, $D = 3.8$ cm, $\delta_\theta/D|_{\mathrm{init}} \simeq 3\times10^{-3}$
  At $x = 5D$, $L_{11}^{(1)} \simeq 0.27\ D \sim$ cm, Kolmogorov scale $l_\eta \simeq 10^{-4}\ D \sim \mu$m

  - Space-time second-order correlation functions $R_{11}(\boldsymbol{x},\boldsymbol{\xi},\tau)$ and $R_{22}(\boldsymbol{x},\boldsymbol{\xi},\tau)$ measured at $\boldsymbol{x}=(6.5D, 0.5D)$ $\quad L_{11}^{(1)} \simeq 2\delta_\theta \quad L_{22}^{(1)} \simeq \delta_\theta$

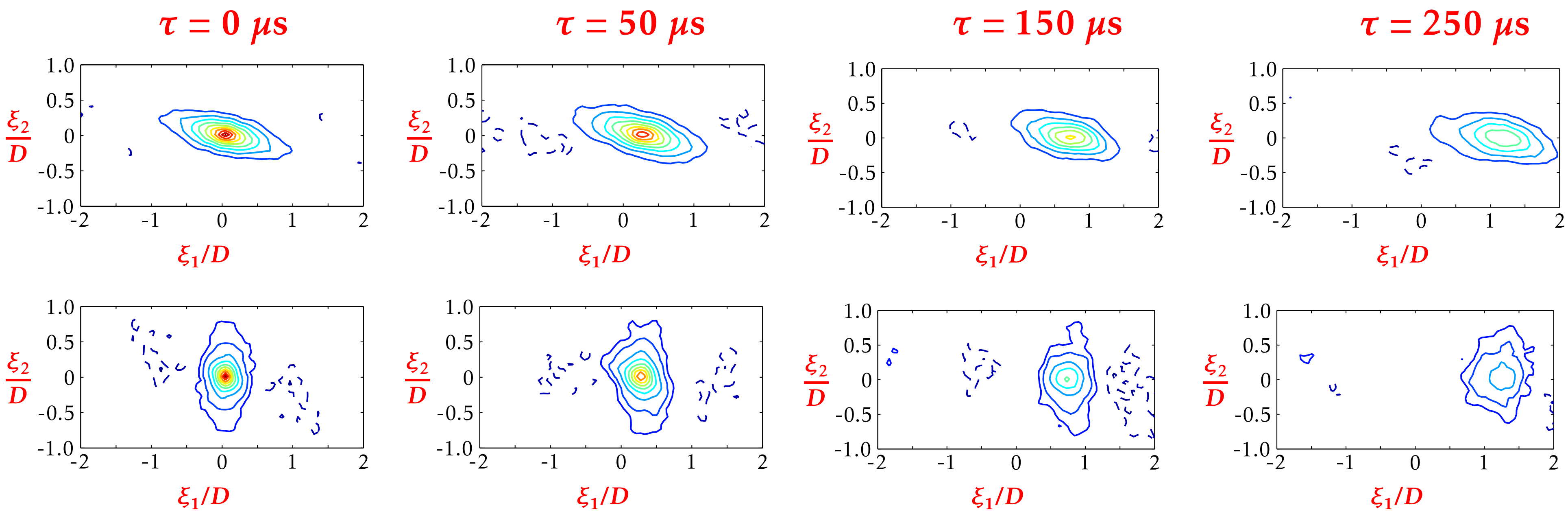

Particle Image Velocimetry (TR-PIV)

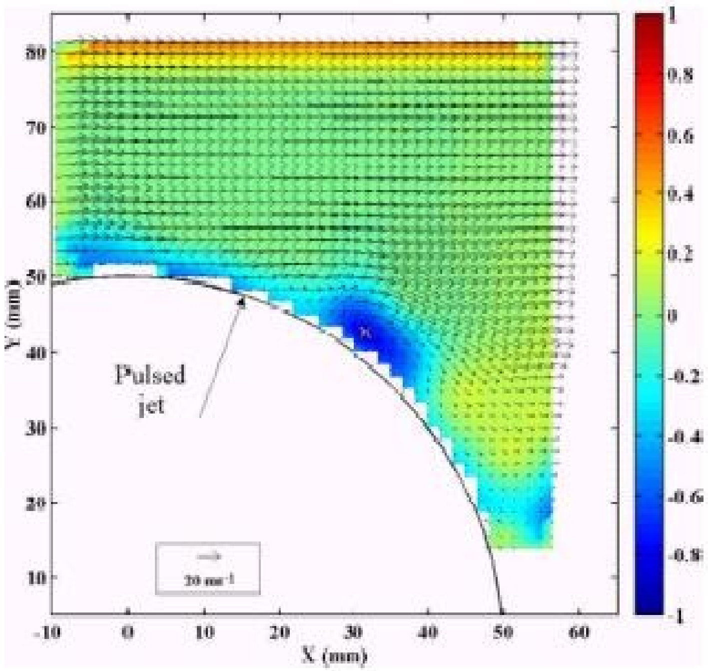

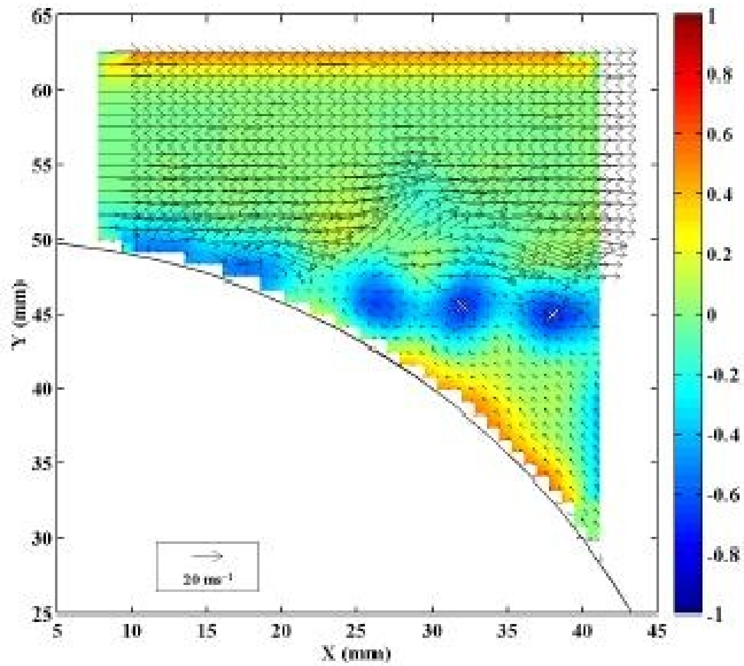

Recollement de la zone séparée en aval d’un cylindre
par effet d’un jet pulsé à 200 Hz, issu d’une fente de 1.5 mm
placé à 110 degrés du point d’arrêt,
diamètre du cylindre 10 cm, vitesse incidente 20 m.s^{-1}

Béra *et al.*, *Eur. J. Mech. B-Fluids* (2000)

Particle Image Velocimetry

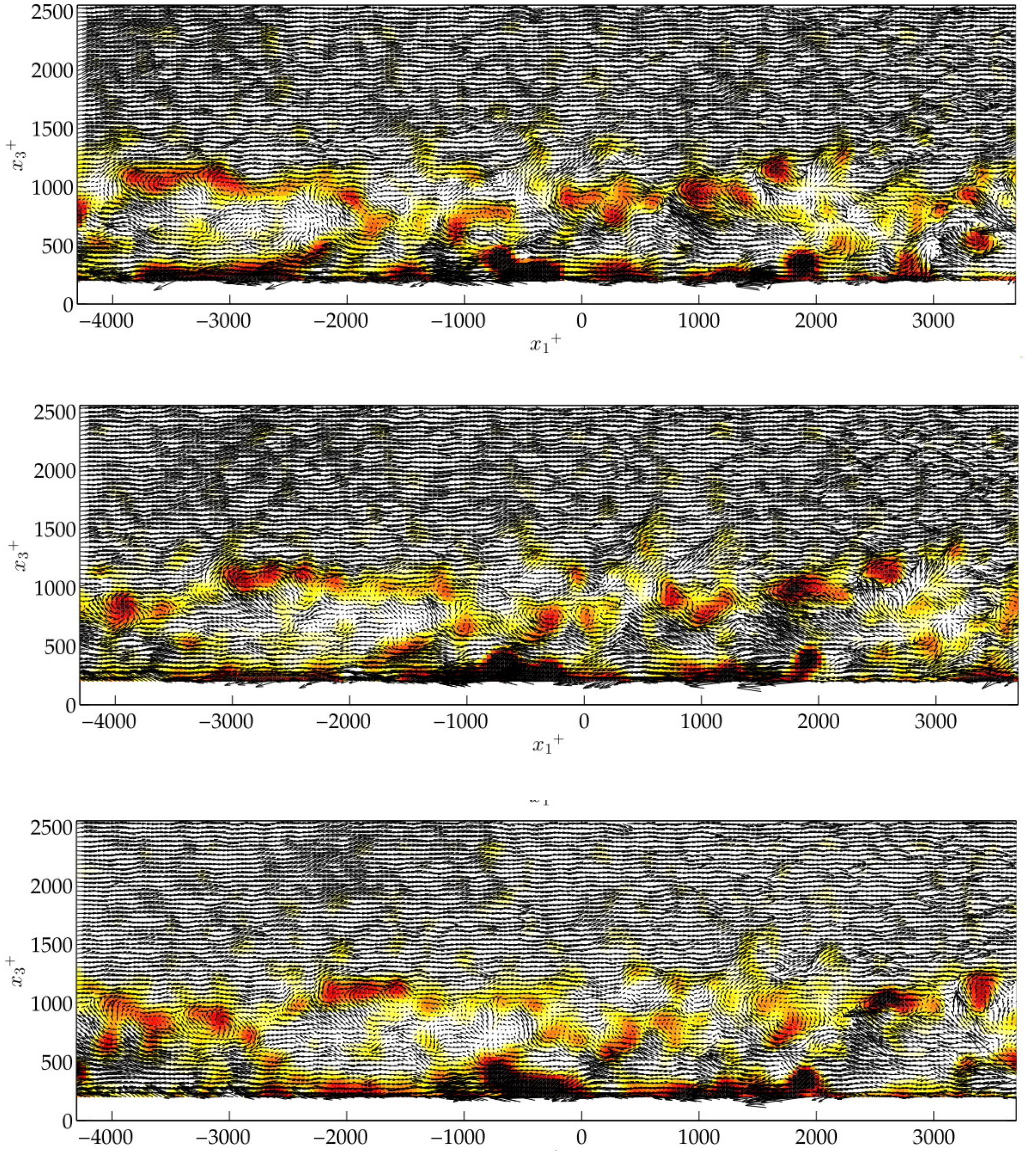

2D-2C PIV measurement in a turbulent boundary layer

Velocity field colored by vorticity magnitude $|\omega_2|$ (the convection velocity $U_c = 0.85 U_\infty$ has been substracted to enlight large structures)

3 velocity fields at $t = 0$, $t = 161\mu$s and $t = 322\mu$s

$\delta \simeq 20$ mm, $U_\infty = 45$ m.s^{-1}

Window size 68×21 mm, pairs of images with a delay of 10 μs @ 6.2 kHz, LaVision software to compute the flow field, cross-correlations on 12×12 pixels with 50% overlap

(E. Salze & E. Jondeau, LMFA)

Various techniques

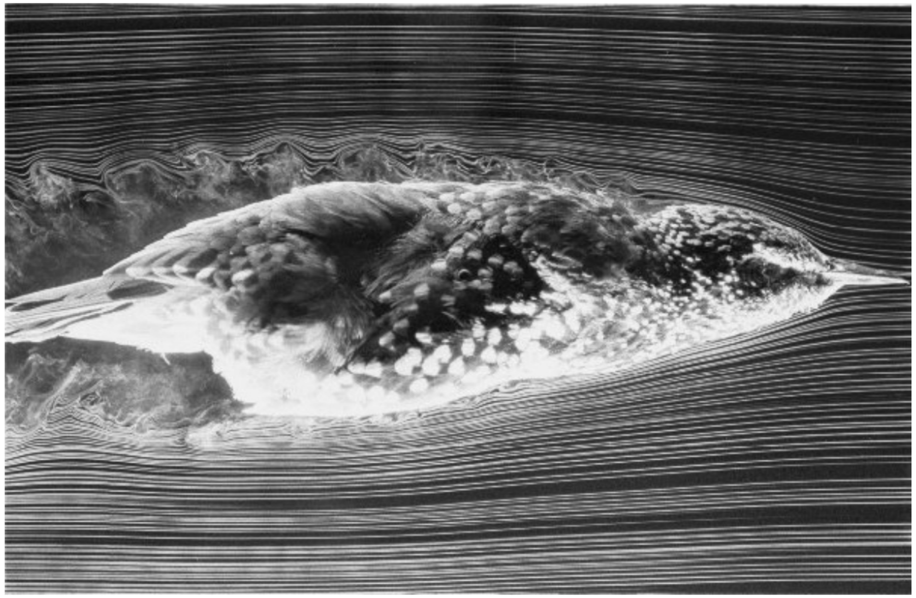

Visualization of airflow over a European starling using the smoke-wire technique
media.efluids.com

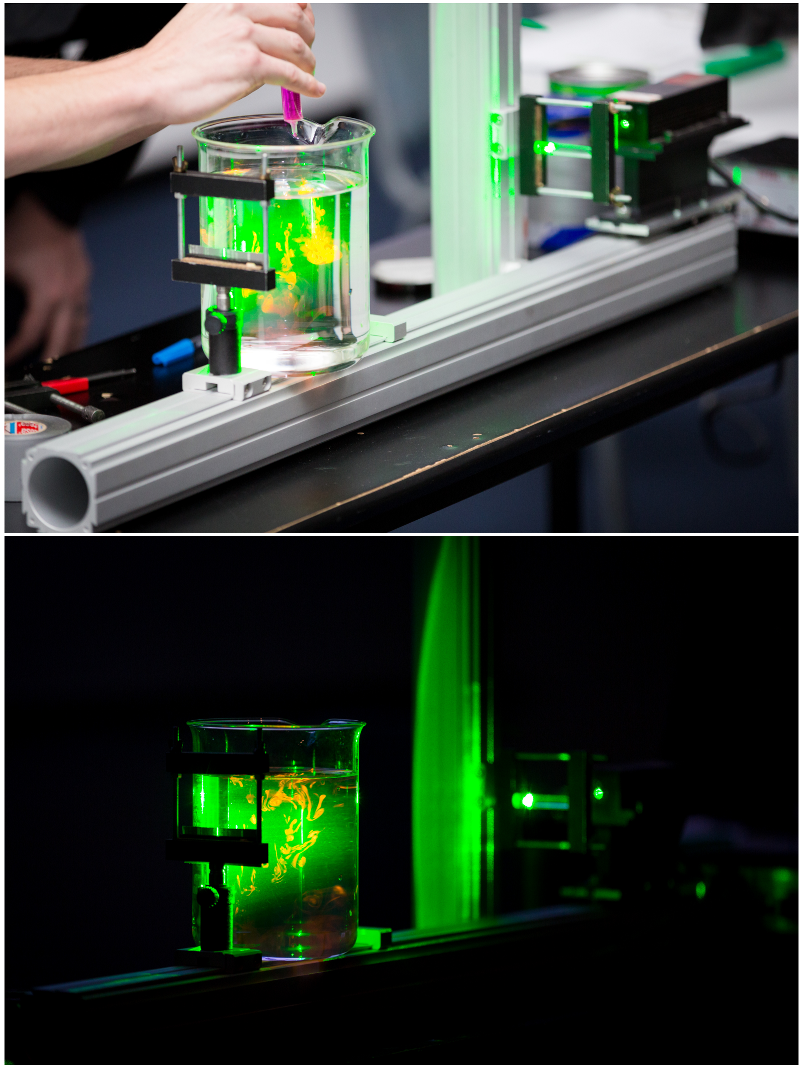

Planar laser induced fluorescence
D. Edgington-Mitchell (Monash Univ)

Shadowgraph of transition on a sharp cone at Mach 4.31

(Schneider, *Prog. Aero. Sci.*, 2004, from Naval Ordnance Lab ballistics range)

A shock wave emanating from the nose of a cone travelling at Mach 4 in a ballistic range shows up as a thin dark line in this Schlieren image ; the sharp jump in density across the shock produces a steep refractive-index gradient, which in turn deflects transmitted light, thereby producing the contrast that we observe in the figure. Also visible are laminar and turbulent boundary layers and the wake. $\mathrm{Re} \simeq 6.2 \times 10^5$

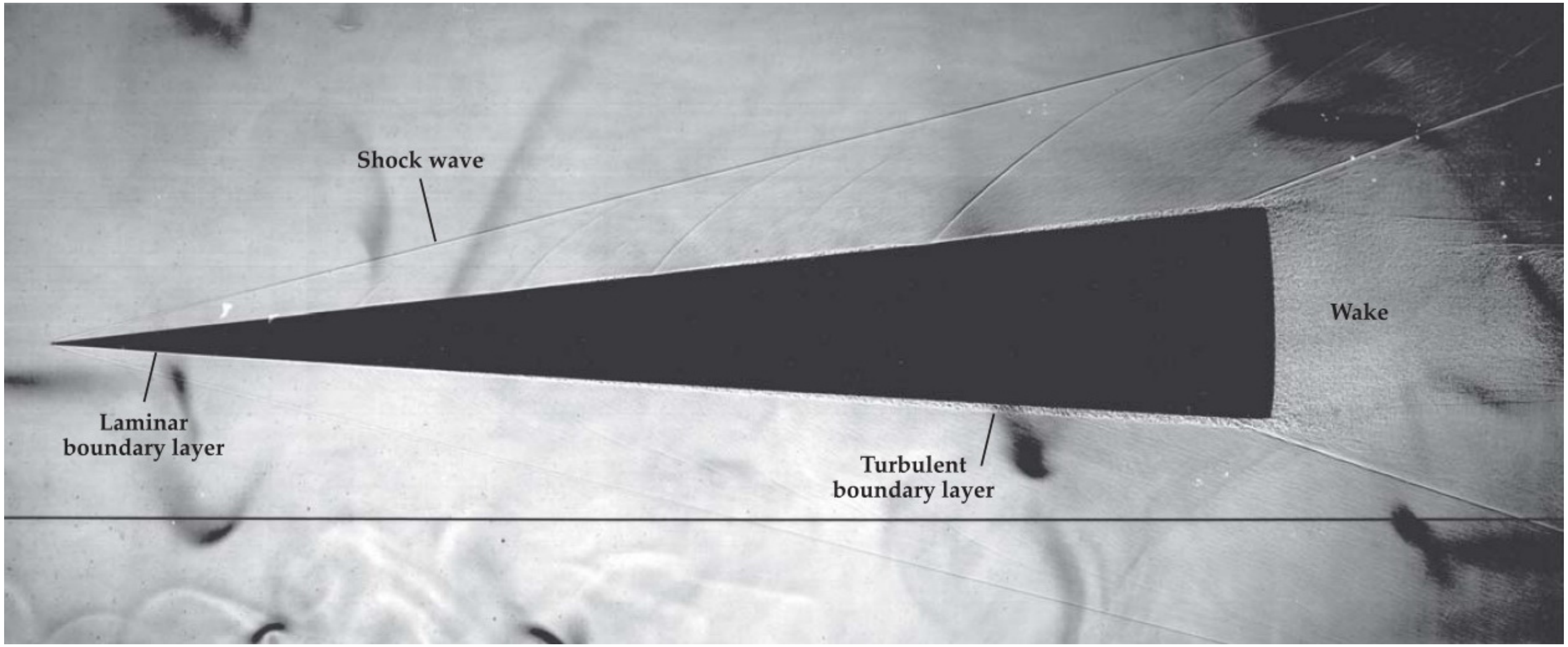

Shadowgraphy (cont.)

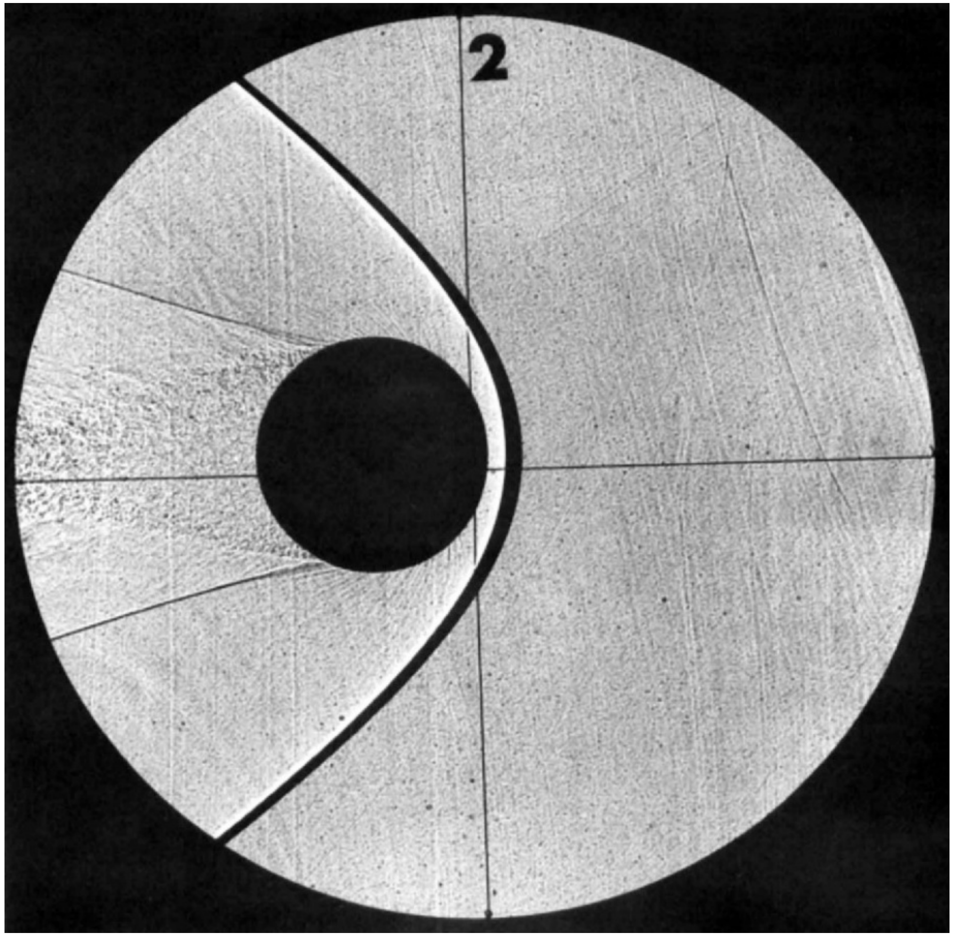

Shadowgraph image of supersonic flow (from the left to the right) at a Mach number $M = 1.7$ past a sphere

(Stilp, 1968 in Merzkirch, 1987, fig. 3.10)

Schlieren vs shadowgraphy

Refraction index n for perfect gas :
Gladstone - Dale law $n - 1 \simeq k\rho$ with $k \simeq 0.226 \times 10^{-3}$ m^3.kg (air)

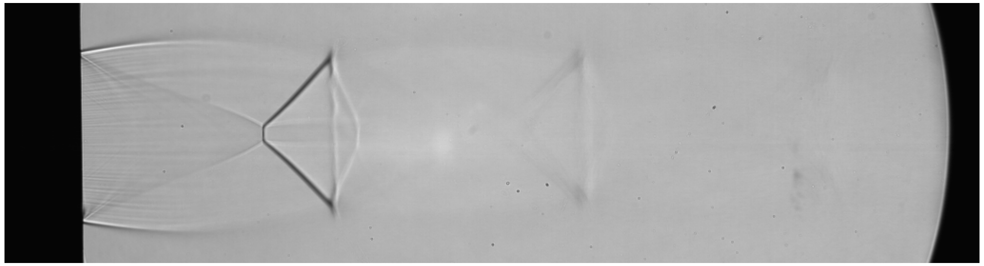

shadowgraphy
illuminance level $\sim \nabla_\perp^2 n \sim \nabla_\perp^2 \rho$

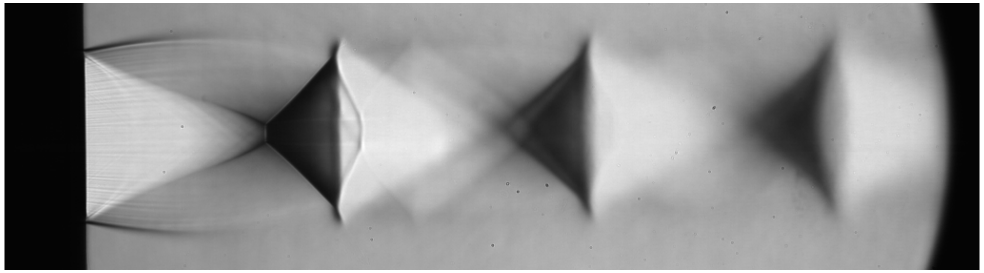

schlieren
illuminance level $\sim \nabla_\perp n \sim \nabla_\perp \rho$

(useful when high sensitivity is required)

NPR = 3.68 $\quad M_j = 1.5 \quad T_t/T_\infty = 1.04$
view obtained by averaging 500 images
$x_\perp$ direction perpendicular to the optical axis of the schlieren system

Z-type schlieren system

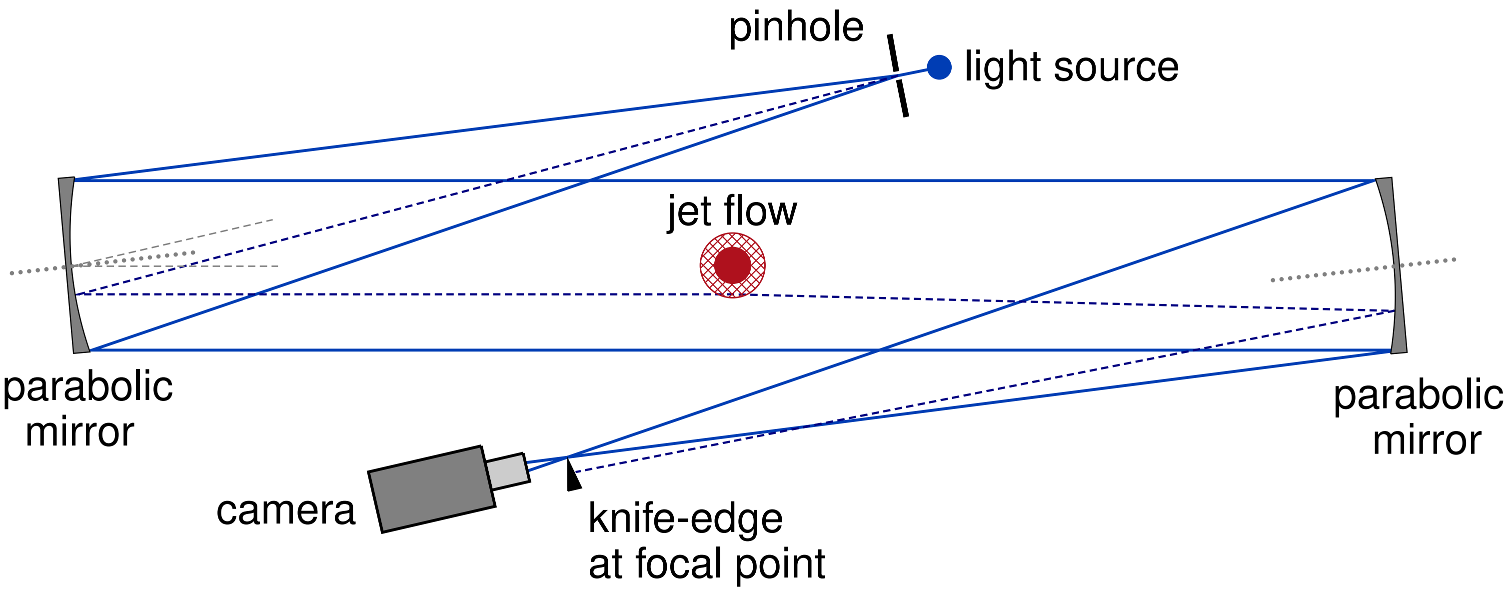

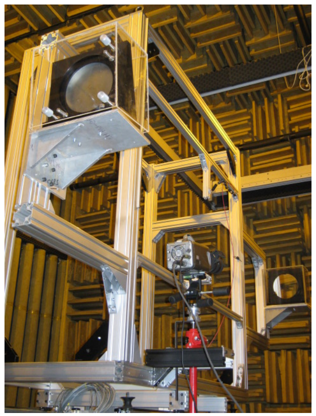

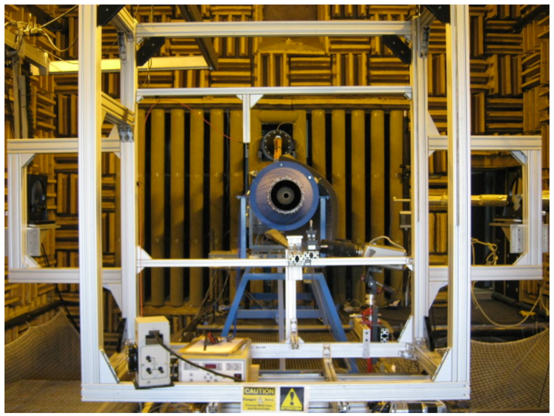

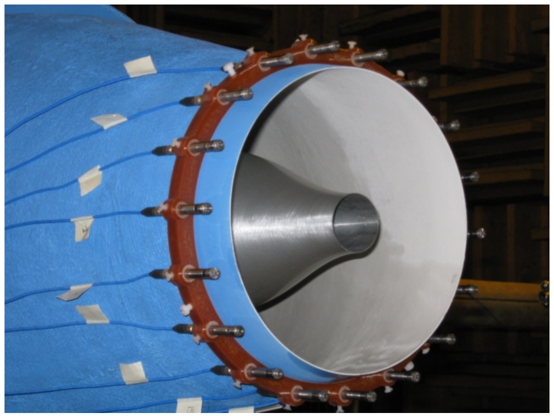

- **Noise of underexpanded screeching jets**
  Time-averaged Schlieren pictures ($D = 38$ mm, $M_j = 1.5$)

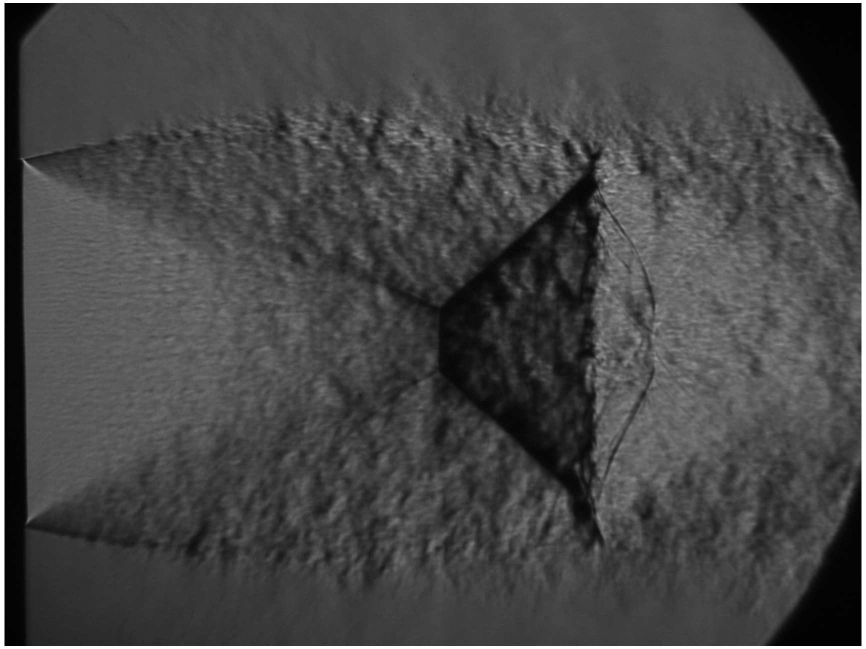
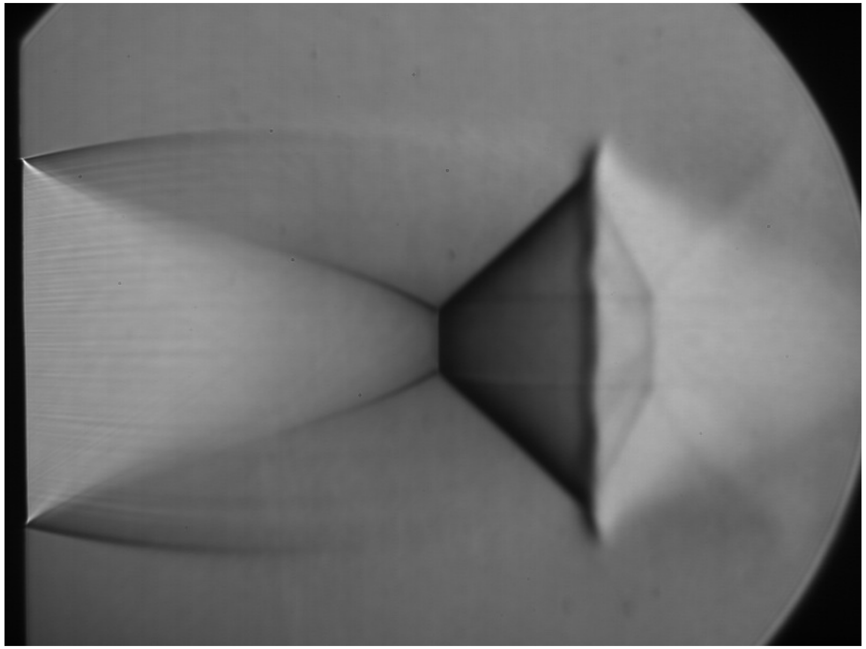

$M_j = 1.5 \;\; M_f = 0.39$ phase average

André *et al.*, 2011, *AIAA Journal*, 49(7)

Concluding remarks

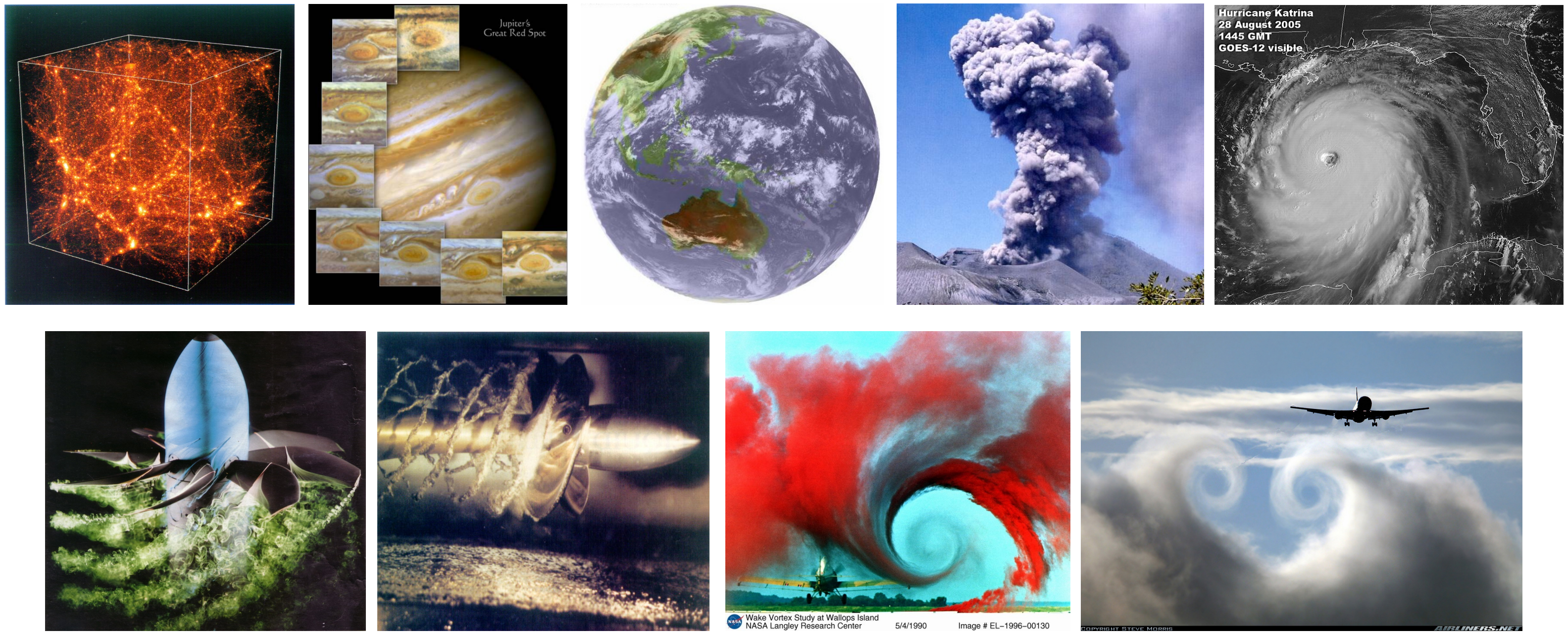

Turbulence and Aeroacoustics

Highly qualified candidates are encouraged to apply at any time !

Contact directly Christophe Bogey (numerics) and Thomas Castelain (experiments)

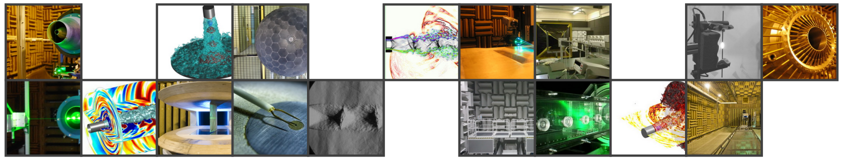

http://acoustique.ec-lyon.fr